SYNTHESIS, CHARACTERISATION AND COORDINATION CHEMISTRY OF NOVEL *N*-ALKYL- AND *N,N*-DIALKYL-*N'*-ACYLTHIOUREAS

A thesis submitted to the

UNIVERSITY OF CAPE TOWN

in fulfilment of the requirements for the degree of

DOCTOR OF PHILOSOPHY

by

TARRON GRIMMBACHER

B.Sc (Hons.) - (University of Cape Town)

Department of Chemistry

University of Cape Town

Rondebosch 7700

South Africa

August 1995

"What we anticipate seldom occurs; what we least expect generally happens"

Benjamin Disraeli

ACKNOWLEDGEMENTS

I would sincerely like to thank :

- My supervisor, Professor Klaus Koch, for all his help, motivation and constant enthusiasm
- Mom and Jannie, who have always stood by me
- Professor Roger Hunter for the fruitful discussions and valuable comments made during the course of this work
- Dr Susan Bourne and Ms Anita Coetzee for determining the crystal structures addressed in this work
- Dr Krassi Dimitrikova for her assistance with the NMR spectra and Dr Christa Loubser for the help with photography
- Mr William Hendriks for his friendly assistance in the laboratory
- Mrs Elizabeth Wilson for her constant interest and moral support
- To all the staff and students of the Chemistry Department, especially those on the third floor, Mr Derek Auer, Mr Jörn Miller, Mr Francois Wevers and Ms Claire Lawrence
- To my friend, Dr Cheryl Sacht for all her interest, enthusiasm and invaluable help throughout my studies
- The University of Cape Town and The Foundation for Research Development for financial assistance.

Most of all I wish to thank my husband, Graham Meyer, for his friendship, encouragement, invaluable moral support and for proof-reading my thesis.

ABSTRACT

A series of *N*-alkyl- and *N,N*-dialkyl-*N'*-acylthioureas are synthesised and characterised. The crystal structure of *N*-butyl-*N'*-benzoylthiourea indicates that an *intra*molecular hydrogen bond locks the potentially bidentate chelate moiety into a planar six-membered ring with an overall rod-like molecular structure.

The rod-like structure of the *N*-alkyl-*N'*-benzoylthioureas is exploited and the synthesis and characterisation of a novel series of liquid crystals based on *N*-(*p*-alkyl(oxy))aniline-*N'*-(*p*-alkyl(oxy))benzoylthiourea is discussed. The liquid-crystalline phases are identified with the aid of Polarising Optical Microscopy and confirmed by Differential Scanning Calorimetry studies. The compounds display nematic, smectic A or a combination of these liquid crystal phases. The X-ray crystal structure of *N*-(*p*-hexyloxy)aniline-*N'*-(*p*-methyloxy)benzoylthiourea shows co-planarity of the aromatic and hydrogen-bonded six-membered rings. *Inter*molecular hydrogen bond interactions between adjacent molecules allow for favourable molecular interaction for the formation of liquid crystal phases.

The *N*-alkyl- and *N,N*-dialkyl-*N'*-acylthioureas show substantially different coordination chemistries, as illustrated by their reactions with Ni (II), Cu (II) and *cis*-$[Pt(PEt_2Ph)_2Cl_2]$. *N,N*-dialkyl-*N'*-acylthioureas react with nickel (II) and copper (II) acetate to yield the corresponding *cis*-$[ML_2]$ complexes. *N*-alkyl-*N'*-acylthiourea does not form nickel (II) complexes under any conditions and reduces Cu (II) to Cu (I). The results of $^{31}P\{^1H\}$ NMR studies suggest that *N,N*-dialkyl-*N'*-acylthiourea compounds react with *cis*-$[Pt(PEt_2Ph)_2Cl_2]$ to form exclusively *cis*-$[Pt(PEt_2Ph)_2(L\text{-}S,O)]$, where L-*S,O* represents the deprotonated ligand coordinated through the sulfur and oxygen atoms. On the other hand, *N*-alkyl-*N'*-acylthioureas react with *cis*-$[Pt(PEt_2Ph)_2(L\text{-}S,O)]$ to form a mixture of complex species with the major products assigned to *trans*-$[Pt(PEt_2Ph)_2(L\text{-}S)_2]$ and *trans*-$[Pt(PEt_2Ph)_2(L\text{-}S)(Cl)]$, where L-*S* represents the deprotonated ligand coordinated through the sulfur atom only.

Protonation of *cis*-bis(*N,N*-dialkyl-*N'*-acylthioureato)platinum(II) complexes, (*cis*-$[Pt(L\text{-}S,O)_2]$), are studied by means of high resolution NMR spectroscopy. The results suggest that protonation with HCl results in ring-opening of the chelate ring with concomitant coordination of Cl^- atoms, and yields mixtures of *cis*- and *trans*-$[Pt(HL\text{-}S)_2Cl_2]$ where HL-*S* represents the protonated ligand bound to Pt through the sulfur atom only. Addition of H_2O yields *cis*-$[Pt(L\text{-}S,O)(HL\text{-}S)Cl]$ in addition to *cis*- and *trans*-$[Pt(HL\text{-}S)_2Cl_2]$. Complete deprotonation with NH_3 or NaOH yields the *cis*-$[Pt(L\text{-}S,O)_2]$ isomer exclusively when L is the *N*-benzoylthiourea ligand, and *cis*-$[Pt(L\text{-}S,O)_2]$ and a small amount of the corresponding *trans*-$[Pt(L\text{-}S,O)_2]$ complex when L represents the *N*-naphthoylthiourea ligand.

A heterocyclic *N*-acylthiourea, *N*-morpholino-*N'*-naphthoylthiourea (**1**), and two novel macrocyclic *N*-acylthioureas, *N*-aza-18-crown-6-*N'*-naphthoylthiourea (**2**) and *N,N*-diaza-18-crown-6-*N'*-naphthoylthiourea (**3**) are synthesised and characterised. The results of ^{1}H NMR spectroscopy, picrate extraction studies and UV spectrometry indicate a weak interaction of the aza- and diaza-crown ether rings of **2** and **3** with K^+ and $CH_3NH_3^+$ or NH_4^+ cations. This poor interaction is explained by the crystal structures of **2** and **3** which indicate that the aza- and diaza-crown ether moieties assume an unusual conformation due to the presence of one and two *intra*molecular hydrogen bonds respectively, between the amide hydrogen and an oxygen atom of the aza- and diaza-crown ether rings.

The platinum coordination chemistry of **1** and **2** is addressed. Elemental analysis, thermogravimetric analysis and proton NMR spectroscopy indicate that two moles of KCl and four moles of H_2O are associated with one mole of *cis*-bis(*N*-aza-18-crown-6-*N'*-naphthoylthioureato)platinum(II). The X-ray crystal structure of the novel *cis*-bis(*N*-morpholino-*N'*-naphthoylthioureato)platinum(II) is described.

LIST OF SYMBOLS AND ABBREVIATIONS

Å	angstrom unit, 10^{-10} m
Hz	hertz, s^{-1}
L	ligand
SH	protonated ligand
M^{n+}	metal cation
X^-	halogen
mp	melting point
ΔG_c	Gibbs free energy change at the coalescence temperature
ΔH	enthalpy change
ΔS	entropy change
K	equilibrium constant
R	Universal gas constant (in association with temperature) or crystallographic R value
wR	weighted crystallographic R value
T	temperature
T_c	coalescence temperature (NMR)
ν	frequency
Z	number of molecules per unit cell
δ	chemical shift (NMR)
^1J	one-bond coupling constant
V	volume
D_c	density
e.s.d	estimated standard deviation
λ_{max}	wavelength
K	temperature in Kelvin
ln	natural logarithm
ppm	parts per million (NMR)
lit.	literature

18-crown-6	1,4,7,10,13,16-hexaoxacyclooctadecane
aza-18-crown-6	1,4,7,10,13-pentaoxa-16-azacyclooctadecane
diaza-18-crown-6	4,7,13,16-tetraoxa-1,10-diazacyclooctadecane
morpholine	16-oxa-13-azacyclohexane
N-morpholino-*N'*-naphthoylthiourea	*N*-naphthoyl-(*N'*-morpholino)thioamide

N-aza-18-crown-6-*N'*-napthoylthiourea	*N*-naphthoyl-(*N'*-aza-18-crown-6)thioamide
N,N-diaza-18-crown-6-*N'*-napthoylthiourea	bis-(*N*-naphthoylthioamide)-*N',N'*-diaza-18-crown-6
$Pt(PEt_2Ph)_2Cl_2$	dichloro-bis(diethylphenylphosphine)platinum(II)
Bu	butyl
Et	ethyl
Me	methyl
Ph	phenyl
tert (*t*)	tertiary
DMSO-d_6	deuterated dimethyl sulfoxide
$CDCl_3$	deuterated chloroform
CD_3COCD_3	deuterated acetone
CH_3CN	acetonitrile
DMF	dimethylformamide
CH_2Cl_2	dichloromethane
Et_3N	triethylamine
D_2O	deuterium oxide
+FAB	positive fast atom bombardment
DSC	differential scanning calorimetry
TGA	thermogravimetric analysis
NOBA	nitrobenzylalcohol
COSY	correlated spectroscopy
DEPT	distortionless enhancement by polarisation transfer
HETCOR	heteronuclear chemical shift correlation

TABLE OF CONTENTS

CHAPTER 1

INTRODUCTION

Introduction

The majority of *N*-substituted thioureas possess a wide spectrum of bioactivity which include antituberculose, hypnotic, antiviral and pesticide properties[1]. In particular, some *N*-acylthioureas have potent fungicidal action[2]. From an analytical point of view the compounds, *N*-alkyl- and *N,N*-dialkyl-*N'*-acylthiourea (Figure 1.1), have recently attracted attention in view of their selective coordination of particularly the softer 2nd and 3rd row transition metals. In this context, the pioneering work of Beyer[3,4] *et al* and Schuster[5-8] *et al* should be mentioned, particularly with regard to the use of *N*-acylthiourea compounds as selective reagents for the solvent extraction of platinum group metals.

Figure 1.1 Schematic representation of *N*-alkyl-*N'*-acylthiourea (**a**) and *N,N*-dialkyl-*N'*-acylthiourea (**b**).

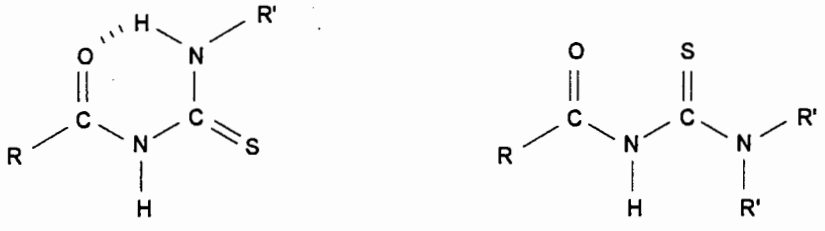

The ease of synthesis from simple and inexpensive starting materials has encouraged and facilitated the study of *N*-acylthioureas. These compounds possess a number of interesting properties. They are potential O and S donor *bidentate* ligands that can coordinate as anionic species with loss of the proton from the acyl-substituted nitrogen. Furthermore, X-ray crystal studies have revealed that *N*-benzoylthioureas form *bis, square-planar* complexes of *cis* conformation[9-14]. However, depending on the nature of the substituent groups, *N*-acylthioureas may act as *unidentate* ligands[15]. These properties of *N*-acylthioureas are reminiscent of the structurally related thioureas, 1,3-diketones, monothio and dithio-β-diketones (Figure 1.2).

Figure 1.2 Schematic representation of thiourea, 1,3-diketone, monothio and dithio-β-diketone compounds.

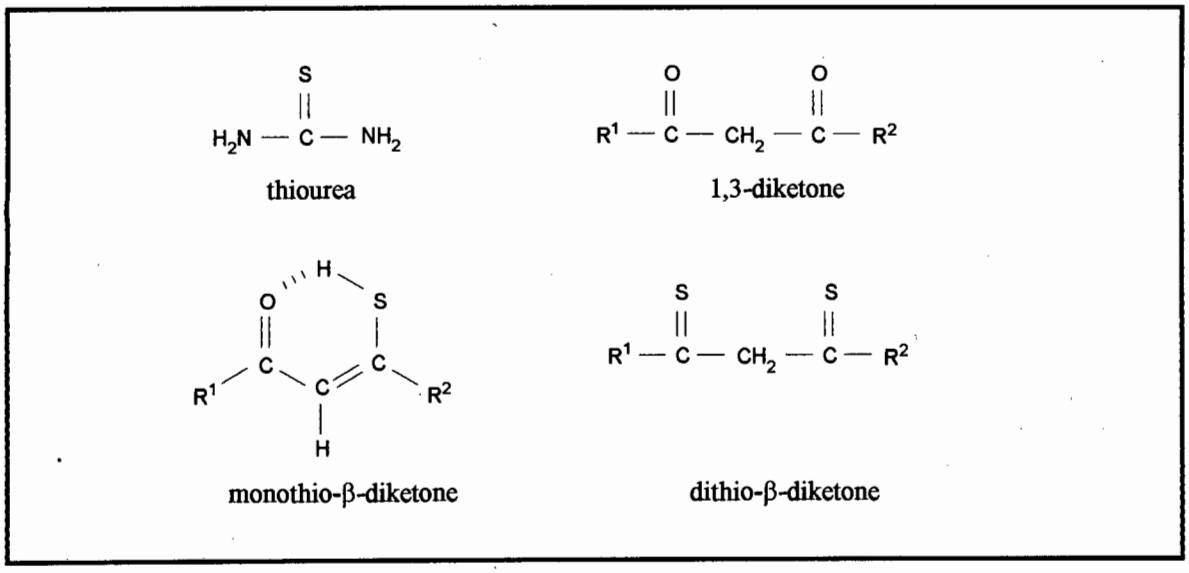

In particular, the *bidentate* nature of *N*-acylthioureas is redolent of 1,3-diketones, monothio- and dithio-β-diketones. Removal of the acidic methylene proton in the keto form and the hydroxyl proton in the enol form of β-diketones, generates 1,3-diketonate anions which are the source of an extremely broad class of coordination compounds generally referred to as β-diketonates[16]. Diketonates are powerful *chelating* species and form complexes with virtually every transition and main group element[16]. X-ray crystallographic studies[17] have shown that η_2 oxygen-bonded diketonate ligands form bis-ligand complexes with a variety of metals that can take up square planar configurations. Furthermore, monothio- and dithio-β-diketones readily form stable square-planar complexes with Ni (II), Pd (II), Pt (II), Hg (II) and Pb (II)[16]. X-ray structural data has established the *cis* square-planar configuration for Pd (II), Pt (II)[18] and Ni (II)[19] complexes.

Under certain conditions, on the other hand, *unidentate* coordination of *N*-acylthioureas is comparable to that observed for thiourea, $(H_2N)_2$-C=S. Thiourea acts as a unidentate ligand forming strong S-bonded complexes with Cu (I), Ag (I), Au (I) and Hg (II). It reduces Cu (II) to Cu (I), Au (III) to Au (I), and Pt (IV) to Pt (II), forming complexes with the metal in the lower oxidation state[20,21].

We have become interested in the design of compounds incorporating the *N*-acylthiourea functional group as central motif and, by exploiting the versatile synthesis of these types of molecules, we hope to prepare a great variety of new compounds with potential applications. Firstly, to familiarise the Author with the chemistry of the deceptively simple *N*-acylthioureas, we decided to systematically study the extent to

which the amine and acyl moieties of these compounds could be altered. Accordingly, Chapter 2 of this thesis deals with the synthesis and characterisation of a series of *N*-alkyl- and *N,N*-dialkyl-*N'*-acylthioureas.

The crystal structure determination of *N*-alkyl-*N'*-benzoylthiourea revealed a rod-shaped molecular geometry similar to that observed in the solid state structures of certain liquid-crystalline materials. This, together with the fact that considerable interest has been shown in the liquid-crystalline behaviour of metal complexes of the structurally related β-diketonates[22], prompted the Author to examine the possibility of designing compounds that possess liquid-crystalline properties. Hence, Chapter 3 deals with the synthesis and characterisation of a series of potential liquid crystal compounds based on the *N*-acylthiourea functional group.

In view of the recent new class of liquid crystals incorporating transition metals[22], we decided to investigate whether *N*-acylthiourea metal (II) complexes exhibit liquid-crystalline behaviour. Thus the complexation of nickel (II), copper (II), platinum (II) and palladium (II) with *N*-alkyl- and *N,N*-dialkyl-*N'*-benzoylthioureas was examined and is described in Chapter 4.

As part of our interest in *N*-acylthiourea compounds with potential applications, we extended our study to incorporate the crown ether functional group. Since Pedersen[23] discovered crown ether molecules in 1967, a variety of macrocyclic molecules have been prepared and widely applied in chemistry, industry and related fields. Employing the general method of synthesis of *N*-acylthioureas, the cyclic analogues, *N*-morpholino-*N'*-naphthoylthiourea, *N*-aza-18-crown-6-*N'*-naphthoylthiourea and *N,N*-diaza-18-crown-6-*N'*-naphthoylthiourea, were synthesised and characterised (Chapter 5). Given the exceptional coordinating ability of crown ethers[23,24], the interaction of K^+ and $CH_3NH_3^+$ with the aza-crown ether moiety of *N*-aza-18-crown-6-*N'*-naphthoylthiourea and *N,N*-diaza-18-crown-6-*N'*-naphthoylthiourea is discussed.

Finally, the platinum coordination chemistry of *N*-morpholino- and *N*-aza-18-crown-6-*N'*-naphthoyl-thiourea is addressed in Chapter 6 and the crystal structure determination of the novel *cis*-bis(*N*-morpholino-*N'*-naphthoylthioureato)platinum(II) is described.

REFERENCES

1 Schroeder, D.C.; *Chem. Rev.*, 1955, **55**, 181.

2 Macías, A.; Rodríquez, Y.; Rivero, R.; Certificado de Invención # 21578, 1986, La Habana, Cuba.

3 Beyer, L.; Hoyer, E.; Liebscher, J.; Hartmann, H.; *Z. Chem.*, 1981, **21**, 81.

4 Mühl, P.; Gloe, K.; Dietze, F.; Hoyer, E.; Beyer, L.; *Z. Chem.*, 1986, **26**, 81.

5 Vest, P.; Schuster, M.; König, K.-H.; *Fresenius' Z. Anal. Chem.*, 1989, **335**, 759.

6 König, K.-H.; Schuster, M.; Schneeweis, G.; Steinbrech, B.; *Fresenius' Z. Anal. Chem.*, 1984, **319**, 66.

7 König, K.-H.; Schuster, M.; Steinbrech, B.; Schneeweis, G.; Schlodder, R.; *Fresenius' Z. Anal. Chem.*, 1985, **321**, 457.

8 Vest, P.; Schuster, M.; König, K.-H.; *Fresenius' Z. Anal. Chem.*, 1991, **339**, 142.

9 Richter, R.; Beyer, L.; Kaiser, J.; *Z. Anorg. Allg. Chem.*, 1980, **461**, 67.

10 Knuuttilla, P.; Knuuttilla, H.; Hennig, H.; Beyer, L.; *Acta Chem. Scand., Ser. A,* 1982, **36**, 541.

11 Irving, A.; Koch, K.R.; Matoetoe, M.; *Inorg. Chim. Acta,* 1993, **206**, 193.

12 Fitzl, G.; Beyer, L.; Sieler, J.; Richter, R.; Kaiser, J.; Hoyer, E.; *Z. Anorg. Allg. Chem.*, 1977, **433**, 237.

13 Sieler, J.; Richter, R.; Hoyer, E.; Beyer, L.; Lindqvist, O.; Andersen, L.; *Z. Anorg. Allg. Chem.*, 1990, **580**, 167.

14 Bensch, W.; Schuster, M.; *Z. Anorg. Allg. Chem.*, 1992, **615**, 93.

15 Koch, K.R.; Bourne, S.; *J. Chem. Soc., Dalton Trans.*, 1993, 2071.

16 Comprehensive Coordination Chemistry, vol 2, (eds.), Wilkinson, G.; Gillard, R.D.; McCleverty, J.P.; Pergamon Press, Oxford, 1987.

17 Mulberger, B.; Haase, W.; *Liq. Cryst.*, 1989, **5**, 251.

18 Shugam, E.A.; Shkol'nikova, L.M.; Livingstone, S.E.; *Zh. Strukt. Khim.*, 1967, **8**, 550.

19 Siiman, O.; Titus, D.D.; Cowman, C.D.; *J. Am. Chem. Soc.*, 1974, **96**, 2353.

20 Livingstone, S.E.; *Q. Rev., Chem. Soc.*, 1965, **19**, 386.

21 Nakamoto, M.; *Infrared Spectra of Inorganic and Coordination Compounds*, 2nd edn., Wiley-Interscience, New York, 1970.

22 Giroud-Godquin, A-M.; Maitlis, P.M.; *Angew. Chem. Int. Ed. Engl.*, 1991, **30**, 375.

23 Pedersen, C.J.; *J. Am. Chem. Soc.*, 1967, **89**, 2495.

24 Moore, C.; Pressman, B.C.; *Biochem. Biophys. Res. Commun.*, 1964, **15**, 562.

CHAPTER 2

SYNTHESIS AND CHARACTERISATION OF *N*-ALKYL- AND *N,N*-DIALKYL-*N'*-ACYLTHIOUREAS

2.1 Introduction

The facile synthesis of *N*-alkyl- and *N,N*-dialkyl-*N'*-acylthioureas in high yields and from inexpensive starting materials, has favoured the study of these compounds. The relative ease of modification, at either the acyl or amine moiety, and the high stability of the corresponding derivatives, potentially gives rise to a large class of new compounds. This may lead to an interesting and dynamic area of research.

The single step synthesis of *N*-acylthioureas[1] (Figure 2.1) involves nucleophilic attack of the isothiocyanate ion on the carbonyl group, thermal isomerism to the thiocyanate ion and subsequent reaction with a secondary or primary amine to afford exclusively the analogous *N,N*-dialkyl-*N'*-acylthiourea or *N*-alkyl-*N'*-acylthiourea.

Figure 2.1 Schematic representation of the stepwise preparation of *N,N*-dialkyl-*N'*-acylthiourea.

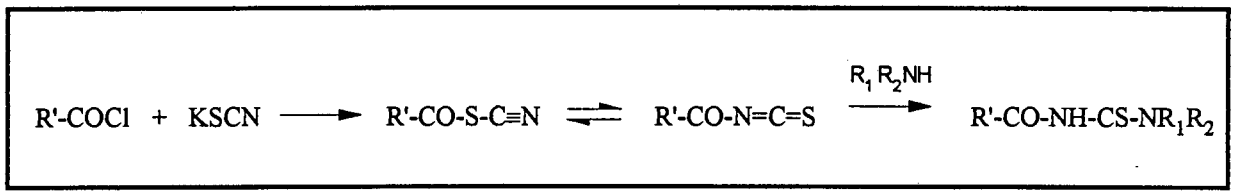

The mechanism of the reaction of an acyl chloride with a thiocyanate ion has been reported by Takamizawa[2] *et al.* In acetone, the thiocyanate ion exists in two forms, (**a**) and (**b**), Figure 2.2. Electrophilic attack by the carbonyl carbon of the acyl chloride is equally possible at the S and N sites, giving rise to the thiocyanate (**c**) or isothiocyanate (**d**) isomers, respectively. The acyl (or aroyl) carbonyl carbon of the thiocyanate isomer is relatively reactive and may therefore interact with more isothiocyanate ($^{-}$N=C=S) to yield (**d**). This results in an entire conversion to the isothiocyanate derivative.

Figure 2.2 Schematic representation of the mechanism of the reaction of an acyl chloride with a thiocyanate ion[2].

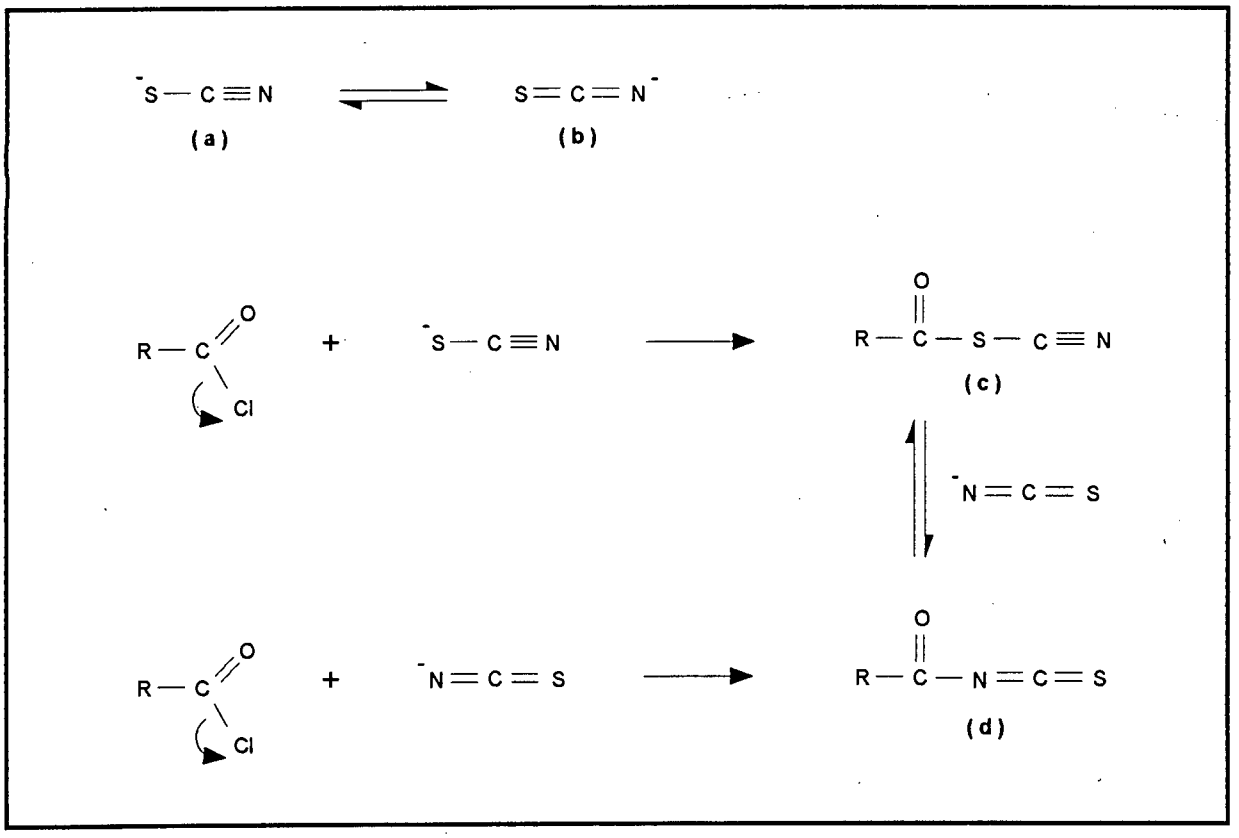

Nucleophilic addition reactions, typical for isothiocyanates, occur as a result of the presence of a strong electrophilic centre at the carbon of the NCS group[3]. Acyl thiocyanates contain two strongly electrophilic centres; one at the NCS carbon and the other at the carbonyl carbon. Accordingly, the reaction of benzoyl isothiocyanate with an amine can in principle afford two products: *N*-benzoylthiourea and *N*-substituted benzamide. However, as found by Elmore and Ogle[4], benzoyl isothiocyanates react with amines, in anhydrous organic solvents, to afford exclusively the corresponding disubstituted *N*-acylthioureas (Figure 2.3, compound A). When the reaction is performed in aqueous dioxane at pH 8.5, the *N*-substituted benzamides (Figure 2.3, compound B) are also isolated.

Figure 2.3 Schematic representation of the reaction of benzoyl isothiocyanate with a primary amine.

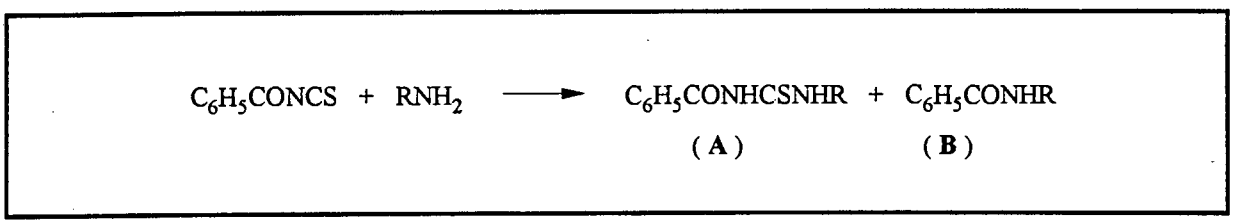

The reaction of carbonyl isothiocyanates with amines has been thoroughly investigated and occurs smoothly, both in polar solvents and in solvents of low polarity on heating[1,5-8]. Reports indicate that the reaction takes place *via* an intermediate donor-acceptor complex of the acyl isothiocyanate with an amine[9] (Figure 2.4). Aliphatic and aromatic amines react with acyl isothiocyanates almost quantitatively and the corresponding *N*-acylthioureas are obtained in yields exceeding 70 %.

Figure 2.4 Schematic representation of the intermediate donor-acceptor complex proposed for the reaction of a carbonyl isothiocyanate with an amine[10].

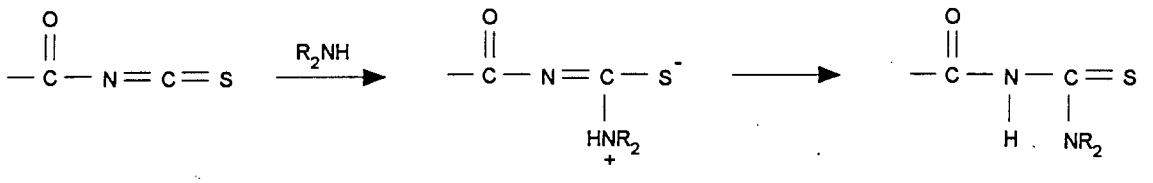

The first paper referring to the synthesis of *N*-acylthioureas was published in 1934, when Douglass and Dains reported the synthesis of *N*-benzoylthiourea[1]. Since this report, a variety of *N*-acylthioureas have been synthesised and characterised, the work of Schuster, Beyer and Sarkis being of particular significance. Schuster[11] *et al* reported the synthesis and characterisation of *N,N*-dimethyl-, *N,N*-diethyl-, *N,N*-dipropyl-, *N,N*-dibutyl and *N,N*-dihexyl-*N'*-benzoylthiourea. Their interest focused on the use of these compounds in selective metal extractions. Beyer[12] *et al* investigated the coordination chemistry of a series of *N*-alkyl-, *N,N*-dialkyl-*N'*-acylthioureas and a variety of heterocyclic analogues, including the piperidino, pyrrolidino and morpholino derivatives. The synthesis and characterisation of *N*-phenyl-*N'*-benzoylthiourea derivatives of potential biological interest was reported by Sarkis[13,14] *et al.*

Dago[15] *et al* reported the first X-ray crystal structure determination of *N*-alkyl-*N'*-acylthiourea. They found that each molecule of *N*-fenyl-*N'*-(*p*-chloro)benzoylthiourea shows an *intra*molecular hydrogen bond between the H atom of the NH group of the amine and the O atom of the carbonyl group. They also found that the compound is characterised by the formation of dimers. One year later, they reported the crystal structure of a related compound, *N*-propyl-*N'*-benzoylthiourea[16], and observed a similar *intra*molecular hydrogen bond and the characteristic formation of dimers.

The high stability of *N*-acylthioureas has promoted the study of these compounds. In particular, *N*-acylthiourea compounds have relatively high thermal stabilities and do not decompose when exposed to air or light. The stability of *N*-acylthioureas with respect to protonation, alkaline hydrolysis and oxidation-reduction reactions have been reported[17-19].

The stability of *N*-acylthioureas in alkaline solutions was studied by Edward[18] *et al.* They showed that *N*-benzoylthiourea and other *N*-acylthioureas ionise in alkaline solution, and are then rapidly hydrolysed to thiourea and the corresponding carboxylic acid (Figure 2.5). Their results indicated that alkaline hydrolysis involves the attack of an hydroxide ion on the un-ionised molecules of *N*-acylthiourea.

Figure 2.5 Schematic representation of the hydrolysis of *N*-acylthiourea, in the presence of hydroxide ions, to yield the corresponding thiourea and carboxylic acid[18].

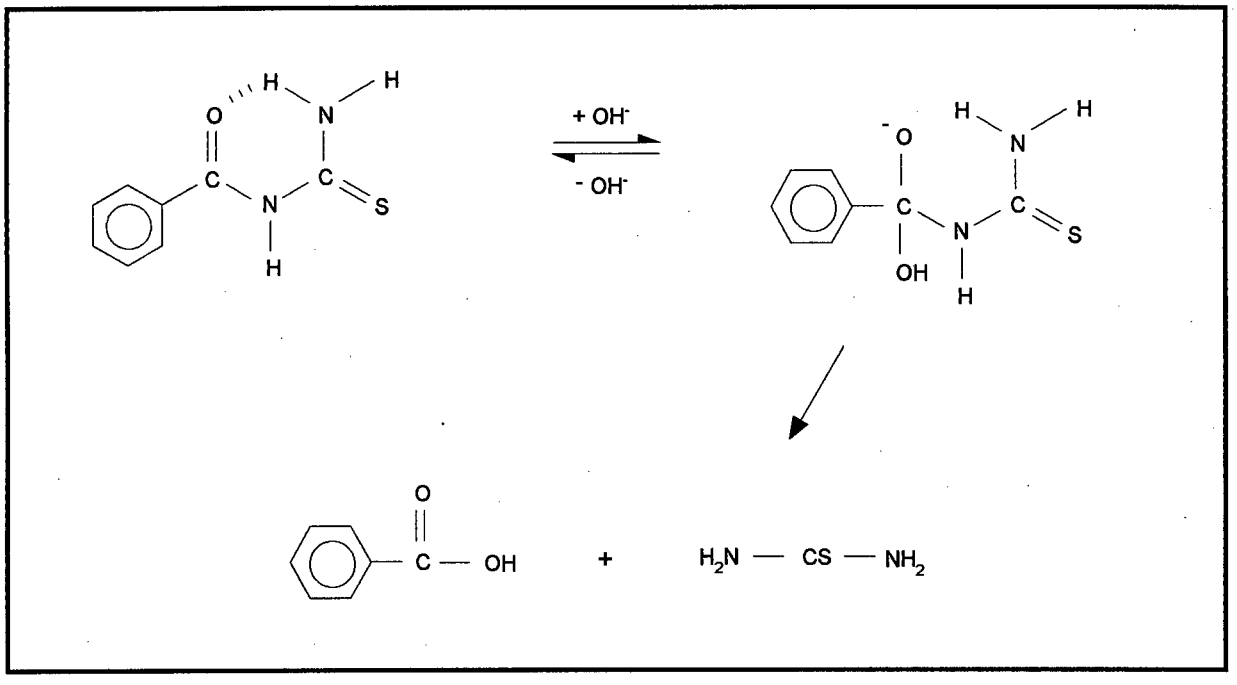

Harris[19] *et al* showed that *N*-acylthioureas are stable to oxidation - reduction reactions. They reported that the treatment of *N*-benzoylthiourea with one-half mole equivalent of bromine, in chloroform or methylene chloride, gives a microcrystalline product which can quantitatively be reduced back to *N*-benzoylthiourea by H_2S (Figure 2.6). Harris[19] predicted that, upon oxidation, the amine proton is lost to form the disulfide derivative.

Figure 2.6 Schematic representation of the reversible redox reactions of *N*-benzoylthiourea[19].

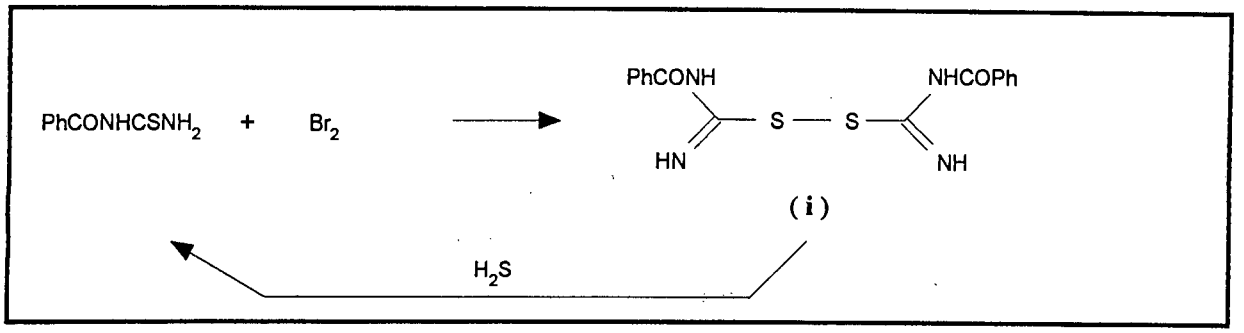

2.1.1 Objectives of the present study

The chemistry of *N*-acylthioureas is still relatively undeveloped, as rather little is known about these deceptively simple compounds. The present study includes the examination of a series of *N*-alkyl-*N'*-benzoylthioureas (**1**) and *N,N*-dialkyl-*N'*-benzoylthioureas (**2**), (Figure 2.7), with the aim of gaining experience in the preparation of *N*-acylthioureas and achieving a better understanding of their physical properties. The alkyl length is systematically changed from C4 to C8 for *N*-alkyl-*N'*-benzoylthiourea and *N,N*-dialkyl-*N'*-benzoylthiourea.

Figure 2.7 Schematic representation of *N*-alkyl-N'-benzoylthiourea (**1**) and *N,N*-dialkyl-*N'*-benzoylthiourea (**2**)

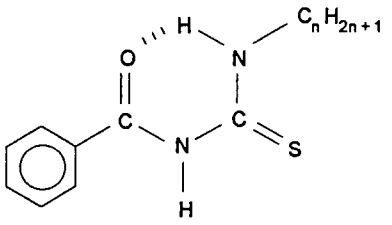

(**1**)

n = 4, 6, 8

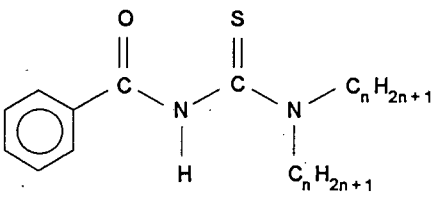

(**2**)

n = 4, 6, 8

Selected *N*-naphthoylthiourea (**3**, **4**) and *N*-anthroylthiourea (**5**) derivatives, (Figure 2.8), have been studied to ascertain the effect, on the physical properties of the compounds, of increasing the steric component of the acyl group.

Figure 2.8 Schematic representation of *N*-alkyl-*N'*-naphthoylthiourea (**3**), *N,N*-dialkyl-*N'*-naphthoyl-thiourea (**4**), and *N,N*-dialkyl-*N'*-anthroylthiourea (**5**), showing the atom numbering for all non-hydrogen atoms.

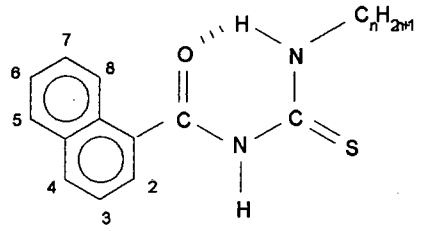

(**3**)

n = 8

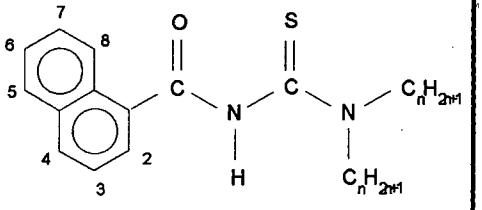

(**4**)

n = 4, 6, 8

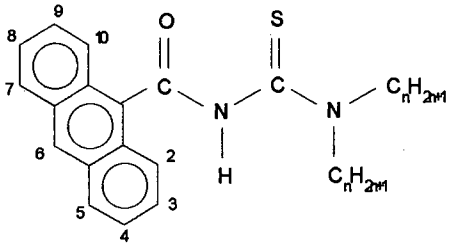

(**5**)

n = 4, 8

2.2 Results and Discussion

2.2.1 Ligand synthesis and characterisation

The *N*-alkyl-*N'*-benzoylthiourea (**1**), *N,N*-dialkyl-*N'*-benzoylthiourea (**2**), (Figure 2.7), *N*-alkyl-*N'*-naphthoylthiourea (**3**), *N,N*-dialkyl-*N'*-naphthoylthiourea (**4**), and *N,N*-dialkyl-*N'*-anthroylthiourea (**5**) compounds (Figure 2.8), were synthesised in 70 - 90 % yield, according to the method reported by Douglass and Dains[1]. The crude products were recrystallised from hot ethanol to yield white crystals, however, *N*-hexyl- and *N*-octyl-*N'*-benzoylthiourea were purified by column chromatography on silica gel using toluene as eluent. All the *N*-acylthiourea compounds prepared were satisfactorily characterised by C, H and N elemental analysis, mass spectrometry and ^{1}H and ^{13}C NMR spectroscopy ($CDCl_3$).

2.2.1.1 *N*-alkyl-*N'*-benzoylthiourea

A series of *N*-alkyl-*N'*-benzoylthioureas, (**1a - 1c**), were synthesised by systematically changing the number of carbon atoms in the alkyl chain from four to eight (Table 2.1). A full characterisation of these compounds is given in the experimental section.

Physical Properties

The melting points of the *N*-alkyl-*N'*-benzoylthiourea compounds are relatively low (Table 2.1). No unusual thermal behaviour is evident from polarising optical microscopy. On heating, the compounds all melt directly from the solid material to the isotropic liquid and super-cooling of the isotropic liquid allows for crystallisation to the solid material.

NMR Spectroscopy

An increase in the length of the alkyl chain of *N*-alkyl-*N'*-benzoylthiourea, (**1**), has practically no influence on the ^{1}H, ^{13}C and ^{15}N NMR spectra. All spectra are practically the same: one example, for *N*-octyl-*N'*-benzoylthiourea, (**1c**), is briefly described below. The atoms are numbered according to the scheme in Figure 2.9.

Table 2.1 Analytical data and properties of the *N*-alkyl-*N'*-benzoylthiourea, (**1a - c**).

compound	n	% yield	mp (°C)	elemental analysis %C/H/N
1a	4	86	48 - 49	*calc*: 61.0; 6.8; 11.9 *obs*: 61.0; 7.0; 11.8
1b	6	71	37 - 39*	*calc*: 63.6; 7.6; 10.6 *obs*: 63.5; 7.6; 10.7
1c	8	78	37 - 41	*calc*: 65.7; 8.3; 9.6 *obs*: 65.4; 7.9; 9.5

* *literature melting point is 37 °C*[20]

Figure 2.9 The numbering scheme of *N*-octyl-*N'*-benzoylthiourea.

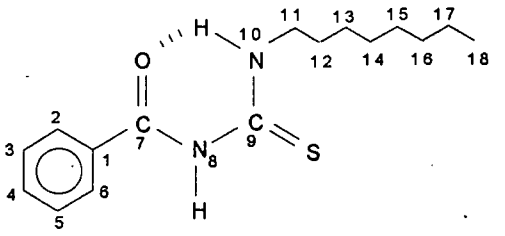

(**1c**)

In general, the ^{1}H assignments for the *N*-alkyl-*N'*-benzoylthiourea compounds are straightforward and are similar to those published by Koch[21] *et al* for *N,N*-dialkyl-*N'*-benzoylthiourea. The H(2) / H(6) protons of *N*-octyl-*N'*-benzoylthiourea are observed as a doublet at 7.83 ppm. The H(3) / H(5) and H(4) protons are evident as two sets of triplets at 7.51 and 7.63 ppm respectively. The signals for the N - H protons, H(8) and H(10), were confirmed by means of irradiation decoupling experiments, where strong coupling between the H(10) and H(11) protons was evident. Accordingly, the broad singlets at 10.77 and 9.07 ppm, in the ^{1}H NMR spectrum, are assigned to H(10) and H(8) respectively.

The ^{13}C NMR shifts of *N*-octyl-*N'*-benzoylthiourea, reported in the experimental section, are similar to those previously published by Koch[21] *et al* for *N,N*-dialkyl-*N'*-benzoylthiourea. The thiocarbonyl peak at 179.66 ppm, and carbonyl peak at 166.86 ppm, are characteristic of the ^{13}C NMR spectrum of *N*-acylthioureas.

Two peaks were observed in a ^{15}N DEPT experiment, at -230.74 and -248.74 ppm, for *N*-octyl-*N'*-benzoylthiourea. The $^{1}J(H - N)$ coupling constant measured was approximately 91 and 89 Hz respectively. Furthermore, correlation between the nitrogen peaks and the respective hydrogen protons are evident from a HETCOR experiment. The peak at -230.74 ppm corresponds to N(8), the acyl substituted nitrogen atom, whereas the peak at -248.74 ppm corresponds to N(10), the nitrogen involved in the hydrogen bond.

2.2.1.2 *N,N*-dialkyl-*N'*-benzoylthiourea

A series of *N,N*-dialkyl-*N'*-benzoylthioureas, (**2a - 2c**), (Table 2.2), were synthesised and the detailed characterisation of these compounds is given in the experimental section.

Physical Properties

The *N,N*-dialkyl-*N'*-benzoylthiourea compounds, (**2a -2c**), show a decrease in melting point as a function of an increase in length of the alkyl chain (Table 2.2). This observation is similar to that observed for the short chained, (C4 - C8), *N*-alkyl-*N'*-benzoylthioureas. No unusual melting behaviour was evident microscopically for **2a - c**. The *N,N*-dialkyl-*N'*-benzoylthiourea compounds have much higher melting points than that observed for the analogous *N*-alkyl-*N'*-benzoylthiourea compounds, e.g. melting point of *N*-butyl-*N'*-benzoylthiourea is 48 - 49 °C, whereas the melting point of *N,N*-dibutyl-*N'*-benzoylthiourea is 91 - 92 °C.

Table 2.2 Analytical data and properties of the *N,N*-dialkyl-*N'*-benzoylthioureas, (**2a - c**).

compound	n	% yield	mp (°C)	elemental analysis %C/H/N
2a	4	86	91 - 92*	*calc*: 65.8; 8.2; 9.5 *obs*: 65.9; 8.2; 9.8
2b	6	81	57 - 58**	*calc*: 68.9; 9.2; 8.1 *obs*: 68.6; 9.3; 8.0
2c	8	87	52 - 54	*calc*: 71.2; 9.9; 6.9 *obs*: 71.7; 9.8; 6.7

* *literature melting point 93 °C*[22]

** *literature melting point 59 °C*[20]

NMR Spectroscopy

The assignment of the ^{1}H and ^{13}C NMR spectra of compounds **2** are straightforward, the ^{13}C shifts comparable to those previously reported by Koch[21,23] *et al.* All spectra are practically the same: one example, *N,N*-dioctyl-*N'*-benzoylthiourea, is given in Figure 2.10. The atoms are numbered according to the scheme in Figure 2.11.

Figure 2.11. Numbering scheme of *N,N*-dioctyl-*N'*-benzoylthiourea.

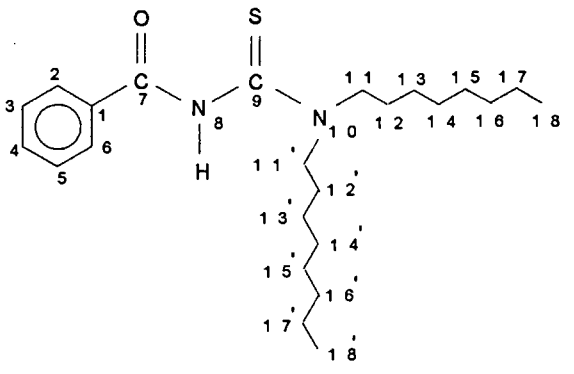

(**2c**)

The ^{1}H NMR spectrum is characterised by a single N - H peak, in the region 8 - 9 ppm. One of the most interesting aspects of the spectrum of *N,N*-dialkyl-*N'*-benzoylthiourea is the observation of separate resonances for H(11) and H(11') of the dialkyl chain (Figure 2.10(a)). Accordingly, it is necessary to address the concept of restricted rotation around an amidic or thio-amidic C - N bond[24]. Consider the two resonance structures (**a**) and (**b**), Figure 2.12.

The C - N bond between the thiocarbonyl group and the nitrogen atom has a significant double bond character[25,26] as is represented by contribution of the resonance hybrid (**b**) to the structure. In the lowest energy configuration, the protons of the methylene groups are in different environments, H(1) and H(1') and H(2) and H(2'), and therefore have different resonance frequencies, v(1) and v(1') and v(2) and v(2'). In the absence of restricted rotation, the chemical shifts of H(1) ~ H(1') and H(2) ~ H(2') due to free internal rotation around the C - N bond. However, because of the high C - N energy barrier to rotation at room temperature, the exchange frequency is low. Therefore the resonance time of the methylene groups in the two environments is relatively long with respect to the NMR time scale and accordingly four separate resonance signals are expected.

Figure 2.12 Resonance structures of a thio-amidic C - N bond due to the electron delocalisation between the nitrogen lone pair and the thiocarbonyl sulfur atom[24].

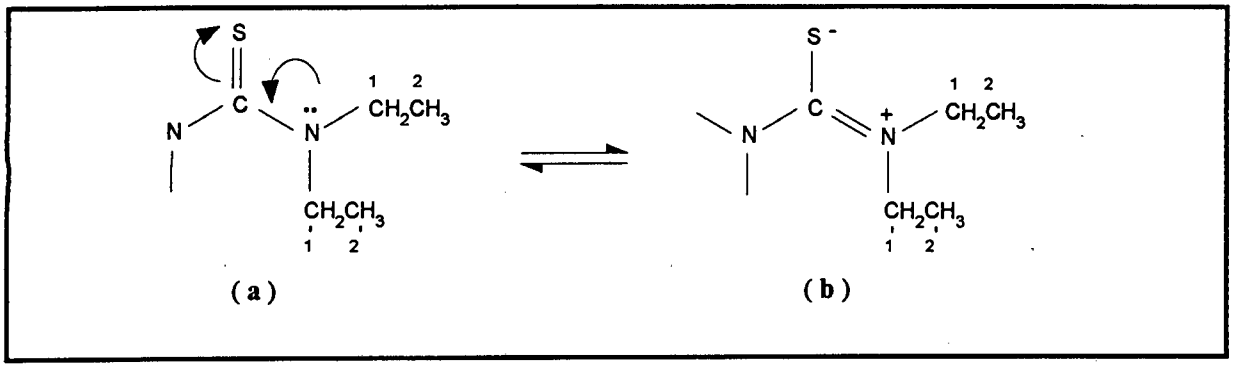

Accordingly, two sets of triplets are observed in the ^{1}H NMR spectrum of *N,N*-dioctyl-*N'*-benzoylthiourea for H(11) and H(11'), at 3.97 and 3.55 ppm, as a result of the partial double bond character of the C(9) - N(10) bond[26]. Moreover, the partial double bond character of the C(9) - N(10) bond is mirrored in the ^{13}C NMR spectrum where C(11) and C(11') signals, at 53.29 and 53.57 ppm, are observed as a result of their different chemical environments (Figure 2.10(b)).

Two signals, at -229.02 and -232.33 ppm, are observed in the ^{15}N NMR spectrum of *N,N*-dioctyl-*N'*-benzoyl-thiourea (Figure 2.10(c)). The peaks at -229.02 and -232.33 ppm were found to correlate, with the aid of a HETCOR experiment, to the amine nitrogen and the acyl substituted nitrogen respectively. The $^{1}J(H - N)$ coupling is 90 Hz. The chelate nitrogen resonance is in approximately the same chemical environment as that of the analogous nitrogen of *N*-octyl-*N'*-benzoylthiourea as confirmed by the similar chemical shifts. The amine nitrogen is, as expected, in a very different chemical environment to that of the *N*-alkyl-*N'*-benzoylthiourea derivative. This is evidenced by the different chemical shifts, i.e. -229.02 ppm for *N,N*-dioctyl-*N'*-benzoylthiourea compared to -248.74 ppm for *N*-octyl-*N'*-benzoylthiourea.

Figure 2.10 (a) ^{1}H (b) ^{13}C and (c) ^{15}N NMR spectra of *N,N*-dioctyl-*N'*-benzoylthiourea in $CDCl_3$, at 25 °C.

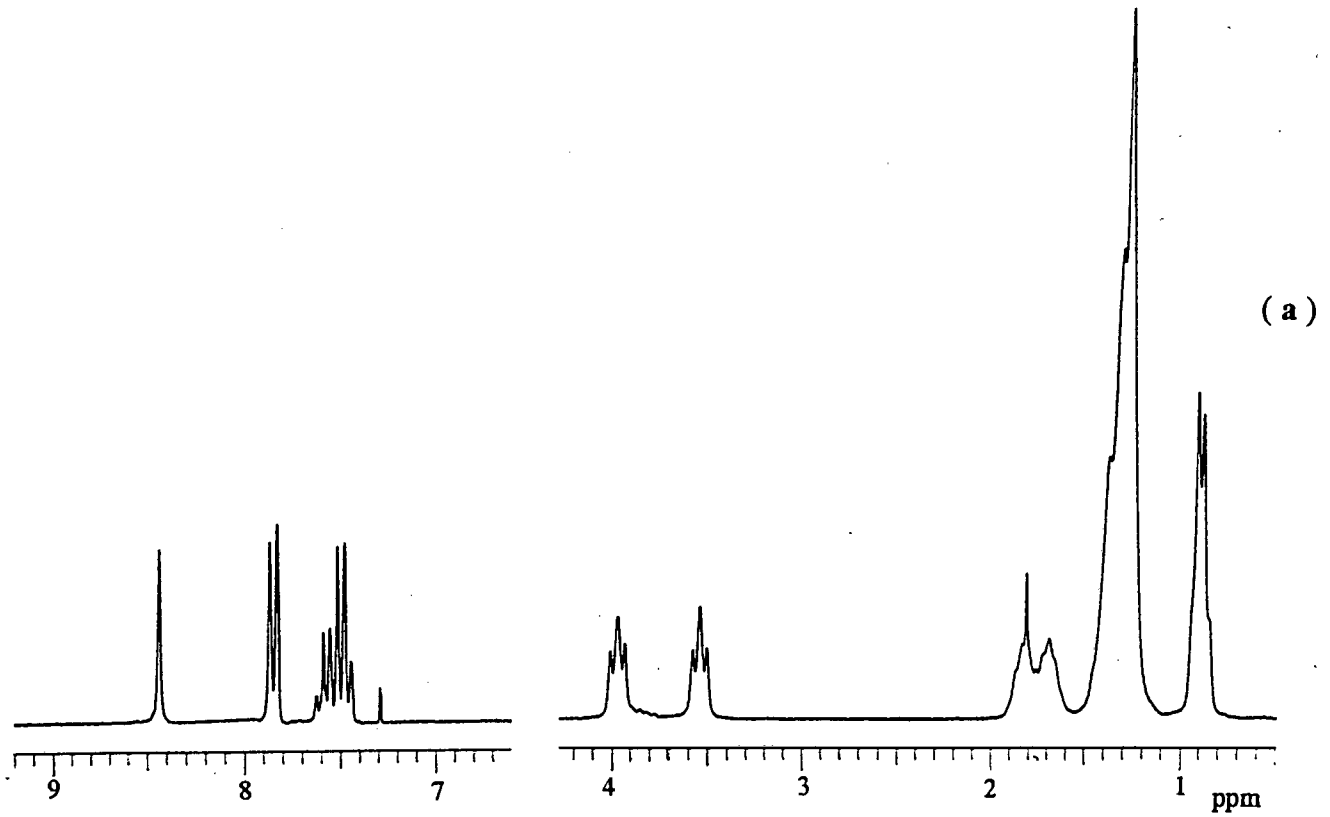

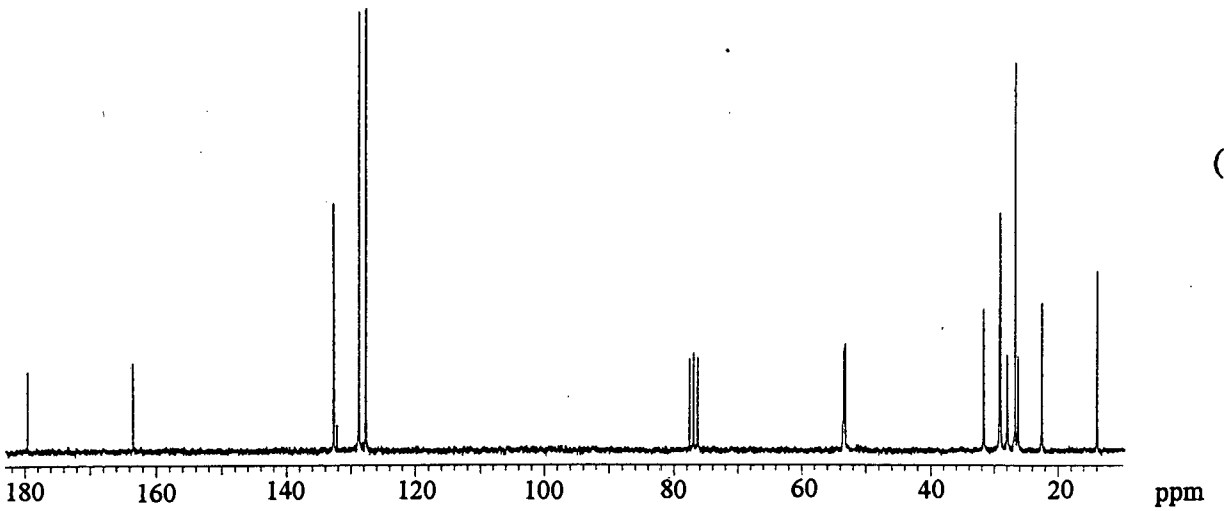

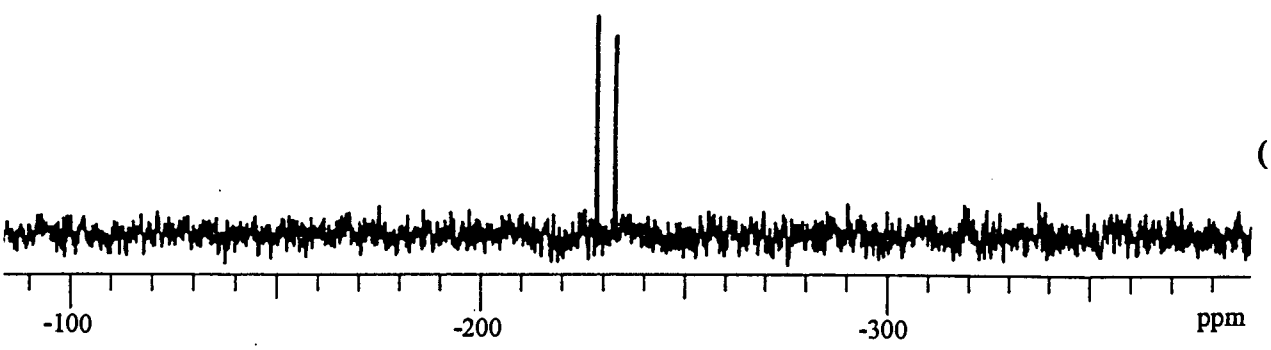

2.2.1.3 *N*-alkyl-, *N,N*-dialkyl-*N'*-naphthoylthiourea and *N,N*-dialkyl-*N'*-anthroylthiourea

Fluorometric and spectrofluorometric methods of analysis, which are unusually sensitive and highly selective, have been applied to the determination of many inorganic and organic molecules in trace amounts[27]. The most intense and most useful molecular fluorescence behaviour is found in compounds containing aromatic rings[28]. Accordingly, the *N*-naphthoylthiourea and *N*-anthroylthiourea compounds (Figure 2.8) were synthesised firstly, to introduce to *N*-acylthioureas a fluorescent probe and secondly, to ascertain the effect a sterically demanding naphthyl or anthracyl moiety has on the physical properties of the compounds. The octyl derivative of *N*-alkyl-*N'*-naphthoylthiourea, the dibutyl, dihexyl and dioctyl derivatives of *N,N*-dialkyl-*N'*-naphthoylthiourea and the dibutyl and dioctyl analogues of *N,N*-dialkyl-*N'*-anthroylthiourea were synthesised. A detailed characterisation of these compounds appears in the experimental section.

Physical Properties

Interestingly, there is very little difference between the melting points of *N*-octyl-*N'*-naphthoylthiourea and *N,N*-dioctyl-*N'*-naphthoylthiourea, as was observed between the *N*-alkyl- and *N,N*-dialkyl-*N'*-benzoylthioureas. A comparison of the melting points of the benzoyl, 1-naphthoyl and 9-anthroyl derivatives of *N,N*-dioctyl-*N'*-acylthiourea indicates that the anthroyl derivatives have lower melting points than either the naphthoyl or benzoyl derivatives, i.e. the melting point of analogous compounds is in the order anthracoyl < benzoyl < naphthoyl. These results suggest that optimal packing in the solid state occurs for the naphthyl compounds, as confirmed by the higher melting points compared to the benzyl and anthracyl compounds. An X-ray crystal structure analysis of the anthracyl derivative may show an interesting and unusual packing arrangement of these compounds, which may explain their unexpectedly low melting points.

Table 2.3 Analytical analyses and properties of *N*-octyl-*N'*-naphthoylthiourea (**3**), *N,N*-dibutyl-*N'*-naphthoylthiourea (**4a**), *N,N*-dihexyl-*N'*-naphthoylthiourea (**4b**), *N,N*-dioctyl-*N'*-naphthoylthiourea (**4c**), *N,N*-dibutyl-*N'*-anthroylthiourea, (**5a**) and *N,N*-dioctyl-*N'*-anthroylthiourea (**5b**).

compound	n	% yield	mp (°C)	elemental analysis %C/H/N
3	8	74	85 - 86	*calc*: 70.1; 7.7; 8.2 *obs*: 70.1; 7.8; 8.1
4a	4	75	97 - 99*	*calc*: 70.1; 7.7; 8.2 *obs*: 69.0; 7.3; 8.4
4b	6	86	71 - 72	*calc*: 72.3; 8.6; 7.0 *obs*: 72.1; 8.8; 7.8
4c	8	79	82 - 83	*calc*: 74.0; 9.3; 6.2 *obs*: 74.5; 9.5; 6.3
5a	4	82	115 - 117	*calc*: 73.4; 7.2; 7.1 *obs*: 72.9; 7.3; 7.0
5b	8	72	43 - 47	*calc*: 76.1; 8.8; 5.6 *obs*: 75.8; 8.8; 5.7

* *literature melting point 95 - 99 °C*[23]

2.2.2 Crystal structure determination of *N*-butyl-*N'*-benzoylthiourea

The X-ray crystal structure of *N*-butyl-*N'*-benzoylthiourea was solved to verify the structure of *N*-alkyl-*N'*-benzoylthiourea as proposed by Dago[15,16] *et al.* Dago reported that *N*-alkyl-*N'*-benzoylthioureas are characterised by a structure with an *intra*molecular hydrogen bond between the H atom of the amine NH group and the O atom of the carbonyl group. Furthermore, they reported that the compounds exist as dimers in the solid state.

The structure of *N*-butyl-*N'*-benzoylthiourea was determined by Dr Susan Bourne (Department of X-ray Crystallography, UCT). The structure was determined by single crystal X-ray diffraction and the numbering scheme is shown in Figure 2.13. Colourless block-like crystals of *N*-butyl-*N'*-benzoylthiourea were obtained by dissolving the compound in ethanol and allowing slow evaporation of the solvent at room temperature. The structure was solved by direct methods using SHELXS-86[29] and refined using SHELX-76[30]. The final model included anisotropic refinement of all non-hydrogen atoms except the carbons of the butyl chain. These showed high thermal motion and were thus modelled isotropically. All hydrogens, except that of H(10) which is involved in the hydrogen bond, were placed in calculated positions and linked to shared isotropic temperature factors. The crystal data, experimental and refinement parameters are summarised in Table 2.1 of Appendix 1. The fractional atomic coordinates for all non-hydrogens, except of H(10), are listed in Table 2.2 of Appendix 1.

Figure 2.13 Perspective view of the molecular structure of *N*-butyl-*N'*-benzoylthiourea showing the atom numbering scheme for all non-hydrogen atoms. The dashed line represents the *intra*molecular hydrogen bond.

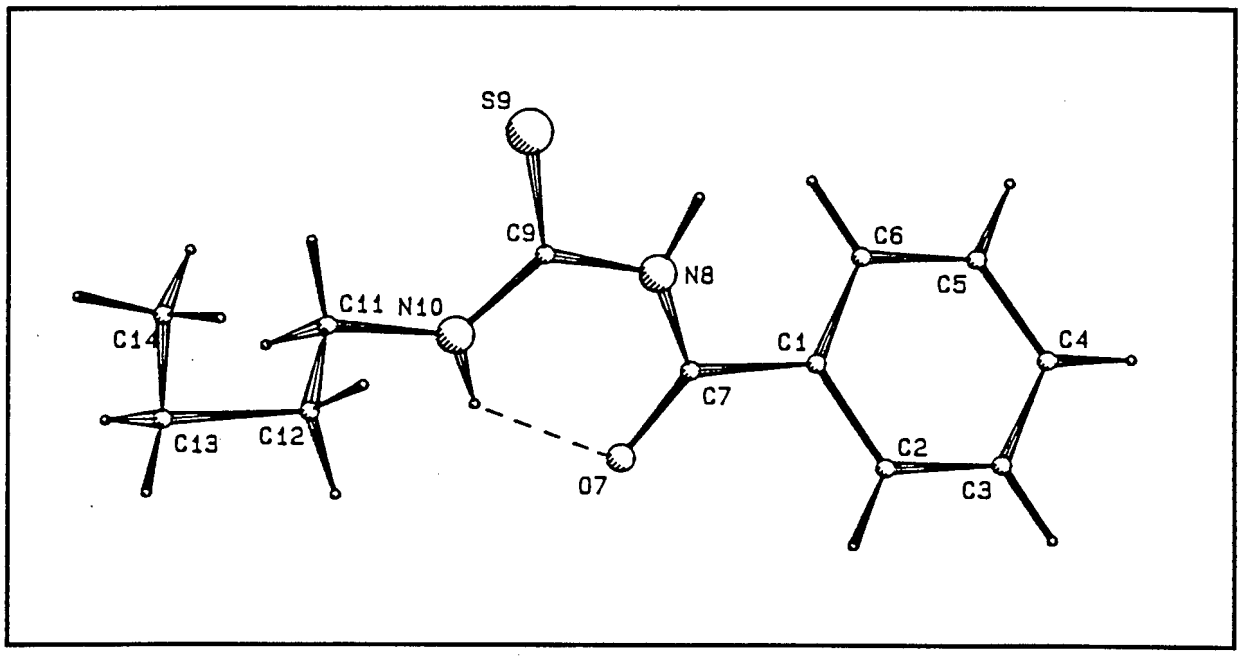

Description of the molecular structure

The crystal system is monoclinic and contains four molecules per unit cell. The bond lengths and bond angles all fall within the expected limits and agree with those reported by Dago[16] *et al* for *N*-propyl-*N'*-benzoylthiourea.

The observed C(7) - N(8) and C(9) - N(10) bond lengths are 1.368(6) and 1.317(6) Å respectively. These bonds are shorter than the usual C - N single bond of 1.47 Å[25] and slightly longer than the usual C = N double bond length reported to be 1.28 Å[25]. It is evident that C(9) - N(10) has a bond length closer to that of a double bond than a single bond. The observed C(9) - S(9) and C(7) - O(7) bond distances are 1.676(5) and 1.226(6) Å respectively (Table 2.4). Accordingly, the C - N, C - S and C - O bond distances indicate that the compound is stabilised by resonance[25] - the four potential resonance structures are depicted in Figure 2.14. The fact that C(7) - N(8) has more single bond character and C(9) - C(10) has more double bond character suggests that resonance form (ii), Figure 2.14, is most likely contributing to the observed structure.

Figure 2.14 Potential resonance structures of *N*-alkyl-*N'*-acylthiourea[16].

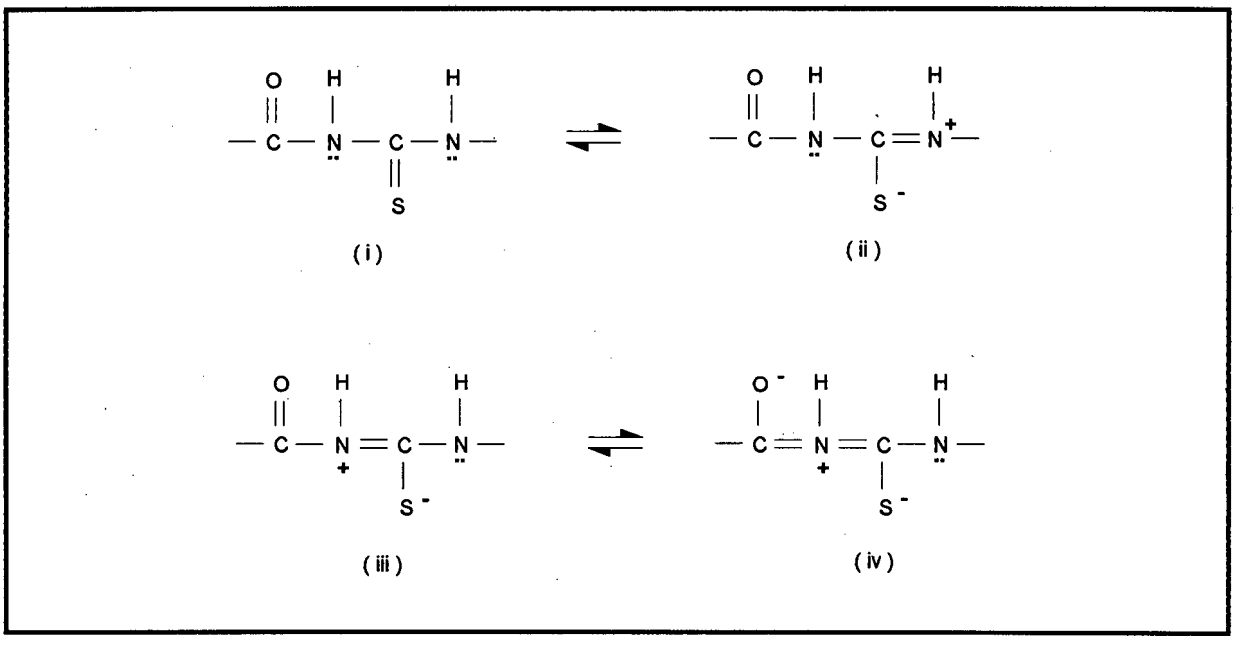

The crystal structure of *N*-butyl-*N'*-benzoylthiourea shows an *intra*molecular hydrogen bond locking O(7) - C(7) - N(8) - C(9) - N(10) - H(10) into a six-membered ring. The ring is planar (Table 2.3 of appendix 2) with deviations from the plane less than 0.1 Å. The dihedral angle between this plane and that of the planar phenyl ring is 43.87(19) °. The angle between the two planes can clearly be seen from the packing diagram in Figure 2.15.

The hydrogen involved in the hydrogen bond, H(10), was located in a difference Fourier map and was constrained to 1.00(2) Å from N(10) with an independent temperature factor. The N(10) - H(10) ... O(7) bond length and bond angle were found to be 2.644(6) Å and 133.5(43) ° respectively. The bond lengths and angles given here agree with those reported by Donohue for N - H...O interactions[30]. It is interesting to note that the N - H...O bond angle is 13 ° smaller than the analogous bond reported by Dago[16].

The molecules pack in a herring-bone configuration (Figure 2.15). There are no significant *inter*molecular contacts between adjacent molecules. This is in contrast to that observed by Dago[16] *et al* who reported that the structure of *N*-propyl-*N'*-benzoylthiourea was shown to be a dimer, formed through two *inter*molecular hydrogen bonds, N(8) - H(8) ... S(9).

Figure 2.15 Packing diagram of *N*-butyl-*N'*-benzoylthiourea. (View Z0 YROT 102.4).

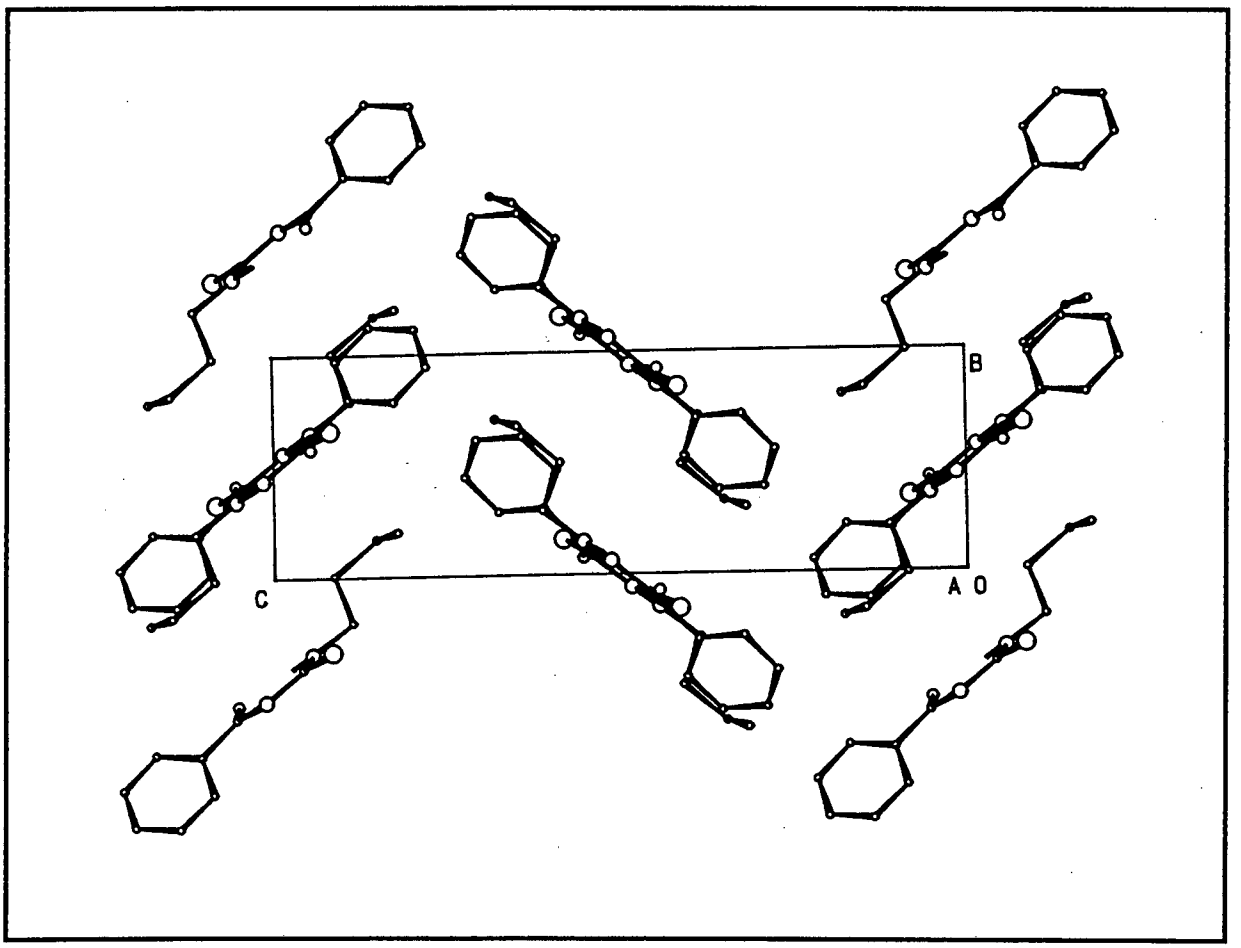

In conclusion, the present study clearly illustrates that *N*-acylthioureas may easily, and in high yield, be modified at either the amine or acyl functional group. A comparison of the melting points of analogous benzyl, naphthyl and anthracyl derivatives confirms that the anthracyl derivatives have lower melting points than the corresponding naphthyl or benzyl derivatives. The melting point of analogous compounds is in the order anthracyl < benzyl < naphthyl.

The crystal structure of *N*-butyl-*N'*-benzoylthiourea has confirmed the existence of a strong *intra*molecular hydrogen bond that allows for the formation of a planar six-membered ring. This conformation may have a significant influence on the coordination chemistry of the *N*-alkyl-*N'*-acylthioureas. Furthermore it allows for an interesting rod-shaped molecular geometry.

2.3 EXPERIMENTAL

The following instrumentation and experimental procedure was used throughout this study for the preparation and characterisation of the *N*-alkyl- and *N,N*-dialkyl-*N'*-acylthioureas.

Melting point determination

All melting points were determined on a Reichert-Jung thermovar attached to a DP-4 digital thermometer and are uncorrected.

Elemental analysis

Elemental analyses for % C, H and N were performed on a Fissons Elemental Analyser EA 1108 by Mr P. Benincasa of the Department of Chemistry, University of Cape Town.

Positive Fast Atom Bombardment (+FAB)

All +FAB spectra were recorded in nitrobenzylalcohol. The analyses were performed at the mass spectral unit at Cambridge University, England.

Nuclear magnetic resonance spectroscopy

All ^{1}H, ^{13}C and ^{15}N spectra were recorded in $CDCl_3$ using 5-mm tubes and a Varian VXR-200 Fourier transform spectrometer, unless otherwise stated, operating at 200, 50.32 and 40.54 MHz respectively at 25 °C. All ^{1}H and ^{13}C chemical shifts were referred to the central line of the solvent resonance of known shifts relative to tetramethylsilane and are estimated to be accurate to ± 0.05 ppm. All ^{15}N DEPT spectra were recorded in the presence of 5 mg chromium tris-acetylacetonate; the shifts are given relative to 95% ^{15}N enriched CH_3NO_2 (δ = 0 ppm) and are estimated to be accurate to ±1 ppm. The ^{1}H and ^{13}C spectra were obtained using a 10-μs pulse width (60° pulse angle), 1 - 1.5 s pulse delay and 12 kHz spectral width; in general, between 2048 and 8192 transients were required, while data was processed with a line broadening of 0.5 - 1 Hz. The ^{15}N DEPT spectra were obtained using a 2 - 2.5 s pulse delay and 15 kHz spectral width while data was processed with a line broadening of 3 Hz. The chemical shifts are recorded in parts per million (ppm).

Differential Scanning Calorimetry (DSC) and Thermogravimetric Analysis (TGA)

All DSC and TGA thermograms were recorded by Ms Rianna Mohamed on a Perkin Elmer - PE 7. The DSC heating and cooling curves were performed at scanning rates of 10 °C.min^{-1} unless otherwise stated.

X-ray crystallography

The crystal structure determinations were performed by Dr Susan Bourne or Ms Anita Coetzee, Department of Crystallography, University of Cape Town. Intensity data was collected on an Enraf-Nonius CAD4 diffractometer using graphite-monochromated Mo Kα radiation (λ = 0.7101 Å) at 20 °C.

Experimental procedure

The acetone was heated to reflux in the presence of K_2CO_3 and type 4Å Linde molecular sieves and distilled prior to use. The reagents are commercially available and were used without any additional purification. The *N*-alkyl- and *N,N*-dialkyl-*N'*-acylthiourea compounds were synthesised according to the method reported by Douglass and Dains[1], in 70 - 90 % yield. Potassium thiocyanate (0.05 mol) was dissolved in dry acetone (40 cm^3) and the acyl chloride (0.05 mol) in 40 cm^3 added dropwise under a nitrogen atmosphere. The reaction mixture was heated to reflux for 30 minutes and the amine (0.052 mol), in dry acetone (20 cm^3) was added dropwise and the mixture heated to reflux for an additional 30 minutes. The mixture was cooled and poured into ice water. The precipitated product was filtered and recrystallised from EtOH, unless otherwise stated, to give a white crystalline material.

***N*-butyl-*N'*-benzoylthiourea (1a)** 86 % yield, mp 48 - 49 °C. Anal. Calcd for $C_{12}H_{16}N_2OS$: C, 61.0; H, 6.8; N, 11.9. Found C, 61.0; H, 7.0; N, 11.8. NMR ($CDCl_3$) ^{1}H δ 1.01 (3H, t, CH_3), 1.49 (2H, m, $\underline{CH_2}CH_3$), 1.74 (2H, m, $\underline{CH_2}CH_2CH_3$), 3.73 (2H, q, NCH_2), 7.54 (2H, t, H(3) / H(5)), 7.66 (1H, t, H(4)), 7.86 (2H, d, H(2) / H(6)), 9.10 (1H, b.s, N(8) - H(8)), 10.75 (1H, t, N(10) - H(10)); ^{13}C δ 14.4, 20.8, 30.9, 46.3, 128.1, 129.7, 132.5, 134.1, 167.5, 180.4.

***N*-hexyl-*N'*-benzoylthiourea (1b)** Pure **1b** was obtained as a white solid after chromatography of the crude product on silica gel using toluene as eluent (71 % yield), mp 37 - 39 °C (lit. 37 °C)[20]. Anal. Calcd for $C_{14}H_{20}N_2OS$: C, 63.6; H, 7.6; N, 10.6. Found C, 63.5; H, 7.6; N, 10.7. NMR ($CDCl_3$) ^{1}H δ 0.88 (3H, t, CH_3), 1.33 (6H, m, CH_2), 1.65 (2H, m, $NCH_2\underline{CH_2}$), 3.67 (2H, q, NCH_2), 7.47 (2H, t, H(3) / H(5)), 7.59 (1H, t, H(4)), 7.84 (2H, d, H(2) / H(6)), 9.12 (1H, b.s, N(8) - H(8)), 10.74 (1H, t, N(10) - H(10)); ^{13}C δ 13.97, 22.48, 26.60, 28.15, 31.37, 58.26, 127.44, 129.05, 131.85, 133.44, 166.92, 179.69.

***N*-octyl-*N'*-benzoylthiourea (1c)** Pure **1c** was obtained as a white solid after chromatography of the crude product on silica gel using toluene as eluent (78 % yield), mp 37 - 41 °C. Anal. Calcd for $C_{16}H_{24}N_2OS$: C, 65.7; H, 8.3; N, 9.6. Found C, 65.4; H, 7.9; N, 9.5. NMR ($CDCl_3$) ^{1}H δ 0.88 (3H, t, CH_3), 1.35 (10H, m, $\underline{CH_2}$), 1.73 (2H, m, $NCH_2\underline{CH_2}$), 3.70 (2H, q, $N\underline{CH_2}$), 7.51 (2H, t, H(3) / H(5)), 7.63 (1H, t, H(4)), 7.83 (2H, d, H(2) / H(6)), 9.07 (1H, b.s, N(8) - H(8)), 10.77 (1H, t, N(10) - H(10)); ^{13}C δ 14.06, 22.61, 26.94, 28.20, 29.12, 29.17, 31.75, 45.96, 127.40, 129.09, 131.85, 133.46, 166.86, 179.66.

***N,N*-dibutyl-*N'*-benzoylthiourea (2a)** 86 % yield, mp 91 - 92 °C (lit. 93 °C)[22]. Anal. Calcd for $C_{16}H_{24}N_2OS$: C, 65.8; H, 8.2; N, 9.5. Found C, 65.9; H, 8.2; N, 9.8. NMR ($CDCl_3$) ^1H δ 0.89 (3H, t, CH_3), 0.98 (3H, t, CH_3'), 1.29 (2H, m, $\underline{CH_2}CH_3$), 1.46 (2H, m, $\underline{CH_2}'CH_3'$), 1.65 (2H, m, $\underline{CH_2}CH_2CH_3$), 1.79 (2H, m, $\underline{CH_2}'CH_2'CH_3'$), 3.52 (2H, m, NCH_2) 3.96 (2H, m, NCH_2'), 7.45 (2H, q, H(3) / H(5)), 7.56 (1H, t, H(4)), 7.82 (2H, d, H(2) / H(6)), 8.66 (1H, s, N - H); ^{13}C δ 13.56, 13.71, 19.89, 28.31, 29.98, 52.85, 53.07, 127.72, 128.63, 132.51, 132.63, 163.57, 179.75.

***N,N*-dihexyl-*N'*-benzoylthiourea (2b)** 81 % yield, mp 57 - 58 °C (lit. 59 °C)[20]. Anal. Calcd for $C_{20}H_{32}N_2OS$: C, 68.9; H, 9.2; N, 8.1. Found C, 68.6; H, 9.3; N, 8.0. NMR ($CDCl_3$) ^1H δ 0.84 (3H, t, CH_3), 0.91 (3H, t, CH_3'), 1.2 - 1.9 (16H, m, CH_2), 3.52 (2H, m, NCH_2), 3.94 (2H, m, NCH_2'), 7.44 (2H, q, H(3) / H(5)), 7.56 (1H, t, H(4)), 7.83 (2H, d, H(2) / H(6)), 8.65 (1H, s, N - H); ^{13}C δ 13.85, 22.33, 22.38, 26.13, 26.32, 27.88, 31.21, 31.32, 53.14, 53.43, 127.71, 128.61, 132.53, 132.60, 163.53, 179.68.

***N,N*-dioctyl-*N'*-benzoylthiourea (2c)** 87 % yield, mp 52 - 54 °C. Anal. Calcd for $C_{24}H_{40}N_2OS$: C, 71.2; H, 9.9; N, 6.9. Found C, 71.7; H, 9.8; N, 6.7. NMR ($CDCl_3$) ^1H δ 0.87 (3H, t, CH_3), 0.91 (3H, t, CH_3'), 1.2 - 1.9 (24H, m, CH_2), 3.55 (2H, m, NCH_2) 3.97 (2H, m, NCH_2'), 7.48 (2H, q, H(3) / H(5)), 7.59 (1H, t, H(4)), 7.85 (2H, d, H(2) / H(6)), 8.44 (1H, s, N - H); ^{13}C δ 14.01, 22.53, 26.29, 26.75, 27.98, 29.09, 31.69, 53.29, 53.57, 127.73, 128.76, 132.67, 132.75, 163.52, 179.65.

***N*-octyl-*N'*-naphthoylthiourea (3)** 74 % yield, mp 85 - 86 °C. Anal. Calcd for $C_{20}H_{26}N_2OS$: C, 70.1; H, 7.7; N, 8.2. Found C, 70.1; H, 7.8; N, 8.1. NMR ($CDCl_3$) ^1H δ 0.89 (3H, t, CH_3), 1.31 (10H, m, CH_2), 1.77 (2H, m, $NCH_2\underline{CH_2}$), 3.74 (2H, q, NCH_2), 7.51 (1H, t, H(7)), 7.60 (1H, t, H(3)), 7.61 (1H, t, H(6)), 7.75 (1H, d, H(5)), 7.92 (1H, d, H(4)), 8.03 (1H, d, H(2)), 8.32 (1H, d, H(8)), 8.94 (1H, s, N(12) - H(12)), 10.73 (1H, b.s, N(14) - H(14)); ^{13}C δ 14.08, 22.63, 27.01, 28.24, 29.15, 29.21, 31.78, 46.03, 124.53, 124.61, 126.14, 126.98, 128.07, 128.72, 129.77, 130.95, 132.90, 133.80, 168.97, 179.73.

***N,N*-dibutyl-*N'*-naphthoylthiourea (4a)** 75 % yield, mp 97 - 99 °C (lit. 95 - 99 °C)[23]. Anal. Calcd for $C_{20}H_{26}N_2OS$: C, 70.1; H, 7.7; N, 8.2. Found C, 69.0; H, 7.3; N, 8.4. NMR (400 MHz, $CDCl_3$) ^1H δ 0.98 (3H, t, CH_3), 1.02 (3H, t, CH_3'), 1.38 (2H, q, $\underline{CH_2}CH_3$), 1.47 (2H, q, $\underline{CH_2}CH_3'$), 1.76 (2H, t, $NCH_2\underline{CH_2}$), 1.83 (2H, t, $NCH_2\underline{CH_2}'$), 3.70 (2H, t, NCH_2), 4.01 (2H, t, NCH_2), 7.51 (1H, t, H(7)), 7.60 (1H, t, H(3)), 7.61 (1H, t, H(6)), 7.75 (1H, d, H(5)), 7.92 (1H, d, H(4)), 8.03 (1H, d, H(2)), 8.45 (1H, d, H(8)), 8.15 (1H, s, N(12) - H(12)), 8.45 (1H, d, H(8)).

***N,N*-dihexyl-*N'*-naphthoylthiourea (4b)** 86 % yield, mp 71 - 72 °C. Anal. Calcd for $C_{24}H_{34}N_2OS$: C, 72.3; H, 8.6; N, 7.0. Found C, 72.1; H, 8.8; N, 7.8. NMR ($CDCl_3$) ^1H δ 0.89 (3H, t, CH_3), 1.31 (10H, m, CH_2), 1.77 (2H, m, CH_2), 3.74 (2H, q, N-CH_2), 7.51 (1H, t, H(7)), 7.60 (1H, t, H(3)), 7.61 (1H, t, H(6)), 7.75 (1H, d, H(5)), 7.92 (1H, d, H(4)), 8.03 (1H, d, H(2)), 8.32 (1H, d, H(8)), 8.94 (1H, s, N(12) - H(12)); ^{13}C δ 14.06, 22.61, 26.98, 28.19, 29.14, 53.23, 53.41, 124.51, 124.57, 126.20, 127.06, 128.09, 128.67, 129.81, 131.05, 132.96, 133.84, 168.86, 179.49.

***N,N*-dioctyl-*N'*-naphthoylthiourea (4c)** 79 % yield, mp 82 - 83 °C. Anal. Calcd for $C_{28}H_{42}N_2OS$: C, 74.0; H, 9.3; N, 6.2. Found C, 74.5; H, 9.5; N, 6.3. NMR ($CDCl_3$) ^1H δ 0.86 (3H, t, CH_3), 0.90 (3H, t CH_3'), 1.31 (20H, m, CH_2), 1.77 (4H, m, CH_2), 3.66 (2H, t, NCH_2), 3.97 (2H, t, NCH_2'), 7.47 (1H, t, H(7)), 7.56 (1H, t, H(3)), 7.59 (1H, t, H(6)), 7.75 (1H, d, H(5)), 7.88 (1H, d, H(4)), 7.98 (1H, d, H(2)), 8.45 (1H, d, H(8)), 8.30 (1H, s, N(12) - H(12)); ^{13}C δ 14.02, 22.57, 26.33, 26.85, 28.12, 29.12, 31.73, 53.54, 53.60, 124.42, 125.12, 126.24, 126.67, 127.67, 128.46, 130.21, 131.62, 132.30, 133.80, 165.10, 179.21.

***N,N*-dibutyl-*N'*-anthracoylthiourea (5a)** 82 % yield, mp 115 - 117 °C. Anal. Calcd for $C_{24}H_{28}N_2OS$: C, 73.4; H, 7.2; N, 7.1. Found C, 72.9; H, 7.3; N, 7.0. NMR ($CDCl_3$) ^1H δ 1.02 (6H, t, CH_3), 1.49 (4H m, $\underline{CH_2}CH_3$), 1.87 (4H, m, $\underline{CH_2}CH_2CH_3$), 3.95 (2H, t, NCH_2), 4.05 (2H, t, NCH_2'), 7.51 (2H, t, H(4) / H(8)), 7.59 (2H, t, H(3) / H(9)), 8.04 (2H, d, H(5) / H(7)), 8.05 (1H, s, H(6)), 8.14 (2H, d, H(2) / H(10)), 8.54 (1H, s, N - H); ^{13}C δ 13.87, 20.33, 28.55, 30.44, 53.77, 124.45, 125.71, 127.40, 128.26, 128.77, 129.49, 130.98, 166.11, 178.71.

***N,N*-dioctyl-*N'*-anthracoylthiourea (5b)** Pure **5b** was obtained as a yellow solid after chromatography on silica gel using chloroform as eluent (72 % yield), mp 43 - 47 °C. Anal. Calcd for $C_{32}H_{44}N_2OS$: C, 76.1; H, 8.8; N, 5.6. Found C, 75.8; H, 8.8; N, 5.7. NMR ($CDCl_3$) ^1H δ 0.89 (6H, t, CH_3), 1.31 (20H, b.m, CH_2), 1.90 (4H, b.s, CH_2), 3.94 (2H, t, NCH_2), 4.03 (2H, t, NCH_2'), 7.51 (2H, t, H(4) / H(8)), 7.58 (2H, t, H(3) / H(9)), 8.04 (2H, d, H(5) / H(7)), 8.06 (1H, s, H(6)), 8.16 (2H, d, H(2) / H(10)), 8.54 (1H, s, N - H); ^{13}C δ 14.07, 22.62, 26.39, 26.96, 27.05, 28.39, 29.23, 29.30, 31.78, 54.01, 124.46, 125.68, 127.36, 128.24, 128.75, 129.43, 130.97, 166.08, 178.62.

REFERENCES

1 Douglass, I.B.; Dains, F.B.; *J. Am. Chem. Soc.*, 1934, **56**, 719.

2 Takamizawa, A.; Hirai, K.; Matsui, K.; *Bull. Chem. Soc. Jpn.*, 1963, **36**, 1214.

3 Drobnica, L.; Kristian, P.; Augustín, J.; *The Chemistry of the Cyanates and Their Thio Derivatives*, (ed.), Patai, S., Wiley-Interscience, New York, 1977.

4 Elmore, D.T.; Ogle, J.R.; *J. Chem. Soc.*, 1958, 1141.

5 Shaw, G.; Warrener, R.N.; *J. Chem. Soc.*, 1958, 157.

6 Douglass, I.B.; Forman, L.E.; *J. Am. Chem. Soc.*, 1934, **56**, 1609.

7 Akiyama, H.; Yoshida, N.; Araki, Y.; Ouchi, K.; *J. Chem. Soc. B*; 1968, 676.

8 Williams, A.; Jencks, W.P.; *J. Chem. Soc., Perkin Trans.2*, 1974, 1753.

9 Lozinskii, M.O.; Pel'kis, P.S.; *Russ. Chem. Rev.*, 1968, **37**, 363.

10 Baker, J.W.; Gaunt, J.; *J. Chem. Soc.*, 1949, 19.

11 König, K.-H.; Schuster, M.; Steinbrech, B.; Schneeweis, G.; Schlodder, R.; *Fresenius' Z. Anal. Chem.*, 1985, **321**, 457.

12 Beyer, L.; *Z. Chem.*, 1980, **20**, 268.

13 Sarkis, G.Y.; Faisal, E.D.; *J. Heterocyclic Chem.*, 1985, **22**, 137.

14 Salmon, S.R.; Sarkis, G.Y.; Faisal, E.D.; *Can. J. Spectrosc.*, 1986, **31**, 167.

15 Dago, A.; Simonov, M.A.; Pobedimskaya, E.A.; Macías, A.; Martín, A.; *Kristallografiya,* 1988, **33**, 1021.

16 Dago, A.; Shepelev, Y.; Fajardo, F.; Alvarez, F.; Pomés, R.; *Acta Crystallogr.*, 1989, **C45**, 1192.

17 Congdon, W.I.; Edward, J.T.; *J. Am. Chem. Soc.*, 1972, **94**, 6096.

18 Congdon, W.I.; Edward, J.T.; *Can. J. Chem.*, 1974, **52**, 697.

19 Harris, R.L.N.; Oswald, L.T.; *Aust. J. Chem.*, 1974, **27**, 1531.

20 Vest, P.; Schuster, M.; König, K.-H.; *Fresenius' Z. Anal. Chem.*, 1989, **335**, 759.

21 Koch, K.R.; Matoetoe, M.C.; *Mag. Res. Chem.*, 1991, **29**, 1158.

22 König, K.-H.; Schuster, M.; Schneeweis, G.; Steinbrech, B.; *Fresenius' Z. Anal. Chem.*, 1984, **319**, 66.

23 Koch, K.R.; du Toit, J.; Caira, M.; Sacht, C.; *J. Chem. Soc., Dalton Trans.*, 1994, 785.

24 Günter, H.; *An Introduction to NMR Spectroscopy*, John Willey & Sons, Chichester, 1980.

25 March, J.; *Advanced Organic Chemistry: Reactions, Mechanisms and Structure*, McGraw-Hill Company, 1968.

26 Beyer, L.; Behrendt, S.; Kleinpeter, E.; Borsdorf, R.; Hoyer, E.; *Z. Anorg. Allg. Chem.*, 1977, **437**, 282.

27 Schulman, S.G.; *Fluorescence and Phosphorescence Spectroscopy*, Pergamon Press, New York, 1977.

28 Skoog, D.A.; West, D.M.; Holler, F.J.; *Fundamentals of Analytical Chemistry*, 5th edn., Saunders College Publishing, New York, 1988.

29 Sheldrick, G.M.; SHELXS-86 in *Crystallographic Computing 3*, (eds.), Sheldrick, G.M.; Kruger, C.; Goddard, R.; Oxford University Press, 1985.

30 Sheldrick, G.M.; SHELX-76. Package for Crystal Structure Determination, University of Cambridge, 1976.

31 Donohue, J.; *Selected Topics in Hydrogen Bonding. Structural Chemistry and Molecular Biology,* (ed.), Rich, A.; Davidson, N.; Freeman, San Francisco, 1968.

CHAPTER 3

POTENTIAL LIQUID CRYSTALS COMPOUNDS BASED ON *N*-ALKYL-*N'*-BENZOYLTHIOUREAS

3.1 Introduction

Matter is generally thought of as existing in one of three states or phases; that is, solid, liquid and gas. However, the phenomenon of 'liquid crystallinity' was discovered more than a hundred years ago, when in 1888 the Austrian botanist Reinitzer first observed the strange melting behaviour of cholesteryl acetate and cholesteryl benzoate[1]. Since these initial discoveries, liquid crystals have become a major, multidisciplinary area of research. It is a constantly expanding field in which the synthesis of new materials tries to meet the demands of industrial applications.

The most well known use of liquid crystals is in the area of electro-optic displays, e.g. in calculators, digital watches and television sets[2]. All liquid crystal display devices produced commercially, contain fluids which are mixtures of several liquid crystal components[3]. Overall, however, relatively few classes of compounds have found commercial usefulness. This arises naturally from the constraints imposed by practical applications: the fluids employed in devices must be stable, colourless, mesomorphic over a wide range in the room temperature region, and operate at low voltage and power levels[3]. The first two criteria alone eliminate a vast number of liquid-crystalline compounds.

In addition to liquid crystal displays, chiral liquid crystals have been used in biomedical thermography[4] as an important diagnostic aid which is used to assist in the identification of a wide range of medical conditions, e.g. breast cancer detection[5], placental location[6] and vascular disorders[7]. Thermal mapping[8] of inanimate objects can provide engineers with useful diagnostic and design information, e.g. heat transfer effects in aerodynamic models[9]. Liquid crystals have been used in radiation leakage detectors which consist of a low thermal mass transducer which converts the radiation into heat energy. The temperature rise is viewed directly as an induced colour change in a film of liquid crystalline material coating the surface[10].

The area of liquid crystals has received an increased amount of attention in recent years. A report[11] indicates that 50 000 mesogenic compounds had been studied by 1990 and more than 2000 papers and 1500 patents are published in the field of liquid crystals each year. However, to the Author's knowledge, no liquid crystal compounds based on the *N*-acylthiourea moiety have been reported to date.

The term 'liquid crystal' is in itself contradictory, but has become an accepted form of terminology to describe a state of matter whose properties are intermediate between a solid and a liquid. Liquid crystals may therefore be considered as either *disordered solids* or *ordered liquids*. They exhibit a molecular order in a size range similar to that of a crystal but act like a viscous liquid. The terms *mesomorph* (Greek for between two states or forms) *liquid crystal phase, mesophase* and *mesomorphous state*[12] are used synonymously; a *mesogen* or *liquid crystal* is a molecule that gives rise to a mesophase[13]. Compounds with liquid-crystalline properties do not undergo a transition from solid to liquid at a sharp melting point. Instead, these compounds assume one or several mesophases with sharp transitional temperatures between the solid and liquid state.

To avoid ambiguity when addressing liquid crystals, the terms melting point, clearing point and isotropic liquid need to be defined. The conventional liquid state is referred to as the *isotropic liquid*. The temperature at which a compound passes from the solid state into an isotropic liquid or a mesophase is referred to as the *melting point*, and that from the highest mesophase to the isotropic liquid as the *clearing point*[13].

3.1.1 Classification of liquid crystals

Organic liquid crystals can be divided into two broad families depending on the method used to destroy the order associated with the solid state, namely the *thermotropics*[3] and the *lyotropics*[4]. The one which will principally concern us in this work is the family of *thermotropic liquid crystals*, where heating the compound to a temperature above which the crystal lattice is no longer stable, causes transitions between the various states, i.e. by thermal effects. Thermotropic liquid crystals usually have structures that are mainly either rod-shaped or disc-shaped[13]. This class of liquid crystals is further divided into two subgroups, *enantiotropic* and *monotropic*[3]. Phases of enantiotropic liquid crystals are reversibly formed by heating the solid crystalline phase or by cooling the isotropic liquid (sequence 1, Figure 3.1). The phases of monotropic liquid crystals can be obtained only by supercooling the isotropic liquid; that is, these liquid crystal phases are not normally observed on heating of the solid crystalline phase (sequence 2, Figure 3.1)[13].

Lyotropic liquid crystals are formed when compounds with amphiphilic properties are treated with a solvent (usually water)[14]. A true solution is not obtained but the resultant state possesses the properties of the liquid-crystalline phase. The appearance of this liquid crystal phase is controlled by the concentration of the compound in solution[13].

Figure 3.1 Schematic representation of enantiotropic and monotropic thermotropic liquid crystals.

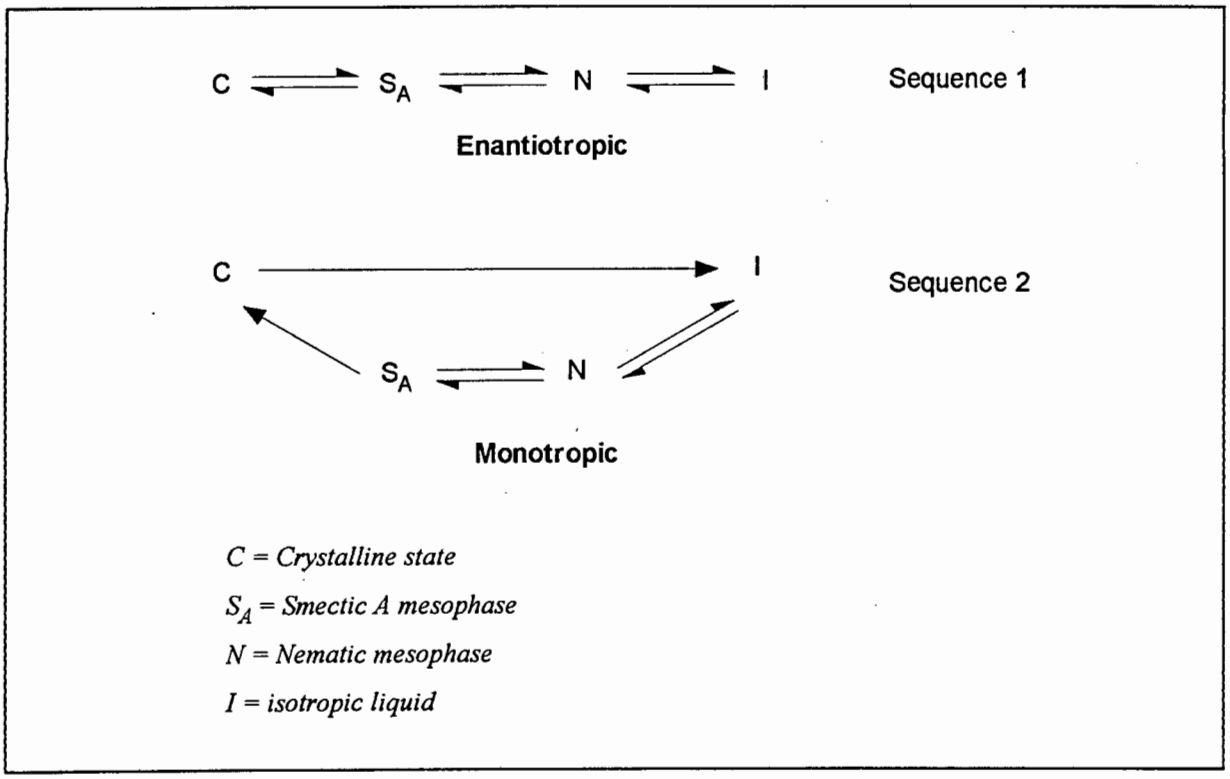

A crystal (**C**) has a defined shape and most of its physical properties are anisotropic because the constituent molecules or ions are ordered with respect to position and orientation i.e. direction dependent. On the other hand, the molecules (or ions) of a true fluid lack positional and orientational order and therefore the physical properties are isotropic (**I**). In a thermotropic liquid crystal phase the positional order is largely absent resulting in the fluidity[13]. However a degree of orientational order is retained which results in anisotropic properties[13]. The anisotropy of optical properties manifests itself in what is called *birefringence* (double refraction in crystals).[15,16]

Thermotropics can further be divided into *calamitic* (rod-like) and *discotic* (disc-like)[17]. Calamitic liquid crystals form three broad classes, *nematic* (**N**), *smectic* (**S**) and *cholesteric* (**Ch**)[18]. Several subgroups of discotic liquid crystals are also known but since they are not pertinent to this study, they will not be discussed further.

Friedel[18] demonstrated that a particular type of mesophase, when observed under a polarising microscope, will adopt one of a limited number of *textures*, the birefringent patterns of liquid-crystalline phases. These textures may be used to establish whether the mesophase under investigation is smectic, nematic or cholesteric. All textures depend on molecular short range order that is in turn dependent on molecular structure[12]. Certain textures, called type-textures[12], are characteristic of a given liquid crystal phase whereas other textures may occur in more than one mesogenic phase.

Figure 3.2 Sub-classification of liquid crystal systems.

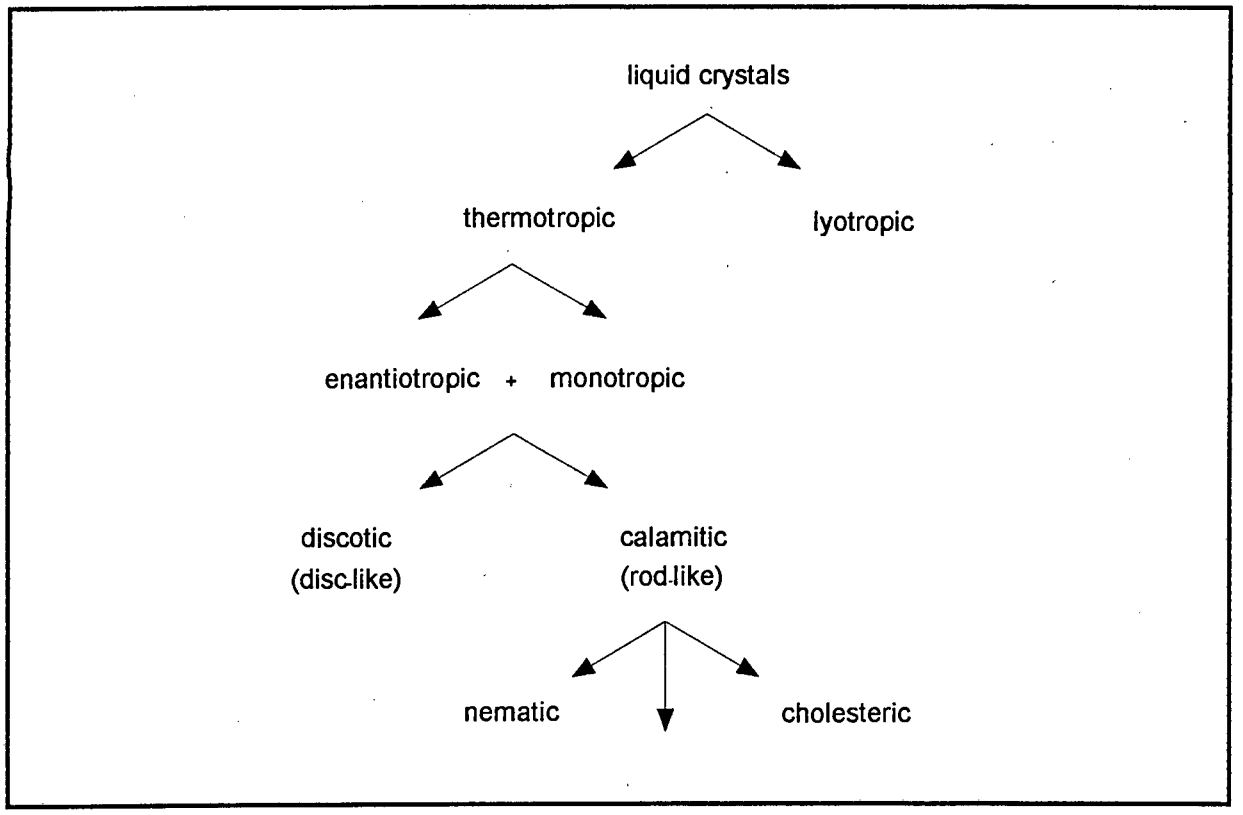

3.1.2 Structure and order in liquid crystals

3.1.2.1 Smectic phase

Friedel introduced the term *smectic* (Greek for soap), to describe the texture of alkali metal salts of long-chain aliphatic carboxylic acids observed under a polarising microscope[18]. The different smectic phases are based on a two-dimensional arrangement and therefore show the highest dimensional order and the most solid-like textures of all the liquid-crystalline phases[19]. The molecules are loosely arrayed in layers, which are roughly as thick as the molecules are long, with the long axes of the molecules orientated in a similar direction[13]. Some smectic phases have their molecules perpendicular to the layers (e.g. Smectic A) (Figure 3.3); in others they are inclined to them (e.g. Smectic C). The high viscosity and surface tension of smectic phases reflects their high degree of order[19].

Figure 3.3 Schematic representation of the phase structure (molecular alignment) in a Smectic A phase[19]. The molecules are perpendicular to the layers, rotate around their longitudinal axis and move freely within their layers[17].

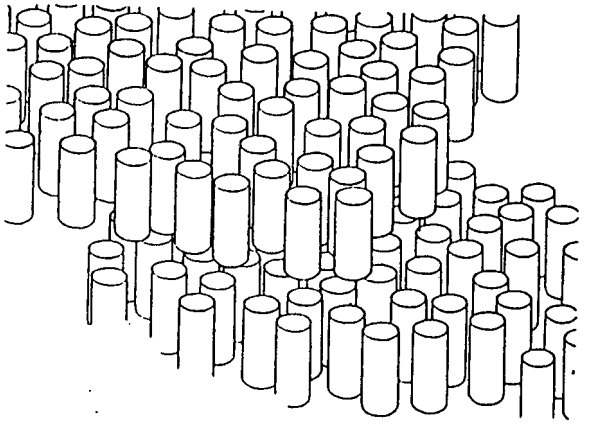

Based on the molecular order within the layers, nine different smectic phases (S_A, S_B, ..., S_I) have been distinguished[20]. The temperature sequence for liquid-crystalline phases is not arbitrary. The order in which the phases follow each other is

$$S_E \text{ or } S_G \text{ or } S_H \rightarrow S_B \rightarrow S_F \rightarrow S_I \rightarrow S_C \rightarrow S_D \rightarrow S_A^{21},$$

with Smectic E (S_E) possessing most order, i.e. most solid-like, and Smectic A (S_A) possessing least order, i.e. most liquid-like. Compounds are known which give up to one nematic and five smectic phases[22]. These different possibilities are termed variants of *polymorphism*[23].

3.1.2.2 Nematic phase

Friedel called the second type of thermotropic, liquid-crystalline phase *nematic* (Greek for thread); because between crossed polarising filters these show thread-like irregularities in the liquid melt and are less viscous than smectic phases[18]. Particularly striking are the highly mobile drops, sparkling bright colours and the so-called schlieren texture[3,20,23] (see section 3.1.5.2). The nematic phase has the simplest structure of all the liquid-crystalline phases, is very fluid and is also the most disordered phase[24]. The nematic phase consists of molecules which are approximately parallel to each other and free to move in all three directions, but can only rotate along their longitudinal axis[19], i.e. it is the long axes which correlate and not the molecules themselves (Figure 3.4).

Figure 3.4 Schematic representation of the phase structure of a nematic liquid crystal[19]. Molecules are nearly parallel to each other but are not arranged in layers.

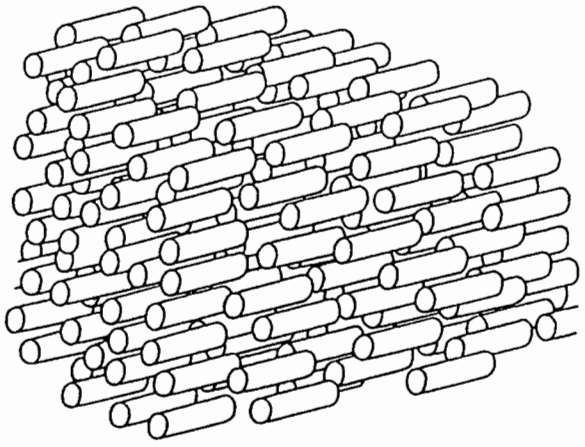

3.1.2.3 Cholesteric phase

A third type of liquid-crystalline phase was first observed with cholesteryl compounds, and was named the cholesteric phase[18]. From the structural point of view, cholesteric liquid crystals are 'twisted' nematics. Cholesteric liquid-crystalline behaviour is only observed in compounds that contain a chiral carbon centre and since we are dealing with achiral compounds, they will not be discussed further.

3.1.3 Structural features of liquid-crystalline materials

Thermotropic materials are held together by weak dipole-dipole and dispersion forces[13]. The magnitude of these forces is critical since when they are too weak or too strong, the liquid-crystalline character is lost. By comparing the chemical constitution and liquid-crystalline properties of a large number of calamitic-thermotropic liquid crystals, the criteria that indicate a molecule's predisposition to forming liquid crystals can be summarised in four points[19]:

- a thin elongated molecular shape is necessary, especially with inflexible molecular frameworks
- branched or angular molecular frameworks reduce or prevent the formation of liquid-crystalline regions

- a high anisotropy of polarisability is necessary since the orientation of the molecules in liquid-crystalline phases is brought about by dispersive forces. This is promoted by permanent dipoles or easily polarisable groups

- in order to avoid supercooled, metastable liquid-crystalline phases (monotropic phases), the melting point should not be too high.

The vast majority of liquid-crystalline substances are based on the general structure in Figure 3.5 and possess[24]:

- rigid , linear building blocks, consisting of two or more aromatic rings

- polar or easily polarizable functional groups, A — B, that bind the rings together

- terminal groups, X and Y, which are mostly unbranched aliphatic chains extending the molecule and lowering the melting point[25].

Figure 3.5 Schematic representation of the general structural design of liquid crystals[13].

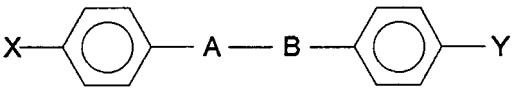

The 1,4-disubstituted benzene ring forms the standard building-block from which the majority of liquid crystal molecular structures are derived[12]. It is highly polarizable and determines the basic rod-shaped structure of the molecule. However, saturated, conformatively mobile rings can also have the necessary rigid linear geometry for mesomorphic behaviour[19]. Polarizable bridging groups also seem essential for mesogenic behaviour, although rigid, linear geometry is of greater importance for the thermal stability of liquid-crystalline phases than easily polarizable groups[19]. There are only a few completely linear bridging groups, more frequently the building blocks are angular allowing a parallel arrangement of the two halves of the molecule[12] (Figure 3.7).

Figure 3.6 The most frequently used building blocks for the preparation of liquid crystals[19].

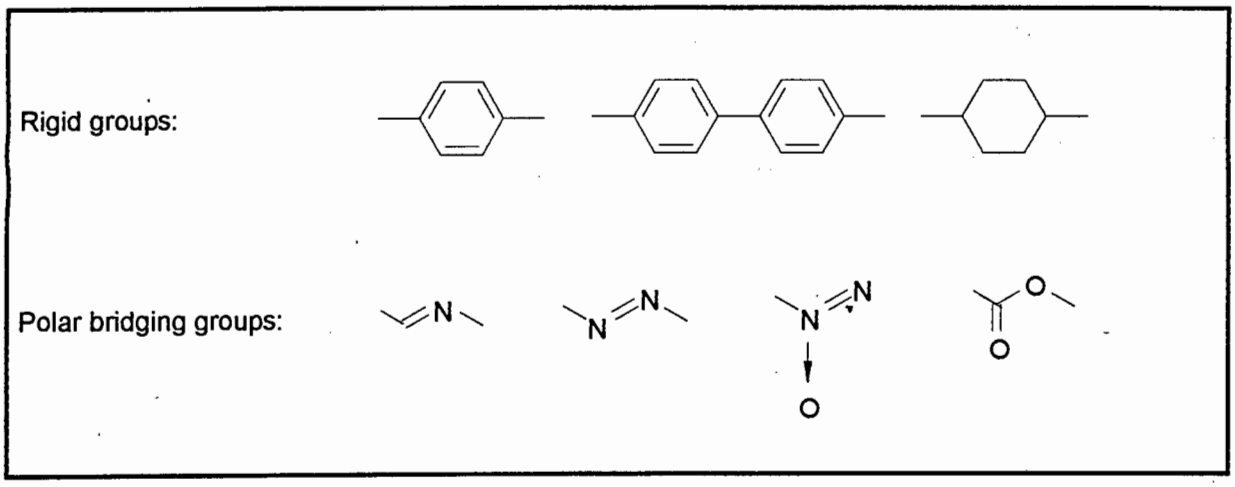

Figure 3.7 Parallel arrangement of two halves of a molecule[12].

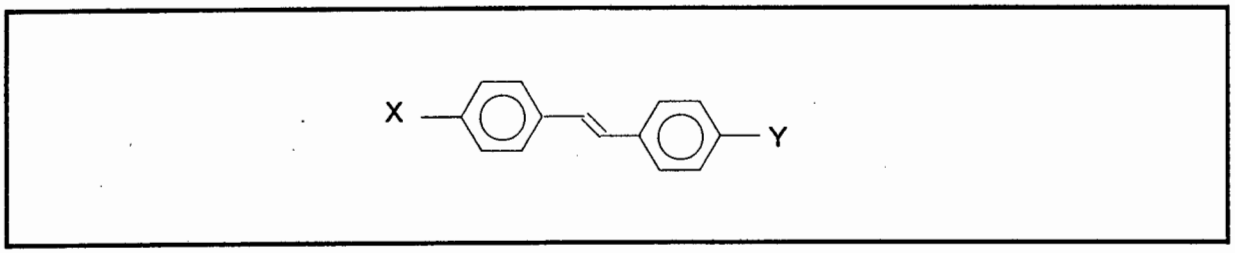

The addition of rings or multiple-bonded units to extend the length of the rigid core of a rod-shaped molecule, results in significant increases in the clearing point temperatures (temperature transition from highest mesophase to the isotropic liquid) of nematics[12]. Terminal n-alkyl or n-alkoxy chains are primarily used to lower the melting point[26]. Generally, lengthening of the alkyl chain of a terminal n-alkyl or n-alkoxy group prevents the molecules from sliding and thus favours the formation of smectics at the expense of nematics. On the other hand, these longer terminal groups tend to coil with increasing length, thus hindering the parallel alignment of the molecules[12].

3.1.4 Identification of the liquid-crystalline phases

Once a compound has been synthesised, there are three different techniques which are used to identify whether the material possesses mesogenic character. These include polarising hot-stage optical microscopy, differential scanning calorimetry and low angle X-ray scattering in the mesophase.

3.1.4.1 Polarised optical microscopy is usually the first technique used to characterise thermotropic mesophases and is indispensable for the observation of liquid crystals[23,29]. The compound is 'sandwiched' between two microscope glass plates and then placed on a temperature-controlled hot-stage through which there is an optical path. The technique makes use of the fact that isotropic liquids and solids and also the free field of vision remain dark, whereas anisotropic materials allow the passage of light and show bright interference colours when placed between two polarising filters whose planes of polarisation are perpendicular to each other (Figure 3.8)[24].

Figure 3.8 Schematic view of a polarised, hot-stage microscope.

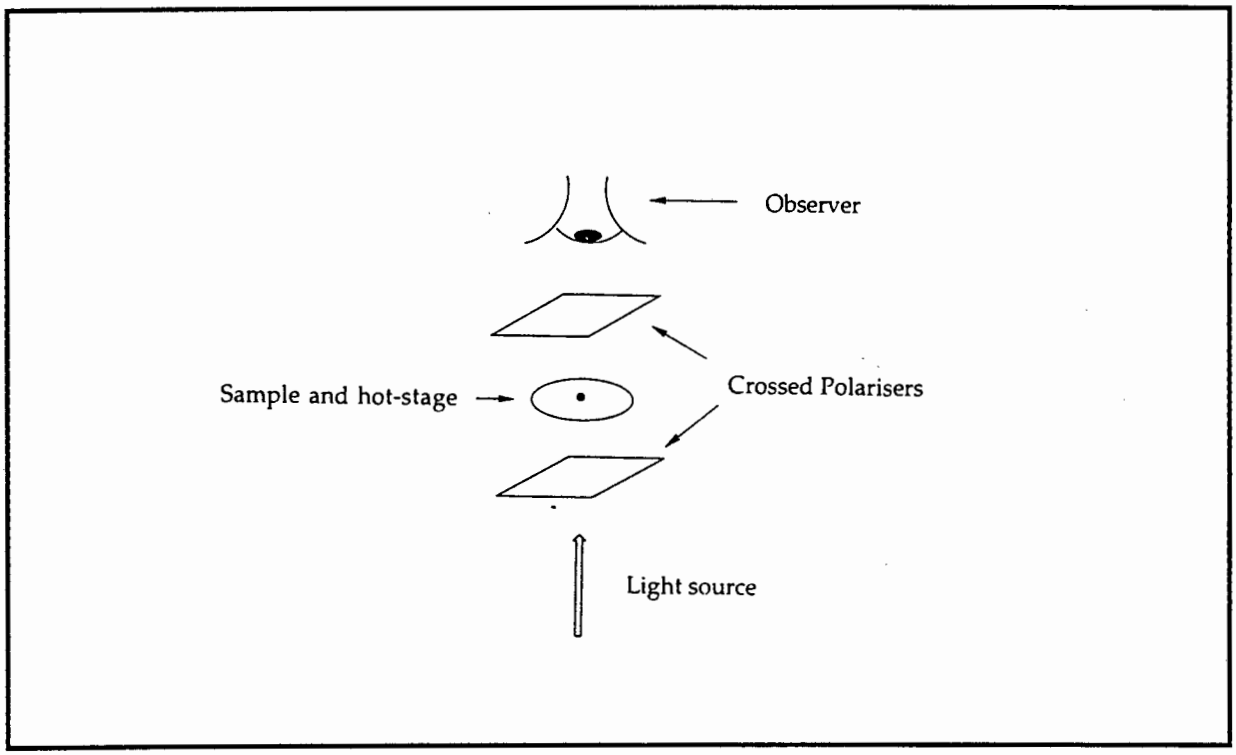

Liquid crystals appear to the naked eye as opalescent, cloudy liquids that are reminiscent of soap solutions due to their frequently white to yellowish colour. In thin films, however, they may become transparent. Nematic phases have low viscosity's similar to that of water, but all smectic phases are highly viscous and in some cases so highly viscous that it is difficult to recognise them as 'liquids'[12]. The investigator frequently finds that scratching free droplets with a sharp object or moving the glass cover slips on closed preparations is necessary to be convinced that the sample is truly liquid. However, it is often found that by moving the glass coverplate, the supercooled substance is transformed into a crystalline one.

The texture a mesophase adopts is dependent on[28]:

- the nature of the material under investigation
- the nature and cleanliness of the supporting surface, i.e. surface treatment of the glass cover slip
- the manner in which the mesophase is produced, i.e. by cooling the isotropic liquid, by cooling the nematic phase or by heating the material from the crystalline state
- the thickness of the sample.

It is thus evident that a liquid crystal can display different microscopic textures for the same mesogenic phase depending on the boundary surfaces, sample thickness, purity and the thermal and temporal pretreatment[12]. Accordingly, considerable skill is necessary to identify the different liquid-crystalline phases. It is important to note that all changes in optical texture do not necessary correspond to a change in mesophase type, while all phase changes do not always lead to an easily identifiable change in texture[24]. It is therefore necessary to compare the results of optical studies with those of Differential Scanning Calorimetry thermograms.

3.1.4.2 Differential scanning calorimetry (DSC) provides an essential supplementary approach to phase identification. DSC directly provides a measurement of the magnitude and temperature at which chemical or physical changes occur in a substance during heating or cooling[29]. The technique measures the difference in electrical power required to maintain a sample pan and empty reference pan at a precisely controlled linearly increasing or decreasing temperature. The differential power input, recorded as a function of temperature, is directly proportional to the energy involved in thermal transitions.

DSC provides for the direct determination of the enthalpy and entropy of each of the mesomorphic phase transitions. The enthalpy is a measure of the relative stability of the mesophases, while the entropy provides a measure of the order of the system. From a thermodynamic point of view, melting transitions are strongly first order while liquid crystal - liquid crystal transitions are weakly first order or may be second order. A first-order phase transition is characterised by an infinite heat capacity at the transition temperature whereas a second-order phase transition is characterised by a zero change in enthalpy, entropy and volume at the phase transition[12]. Information about the phase transition may therefore be derived from the relative magnitudes of the transition enthalpies, so that the melting enthalpies are much larger than those found for the N - I transition. While such information is useful, *it does not allow generalisations to be made.*

3.1.4.3 X-ray scattering is an additional method of mesophase identification and relies on the fact that mesomorphic structures are periodic and can therefore diffract[24]. Thus for a smectic phase, diffraction lines corresponding to both the layer periodicity and side-to-side periodicity can be observed; comparison between the calculated molecular length and the observed layer periodicity can give information about the tilt angles and interdigitation.

Finally, impurities in a sample can induce the appearance of a mesophase where none truly exists in a purer sample, or can inhibit the formation of a mesophase which would be present[29]. Small amounts of impurity may greatly broaden and shift the mesophase transition to lower temperatures by several degrees. Thus it is important to ensure the absolute purity of the material when studying the potential mesogenic behaviour of the compound.

3.1.5 Structure and textures of thermotropic liquid crystals

In view of the fact that nine different smectic phases have been reported, each with different structures and textures, I have limited the discussion of the smectic phases to the structure and textures of the liquid-crystalline phases pertinent to the present study. Hence, only the smectic A and nematic phases are described.

3.1.5.1 Structure and textures of the smectic A phase

The smectic A phase, (S_A), is the smectic polymorphic modification which possesses least order[26]. If a liquid-crystalline phase sequence includes a smectic A phase, this phase precedes all other smectic phases upon cooling either the isotropic liquid or the nematic phase.

The smectic A phase, together with the smectic C phase, are the most frequently observed of the presently known smectic phases. The textures of smectic A are compatible with its layered structure[23]. There are two important microscopic textures exhibited by the smectic A phase — the homeotropic or pseudoisotropic texture and the focal-conic fan texture.

- *The homeotropic or pseudoisotropic texture*

  The simplest configuration of a smectic A texture is an arrangement with the layers of molecules parallel to the surfaces of the glass coverplates[23]. The molecules are aligned with perpendicular orientation with respect to the layers. The homeotropic texture *appears black* when observed through a polarising microscope and crossed polarisers. Bright birefringent regions usually appear only at the edges of the specimen or around air bubbles and particles of impurity[27].

- *The focal-conic fan texture*

The focal-conic fan texture is probably the most commonly observed texture of the smectic A phase[3]. The phase usually separates out (on cooling the isotropic liquid or the nematic phase) in the form of *bâtonnets* which are rod-shaped with cylindrically symmetrical protrusions[28] (Figure 3.9). The bâtonnets join together to form larger structures which coalesce and build up the *focal-conic texture*. The backs of the fans are usually grained, giving a radiating pattern along the length of a fan-shaped area. The focal-conic fan texture contains optical discontinuities which are visible in ordinary light and with crossed polarisers.

Figure 3.9 Drawings of three typical smectic bâtonnets[28].

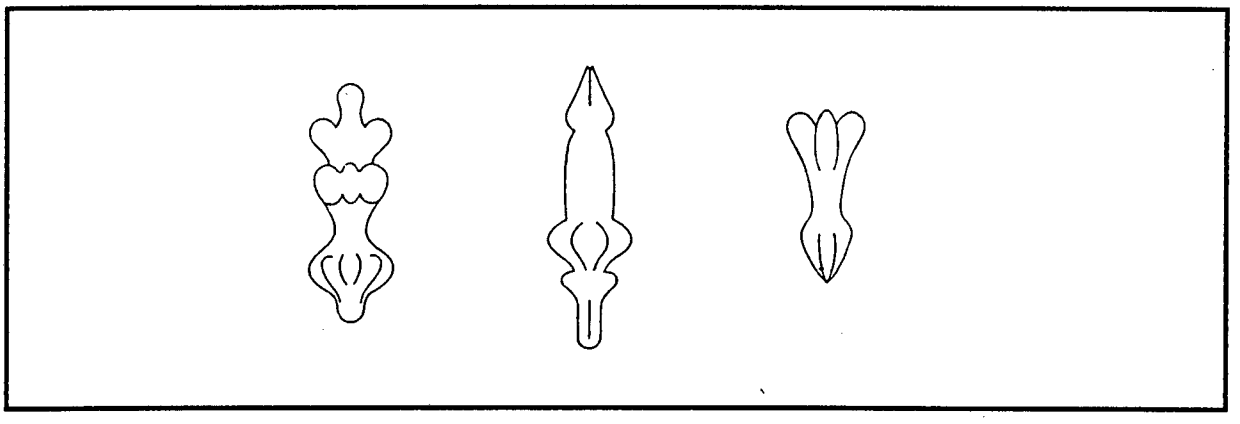

3.1.5.2 The structure and textures of the nematic phase

A nematic phase can be recognised microscopically by a *visible increase in fluidity* with respect to the smectic phases. There are four important microscopic textures exhibited by the nematic phase — the homeotropic texture, nematic droplets, the schlieren texture and the marbled texture.

- *The homeotropic texture*

Like smectic A phases, the nematic phase easily forms the homeotropic texture[12], appearing extinct when viewed through crossed polarisers. If the preparation is subjected to mechanical stress, the field of view instantly brightens but after the release of the stress the field of view once again becomes extinct when viewed through crossed polarisers.

- *Nematic droplets*

The nematic phase is most easily identified by the presence of nematic droplets and the schlieren texture[12]. Nematic droplets characterise a *type-texture* of the nematic phase since they occur nowhere else. Upon cooling an isotropic liquid, the nematic phase begins to separate at the clearing point in the form of typical free-form droplets (Figure 3.10).

Figure 3.10 Nematic droplets which characterise a type-texture of the nematic phase[12].

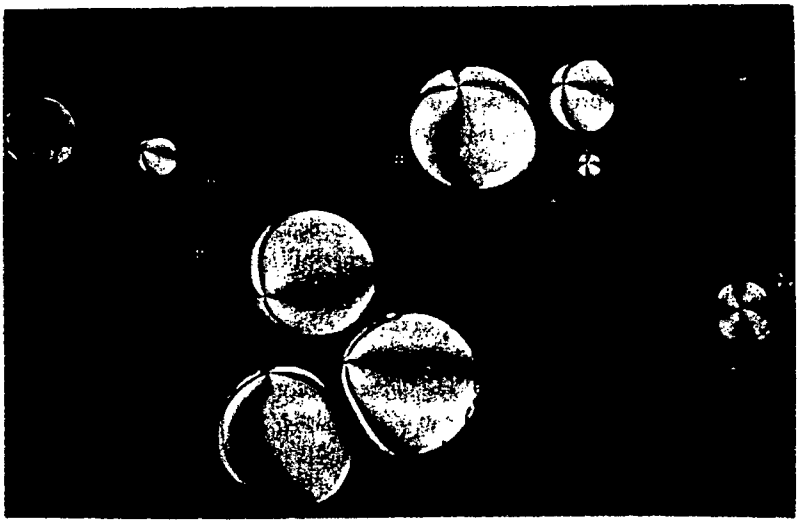

- *Schlieren texture*

Schlieren texture appears in the smectic C and B phases as well as in the nematic phase[27]. A typical schlieren texture of the nematic phase is shown in Figure 3.11. The black bands or schlieren occurring throughout the texture are regions of extinction and are often referred to as 'schlieren brushes.' These brushes meet at point singularities on the surface of the preparation. Two types of point singularities are observed for schlieren textures in nematic phases - one in which two brushes originate from the centre and the other in which four brushes originate from the centre (Figure 3.12). The schlieren texture of the nematic phase flashes when subjected to mechanical stress due to a change in the birefringence of the sample[27].

Figure 3.11 Schlieren texture of the nematic phase[23].

Figure 3.12 Representation of point singularities with (a) 4-schlieren brushes and (b) 2-schlieren brushes observed in schlieren liquid crystal textures[27].

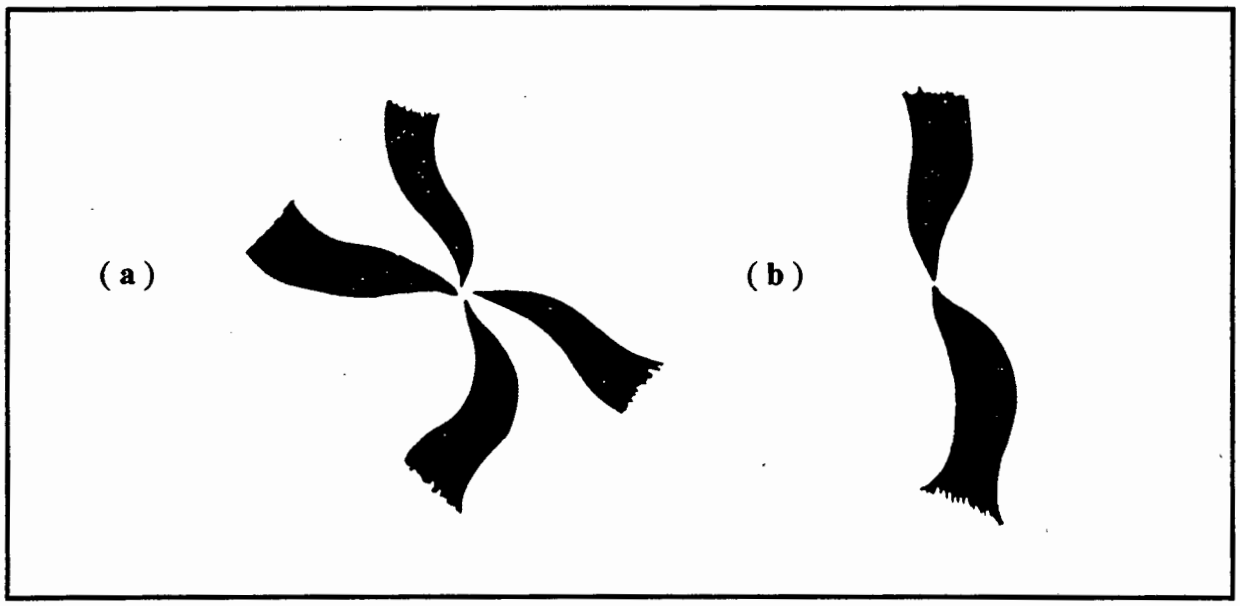

- *Marbled texture*

Nematic marbled textures consist of several areas with different molecular orientations[23]. The marbled texture, when viewed under a polarising microscope, exhibits sharp, straight bordered areas with a nearly constant interference colour resulting in a rock-like appearance[12,23].

3.1.6 Acyl Thioureas as Potential Liquid Crystals

The *N*-acylthiourea compounds **1** - **6**, shown in Figure 3.13, have a thin elongated molecular shape, a reasonably rigid core and easily polarisable groups which lends itself to exhibit liquid-crystalline behaviour. A prerequisite for the desired rod-like structure is the *intra*molecular hydrogen bond locking the potential chelate moiety into a planar six-membered ring (Chapter 2). In designing the compounds based on the structures in Figure 3.13, it was anticipated that the hydrogen-bonded six-membered *N*-acylthiourea chelate ring would behave like a phenyl ring. Hence, the overall arrangement of the molecules based on structures **2**, **4**, **5** and **6** in Figure 3.13 are reminiscent of the organic 4,4'-dialkylterphenyls, which have been reported to form smectic phases[30].

Figure 3.13 Schematic representation of the general structure of the compounds prepared in this work.

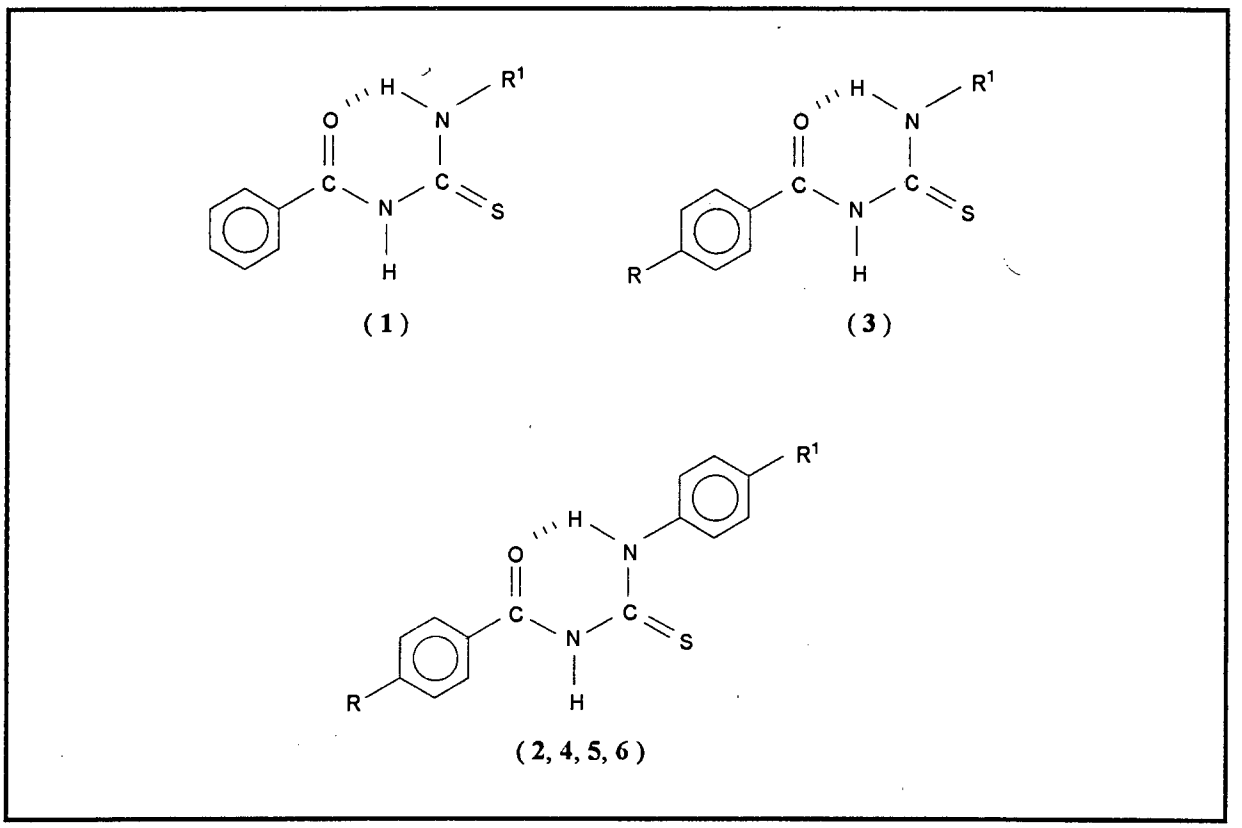

The main aim of this investigation was to synthesise *N*-acylthioureas with potential mesogenic properties and to determine the effect, if any, of the substituents R and R^1, on the liquid-crystalline behaviour of the compounds. R and R^1, (Figure 3.13), were varied as follows:

- compound **1** — R^1 = alkyl
- compound **2** R = alkyl, R^1 = alkyl
- compound **3** R = alkyloxy, R^1 = alkyl
- compound **4** R = alkyloxy, R^1 = alkyl
- compound **5** R = alkyl, R^1 = alkyloxy
- compound **6** R = alkyloxy, R^1 = alkyloxy

All liquid-crystalline compounds were characterised with respect to their mesogenic phases. Furthermore, the entropy and enthalpy involved with these phase transitions are addressed. Characterisation techniques include:

- optical microscopy - to identify the mesophase
- differential Scanning Calorimetry - to provide information regarding phase transition temperatures, entropy and enthalpy values
- crystallographic analysis - to ascertain the relative orientation of the molecules in the solid state.

3.2 Results and Discussion

All compounds were synthesised according to an earlier method reported by Douglass and Dains[31] and characterised by C, H and N elemental analysis and in some cases ^{1}H and ^{13}C NMR spectroscopy. Analytical data of all new compounds, (**1 - 6**), is recorded in the experimental section. Each compound was studied with the aid of a Reichert-Jung polarising optical microscope and Differential Scanning Calorimetry (DSC). All DSC experiments were performed by Ms R. Mohamed (Physical Chemistry Department, UCT) on a Perkin-Elmer - PE 7. All photographs of mesogenic phases were obtained with a Nikon Optiphot - POL.

Optical polarising microscopy, with a temperature-controlled hot-stage, was used to determine whether the compound under study was a liquid crystal and if so, the liquid-crystalline phase it formed. DSC studies were performed to confirm that the compound was mesogenic and to determine the temperatures at which the respective phase transitions occurred. Furthermore an estimation of the enthalpy and entropy associated with each phase transition was determined from the DSC thermograms. From the heat flow ($J.g^{-1}$) associated with each phase transition, the corresponding enthalpy and entropy were calculated accordingly to the following equations:

$$\Delta H\ (Jmol^{-1}) = \text{heat flow x molar mass}$$

$$\Delta S\ (JK^{-1}.mol^{-1}) = \Delta H \div T \qquad (T = \text{phase transition temperature in Kelvin})$$

It is interesting to note that the transition temperatures recorded with the aid of optical microscopy are often slightly different to the analogous transition temperatures observed in the DSC thermogram. This suggests that either different heating/cooling rates were used in the DSC and optical microscopy experiments or, alternatively, that the polarising optical microscope and DSC instrument were calibrated differently. However, a number of transition temperatures were similar whether recorded optically or observed from the DSC thermogram, which suggests that differences in analogous transition temperatures are due to different heating/cooling rates.

3.2.1 Characterisation of *N*-alkyl-*N'*-benzoylthiourea (1)

The short chained *N*-alkyl-*N'*-benzoylthioureas (*N*-butyl-, *N*-hexyl- and *N*-octyl-) discussed in Chapter 2, did not show any unusual melting behaviour. In continuing this series of compounds, the *N*-decyl- to *N*-octadecyl-*N'*-benzoylthioureas (**1d - 1h**) were synthesised to investigate whether the longer chained molecules exhibited mesogenic properties. The observed melting points are recorded in Table 3.1.

Figure 3.14 Schematic representation of *N*-alkyl-*N'*-benzoylthiourea, **1d - 1h**.

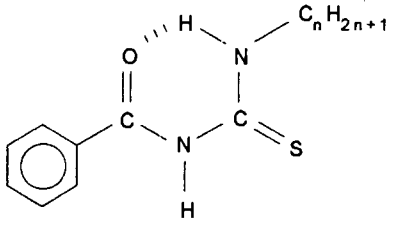

(1d) n = 10 **(1f)** n = 14 **(1h)** = 18

(1e) n = 12 **(1g)** n = 16

The melting point of compounds **1a - 1h** is relatively low. Interestingly, the melting point decreases, with an increase in alkyl chain length, to a minimum at n = 10, and then increases with an increase in alkyl chain length (Table 3.1 and Table 2.1 of Chapter 2). No mesogenic properties were observed with the aid of polarising optical microscopy. In other words, heating of these compounds resulted in a direct transition from the solid state into the isotropic liquid at a sharp melting point, and slow cooling of the isotropic liquid did not result in mesophase formation. The compounds generally remained in the isotropic liquid phase on cooling to room temperature.

Table 3.1 A comparison of the melting points (°C) for the non-mesogenic compounds *N*-alkyl-*N'*-benzoylthiourea (**1d - 1h**).

Compound	n	mp (°)
1d	10	32 - 34
1e	12	42 - 44
1f	14	51 - 52
1g	16	58 - 60
1h	18	65 - 67

The absence of mesogenic behaviour for **1a - 1h** was confirmed with the aid of DSC experiments. A typical DSC heating and cooling curve is shown in Figure 3.15. Only one endothermic peak, representing melting, was observed on heating the compounds and no endothermic peaks were evident on cooling the isotropic liquid. This confirms the optical observations that the compounds remain in a liquid state on cooling to room temperature.

Figure 3.15 DSC heating **(a)** and cooling **(b)** curves with scanning rate 5 °C.min^{-1} for *N*-octadecyl-*N'*-benzoylthiourea.

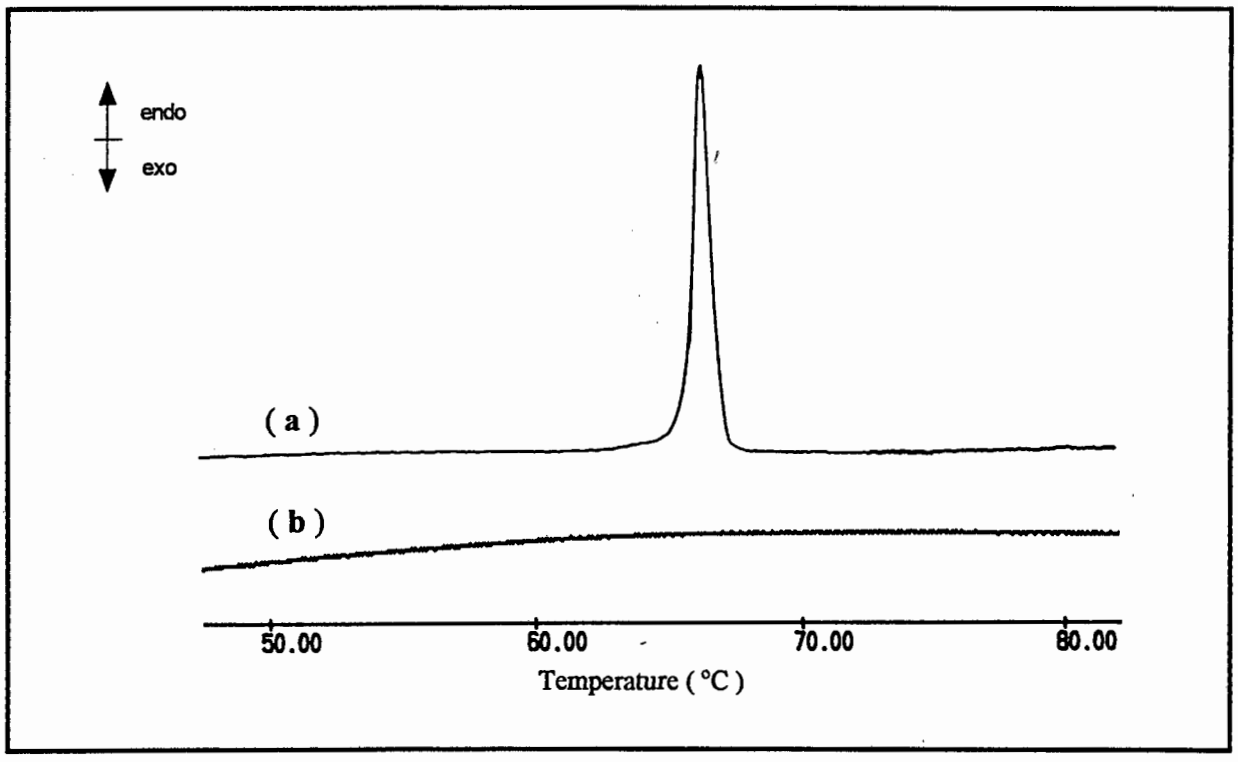

3.2.2 Characterisation of *N*-(*p*-alkyl)aniline-*N'*-(*p*-alkyl)benzoylthiourea (2)

In view of the fact that the *N*-alkyl-*N'*-benzoylthioureas did not show any mesogenic character, we decided to ascertain whether the inclusion of an additional rigid phenyl ring induced liquid-crystalline properties. It is well known that the majority of liquid-crystalline substances possess rigid, linear building blocks consisting of two or more aromatic rings[24]. Accordingly, the *N*-(*p*-alkyl)aniline-*N'*-(*p*-alkyl)benzoylthiourea compounds were synthesised.

The *N*-(*p*-alkyl)aniline-*N'*-(*p*-alkyl)benzoylthiourea compounds, (**2a, b, c** and **d**), (Figure 3.16), were synthesised where the alkyl chain of the benzyl group was systematically changed from butyl to heptyl respectively. The melting points of compounds **2a - 2d** are recorded in Table 3.2.

Figure 3.17 DSC heating (**a**) and cooling (**b**) curves with scanning rate 5 °C.min^{-1} for *N*-(*p*-dodecyl)aniline-*N'*-(*p*-heptyl)benzoylthiourea (**2d**).

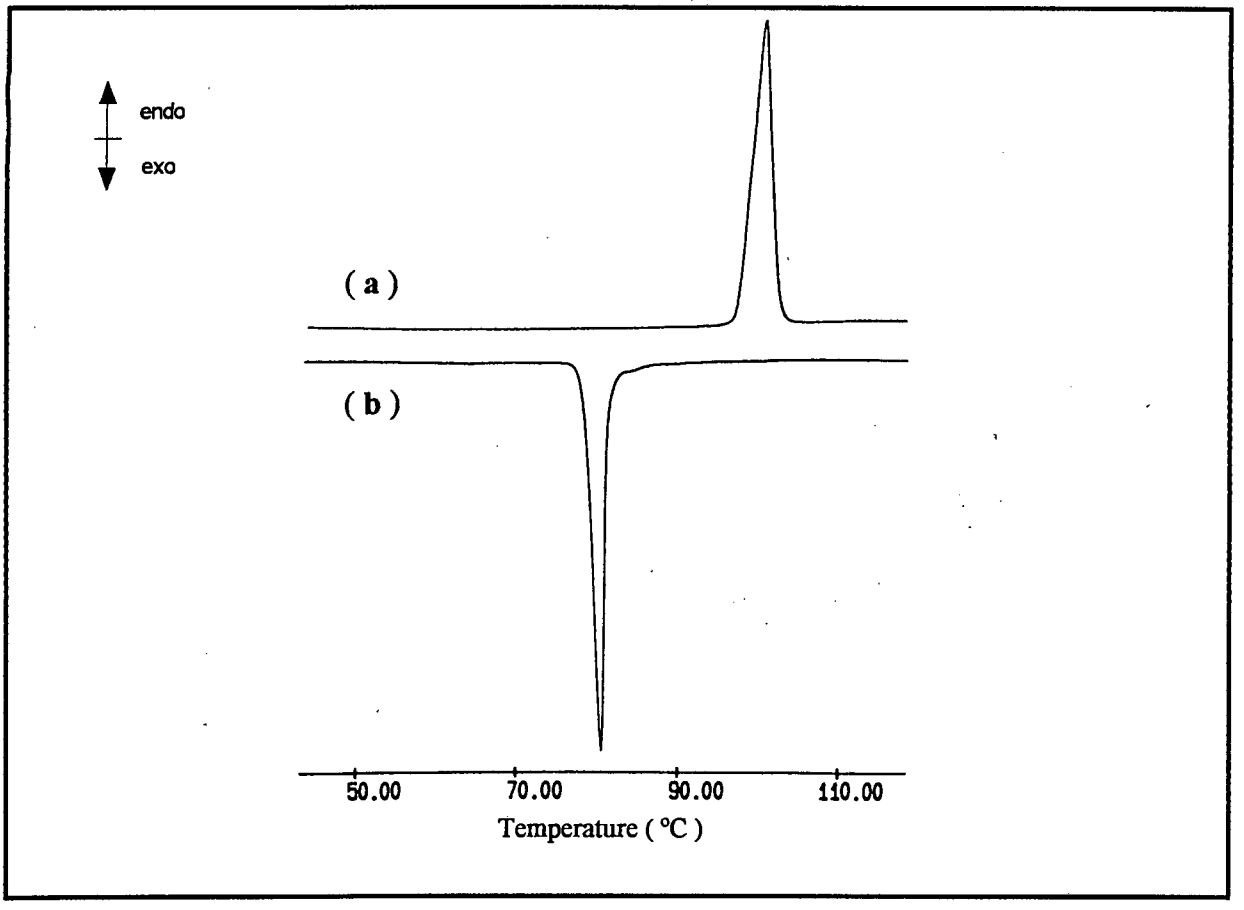

3.2.3 Characterisation of *N*-alkyl-*N'*-(*p*-alkyloxy)benzoylthiourea (3)

Due to a large number of calamitic liquid crystals possessing unbranched alkoxy chains[19], the general structure of the *N*-acylthioureas was modified to include an alkoxy chain. Accordingly, the *N*-alkyl-*N'*-(*p*-alkyloxy)benzoylthioureas (**3**), *N*-(*p*-alkyl)aniline-*N'*-(*p*-alkyloxy)benzoylthioureas (**4**), *N*-(*p*-alkyloxy)-aniline-*N'*-(*p*-alkyl)benzoylthioureas (**5**) and *N*-(*p*-alkyloxy)aniline-*N'*-(*p*-alkyloxy)benzoylthioureas (**6**) were prepared.

The *N*-octyl-*N'*-(*p*-dodecyloxy)benzoylthiourea (**3**) (Figure 3.18) was synthesised to determine to what extent the alkyloxybenzyl moiety influenced the potential liquid-crystalline behaviour of the compound. This compound is the alkyloxybenzyl derivative of the compounds described in section 3.2.1.

Table 3.2 A comparison of the melting points of the non-mesogenic compounds **2**.

Ligand	m	n	mp (°C)
2a	4	12	94 - 95
2b	5	12	89 - 92
2c	6	12	95 - 97
2d	7	12	101 - 102

Figure 3.16 Schematic representation of *N*-(*p*-alkyl)aniline-*N'*-(*p*-alkyl)benzoylthiourea, (**2**).

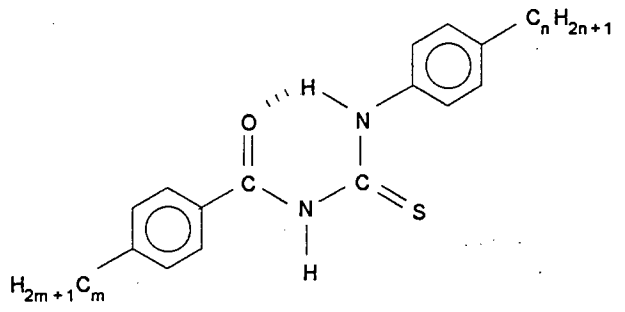

(**2**)

(a) n = 12, m = 4 **(c)** n = 12, m = 6

(b) n = 12, m = 5 **(d)** n = 12, m = 7

It is evident from Table 3.2 that an increase in the length of the alkylbenzyl chain, from butyl to heptyl, results in a linear increase in the melting point of the compounds. Polarising optical microscopy revealed that these compounds do not show any liquid-crystalline behaviour and this observation was further verified by the corresponding DSC thermograms. A typical DSC thermogram is given in Figure 3.17. On heating, the compounds melt directly from the solid state into an isotropic liquid. Slow cooling of the isotropic liquid results in crystallisation to the solid material. A single endothermic peak, representing melting of the sample, and a single exothermic peak, corresponding to crystallisation of the melt, is evident from the DSC thermogram.

Giroud-Godquin[32] *et al* and Ohta[33] *et al* synthesised 1,3-di(*p*-alkylphenyl)propan-1,3-dione of varying alkyl length and observed smectic liquid-crystalline behaviour. It was therefore surprising and rather disappointing that the series of *N*-(*p*-dodecyl)aniline-*N'*-(*p*-alkyl)benzoylthiourea compounds, (**2a - 2d**), did not show any mesogenic properties.

Figure 3.17 DSC heating (**a**) and cooling (**b**) curves with scanning rate 5 °C.min^{-1} for *N*-(*p*-dodecyl)aniline-*N'*-(*p*-heptyl)benzoylthiourea (**2d**).

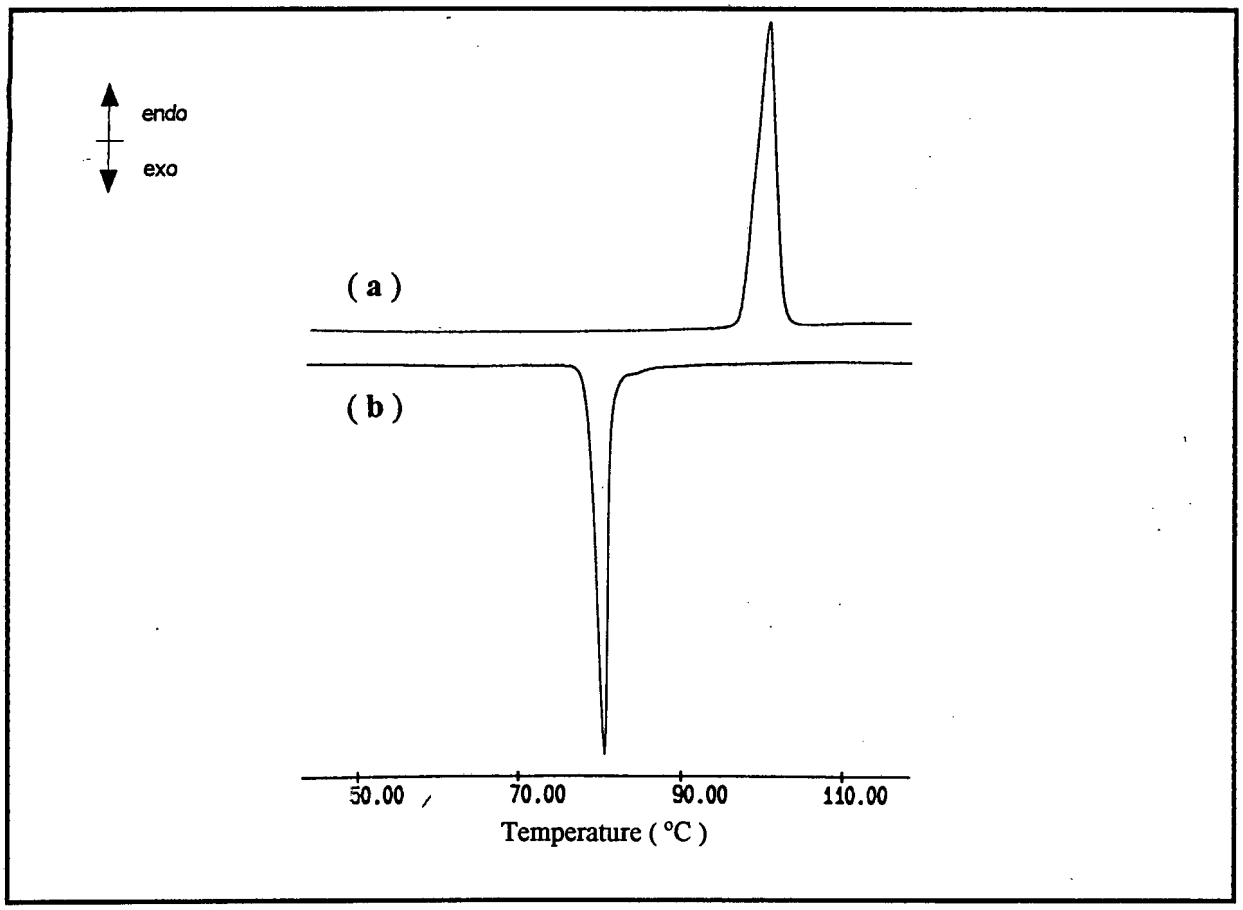

3.2.3 Characterisation of *N*-alkyl-*N'*-(*p*-alkyloxy)benzoylthiourea (3)

Due to a large number of calamitic liquid crystals possessing unbranched alkoxy chains[19], the general structure of the *N*-acylthioureas was modified to include an alkoxy chain. Accordingly, the *N*-alkyl-*N'*-(*p*-alkyloxy)benzoylthioureas (**3**), *N*-(*p*-alkyl)aniline-*N'*-(*p*-alkyloxy)benzoylthioureas (**4**), *N*-(*p*-alkyloxy)-aniline-*N'*-(*p*-alkyl)benzoylthioureas (**5**) and *N*-(*p*-alkyloxy)aniline-*N'*-(*p*-alkyloxy)benzoylthioureas (**6**) were prepared.

The *N*-octyl-*N'*-(*p*-dodecyloxy)benzoylthiourea (**3**) (Figure 3.18) was synthesised to determine to what extent the alkyloxybenzyl moiety influenced the potential liquid-crystalline behaviour of the compound. This compound is the alkyloxybenzyl derivative of the compounds described in section 3.2.1.

Figure 3.18 Schematic representation of *N*-alkyl-*N'*-(*p*-alkyloxy)benzoylthiourea.

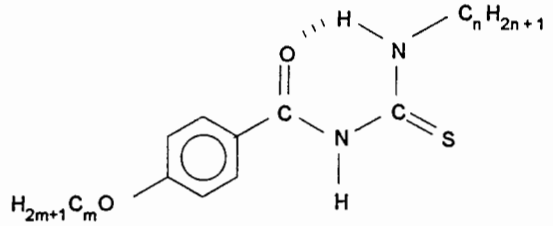

(3)

m = 12, n = 8

No mesogenic behaviour was observed for compound (**3**) with the aid of polarising optical microscopy, on either heating the crystalline solid or slow cooling of the isotropic liquid. This result suggests that firstly, the addition of an alkyloxybenzyl moiety to the general structure of compound **1** does not induce liquid-crystalline behaviour, and secondly, that the absence of mesogenic properties suggests that the benzyl and hydrogen-bonded six-membered ring do not lend sufficient rigidity to the centre core of the compound. It may thus be reasonable to anticipate that a second aromatic group, introduced to increase the rigidity of the centre core, in addition to an alkyloxy chain, could induce liquid-crystalline properties. Accordingly, a series of *N*-(*p*-alkyl)aniline-*N'*-(*p*-alkyloxy)benzoylthioureas were synthesised.

3.2.4 Characterisation of *N*-(*p*-alkyl)aniline-*N'*-(*p*-alkyloxy)benzoylthiourea (4)

It is noteworthy that in 1984, Ohta[33] *et al* reported the synthesis and characterisation of the octyl and octyloxy derivatives of bis(*p*-alkylbenzoyl)methane and found that these compounds showed a smectic liquid-crystalline phase. It may therefore be reasonable to anticipate that derivatives of *N*-(*p*-alkyl)aniline-*N'*-(*p*-alkyloxy)benzoylthiourea could exhibit mesogenic properties. Accordingly, compounds **4a** - **4f** were prepared and each of these compounds examined for liquid-crystalline behaviour with the aid of polarising optical microscopy and DSC.

Figure 3.19 Schematic representation of the series of *N*-(*p*-alkyl)aniline-*N'*-(*p*-alkyloxy)benzoylthioureas prepared in this work.

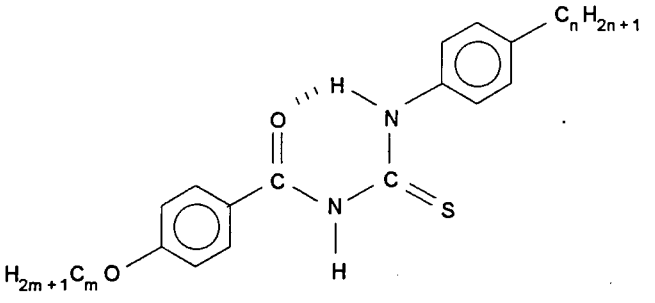

(4a) m = 7, n = 6 **(4c)** m = 12, n = 6 **(4e)** m = 12, n = 10

(4b) m = 7, n = 12 **(4d)** m = 12, n = 8 **(4f)** m = 12, n = 12

Polarising optical microscopy of the *N*-(*p*-alkyl)aniline-*N'*-(*p*-alkyloxy)benzoylthioureas

Compound **4a** failed to exhibit mesogenic behaviour on either heating the solid or cooling the isotropic liquid. The compound was transformed from the solid state directly to the isotropic liquid on heating to 119 °C. Cooling to 102 °C resulted in crystallisation of the isotropic liquid. DSC studies confirmed the optical observations that **4a** shows no liquid-crystalline behaviour, i.e. the DSC plot shows, on heating the solid material, one endothermic peak corresponding to the melting point and, on cooling the isotropic liquid, one exothermic peak representing crystallisation to the solid material. It is noteworthy that a second exothermic peak, at a temperature below that of solidification, (33.8 °C), is observed in the DSC cooling curve. This is not an isolated phenomenon as similar exotherms are observed in the DSC cooling curves of other compounds prepared in this work on liquid crystals. These exothermic peaks could represent solid-solid transitions.

N-(*p*-dodecyl)aniline-*N'*-(*p*-heptyloxy)benzoylthiourea (**4b**) does not exhibit mesogenic behaviour on heating the crystalline material. The compound melts directly from the solid state to the isotropic liquid at a sharp melting point. However, cooling of the isotropic liquid gives rise to a distinct liquid-crystalline phase; hence **4b** displays a monotropic liquid-crystalline phase. A monotropic mesophase is a supercooled state that is thermodynamically unstable[34]. The clearing point of the mesophase of **4b** is at a lower temperature than the observed melting point, which is in accordance with that observed for monotropic liquid crystals[12].

The mesophase formed by **4b** was identified as the *smectic A* phase by means of polarising microscopy . On cooling the isotropic liquid of **4b** to 106 °C, the mesogenic phase separates out in the form of *bâtonnets*. The bâtonnets are elongated, irregularly shaped birefringent bodies which differ widely in shape and are only rarely cylindrical (**photograph 1**). Their surfaces are curved and they are often symmetrical about their long axes. As the temperature falls the bâtonnets crowd together and finally coalesce to form the *focal-conic fan texture* (**photograph 2**). The full transition, from the appearance of the bâtonnets to the formation of the focal-conic fan texture, occurs within a 1 °C drop in temperature. The mesophase is fairly viscous and the focal-conic texture contains optical discontinuities that are visible in ordinary light as well as with crossed polarisers. The backs of the fans are grained which is due to the occurrence of parabolic effects[27]. The displacement of the cover slip of a focal-conic preparation results in the formation of birefringent bands which resemble oily streaks or smears. Gray[28] has found that these are simply chains of small focal-conic groups. Further cooling to 104 °C allows for crystallisation of the mesophase to a solid material.

The mesophase was identified as a smectic A phase due to:

- the viscosity of the phase and
- the formation of bâtonnets which coalesce to form a grained focal-conic fan texture[14].

The remaining *N*-(*p*-alkyl)aniline-*N'*-(*p*-alkyloxy)benzoylthiourea compounds, **4c - 4f,** show monotropic liquid-crystalline behaviour on cooling of the isotropic liquid. The mesophases are formed in a similar manner to that of **4b** described above. Cooling of the isotropic liquid allows for the formation of bâtonnets which coalesce to form a grained focal-conic fan texture. The liquid crystal phase of these compounds was therefore also identified as the *smectic A* phase.

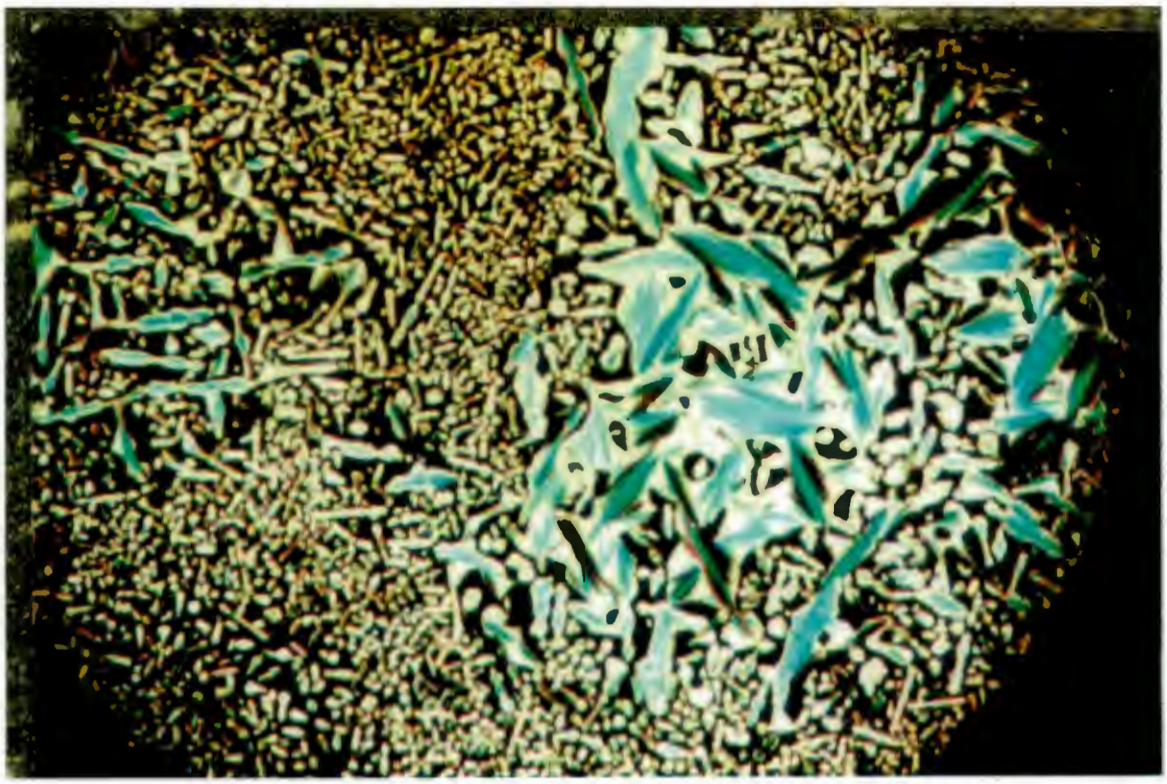

Photograph 1 Formation of bâtonnets (top left-hand side) of the smectic A phase of *N*-(*p*-dodecyl)aniline-*N'*-(*p*-heptyloxy)benzoylthiourea. Focal-conic fan texture present in centre of photograph.

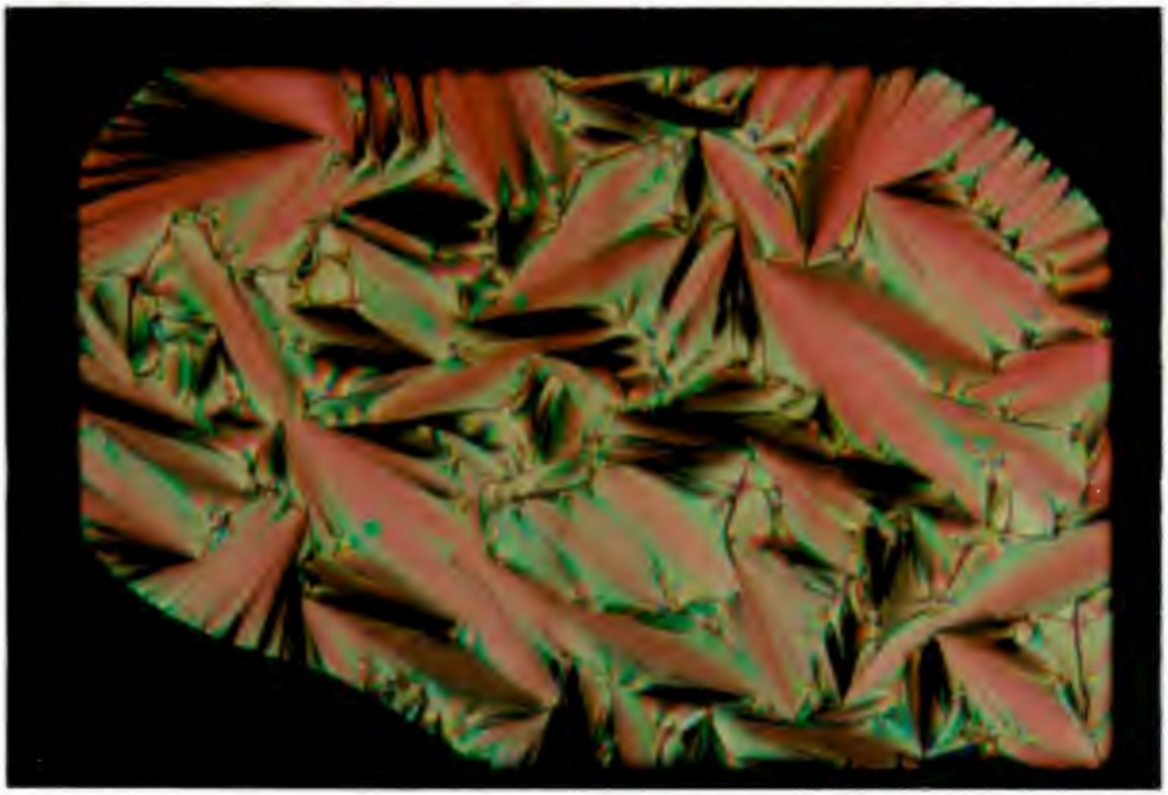

Photograph 2 The focal-conic fan texture of the smectic A phase of *N*-(*p*-dodecyl)aniline-*N'*-(*p*-heptyloxy)benzoylthiourea.

Differential scanning calorimetry (DSC) of *N*-(*p*-alkyl)aniline-*N'*-(*p*-alkyloxy)benzoylthiourea

The enthalpy and entropy changes estimated from the DSC thermograms are recorded in Table 3.3. A typical DSC heating and cooling thermogram of *N*-(*p*-dodecyl)aniline-*N'*-(*p*-heptyloxy)benzoylthiourea is given in Figure 3.20. The heating plot indicates a single endotherm at 118.9 °C. Cooling the isotropic liquid produces one small and two large exothermic peaks at 106.7, 104.5 and 103.0 °C respectively. The small exothermic peak at 106.7 °C corresponds to the formation of the S_A phase. The enthalpy associated with this peak, 0.8 kJ.mol^{-1}, is significantly smaller than is expected for an I - S_A phase transition. Goodby and Gray[27] state that the enthalpy associated with a first order transition from the smectic A phase to the nematic or isotropic phase is usually about 4 - 6 kJ.mol^{-1}. The smaller enthalpy change associated with the I - S_A transition of **4b** suggests that this is a second-order transition since it is much weaker in magnitude. The large exothermic peak at 104.5°C is at a similar temperature to the Smectic A - crystalline transition observed microscopically. Accordingly, this exotherm is assigned to the S_A - C transition. The exothermic peak at 103.0 °C is considered to be due to a solid-solid transition. These observations are schematically summarised in Figure 3.21.

Figure 3.21 Phase changes and transition temperatures (°C) observed from the DSC curves of the monotropic liquid crystal, *N*-(*p*-dodecyl)aniline-*N'*-(*p*-heptyloxy)benzoylthiourea (**4b**).

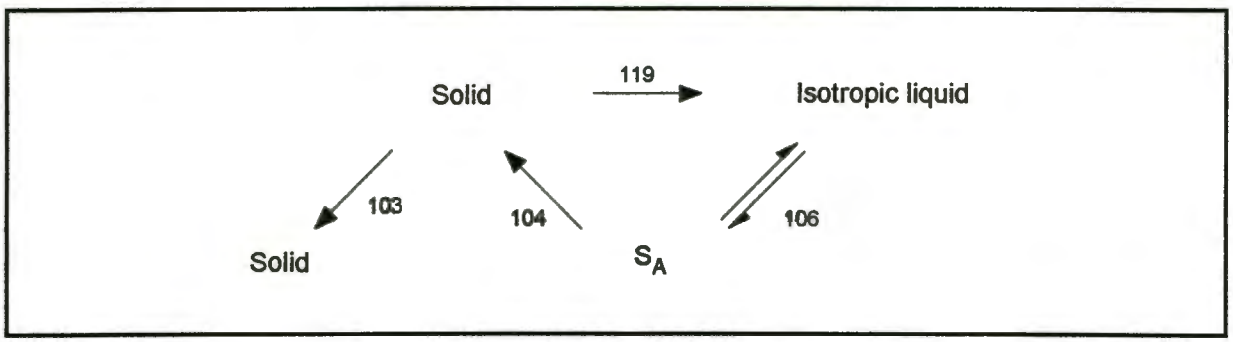

DSC thermograms of compounds **4c - 4f** confirmed the existence of a monotropic liquid crystal phase which in every case has a clearing temperature below the melting point temperature. Furthermore, the DSC curves of **4c - 4f** all exhibited exotherms at temperatures below the crystallisation temperature, which are thought to represent solid-solid transitions.

Figure 3.20 The DSC (**a**) heating and (**b**) cooling thermogram, at 10 °C.min^{-1}, of *N*-(*p*-dodecyl)aniline-*N'*-(*p*-heptyloxy)benzoylthiourea (**4b**).

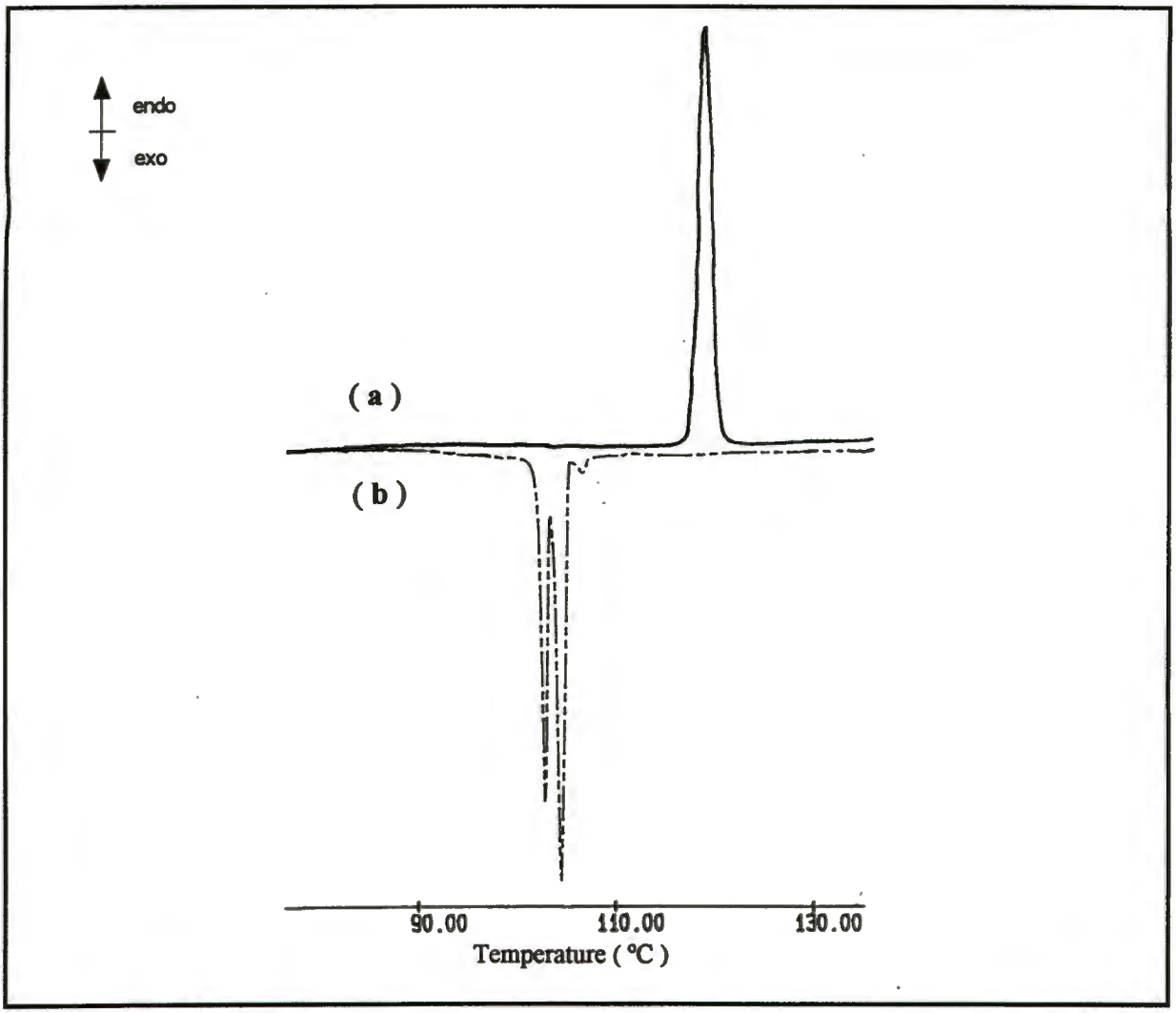

The enthalpy associated with the I - S_A transitions of **4c - 4f**, in the range 7.5 to 8.7 kJ.mol^{-1}, is slightly higher than the values recorded by Gray[27] of 4 - 6 kJ.mol^{-}. The I - S_A transitions of **4c - 4f** all seem to be first-order in nature as indicated by their large enthalpy changes. These isotropic - smectic A transition energies remain essentially constant (average 7.9 kJ.mol^{-1}), which implies that the forces involved in maintaining a constant orientation of the molecules do not depend on the alkyl chain length for these long chained *N*-(*p*-alkyl)aniline-*N'*-(*p*-alkoxy)benzoylthioureas[35].

The reason these enthalpy changes are large as opposed to the small enthalpy change observed for **4b**, is not currently understood. Compound **4b** and **4c** have a similar total number of carbon atoms in their side chains, i.e. 19 and 18 respectively which suggests that the chain length cannot account for the difference in enthalpy change in this case. However, the fact that **4b** has an odd number of carbon atoms in the alkyloxybenzyl

chain whereas **4c - 4f** all have even numbered alkyl and alkyloxy carbon chains may in some way influence the enthalpy of the I - S_A transition.

It is evident for compounds **4c - 4f** that the clearing temperature of the smectics is nearly constant (Table 3.3). This is in accordance with Kelker and Hatz[12] who reported that the clearing temperature of smectics in a homologous series generally rises initially with increasing chain length. It reaches a maximum at moderate chain length, then decreases slightly, and finally acquires a nearly constant value in very long chains.

The magnitude of the enthalpy change associated with the S_A - C transition decreases with an increase in chain length, i.e. enthalpy of **4c** > **4d** > **4e** > **4f**. Data from additional homologues is obviously required to validate this trend. It is not obvious why the solid - smectic A transition energy should alter much with chain length. If another type of change occurred simultaneously in the shorter chained compounds, e.g. onset of chain rotation, then this may explain the observed results[35].

The melting points of the compounds, **4a - 4f**, are all within a few degrees Celsius, i.e. they range from 111 to 118 °C (experimental section). The observed melting point of *N*-(*p*-dodecyl)aniline-*N'*-(*p*-heptyloxy)benzoylthiourea **4b**, 115 - 116 °C, is approximately 15 °C higher than that of the corresponding alkyl derivative, *N*-(*p*-dodecyl)aniline-*N'*-(*p*-heptyl)benzoylthiourea, **2d**. This increase in the melting point of the alkyloxy compound compared to the alkyl compound may possibly be attributed to the greater conjugation provided by the lone pairs of electrons on the oxygen atom[3], as shown in Figure 3.22. The addition of an alkyloxy chain, in addition to the highly polarisable aromatic rings, increases the overall polarisability of the compound and tends to stabilise the crystal phase and any potential mesophases. However, even though this seems to be a simple explanation of the behaviour of the alkyloxy derivative, due caution must be taken before drawing conclusions based on it[36].

Figure 3.22 Schematic representation of the mesomeric forms of *N*-(*p*-alkyl)aniline-*N'*-(*p*-alkyloxy)benzoylthiourea.

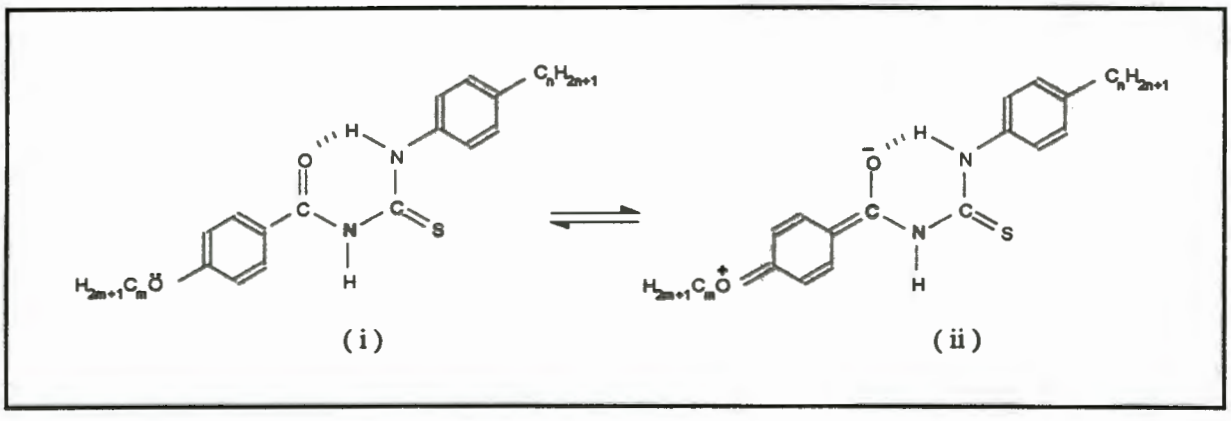

Table 3.3 Transition temperatures, enthalpies and entropies of **4a - 4f** calculated from the DSC cooling curves.

Compound	m	n	transition	T (°C)	ΔH	ΔS
4a	7	6	I - C	104.5	40.7	107.7
			C - C	33.8	2.6	8.4
4b	7	12	I - S_A*	106.7	0.8	2.1
			S_A - C	104.5	23.2	61.4
			C - C	103.0	13.2	2.1
4c	12	6	I - S_A*	110.6	7.8	20.3
			S_A - C	97.3	33.4	90.2
			C - C	54.0	2.0	6.2
			C - C	34.7	9.6	31.1
4d	12	8	I - S_A*	110.8	7.9	20.7
			S_A - C	101.3	30.7	81.9
			C - C	98.0	2.4	6.4
			C - C	35.4	14.2	45.9
4e	12	10	I - S_A*	109.9	7.5	19.6
			S_A - C	97.6	27.7	74.7
			C - C	93.0	6.9	18.8
4f †	12	12	I - S_A*	110.0	8.6	23.0
			S_A - C	104.3	21.7	57.3
			C - C	103.0	0.7	1.8
			C - C	51.1	2.5	7.7

Transition temperatures and enthalpy values are obtained from DSC plots at a cooling rate of 10.0 °C.min^{-1} unless otherwise specified

† *Transition temperatures and enthalpy values are obtained from the DSC plot at a cooling rate of 5.0 °C.min^{-1}*

* *Monotropic transition*

ΔH in kJ.mol^{-1} and ΔS in J.K^{-1}.mol^{-1}

3.2.5 Characterisation of *N*-(*p*-alkyloxy)aniline-*N'*-(*p*-alkyl)benzoylthiourea (5)

Compounds **5a** and **5b**, Figure 3.23, were synthesised to ascertain whether an alkyloxy chain attached to the aniline ring, as opposed to the alkyloxy chain attached to the benzyl moiety, had any effect on the liquid crystal properties, i.e. does the position of the alkyloxy chain in the molecule influence the liquid crystal properties?

Figure 3.23 Schematic representation of *N*-(*p*-alkyloxy)aniline-*N'*-(*p*-alkyl)benzoylthiourea.

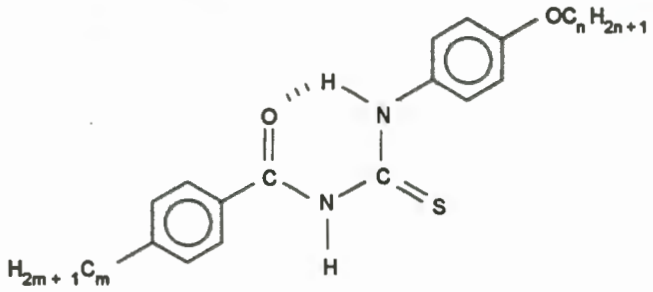

(5a) m = 7, n = 5

(5b) m = 7, n = 6

Polarising optical microscopy of *N*-(*p*-alkyloxy)aniline-*N'*-(*p*-alkyl)benzoylthiourea

Polarising optical microscopic studies revealed that compounds *N*-(*p*-pentyloxy)aniline-*N'*-(*p*-heptyl)benzoyl-thiourea and *N*-(*p*-hexyloxy)aniline-*N'*-(*p*-heptyl)benzoylthiourea are liquid crystals and show monotropic mesogenic behaviour on cooling of the isotropic liquid. Heating the crystalline material of **5a** results in a direct transition from the solid state into the isotropic liquid at 109 °C. Slow cooling of the isotropic liquid to 84 °C allows for the formation of very small *nematic droplets* in the isotropic liquid (**photograph 3**). These droplets rapidly coalesce to form areas of schlieren texture surrounded by homeotropic regions (**photograph 4**). Further coalescence of the nematic droplets results in the formation of a *schlieren texture* (**photograph 5**). Brightly coloured droplets containing black four-brushed schlieren are evident on the periphery of the preparation (**photograph 6**). As the temperature is further lowered, the coloured droplets form white droplets with black crosses of extinction (**photograph 7**). The phase is stable over a 3 °C drop in temperature to 81 °C, where crystallisation to the solid material occurs.

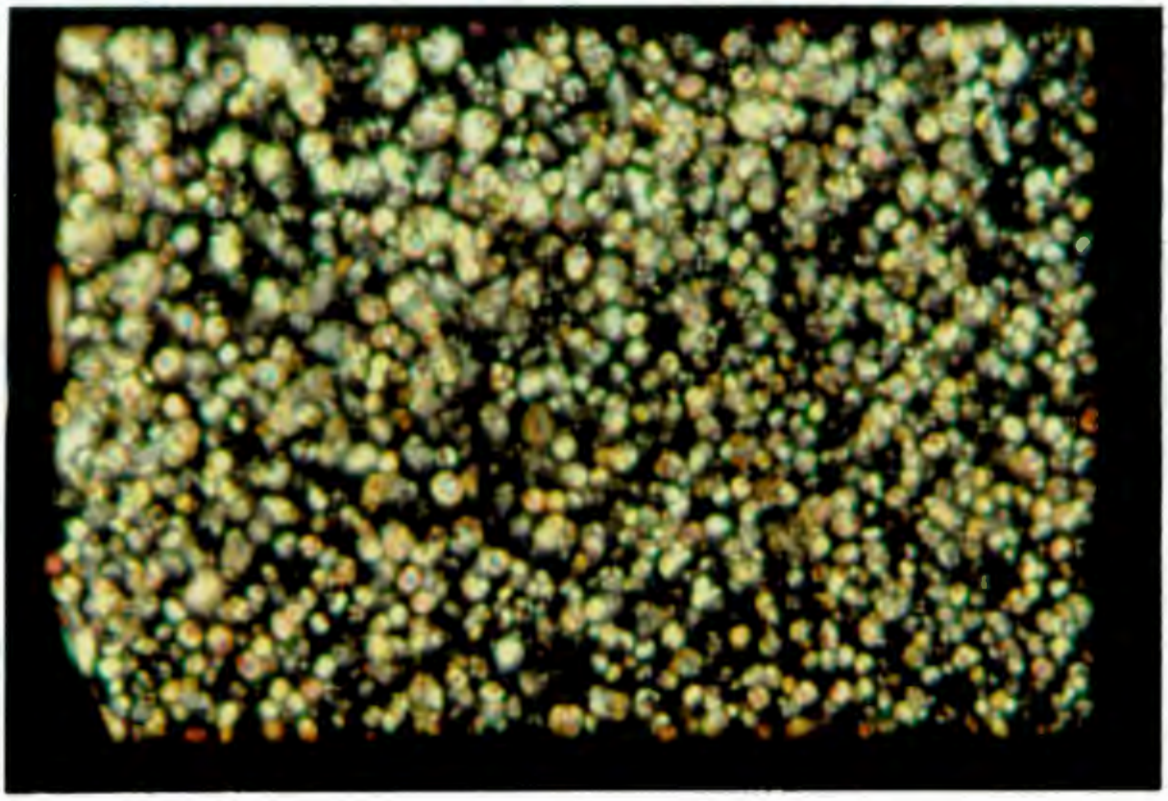

Photograph 3 Cooling of the isotropic liquid of *N*-(*p*-pentyloxy)aniline-*N'*-(*p*-heptyl)benzoylthiourea, **5a**, allows for the formation of numerous, small nematic droplets.

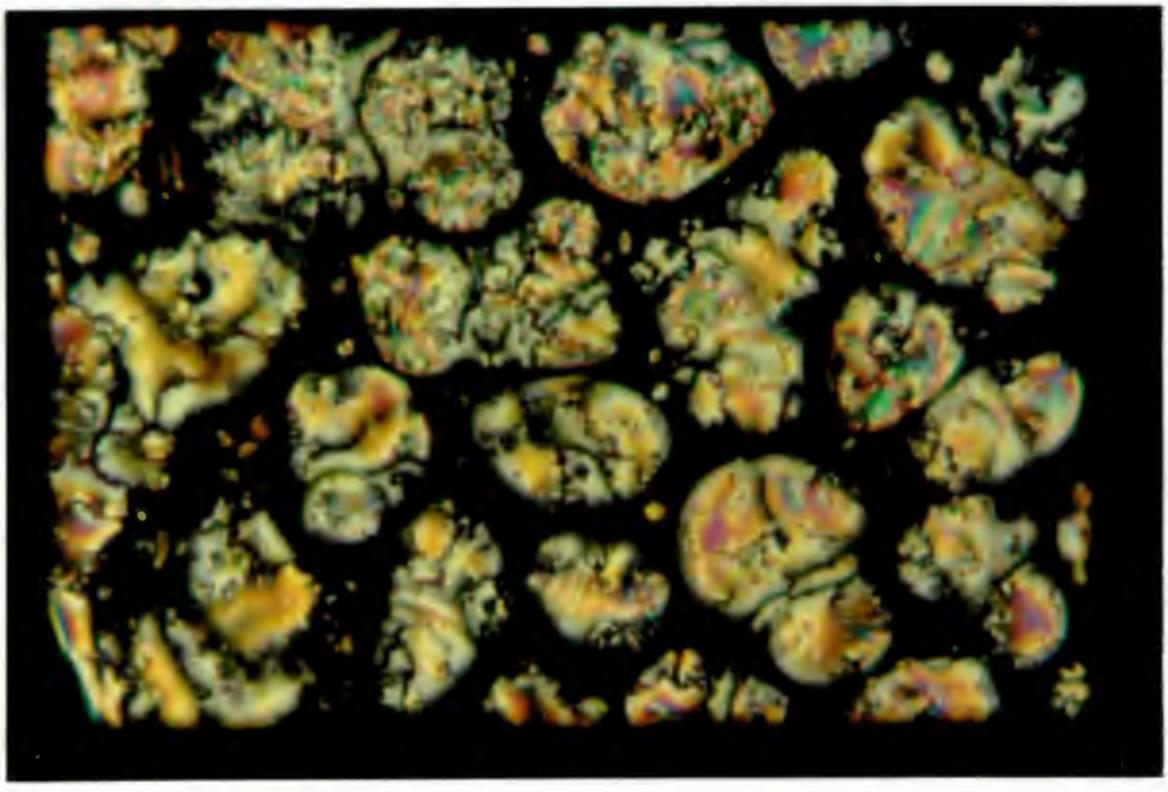

Photograph 4 Coalescence of nematic droplets of *N*-(*p*-pentyloxy)aniline-*N'*-(*p*-heptyl)benzoylthiourea, **5a**, results in schlieren texture and homeotropic regions.

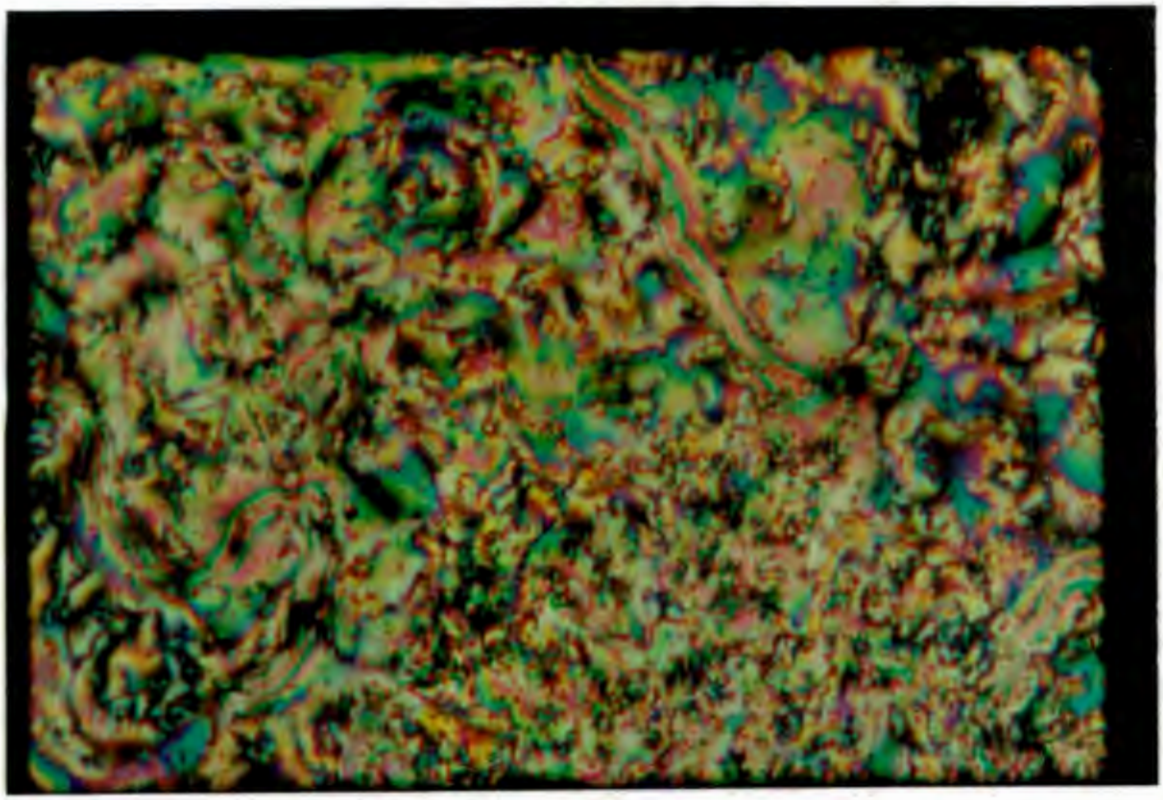

Photograph 5 Further coalescence of *N*-(*p*-pentyloxy)aniline-*N'*-(*p*-heptyl)benzoylthiourea allows for formation of schlieren texture.

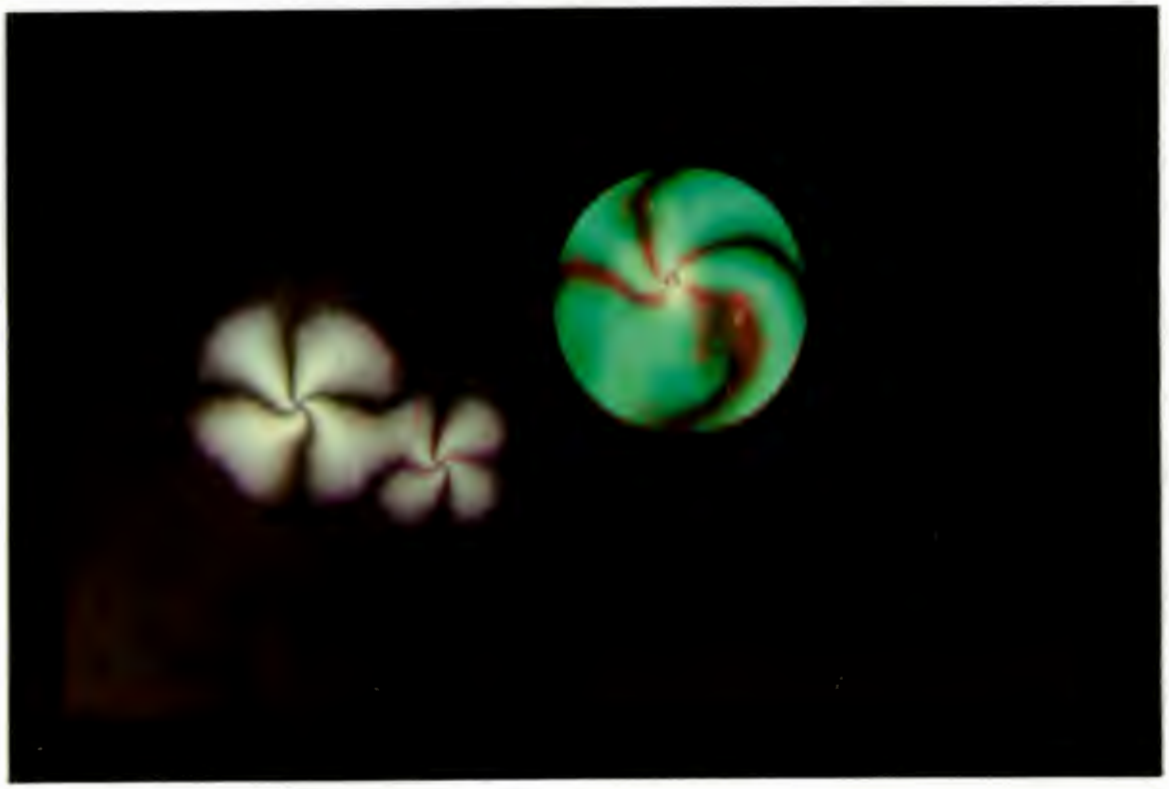

Photograph 6 Brightly coloured droplets of *N*-(*p*-pentyloxy)aniline-*N'*-(*p*-heptyl)benzoylthiourea showing crosses of extinction.

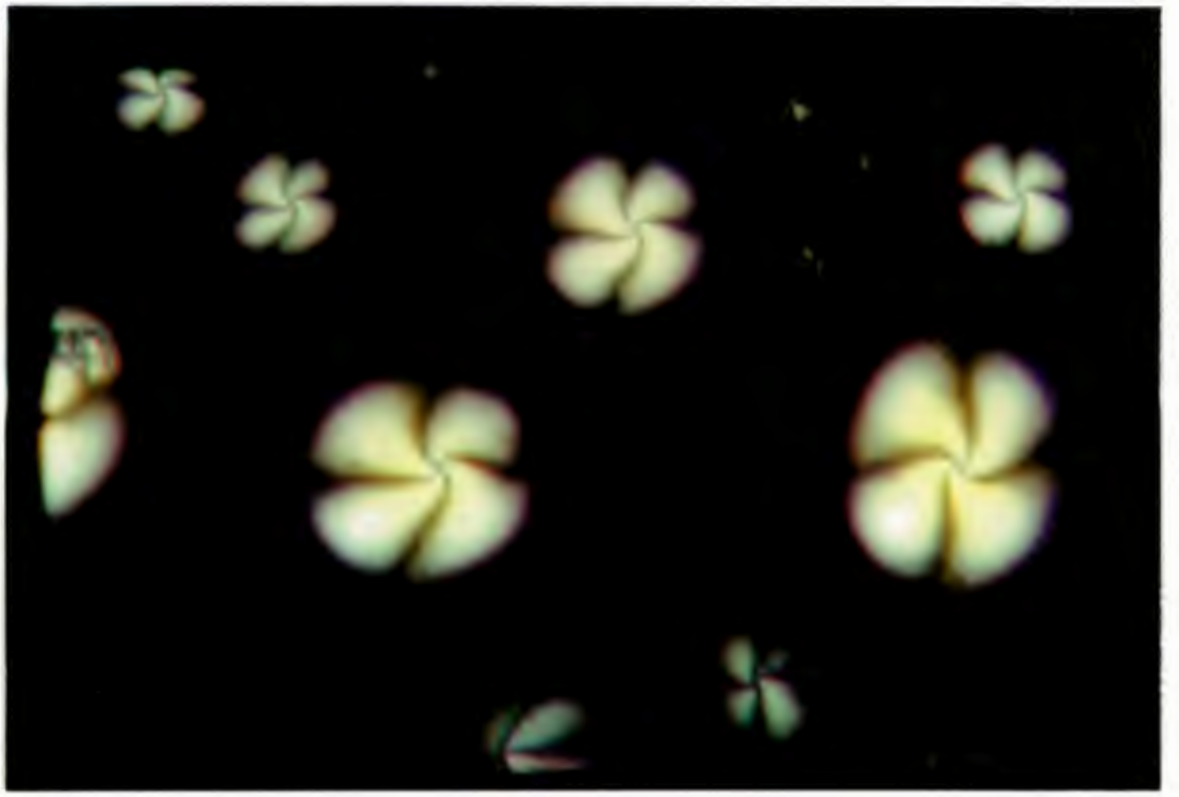

Photograph 7 White droplets of *N*-(*p*-pentyloxy)aniline-*N'*-(*p*-heptyl)benzoylthiourea exhibiting black crosses of extinction.

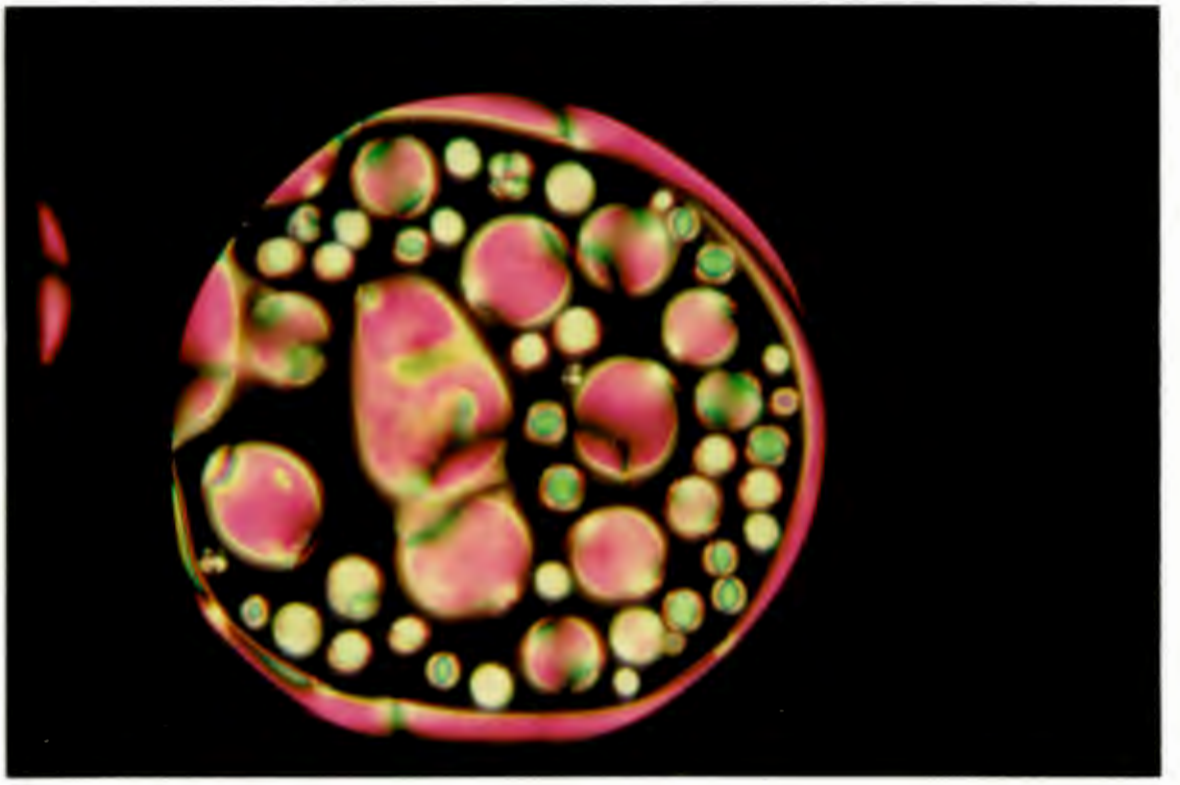

Photograph 8 Nematic droplets of *N*-(*p*-hexyloxy)aniline-*N'*-(*p*-heptyl)benzoylthiourea, **5b**, formed on cooling the isotropic liquid.

Heating of compound **5b** to 109 °C results in a direct transformation from the solid phase to the isotropic liquid. However, cooling of the isotropic liquid from 109 °C to 89 °C allows for the separation of *nematic droplets* from the isotropic liquid (**photograph 8**). Each of these tiny, spherical droplets show a cross with arms and when the preparation is rotated, the cross does not move. Thus the drop must correspond to a true sphere which is suspended in the bulk of the mesophase and which is unattached to the surfaces[25]. **Photographs 3** and **8** illustrate how different the same mesogenic phase may appear to the investigator. The nematic droplets rapidly coalesce to give a typical *schlieren texture*. The schlieren texture shows a high degree of fluidity, i.e. a high degree of Brownian motion, and it flashes when subjected to mechanical stress. Under certain conditions mechanical stress results in a *thread-like texture* in some areas of the preparation. As the temperature is lowered to 88 °C some of the schlieren texture becomes *homeotropic*; it appears extinct through crossed polarisers. The mesophase crystallises at 87 °C.

Optical microscopy suggests that the mesogenic phase formed upon cooling of the isotropic liquids of compounds **5a** and **5b** is a *nematic* phase. The liquid-crystalline phase was identified as nematic on the basis of:

- the formation of nematic drops upon cooling of the isotropic liquid
- the coalescence of the nematic droplets to form the schlieren texture showing two- and four-brushed schlieren
- the fluidity of the phase.

It is difficult and unreliable to draw conclusions from only two compounds, but the mesogenic studies of these two compounds indicate that **5b**, incorporating an uneven number of carbon atoms in its two alkyl chains, has a more stable mesophase than **5a** which possesses an even number of carbon atoms in its two alkyl chains. However, to substantiate this speculation, additional data from other compounds in the series must be taken into consideration.

Differential scanning calorimetry of *N*-(*p*-alkyloxy)aniline-*N'*-(*p*-alkyl)benzoylthiourea

Transition temperatures and thermodynamic data for **5a** and **5b** are summarised in Table 3.4. The DSC thermogram of **5a** (Figure 3.24) confirms the liquid-crystalline behaviour observed optically. The thermogram shows three exothermic peaks at 84.3, 82.5 °C and 79.4 °C, on cooling of the isotropic liquid. The large exotherm at 82.5 °C represents crystallisation, whereas the small exotherm at 84.3 °C is assigned to a monotropic mesophase. This mesophase was identified as the nematic phase with the aid of optical polarising microscopy. The phase identification is substantiated by the ΔH value of 1.3 $kJ.mol^{-1}$ estimated from the DSC thermogram. The magnitude of the N - I transition enthalpy is in the known range[37] and

agrees with those values reported by Hoshino[38] *et al* of 1.1 - 1.9 kJ.mol^{-1}. The exotherm at 79.4 °C may be due to a solid-solid transition.

Figure 3.24 DSC (**a**) heating and (**b**) cooling thermogram, at a scanning rate of 5 °C.min^{-1}, of *N*-(*p*-pentyloxy)aniline-*N'*-(*p*-heptyl)benzoylthiourea, (**5a**)

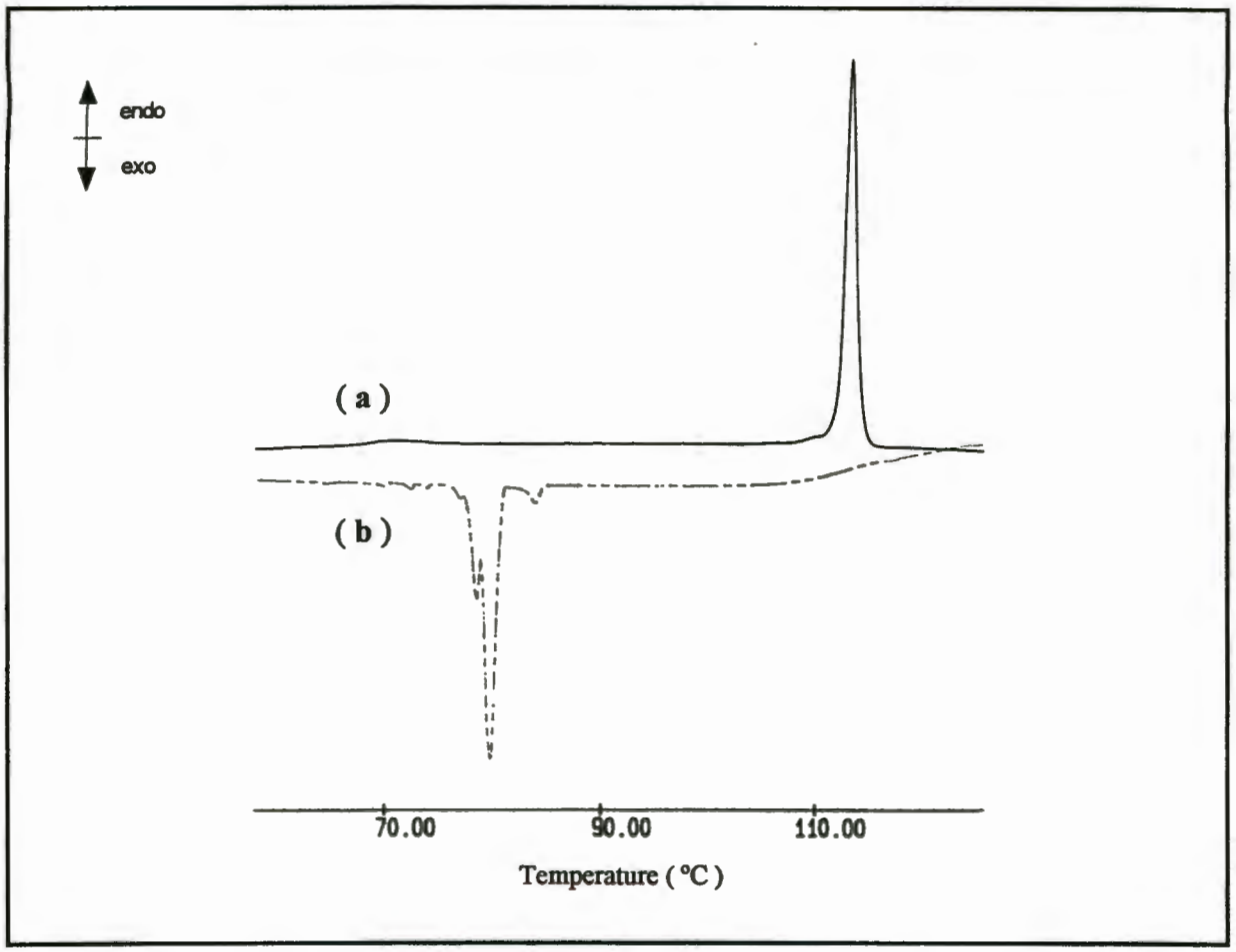

Similarly, the DSC plot of **5b** substantiates the proposed existence of a monotropic nematic phase. A very small exothermic peak at 90.0 °C and a large exotherm at 88.9 °C is evident in the thermogram on cooling the isotropic liquid. Crystallisation of the solid material is represented by the large exothermic peak, whereas the small peak is due to mesophase formation. The enthalpy associated with the small exotherm is 0.8 kJ.mol^{-1} which is slightly less than that observed by Hoshino[38] *et al* for a I - N transition.

Table 3.4 Transition temperatures, mesophases and thermodynamic data for **5a** and **5b**.

Compound	m	n	Transition	T (°C)	ΔH	ΔS
5a	7	5	I - N*	84.3	1.3	3.6
			N - C	82.5	25.5	71.7
			C - C	79.4	11.1	31.7
5b	7	6	I - N*	90.0	0.8	2.3
			N - C	88.9	44.4	122.7

* *Monotropic transition*

Transition temperatures and enthalpy values obtained from DSC plots at a cooling rate of 5 °C.min^{-1} for ***5a*** *and 2 °C.min^{-1} for* ***5b****.*

ΔH in kJ.mol^{-1} and ΔS in J.K^{-1}.mol^{-1}

3.2.6 *N*-(*p*-alkyloxy)aniline-*N'*-(*p*-alkyloxy)benzoylthiourea, (6)

In view of the fact that *N*-(*p*-hexyloxy)aniline-*N'*-(*p*-heptyl)benzoylthiourea exhibits mesogenic properties whereas the analogous *N*-(*p*-hexyl)aniline-*N'*-(*p*-heptyloxy)benzoylthiourea is non-mesogenic, we decided to determine what effect, if any, the presence of two alkyloxy chains in the molecule has on the mesogenic character. Thus, the *N*-(*p*-alkyloxy)aniline-*N'*-(*p*-alkyloxy)benzoylthiourea compounds (**6a - 6c**), (Figure 3.25), were synthesised.

Figure 3.25 Schematic representation of *N*-(*p*-alkyloxy)aniline-*N'*-(*p*-alkyloxy)benzoylthiourea (6).

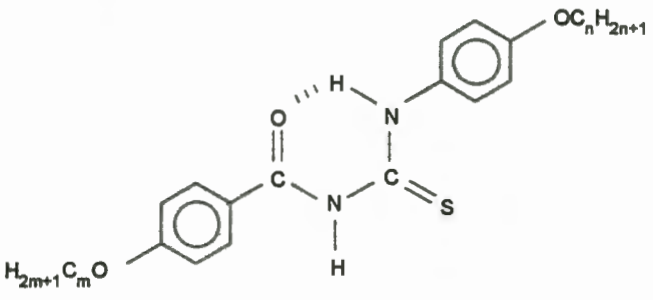

(6a) m = 1, n = 6

(6b) m = 7, n = 5

(6c) m = 7, n = 6

Polarising optical microscopy of *N*-(*p*-alkyloxy)aniline-*N'*-(*p*-alkyloxy)benzoylthiourea

Heating of compound **6a** to 114 °C results in a direct transformation from the solid state into an isotropic liquid. Cooling of the isotropic liquid allows for the crystallisation to the solid material at 105 °C. However, *very slow cooling* (<< 1 °C.min^{-1}) of a thin film of the isotropic liquid to 98 °C allows for the formation of a mesophase. Small *nematic droplets* form in the isotropic liquid on slow cooling. These droplets rapidly coalesce to form a nematic *schlieren texture* consisting of two- and four-brushed schlieren (**photograph 9**). In some areas of the preparation, a *homeotropic texture* (appears extinct through crossed polarisers) replaces the nematic schlieren texture. The phase is fluid and the mesophase flashes when subjected to mechanical stress. The fluidity and observed texture suggest that the mesophase is *nematic*. Crystallisation of the sample occurs at 88 °C.

Compound **6b** melts directly from the solid state to an isotropic liquid, at 118 °C, on heating of the sample. Slow cooling of the isotropic liquid of **6b** to 113 °C allows for the separation of *nematic droplets* from the isotropic liquid. These droplets rapidly coalesce to form a typical *schlieren texture*. It is evident from **photograph 10** that two types of point singularity are observed, one in which two brushes originate from the centre and the other in which four brushes originate from the centre. **Photographs 9** and **10** illustrate how very different the same texture can appear to the investigator. The phase is fluid and a white flash of light is observed in the field of view when the preparation is subjected to mechanical stress. The high fluidity of the phase, the formation of the nematic droplets, and the fact that two- and four-brushed schlieren are evident suggests that this is a *nematic* phase. In some areas of the preparation the schlieren brushes are replaced by threaded regions (*threaded texture*), which is the general texture obtained when nematic droplets coalesce[23]. At 112 °C the nematic phase is replaced by the grained *focal-conic fan texture* of the smectic A phase. Small highly coloured spherulitic domains on the edges of the preparation are also evident. In some areas of the preparation it was possible to observe both the nematic and smectic A mesophases simultaneously (**photograph 11**). The preparation crystallises at 101 °C.

Slow cooling of the isotropic liquid of **6c** to 115 °C allows for the formation of small *nematic droplets* which coalesce to form *two- and four-brushed schlieren*. The phase is fluid and flashes when subjected to mechanical stress. It was therefore identified as the *nematic* phase. Further cooling to 114 °C results in the transformation of the schlieren texture into a grained *focal-conic fan texture*. In some areas of the preparation the *homeotropic texture* is observed in addition to the focal-conic fan texture. This phase is more viscous than the nematic phase but proved to be a liquid when subjected to mechanical stress. Accordingly, the phase was identified as *smectic A*. Further cooling results in crystallisation of the mesogenic phase at 104 °C.

The optical studies of compounds **6a**, **6b** and **6c** have shown that the short chained compound **6a**, exhibits a nematic phase only, whereas the slightly longer chained compounds **6b** and **6c**, show both nematic and smectic A phases. These observations are consistent with those usually observed for a series of homologous compounds[24]. In general, nematic phases are favoured for the shorter alkyl(oxy) chain lengths, as the effect of the core predominates and the molecules are more like rigid rods. As the alkyl(oxy) chain length is increased, the nematic phase is stabilised until the association promoted by mutual attraction of the alkyl(oxy) chains begins stabilising the formation of layers. At this stage the smectic phase appears. As the chains get longer and the smectic phases stabilise, the nematic phase will disappear[24].

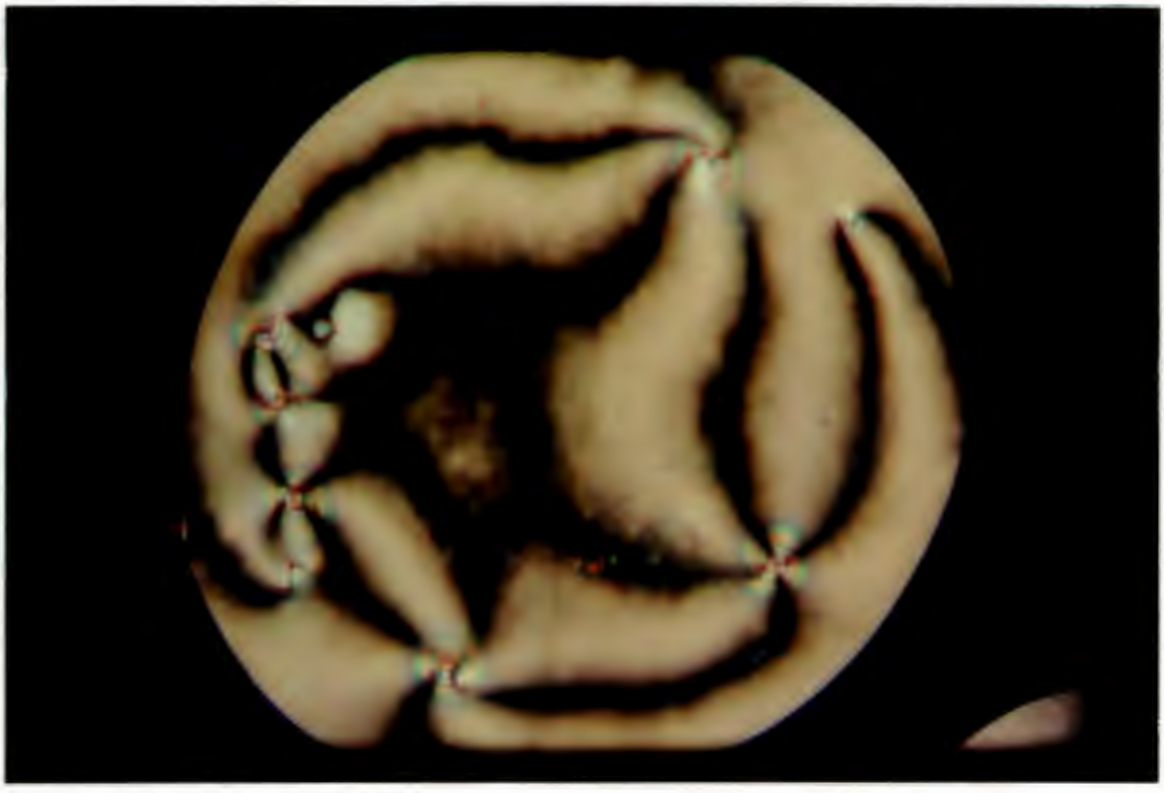

Photograph 9 Schlieren texture of nematic phase of *N*-(*p*-hexyloxy)aniline-*N'*-(*p*-methyloxy)-benzoylthiourea **6a**, showing two- and four-brushed schlieren.

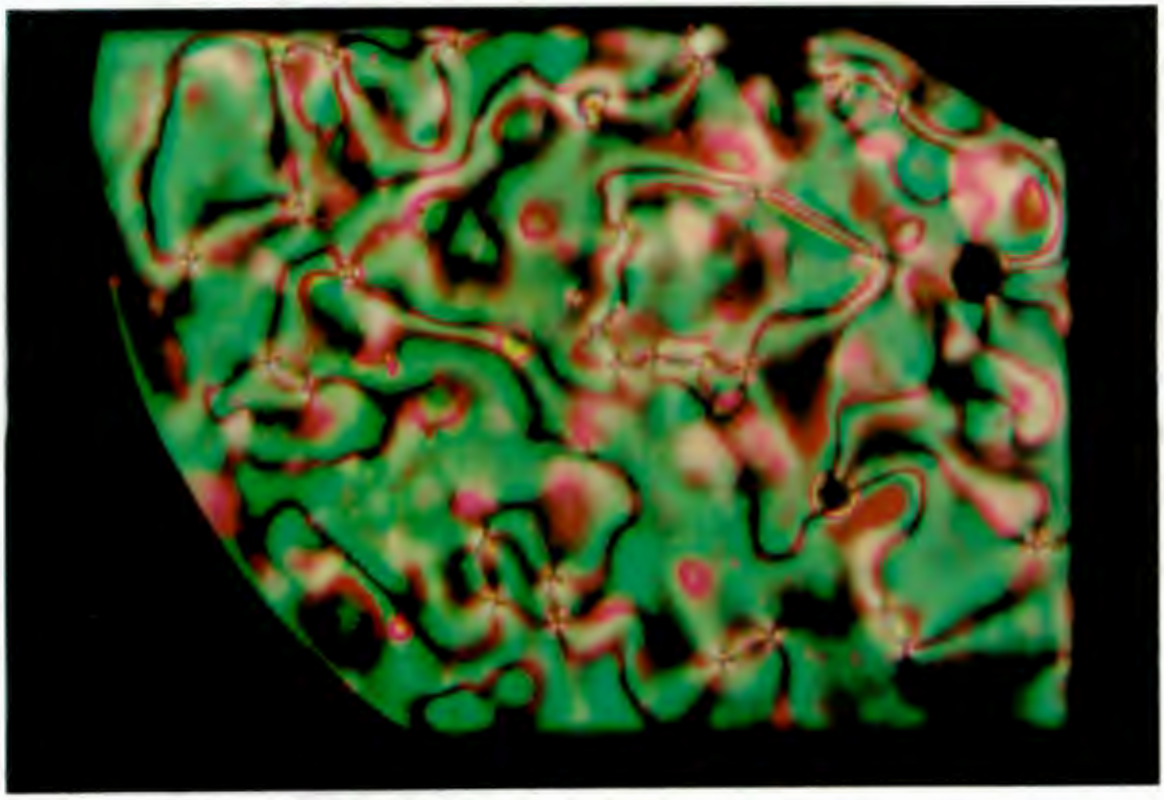

Photograph 10 Schlieren texture of *N*-(*p*-pentyloxy)aniline-*N'*-(*p*-heptyloxy)benzoylthiourea **6b**, exhibiting two and four brushed schlieren.

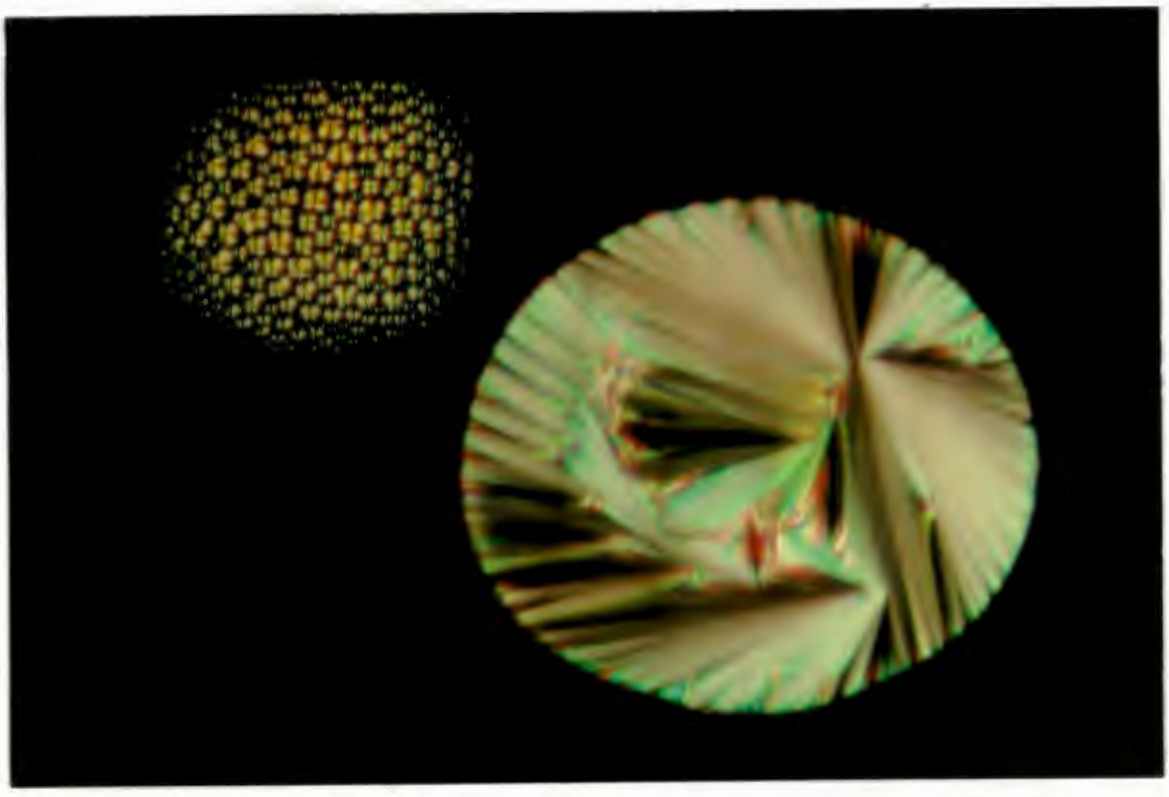

Photograph 11 Nematic droplets, of nematic phase, and focal-conic fan texture, of smectic A phase, evident in a preparation of *N*-(*p*-pentyloxy)aniline-*N'*-(*p*-heptyloxy)benzoylthiourea on cooling of the isotropic liquid.

Differential scanning calorimetry

The transition temperatures and associated thermodynamic data for the *N*-(*p*-alkyloxy)aniline-*N'*-(*p*-alkyloxy)benzoylthioureas is summarised in Table 3.5.

Table 3.5 Transition temperatures, mesophases and thermodynamic data for (**6a, b** and **c**).

Compound	m	n	Transition	T (°C)	ΔH	ΔS
6a	1	6	I - N*	98†	—	—
			N - C	88†	—	—
6b	7	5	I - N	111.7	2.0	5.2
			N - S_A	110.7	0.6	1.5
			S_A - C	103.3	39.4	104.7
6c	7	6	I - N*	114.1	2.1	5.5
			N - S_A*	112.4	0.6	1.5
			S_A - C	103.2	44.4	118.1
			C - C	101.6	1.8	4.7

Transition temperatures and enthalpy values obtained from DSC plots at a cooling rate of 2 °C.min^{-1}

ΔH in kJ.mol^{-1} and ΔS in J.K^{-1}.mol^{-1}

† *Transition temperatures observed microscopically*

* *Monotropic transition*

The DSC heating curve of *N*-(*p*-hexyloxy)aniline-*N'*-(*p*-methyloxy)benzoylthiourea **6a** shows the presence of three endothermic peaks at 82.0, 113.6 and 115.3 °C (Figure 3.25). It is postulated that the peak at 82.0 °C, at a temperature lower than the melting temperature, is due to a solid-solid transition. The large endotherm at 113.6 °C is assumed to be due to melting, since it occurs at a similar temperature to that observed optically and also involves that largest enthalpy change. However, particularly noticeable is the relatively small endotherm at 115.3 °C, two degrees higher than the melting endothermic peak. It may be reasonable to anticipate that this endotherm represents an *enantiotropic* mesogenic transition. Unfortunately, this transition was not detected by optical polarising microscopy. However, it is noteworthy that all phase changes do not always lead to an easily identifiable change in texture[24]. In view of the fact that a nematic phase is observed optically, on cooling of the isotropic liquid, it is postulated that the endotherm at 115 °C represents the nematic - isotropic transition. The enthalpy associated with this transition is approximately 6.3 kJ.mol^{-1} which is substantially larger than the monotropic I - N transitions estimated for compounds **6b** and **6c**.

Unfortunately, the DSC cooling curve of **6a**, is not conclusive with reference to mesophase formation, as the exotherm representing the I - N phase transition is not well-defined (Figure 3.25).

Figure 3.25 DSC heating (a) and cooling (b) curves, at a scanning rate of 1 °C.min^{-1}, of *N*-(*p*-hexyloxy)aniline-*N'*-(*p*-methyloxy)benzoylthiourea, (**6a**).

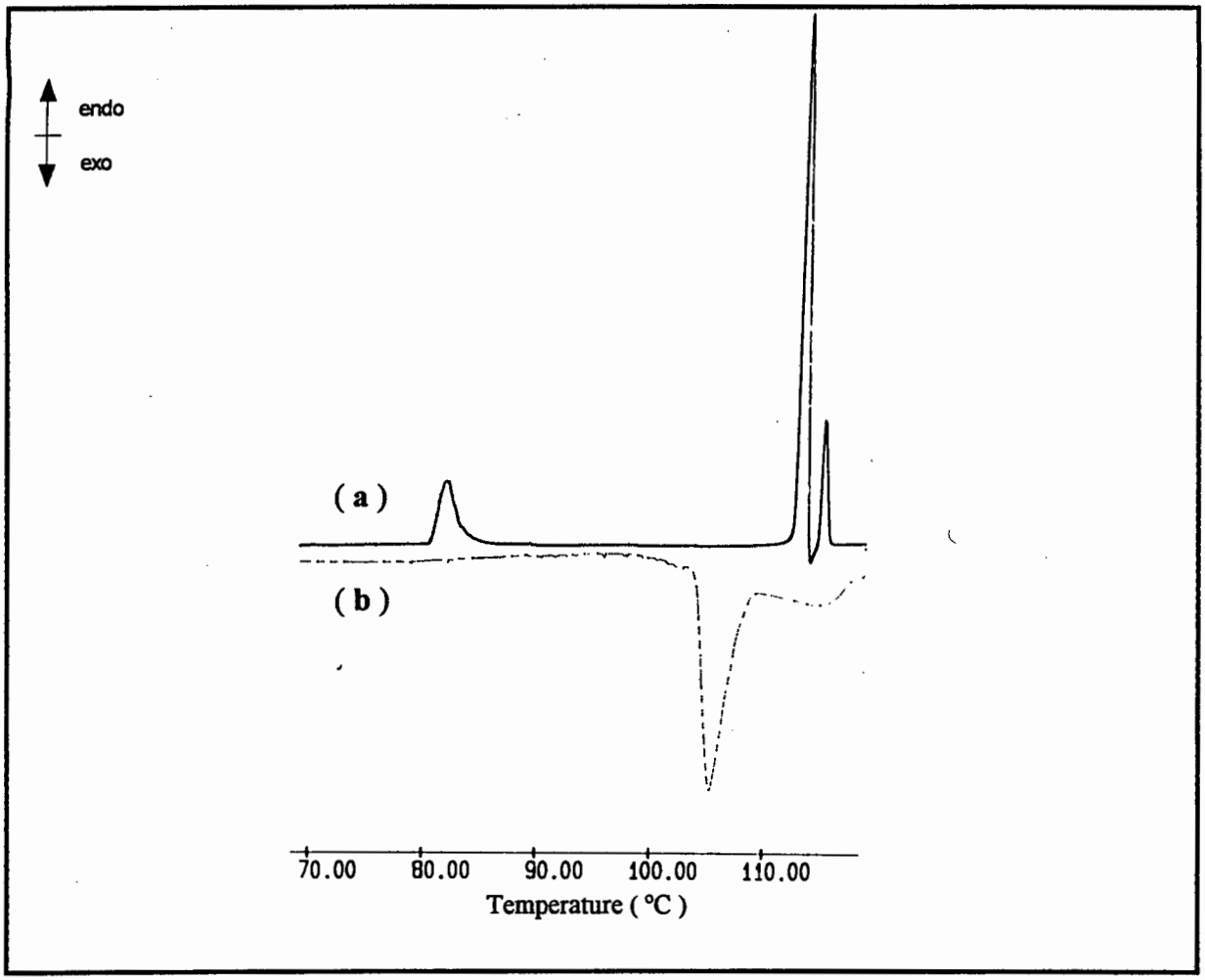

The DSC cooling curve of **6b** showed evidence of two monotropic mesogenic phases. Cooling of the isotropic liquid at 2 °C.min^{-1} results in the formation of a mesogenic phase between 112.2 and 111.2 °C. The enthalpy associated with this transition is 2.0 kJ.mol^{-1}. The results of optical microscopy, together with the size of the transition enthalpy, suggests that the phase under discussion is nematic. Further cooling allows for the transformation of this phase into a different phase which exists between 111.2 and 109.9 °C. The enthalpy associated with this transition is 0.6 kJ.mol^{-1}. Together with optical microscopy, this value suggests that this is a smectic A phase. Further cooling of the sample to 103.3 °C results in crystallisation to the solid material. The energy associated with the smectic A - solid transition is 39.4 kJ.mol^{-1}.

The DSC thermogram of **6c** indicates three small and one large exothermic peaks at 114.1, 112.4, 102.1 and 103.2 °C respectively, upon slow cooling of the isotropic liquid at 2 °C.min^{-1}. A phase exists from 115.0 - 113.3 °C and the enthalpy associated with the transition from the isotropic liquid to this phase is 2.1 kJ.mol^{-1}. The phase was identified as nematic from optical microscopy. Further cooling allows for the transformation from the nematic phase into the smectic A phase (from optical microscopy). This phase change is evident in the DSC plot between 113.3 and 110.9 °C and the enthalpy associated with it is 0.6 kJ.mol^{-1}. Further cooling to 103.2 °C allows for the crystallisation to the solid material; the energy involved is 44.4 kJ.mol^{-1}. A small exotherm, at 101.6 °C, which may represent a solid-solid transition of 1.8 kJ.mol^{-1} is also evident in the DSC thermogram. This phase change is not observed microscopically on either heating the solid material or cooling the isotropic liquid.

3.2.7 The effect of the position of the oxygen atom in the molecule on the observed mesogenic character

Finally, the effect of the position of the oxygen atom has on the observed liquid-crystalline behaviour of the *N*-acylthioureas discussed earlier in this chapter, can be illustrated by comparing compounds of identical alkyl chain lengths. A comparison of *N*-(*p*-hexyl)aniline-*N'*-(*p*-heptyloxy)benzoylthiourea **4a**, *N*-(*p*-hexyloxy)-aniline-*N'*-(*p*-heptyl)benzoylthiourea **5b** and *N*-(*p*-hexyloxy)aniline-*N'*-(*p*-heptyloxy)benzoylthiourea **6c** (Table 3.6), suggests that the position of the oxygen atom in the molecule determines the mesogenic behaviour exhibited on cooling of the isotropic liquid. Compound **4a,** which has an alkyloxy chain attached to the acyl ring and an alkyl chain attached to the aniline ring, does not show any mesogenic behaviour on either heating of the solid material or slow cooling of the isotropic liquid. Compound **5b**, on the other hand, which has an alkyloxy chain attached to the aniline group and an alkyl chain attached to the acyl group, shows a *nematic phase* on cooling of the isotropic liquid. This phase is stable over a 1 °C drop in temperature. Compound **6c**, which has an alkyloxy chain attached to both the acyl and aniline rings, shows both a *nematic* and *smectic A* phase upon cooling of the isotropic liquid. The nematic phase is stable over a 2 °C drop in temperature and transforms into a smectic A phase, stable over a 9 °C drop in temperature.

Table 3.6 Transition temperatures (°C) and observed phase changes for **4a, 5b** and **6c**.

compound	m	n	C - I	I - N	N - S_A	C
4a	7	6	121.8	—	—	104.5
5b	7	6	111.7	90.0	—	88.9
6c	7	6	123.6	114.1	112.4	103.2

Similar trends are observed on comparing *N*-(*p*-pentyloxy)aniline-*N'*-(*p*-heptyl)benzoylthiourea **5a** and *N*-(*p*-pentyloxy)aniline-*N'*-(*p*-heptyloxy)benzoylthiourea **6b**, (Table 3.7). Compound **5a**, which has an alkoxy chain attached to the aniline group and an alkyl chain attached to the acyl group, shows a *nematic phase*, stable over a 2 °C drop in temperature, upon cooling of the isotropic liquid. Compound **6b**, on the other hand, which has an alkyloxy chain attached to both the acyl and the aniline groups, allows for the formation of both a *nematic* and *smectic A* phase on cooling the isotropic liquid. The nematic phase is stable over a 1 °C drop in temperature and the smectic A phase stable over a 7 °C drop in temperature.

Table 3.7 Transition temperatures (°C) and observed phase changes for compounds **5a** and **6b**.

compound	m	n	C - I	I - N	N - S_A	C
5a	7	5	112.0	84.3	—	82.5
6b	7	5	124.0	111.7	110.7	103.3

In summary, these results clearly illustrate that the position of the oxygen atom in the molecule has a significant effect on firstly, whether the molecule is mesogenic, and secondly, the mesogenic phases exhibited on cooling the isotropic liquid.

3.2.8 1,6-Bis(*N,N*-dioctylthiourea)-hexan-1,6-dione (7)

1,6-Bis(*N,N*-dioctylthiourea)-hexan-1,6-dione (7), (Figure 3.26), was synthesised primarily to satisfy the Author's intellectual curiosity. In the absence of a rigid core, the conformations that the molecule can adopt are numerous and thus liquid-crystalline properties were not expected for this compound.

Figure 3.26 Schematic representation of 1,6-bis(*N,N*-dioctylthiourea)-hexan-1,6-dione (7).

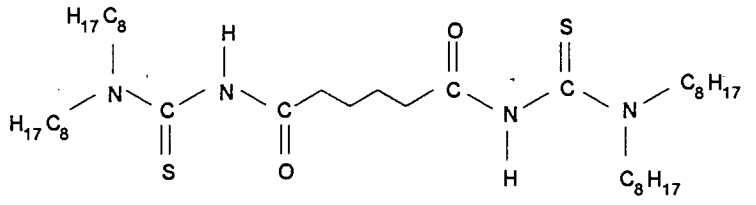

(7)

It was thus with great delight that we discovered that 1,6-bis(*N,N*-dioctylthiourea)-hexan-1,6-dione displays mesogenic behaviour. Heating of the solid crystalline material results in a direct solid to isotropic liquid transition at 77 °C. Slow cooling of the isotropic liquid to 48 °C allows for the formation of highly coloured *spherulites* each carrying a familiar cross of extinction. Upon further cooling, the spherulites coalesce to form a pronounced *pseudo-focal-conic texture*[39] (**photograph 12**). The backs of the fans of the focal-conic texture are smooth. The mesophase appears at a relatively slow rate on cooling of the isotropic liquid and remains in this liquid-crystalline state for several hours at room temperature. The structure of this monotropic mesophase with the spherulitic texture is not currently known and deserves further investigation.

Recently, Stebani and Lattermann[39] synthesised 3,4-bis(alkoxy)benzoyl substituted diethylenetriamine compounds which show monotropic liquid-crystalline phases exhibiting a pseudo-focal-conic texture similar to that observed for compound **7**. Their preliminary X-ray measurements indicated a smectic / lamellar structure. It is thus apparent that X-ray measurements must be performed in order to identify the structure of the monotropic mesophase of 1,6-bis(*N,N*-dioctylthiourea)-hexan-1,6-dione.

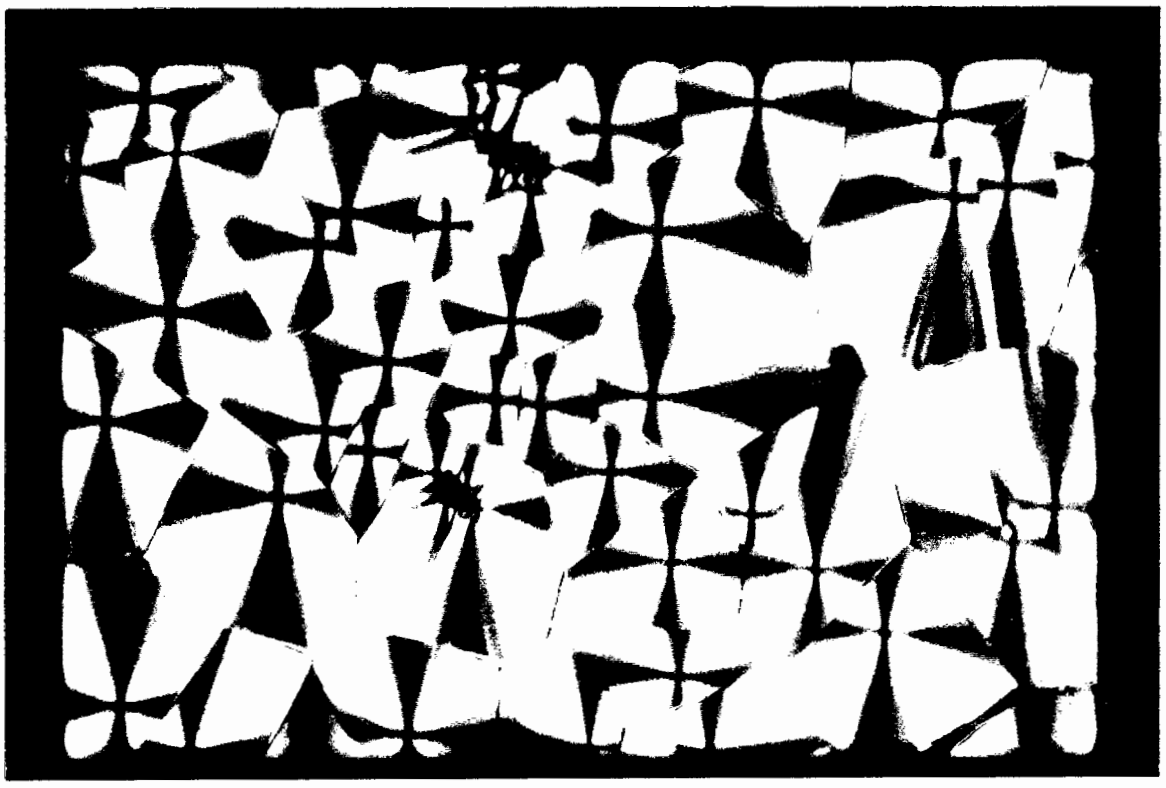

Photograph 12 Pseudo-focal-conic texture of 1,6-bis(*N,N*-dioctylthiourea)-hexan-1,6-dione (**7**) after standing for several hours at room temperature.

Unfortunately, no mesogenic behaviour of 1,6-bis(*N,N*-dioctylthiourea)-hexan-1,6-dione could be inferred from the DSC heating or cooling thermograms. A single endotherm at 78 °C, assigned to the melting temperature, was evident in the heating curve, but no exothermic peaks corresponding to mesophase formation or crystallisation were observed in the DSC cooling thermogram. The absence of exothermic peaks may be attributed to the extremely slow rate of formation of the mesophase as observed microscopically.

3.3 Crystal and molecular structure of *N*-(*p*-hexyloxy)aniline-*N'*-(*p*-methyloxy)benzoylthiourea (6a)

The importance of an elongated, rod-like molecular shape in relation to liquid crystal phases was clearly established early in this century[3]. The relationship between structure and mesogenic properties is very clear - the molecules contain rings and double bonds with strong π-character to enhance rigidity and help to prevent the molecules from adopting non-linear configurations that would militate against the parallel packing of rods needed for formation of liquid crystal phases. In addition, the molecules may also contain para-arranged lateral groups or chains to promote linear molecules[40]. It can therefore be expected that the way in which the molecules pack in the crystal lattice would be important in determining the type of mesophase(s) exhibited by the compound.

The strength of the long range interactions depend on the molecular separation, which amongst other factors, is governed by steric interactions. Steric factors therefore influence molecular packing and determine whether or not a layered structure is attainable. Only in the crystalline phase is it possible to accurately determine the molecular conformation and packing of the molecules in the solid state. Liquid-crystalline compounds may retain some of the order of the crystalline phase[41,42] on melting, such as linearity, layering and relative orientation of molecules. Intermolecular interactions contribute greatly to the formation of ordered molecular aggregates. A proper combination of the shape of a molecule and the magnitude and direction of molecular interactions between molecules, determines whether a compound will show liquid-crystalline behaviour[12].

In view of the fact that certain *N*-acylthioureas exhibit mesogenic behaviour whereas others do not, we decided to compare the X-ray crystal structure of a mesogenic compound to the crystal structure of the non-mesogenic *N*-butyl-*N'*-benzoylthiourea described in Chapter 2. The structure of *N*-(*p*-hexyloxy)aniline-*N'*-(*p*-methyloxy)benzoylthiourea (**6a**) was determined by single-crystal x-ray diffraction and the numbering scheme is shown in Figure 3.27. Colourless cubic crystals of **6a** were obtained by dissolving the compound in a chloroform - ethanol solution and allowing slow evaporation of the solvent at room temperature. The structure was solved (Dr Susan Bourne, Crystallography Department at UCT), by direct methods using SHELXS-86[43] and refined by full-matrix least squares based on F^2 using SHELXL-93[44]. The final model included anisotropic refinement of all non-hydrogen atoms. The crystal data, experimental and refinement

parameters are summarised in Table 2.1 of Appendix 2. The fractional atomic coordinates for all non-hydrogens are listed in Table 2.2 of Appendix 2.

Figure 3.27 Perspective view of the molecular structure of *N*-(*p*-hexyloxy)aniline-*N'*-(*p*-methyloxy)benzoylthiourea showing the atom numbering scheme for all non-hydrogen atoms.

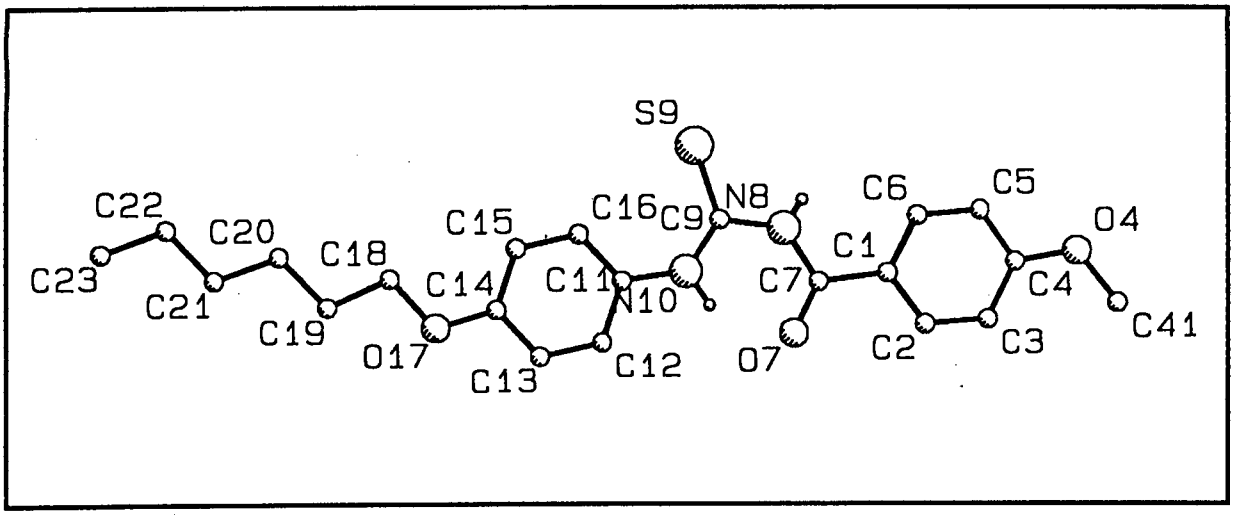

The unit cell is triclinic and contains two molecules related through a centre of inversion. The bond lengths and bond angles all fall within the expected limits and are reported in Table 2.3 of Appendix 2. The aromatic rings, C(1) - C(6) and C(11) - C(16), are planar with maximum deviations from the least squares plane of 0.010(2) and 0.003(2) Å respectively. O(7) - C(7) - N(8) - C(9) - N(10) - H(10) is also planar with deviations from the plane less than 0.010 Å. It is interesting to note that these three rings are almost co-planar; the angle between the aromatic plane C(1) - C(6) and the O(7) - H(10) 6-membered ring is 19° and that between O(7) - H(10) and the aromatic plane C(11) - C(16) is 6°. This is in contrast to that for *N*-butyl-*N'*-benzoylthiourea where a dihedral angle of 43.87(19)° was observed between the aromatic ring and O(7) - C(7) - N(8) - C(9) - N(10) - H(10) hydrogen-bonded 6-membered ring (Chapter 2). This suggests that the planarity of the molecules of compound **6a** allows for a favourable parallel molecular arrangement and optimal packing in the solid state (Figure 3.28). As mentioned in the introduction, such an arrangement of molecules is important in attaining liquid-crystalline phases.

The linear and extended molecular geometry of the molecule is as a result of an *intra*molecular hydrogen bond N(10) - H(10) ... O(7) locking O(7) - C(7) - N(8) - C(9) - N(10) - H(10) into a six-membered ring. This *intra*molecular hydrogen bond allows for the formation of a rigid central core and a parallel arrangement of the alkyloxy chains. In the absence of this strong *intra*molecular hydrogen bond it is hypothesised that the molecules will adopt non-linear conformations. This is considered deleterious to mesogenic behaviour.

The hydrogen attached to N(10) was located in the difference Fourier map and refined isotropically. The N(10) - H(10) bond length was found to be 0.89(3) Å and the N(10) - H(10) ... O(7) bond length 2.668(2) Å. The present N(10) - H(10) ... O(7) bond length is 0.024 Å longer than that observed for *N*-butyl-*N'*-benzoylthiourea and 0.004 Å shorter than that observed for *N*-propyl-*N'*-benzoylthiourea[45] (Table 3.8). The N(10) - H(10) ... O(7) bond angle was 144(2) ° compared to 133.5(43)° for *N*-butyl-*N'*-benzoylthiourea.

Figure 3.28 Packing diagram of *N*-(*p*-hexyloxy)aniline-*N'*-(*p*-methyloxy)benzoylthiourea.

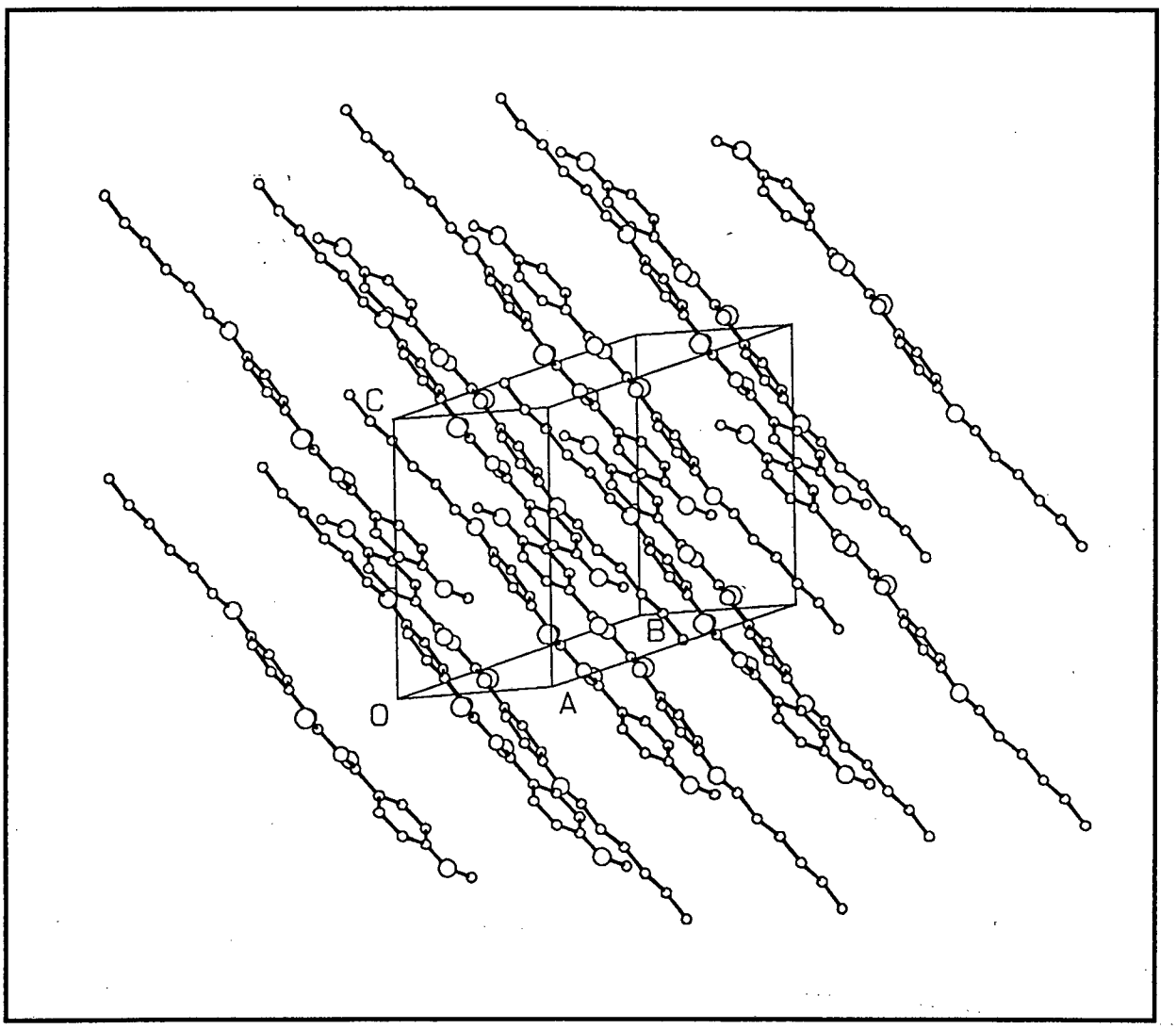

There is a second *inter*molecular hydrogen bond between N(8) - H(8) and S(9) on an adjoining molecule. It is interesting to note that this interaction was not observed in the crystal structure of *N*-butyl-*N'*-benzoylthiourea (Chapter 2). The hydrogen attached to N(8), in the present structure, was located in the difference Fourier map and refined isotropically. The N(8) - H(8) and N(8) - H(8)...S(9) bond lengths were found to be 0.75(3) and 3.597(2) Å respectively (Table 3.8). The N(8) - H(8)...S(9) bond distance is approximately 0.13 Å longer than that reported for the analogous interaction by Dago[45] for *N*-propyl-*N'*-benzoylthiourea. The N(8) - H(8) ... S(9) bond angle was 148(3) ° whereas the corresponding angle in *N*-propyl-*N'*-benzoylthiourea was 161(5)° [45].

Figure 3.29 The structure of the extended mesogen formed by both *inter*- and *intra*molecular hydrogen bonding of *N*-(*p*-hexyloxy)aniline-*N'*-(*p*-methyloxy)benzoylthiourea. The dashed lines represent the *inter*molecular hydrogen bonds.

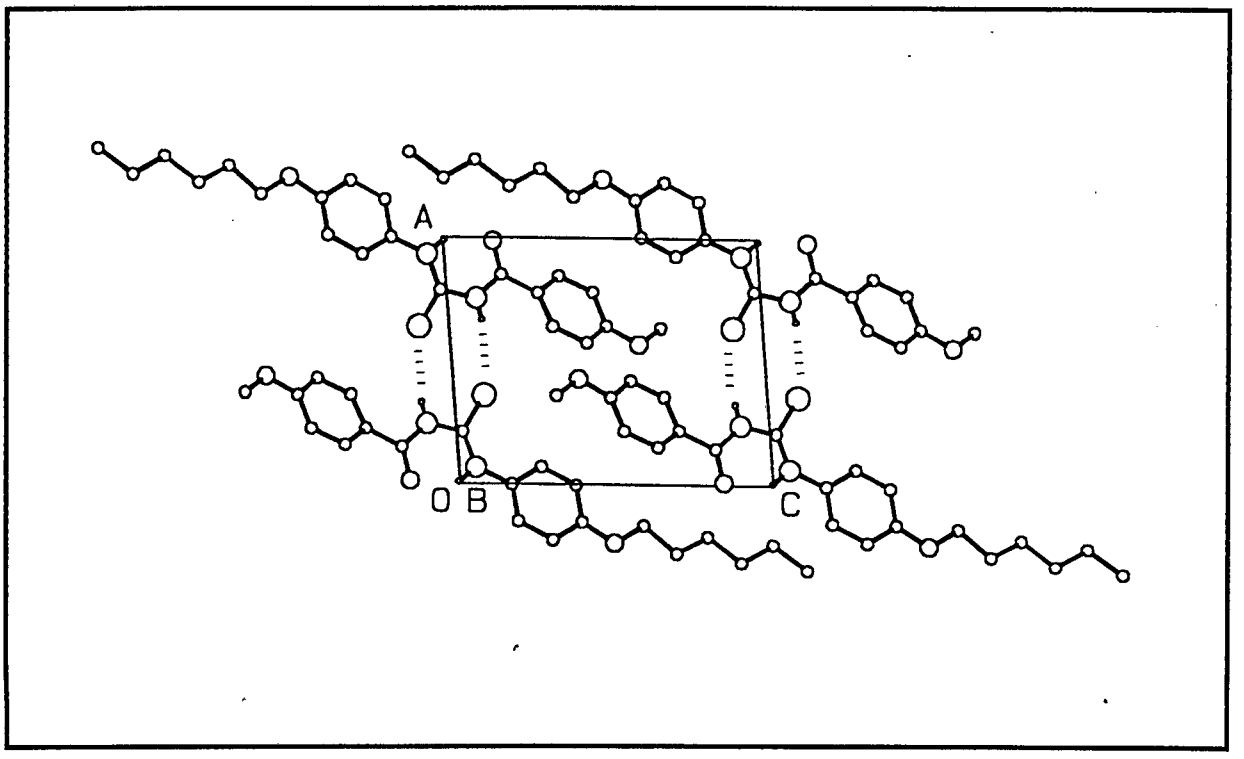

Two *inter*molecular hydrogen bonds between two adjacent molecules results in the formation of a dimeric structure (Figure 3.29). The molecules of the dimer are arranged parallel to each other in a head-to-tail configuration. Two sets of dimers are arranged with the methyloxybenzoyl moiety of one molecule in close proximity to the methyloxybenzoyl moiety of the molecule of a dimer in a neighbouring layer. In contrast to this, the molecules of *N*-butyl-*N'*-benzoylthiourea pack in a herring-bone conformation.

The observed *inter*molecular association between two molecules in neighbouring layers results in the formation of an overall extended S-shape geometry with the aromatic and six-membered rings forming the rigid "core" of the dimer. The remainder of each molecule extends in opposite but parallel directions. A parallel arrangement of molecules in the crystal is known to be necessary in order for the compound to produce a nematic liquid-crystalline phase[12].

The crystal structure determination of *N*-(*p*-hexyloxy)aniline-*N'*-(*p*-methyloxy)benzoylthiourea suggests that the following factors are important in giving rise to liquid-crystalline behaviour:

- the *intra*molecular hydrogen bond, N(10) - H(10) ... O(7), locking O(7) - C(7) - N(8) - C(9) - N(10) - H(10) into a six-membered ring
- the planarity of the aromatic groups and hydrogen bonded six-membered group allowing parallel molecular packing
- the *inter*molecular interactions between adjacent molecules.

In summary the X-ray crystal study has shown that the mesogenic *N*-(*p*-hexyloxy)aniline-*N'*-(*p*-methyloxy)-benzoylthiourea forms a new and extended mesogen through both *intra*- and *inter*molecular hydrogen bonding, allowing favourable molecular orientation and packing of molecules for the formation of liquid crystal phases.

3.4 Conclusion

We have successfully shown that *N*-acylthioureas may be modified to display liquid-crystalline properties. These modifications are synthetically easy to achieve and give products in high yields. The liquid-crystalline phases produced are monotropic, i.e. they are thermodynamically unstable and only appear on cooling of the isotropic liquid. However, the DSC heating curve of *N*-(*p*-hexyloxy)aniline-*N'*-(*p*-methyloxy)benzoylthiourea indicates the presence of an endothermic peak at a temperature higher than the melting temperature, which suggests mesogenic character. Although it has not been possible to establish unambiguously that this small endothermic peak represents mesophase formation, it nevertheless suggests that *N*-(*p*-hexyloxy)aniline-*N'*-(*p*-methyloxy)benzoylthiourea is an enantiotropic liquid crystal.

We have been able to establish that an alkyloxy chain and two phenyl groups are essential for mesogenic behaviour. The position of the alkyloxy chain in the molecule determines the type of mesogenic phase exhibited. The results of polarising optical microscopy and DSC indicate that nematic and smectic A phases are formed in the present series of mesogenic *N*-acylthioureas.

The crystal structure determination of *N*-(*p*-hexyloxy)aniline-*N'*-(*p*-methyloxy)benzoylthiourea suggests that the strong *intra*molecular hydrogen bond is essential for the formation of a rigid central core and rod-like geometry of the molecules. In the absence of this bond it is postulated that the 'centre' of the structure will be flexible. This flexibility is usually considered deleterious to mesogenic behaviour because of the large number of non-linear geometries the molecule may adopt.

A rare mesophase was observed in a related *N*-acylthiourea which does not possess a central rigid core. A pronounced pseudo-focal-conic fan (spherulitic) texture was observed on cooling of the isotropic liquid of 1,6-bis(*N,N*-dioctylthiourea)-hexan-1,6-dione. The monotropic mesophase is stable for several hours at room temperature. The structure of this mesophase is unknown.

In conclusion, the series of liquid-crystalline *N*-acylthioureas discussed in this chapter do not have any practical use because of their high melting points and generally observed monotropic mesogenic behaviour. Although *inter*molecular hydrogen-bonded mesogens have previously been reported[46-49], the monotropic *N*-acylthioureas are to the Author's knowledge the first examples of *intra*- and *inter*molecular hydrogen-bonded mesogens.

3.5 Experimental

General procedure for synthesising *N*-acylthioureas

The *N*-acylthioureas were synthesised according to the procedure of Douglass and Dains *et al*[53] reported in Chapter 2. The products were analysed by means of C, H and N elemental analysis. Proton NMR shifts of selected compounds are recorded in the experimental section.

***N*-decyl-*N'*-benzoylthiourea (1d)** 87 % yield, mp 32 - 34 °C. Anal. Calcd for $C_{18}H_{28}N_2OS$: C, 67.5; H, 8.8; N, 8.7. Found C, 66.9; H, 8.9; N, 8.7. NMR ($CDCl_3$) ^1H δ 0.88 (3H, t, CH_3), 1.27 (14H, b.m, CH_2), 1.72 (2H, m, CH_2), 3.69 (2H, q, NCH_2), 7.51 (2H, t, H(3)/H(5)), 7.58 (1H, t, H(4)), 7.86 (2H, d, H(2)/H(6)), 9.05 (1H, b.s, N(8) - H(8)), 10.72 (1H, t, N(10) - H(10)); ^{13}C δ 14.03, 22.60, 26.89, 28.15, 29.16, 29.22, 29.41, 29.45, 31.81, 45.91, 127.36, 129.03, 131.82, 133.41, 166.79, 179.61.

***N*-dodecyl-*N'*-benzoylthiourea (1e)** 72 % yield, mp 42 - 44 °C. Anal. Calcd for $C_{20}H_{32}N_2OS$: C, 68.9; H, 9.3; N, 8.0. Found C, 69.3; H, 8.7; N, 8.2. NMR ($CDCl_3$) ^1H δ 0.87 (3H, t, CH_3), 1.26 (18H, m, CH_2), 1.72 (2H, m, CH_2), 3.75 (2H, q, NCH_2), 7.51 (2H, t, H(3)/H(5)), 7.62 (H, t, H(4)), 7.81 (2H, d, H(2)/H(6)), 8.99 (1H, b.s, N(8) - H(8)), 10.76 (1H, t, N(10) - H(10)); ^{13}C δ 14.07, 22.64, 26.92, 28.19, 29.19, 29.30, 29.49, 29.52, 29.59, 31.88, 45.97, 127.34, 129.10, 131.84, 133.47, 166.77, 179.62.

***N*-tetradecyl-*N'*-benzoylthiourea (1f)** 84 % yield, mp 51 - 52 °C. Anal. Calcd for $C_{22}H_{36}N_2OS$: C, 70.2; H, 9.6; N, 7.4. Found C, 70.5; H, 10.4; N, 6.8. NMR ($CDCl_3$) ^1H δ 0.92 (3H, t, CH_3), 1.20 (22H, m, CH_2), 1.69 (2H, m, CH_2), 3.69 (2H, q, NCH_2), 7.48 (2H, t, H(3)/H(5)), 7.61 (1H, t, H(4)), 7.86 (2H, d, H(2)/H(6)), 9.41 (1H, b.s, N(8) - H(8)), 10.79 (1H, t, N(10) - H(10)); ^{13}C δ 14.05, 22.67, 26.91, 29.23, 29.46, 29.55, 29.61, 29.66, 31.93, 45.89, 127.36, 129.19, 131.87, 133.49, 166.75, 179.61.

***N*-hexadecyl-*N'*-benzoylthiourea (1g)** 89 % yield, mp 58 - 60 °C. Anal. Calcd for $C_{24}H_{40}N_2OS$: C, 71.2; H, 9.9; N, 6.9. Found C, 71.4; H, 9.9; N, 7.2. NMR ($CDCl_3$) ^1H δ 0.87 (3H, t, CH_3), 1.24 (26H, m, CH_2), 1.73 (2H, m, CH_2), 3.76 (2H, q, NCH_2), 7.49 (2H, t, H(3)/H(5)), 7.61 (1H, t, H(4)), 7.82 (2H, d, H(2)/H(6)), 8.98 (1H, b.s, N(8) - H(8)), 10.74 (1H, t, N(10) - H(10)).

***N*-octadecyl-*N'*-benzoylthiourea (1h)** Pure **1h** was obtained as a white solid after chromatography of the crude product on silica gel using 60% $CHCl_3$ / hexane as eluent (82 % yield), mp 65 - 67 °C. Anal. Calcd for $C_{26}H_{44}N_2OS$: C, 72.2; H, 10.3; N, 6.5. Found C, 71.9; H, 10.3; N, 6.4. NMR ($CDCl_3$) ^1H δ 0.88 (3H, t, CH_3), 1.25 (30H, m, CH_2), 1.76 (2H, m, CH_2), 3.70 (2H, q, NCH_2), 7.51 (2H, t, H(3)/H(5)), 7.63 (1H, t, H(4)), 7.84 (2H, d, H(2)/H(6)), 8.98 (1H, b.s, N(8) - H(8)), 10.71 (1H, t, N(10) - H(10)).

***N*-(*p*-dodecyl)aniline-*N'*-(*p*-butyl)benzoylthiourea (2a)** 81 % yield, mp 94 - 95 °C. Anal. Calcd for $C_{30}H_{44}N_2OS$: C, 74.95; H, 9.23; N, 5.83; S, 6.66. Found C, 74.87; H, 9.19; N, 5.91; S, 6.63.

***N*-(*p*-dodecyl)aniline-*N'*-(*p*-pentyl)benzoylthiourea (2b)** 73 % yield, mp 89 - 92 °C. Anal. Calcd for $C_{31}H_{46}N_2OS$: C, 75.25; H, 9.38; N, 5.66; S, 6.47. Found C, 75.32; H, 9.47; N, 5.71; S, 6.49.

***N*-(*p*-dodecyl)aniline-*N'*-(*p*-hexyl)benzoylthiourea (2c)** 82 % yield, mp 95 - 97 °C. Anal. Calcd for $C_{32}H_{48}N_2OS$: C, 75.53; H, 9.52; N, 5.51; S, 6.29. Found C, 75.52; H, 9.52; N, 5.59; S, 6.28.

***N*-(*p*-dodecyl)aniline-*N'*-(*p*-heptyl)benzoylthiourea (2d)** 71 % yield, mp 101 - 102 °C. Anal. Calcd for $C_{33}H_{50}N_2OS$: C, 75.80; H, 9.65; N, 5.36; S, 6.13. Found C, 75.96; H, 9.61; N, 5.31; S, 6.12.

***N*-octyl-*N'*-(*p*-dodecyloxy)benzoylthiourea (3)** Pure **3** was obtained as a white solid after chromatography of the crude product on a thin layer preparative glass plate using $CHCl_3$ as the eluent (51 % yield), 86 - 87 °C. Anal. Calcd for $C_{28}H_{48}N_2O_2S$: C, 70.49; H, 10.15; N, 5.87; S, 6.71. Found C, 70.63; H, 10.18; N, 5.94; S, 6.69.

***N*-(*p*-hexyl)aniline-*N'*-(*p*-heptyloxy)benzoylthiourea (4a)** 84 % yield, mp 117 - 118 °C. Anal. Calcd for $C_{27}H_{38}N_2O_2S$: C, 71.32; H, 8.43; N, 6.16; S, 7.04. Found C, 71.28; H, 8.52; N, 6.18; S, 6.99.

***N*-(*p*-dodecyl)aniline-*N'*-(*p*-heptyloxy)benzoylthiourea (4b)** 94 % yield, mp 115 - 116 °C. Anal. Calcd for $C_{33}H_{50}N_2O_2S$: C, 73.55; H, 9.36; N, 5.20; S, 5.94. Found C, 73.45; H, 9.44; N, 5.30; S, 5.78.

***N*-(*p*-hexyl)aniline-*N'*-(*p*-dodecyloxy)benzoylthiourea (4c)** 91 % yield, mp 113 - 115 °C. Anal. Calcd for $C_{32}H_{48}N_2O_2S$: C, 73.18; H, 9.22; N, 5.34. Found C, 73.12; H, 9.25; N, 5.38.

***N*-(*p*-octyl)aniline-*N'*-(*p*-dodecyloxy)benzoylthiourea (4d)** 92 % yield, mp 114 - 116 °C. Anal. Calcd for $C_{34}H_{52}N_2O_2S$: C, 73.86; H, 9.49; N, 5.09. Found C, 73.95; H, 9.59; N, 4.99.

***N*-(*p*-decyl)aniline-*N'*-(*p*-dodecyloxy)benzoylthiourea (4e)** 89 % yield, mp 111 - 112 °C. Anal. Calcd for $C_{36}H_{56}N_2O_2S$: C, 74.42; H, 9.72; N, 4.82. Found C, 74.43; H, 9.88; N, 4.79.

***N*-(*p*-dodecyl)aniline-*N'*-(*p*-dodecyloxy)benzoylthiourea (4f)** 81 % yield, mp 112 - 113 °C. Anal. Calcd for $C_{38}H_{60}N_2O_2S$: C, 74.94; H, 9.94; N, 4.60. Found C, 74.89; H, 9.99; N, 4.57. NMR ($CDCl_3$) ^1H δ 0.88 (6H, t, CH_3), 1.26 (36H, b.s, CH_2), 1.61 (2H, q, ϕCH_2), 1.82 (2H, q, OCH_2), 2.61 (2H, t, ϕCH_2), 4.04 (2H, t, NCH_2), 6.99 (2H, d, H(3)/H(5)), 7.29 (2H, d, H(12)/H(16)), 7.60 (2H, d, H(13)/H(15)), 7.84(2H, d, H(2)/H(6)), 9.00 (1H, s, N(8) - H(8)), 12.59 (1H, s, N(10) - H(10)).

***N*-(*p*-pentyloxy)aniline-*N'*-(*p*-heptyl)benzoylthiourea (5a)** 71 % yield, mp 108 - 109 °C. Anal. Calcd for $C_{26}H_{36}N_2O_2S$: C, 70.86; H, 8.24; N, 6.36; S, 7.27. Found C, 69.97; H, 8.28; N, 6.43; S, 7.26.

***N*-(*p*-hexyloxy)aniline-*N'*-(*p*-heptyl)benzoylthiourea (5b)** 77 % yield, mp 109 - 110 °C. Anal. Calcd for $C_{27}H_{38}N_2O_2S$: C, 71.32; H, 8.43; N, 6.16; S, 7.04. Found C, 71.28; H, 8.30; N, 6.05; S, 7.15.

***N*-(*p*-hexyloxy)aniline-*N'*(*p*-methyloxy)benzoylthiourea (6a)** 83 % yield, mp 112 - 114 °C. Anal. Calcd for $C_{21}H_{26}N_2O_3S$: C, 65.25; H, 6.79; N, 7.25; S, 8.29. Found C, 65.35; H, 6.94; N, 7.17; S, 8.42.

***N*-(*p*-pentyloxy)aniline-*N'*-(*p*-heptyloxy)benzoylthiourea (6b)** (71 % yield, mp 120 - 121 °C. Anal. Calcd for $C_{26}H_{36}N_2O_3S$: C, 68.38; H, 7.95; N, 6.14; S, 7.01. Found C, 68.35; H, 7.94; N, 6.17; S, 6.93.

***N*-(*p*-hexyloxy)aniline-*N'*-(*p*-heptyloxy)benzoylthiourea (6c)** 84 % yield, mp 120 - 121 °C. Anal. Calcd for $C_{27}H_{38}N_2O_3S$: C, 68.89; H, 8.14; N, 5.95; S, 6.80. Found C, 68.43; H, 8.25; N, 5.78; S, 6.73.

1,6-Bis-(*N,N*-dioctylthiourea)-hexan-1,6-dione (7) 74 % yield, mp 76 - 77 °C. Anal. Calcd for $C_{40}H_{78}N_4OS_2$: C, 67.54; H, 11.06; N, 7.88; S, 9.01. Found C, 67.64; H, 11.03; N, 7.71; S, 8.91.

REFERENCES

1 Reinitzer, F.; *Monatsh. Chem.*, 1888, **9**, 421.

2 Sage, I.; *Crit. Rep. Appl. Chem.*, 1987, **22**, 64.

3 Gray, G.W. (ed.); *Thermotropic Liquid Crystals*, vol. 22, Wiley, New York, 1987.

4 Nyirjesy, I.; Abernathy, M.R.; Billingsley, F.S.; Bruns, P.; *J. Reproductive Med.*, 1977, **18**, 165.

5 Gautherie, M.; Gros, C.M.; *Cancer*, 1980, **45**, 51.

6 Margolis, R.C.; Shaffer, L.S.; *J. Am. Obstetrics Assn.*, 1974, **73**, 910.

7 Ambrosi, C.; Bourcle, C.; *Gaz. Med. France*, 1975, **82**, 628.

8 Dixon, G.D.; *Mater. Eval.*, 1977, **35**, 51.

9 Ireland, P.; Jones, T.V.; *Heat Transfer and Cooling in Gas Turbines*, AGARD Conf. Proc. CP390, 1985.

10 Tolmachev, A.V.; Govorun, E.Y.; Kuzmichev, V.M.; *Zh. Eksp. Teor. Fiz.*, 1972, **63**, 583.

11 Vill, V., *Adv. Mater.*, 1994, **6**, 527.

12 Kelker, H.; Hatz, R.; *Handbook of Liquid Crystals*, Verlag Chemie, Weinheim, 1980.

13 Giroud-Godquin, A-M.; Maitlis, P.M.; *Angew. Chem. Int. Ed. Engl.*, 1991, **30**, 375.

14 Tiddy, G.J.D.; *Phys. Rev.*, 1980, **57C**, 1.

15 Bergmann, L.; Schäfer, C.; *Experimentalphysik, Band III, Optik*, 5.Aufl., De Gruyter, Berlin, 1972.

16 Westphal, W.H.; *Physik*, 25/26 Aufl., Springer, Berlin, 1970.

17 Billard, J.; *C.R. Acad. Sci. Ser.2*, 1984, **299**, 905.

18 Friedel, G.; *Ann. Phys.*; 1922, **18**, 273.

19 Vögtle, F.; *Supramolecular Chemistry*, John Wiley & Sons, New York, 1991.

20 Brown, G.H.; Crooker, P.P.; *Chem. Eng. News*, 1983, **61**, 24.

21 Loesche, A.; *Wiss. Z. Karl-Marx-Univ., Leipzig, Math. Nat. Reihe*, 1976, **25**, 60.
[Chem.Abstr., 1977, **86**, 198053m].

22 Sackmann, H.; Demus, D.; *Mol. Cryst. Liq. Cryst.*, 1973, **21**, 239.

23 Demus, D.; Richter, L.; *Textures in Liquid Crystals*, Verlag Chemie, New York, 1978.

24 Bruce, D.W.; O'Hare, D.; (eds.); *Inorganic Materials*, John Wiley & Sons, New York, 1992.

25 Deutscher, D.J.; Vorbrodt, H.M.; Zaschke, H.; *Z. Chem.*, 1981, **21**, 9.

26 Boettcher, J.; Hartmann, R.; Vögtle, F.; *Chem. Ber.*, 1992, **125**, 1865.

27 Gray, G.W.; Goodby, J.W.G.; *Smectic Liquid Crystals - Textures and Structures*, Leonard Hill, Glasgow, 1984.

28 Gray, G.W.; *Molecular Structure and Properties of Liquid Crystals*, Academic Press, London, 1962.

29 Brennan, W.P.; Gray, A.P.; *Liquid Crystals - The Mesomorphic State*, Perkin-Elmer Corp. Newsletter, Conneticut.

30 Schubert, H.; Lorenz, H.J.; Hoffmann, R.; Franke, F.; *Z. Chem.*, 1955, **6**, 337.

31 Douglass, I.B.; Dains, F.B.; *J. Am. Chem. Soc.*, 1934, **56**, 719.

32 Giroud-Godquin, A.M.; Billard, J.; *Mol. Cryst. Liq. Cryst.*, 1981, **66**, 147.

33 Ohta, K.; Ishii, A.; Yamamoto, I.; Matsuzaki, K.; *J. Chem. Soc., Chem. Commun.*, 1984, 1099.

34 Espinet, P.; Esteruelas, M.A.; Oro, L.A.; Serrano, J.L.; Sola, E.; *Coord. Chem. Rev.*, 1992, **117**, 215.

35 Herbert, A.J.; *J. Chem. Soc.*, 1966, 555.

36 Dewar, M.J.S.; Griffin, A.C.; *J. Chem. Soc., Perkin Trans. 2.*, 1976, 710 and 713.

37 Gray, G.W.; Harrison, K.J.; Nash, J.A.; *Electron. Lett.*, 1973, **9**, 130.

38 Hoshino, N.; Murakami, H.; Matsunaga, Y.; Inabe, T.; Maruyama, Y.; *Inorg. Chem.*, 1990, **29**, 1177.

39 Stebani, U.; Lattermann, G.; Wittenberg, M.; Festag, R.; Wendorff, J.H.; *Adv. Mater.*, 1994, **6**, 572.

40 Chandrasekhar, S.; *Liquid Crystals*, Cambridge University Press, Cambridge, 1977.

41 Romain, F.; Gruger, A.; Guilhem, J.; *Mol. Cryst. Liq. Cryst.*, 1986, **135**, 111.

42 Sciau, P.P.; Lapasset, J.; Moret, J.; *Acta Cryst.*, 1988, **C44**, 1089.

43 Sheldrick, G.M.; SHELXS-86 in *Crystallographic Computing 3*, (eds.), Sheldrick, G.M.; Kruger, C.; Goddard, R. Oxford University Press, 1985.

44 Sheldrick, G.M.; SHELXL-93. In preparation for *J. Appl. Cryst.*, 1993.

45 Dago, A.; Shepelev, Y.; Fajardo, F.; Alvarez, F.; Pomés, R.; *Acta Cryst.*, 1989, **C45**, 1192.

46 Kato, T.; Fréchet, J.M.J.; *J. Am. Chem. Soc.*, 1989, **111**, 8533.

47 Jeffrey, J.A.; *Acc. Chem. Res.*, 1986, **19**, 168.

48 Goodby, J.W.G.; *Mol. Cryst. Liq. Cryst.*, 1984, **110**, 205.

49 Gray, G.W.; Jones, B.J.; *J. Chem. Soc.*, 1953, 4179.

CHAPTER 4

COORDINATION CHEMISTRY OF *N*-ALKYL- AND *N,N*-DIALKYL-*N'*-ACYLTHIOUREA

4.1 Introduction

N-Acylthioureas have given rise to many investigations because of the ability of these molecules to coordinate with several metals[1,2-5]. Studies involving liquid-liquid extraction[6,7] of the platinum group metals as well as the pre-concentration and separation[8] of platinum-group metals from each other, have been reported. Schuster[9] *et al* reported the synthesis of a series of *N,N*-dialkyl-*N'*-benzoylthioureas and found that they are very good reagents for pH-selective extractions of the platinum group metals from interfering metals such as copper, iron and nickel. Furthermore, Schuster[10] *et al* reported that *N*-benzoylthioureas, in particular *N,N*-dihexyl-*N'*-benzoylthiourea / toluene, are excellent reagents for the solvent extraction of gold.

Various studies have shown that the potentially bidentate *N,N*-dialkyl-*N'*-benzoylthioureas form stable, neutral complexes with a variety of transition metals[3]. The large *trans*-influence of the highly polarisable sulfur donor atoms will tend to make the *cis* configuration for square planar ML_2 complexes thermodynamically more stable than the corresponding *trans* configuration[11]. The *trans*-influence of a ligand in a metal complex is defined as the extent to which that ligand weakens the bond *trans* to itself in the equilibrium state of that complex[12]. Accordingly, two sulfur ligands in mutually *trans*-positions will have a destabilising effect on each other when attached to a metal centre[13]. This phenomenon is illustrated in the reported crystal and molecular structures of exclusively the *cis* metal complexes of *N,N*-dialkyl-*N'*-benzoylthiourea. Some recently reported ML_2 and ML_3 complexes include the metals Cu(II)[14], Ni(II)[15], Pt(II)[11], Pd(II)[16], Ru(III)[17] and Rh(III)[18].

The crystal structure of bis(*N,N*-diethyl-*N'*-benzoylthioureato)copper(II) shows that coordination around the metal atom is tetrahedral. The sulfur and oxygen atoms are arranged in a *cis* conformation and the chelate rings are not planar but distorted in the characteristic manner[14]. Similarly, the crystal structures of Ni(II)[15], Pt(II)[11] and Pd(II)[16] show coordination through the sulfur and oxygen atoms, forming a six-membered rings of *cis* configuration. However, coordination around the nickel, platinum and palladium atoms is square planar.

Due to our interest in liquid-crystalline materials and our successful synthesis and characterisation of a few mesogenic *N*-alkyl-*N'*-acylthioureas, we decided to examine the effect of introducing a metal into *N*-alkyl- and *N,N*-dialkyl-*N'*-acylthioureas with the intention of preparing metal-containing liquid crystals. Metal complexes of organic ligands which exhibit liquid-crystalline character are commonly known as *metallomesogens*[19]. In some cases the ligands themselves are mesogenic, but this is not a requirement for producing metallomesogens[19]. Metal-containing liquid crystals are in general terms no different from purely organic mesogens in that they form the same types of mesophases.

Although metallomesogens have been known for more than eighty years[20], this field of research has only recently become prominent. The introduction of a metal into a liquid crystal can result in many new properties. These include:

- new geometries and shapes not usually found in organic chemistry
- coloured and paramagnetic compounds for the d- and f-block transition metals
- a large and polarisable electron density which is a feature of every metal atom.

Polarisibility is one of the most important features of molecules which form liquid crystals and as observed in Chapter 3, any change in polarisibility will have profound effects on the physical characteristics of the compound, with particular reference to the liquid crystal phases produced[19].

A major requirement for metallomesogens to find applications in new device technology is that the metal-ligand bonds are strong and inert, and the complexes stable. This may therefore be accomplished with chelating ligands and the 5d metals[21]. Hence we attempted the synthesis of nickel (II), copper (II), copper (I), platinum (II) and palladium (II) complexes of the potentially chelating *N*-alkyl- and *N,N*-dialkyl-*N*-acylthioureas with the view to preparing metallomesogens. Accordingly, the coordination chemistry of these transition metals is briefly addressed.

Generally nickel compounds in the solid state and almost all in aqueous solution contain the metal in the oxidation state +2, which by consequence, can be considered the ordinary oxidation state for nickel in all its compounds[22]. Nearly all nickel (II) complexes have coordination numbers of four, five and six. Almost all the six-coordinate complexes of nickel (II) have a pseudo-octahedral stereochemistry[22]. The five-coordinate nickel (II) complexes have structures that are generally near to square pyramidal and trigonal bipyramidal. The majority of four-coordinate nickel (II) complexes are square planar[22]. Planar complexes of nickel (II) are often red or yellow and the majority of them formed by either chelate ligands or tetradentate macrocyclic ligands. Nickel (II) is generally considered to be a 'hard' acid[23] and thus preferentially forms complexes with ligands that act as 'hard' bases (HSAB principle)[23].

On the other hand, copper occurs in a range of oxidation states and readily forms complexes yielding an extensive variety of coordination compounds. Copper (I) and copper (II) oxidation states are by far the most abundant; copper (II) is more stable under normal conditions and forms a wealth of simple compounds and coordination complexes[24]. The copper (I) state is less extensive and is readily oxidised to the copper (II) state[24,25]. While copper (II) is generally considered a borderline 'hard' acid, copper (I) clearly behaves like a 'soft' acid and forms stable complexes with class b ligands ('soft' bases)[26]. In general, oxygen and nitrogen

ligands therefore dominate the chemistry of copper (II)[27], whereas sulfur and phosphorus ligands are more frequent in copper (I) chemistry[28].

Complexes of platinum are commonly in oxidation states 0, II or IV. Platinum (II) is classified as a 'soft' metal centre[13] which forms stable, four-coordinate complexes with polarisable ligands[26]. In this general classification, sulfur ligands, e.g. thiolates and thioureas, will form stable complexes with platinum (II) whereas oxygen ligands will form the most stable complexes with the lighter transition metals[23].

Palladium differs from platinum in that it is more reactive and this is reflected in the chemistry of the metal in various oxidation states. Palladium has a well-established chemistry in the 0, I, II and IV oxidation states[22]. Palladium (II) is the dominant oxidation state and is generally regarded as a class b ('soft') metal. This is illustrated in the rich chemistry with sulfur and phosphorus donor ligands[26], whereas few palladium (II) complexes with hard ligands such as oxygen are reported[22].

The *N*-acylthiourea molecule is a potentially bidentate ligand, incorporating sulfur, a 'soft' donor atom, and oxygen, a 'hard' donor atom. The chelate effect is known to lead to a greater number of stable complexes for bidentate ligands[21]. Thus, oxygen donor complexes with 'soft' metals can be stabilised by incorporation into bidentate ligands with other more strongly binding 'soft' atoms such as nitrogen or sulfur[21]. Similarly, sulfur donor complexes with 'hard' metals can be stabilised by incorporation in bidentate ligands with other more strongly bonding 'hard' atoms. It is therefore expected that *N*-acylthioureas will bind relatively strongly to 'hard' metals such as nickel (II), the borderline 'hard' metal copper (II), and 'soft' metals such as platinum (II) and palladium (II).

Continuing the investigation of the chemistry of *N*-alkyl- and *N,N*-dialkyl-*N'*-acylthioureas, we attempted the preparation of selected divalent metal complexes with the aim of preparing metal-containing liquid crystals. Accordingly, the present study includes:

- the synthesis and characterisation of Ni (II), Cu(II), Pt (II) and Pd (II) complexes of *N*-alkyl-*N'*-acylthiourea and *N,N*-dialkyl-*N'*-acylthiourea
- the influence of the alkyl chain length, acyl moiety and coordinated metal on the physical properties of the complexes
- an examination of the differences in metal coordination chemistry between the *N*-alkyl-*N'*-acylthiourea and *N,N*-dialkyl-*N'*-acylthiourea.

4.2 Results and Discussion

4.2.1 Coordination chemistry of *N,N*-dialkyl-*N'*-benzoylthiourea

The nickel (II), copper (II), platinum (II) and palladium (II) complexes of the dibutyl, dihexyl and dioctyl derivatives of *N,N*-dialkyl-*N'*-benzoylthiourea were synthesised in 70 - 90 % yield and characterised by C, H and N elemental analysis and, for certain complexes, mass spectrometry and NMR spectroscopy. A detailed account of the characterisation of the complexes is recorded in the experimental section.

The nickel and copper complexes were synthesised by reacting two equivalents of ligand with one equivalent of metal acetate in DMF/water mixtures[1]. The *N,N*-dialkyl-*N'*-acylthiourea ligands form purple nickel (II) complexes and dark green copper (II) complexes. The platinum and palladium complexes were synthesised by reacting two equivalents of the ligand with one equivalent of potassium tetrachloroplatinate or potassium tetrachloropalladate in dioxane / water mixtures[29]. The *N,N*-dialkyl-*N'*-benzoylthiourea ligands form yellow platinum (II) complexes and orange / brown palladium (II) complexes.

In accordance with previous studies[11,14-17], the C, H and N elemental analysis and ^{1}H and ^{13}C NMR, of the Pt(II), Pd(II) and Ni(II) complexes, suggests that the products are the deprotonated bis chelates. Furthermore, positive fast atom bombardment (+FAB) analyses of selected nickel complexes of *N,N*-dialkyl-*N'*-benzoylthiourea displayed peaks corresponding to NiL_2, consistent with bis(*N,N*-dialkyl-*N'*-benzoyl-thioureato)nickel(II). The chemical shifts of the signals in the ^{1}H and ^{13}C NMR spectra of the nickel (II), platinum (II) and palladium (II) complexes of *N,N*-dialkyl-*N'*-benzoylthiourea, are similar to those previously reported by Koch[30] *et al* for *cis-(N,N*-dibutyl-*N'*-benzoylthioureato)platinum (II) and palladium (II). Hence it is assumed that the present complexes all have the *cis* conformation of ligands around the central metal ion (Figure 4.1).

Figure 4.1 Schematic representation of the structure of a *cis*-bis(*N,N*-dialkyl-*N'*-benzoylthioureato)metal(II) complex[11,14-17]. Note the *cis* arrangement of atoms around the metal ion.

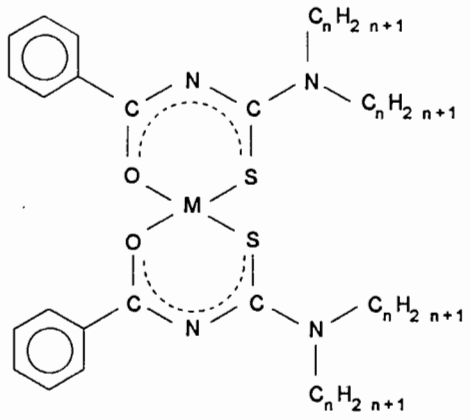

The melting points of the nickel, platinum and palladium complexes are higher than that of the analogous ligands, whereas the melting points of the copper complexes are approximately equal to or lower than that of the parent ligand (Table 4.1). The melting point of the metal (II) complexes decreases in the order PtL_2 > PdL_2 > NiL_2 > CuL_2.

Table 4.1 Melting point (°C) of *N,N*-dibutyl- (n=4), *N,N*-dihexyl- (n=6) and *N,N*-dioctyl-*N'*-benzoyl-thiourea (n=8) and their Cu(II), Ni(II), Pd(II), Pt(II) metal complexes.

n	L	$Cu(II)L_2$	$Ni(II)L_2$	$Pd(II)L_2$	$Pt(II)L_2$
4	91-92	94-96	132-134	142 - 144	162 - 163
6	57-58	39-41	74-76	83 - 84	95 - 97
8	52-54	liquid	75-77	92 - 94	91 - 93

No liquid-crystalline behaviour was observed for the *cis*-bis(*N,N*-dialkyl-*N'*-benzoylthioureato)metal(II) complexes of nickel, copper, platinum and palladium with the aid of polarising optical microscopy. In other words, heating of the complexes results in a direct transformation from the crystalline state into the isotropic liquid without passing through any mesogenic phases. Supercooling of the isotropic liquid allows for the crystallisation to a solid material.

The absence of mesogenic behaviour for the *cis*-bis(*N,N*-dialkyl-*N'*-benzoylthioureato)metal(II) complexes was confirmed with the aid of DSC experiments. The DSC heating curve of *cis*-bis(*N,N*-dihexyl-*N'*-benzoylthioureato)nickel(II) is shown in Figure 4.2. It is interesting to note that the heating thermogram of *cis*-bis(*N,N*-dibutyl-*N'*-benzoylthioureato)nickel(II) and *cis*-bis(*N,N*-dihexyl-*N'*-benzoylthioureato)nickel(II) shows two endothermic peaks at 129.5 and 134.7 °C, and 52.0 and 78.9 °C respectively. At the first endothermic peak, the crystals transform irreversibly to a more stable crystalline phase. This is confirmed by the second run, in which the samples heated to 140 and 80 °C respectively, and then cooled to room temperature, were re-heated. The second heating thermogram shows only a single endothermic peak, representing melting, at 134.7 and 78.9 °C respectively for *cis*-bis(*N,N*-dibutyl-*N'*-benzoylthioureato)nickel(II) and *cis*-bis(*N,N*-dihexyl-*N'*-benzoylthioureato)nickel(II).

Figure 4.2 The DSC heating curve with a scanning rate of 10 °C.min^{-1} for (**a**) crystals of *cis*-bis(*N,N*-dihexyl-*N'*-benzoylthioureato)nickel(II) and (**b**) the specimen previously heated to 80 °C and then cooled to room temperature.

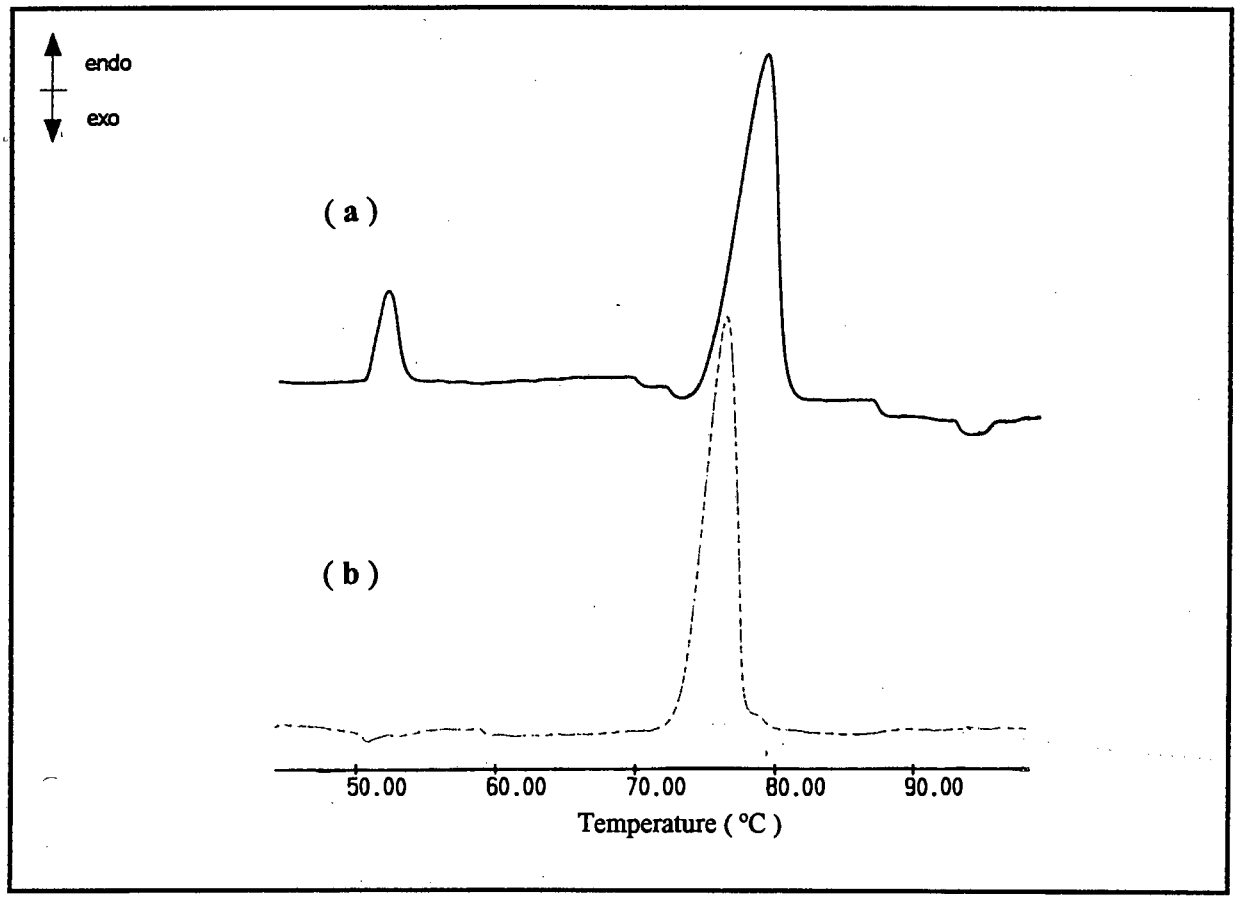

The absence of mesogenic character for the *cis*-bis(*N,N*-dialkyl-*N'*-benzoylthioureato)metal(II) complexes was disappointing. However, in view of the fact that the majority of mesogenic β-diketonato complexes show a *trans* arrangement of ligands around the central metal atom[19], we decided to investigate whether we could prepare the corresponding *trans*-bis(*N,N*-dialkyl-*N'*-benzoylthioureato)metal(II) complexes.

4.2.2 Protonation Studies

The *cis* isomers of *cis*-bis(*N,N*-dialkyl-*N'*-benzoylthioureato)metal(II) are thermodynamically more stable than the corresponding *trans* isomers as a result of the *trans*-influence of the sulfur groups[11]. However *trans*-$[ML_2]$ might be expected to be isolable when considering the formation of *cis* and *trans* thiourea complexes in the Kurnakov test[31], where the reaction of thiourea with *cis*-$[Pt(NH_3)_2Cl_2]$ yields $[Pt(tu)_4]^{2+}$, whereas with *trans*-$[Pt(NH_3)_2Cl_2]$ it reacts to give *trans*-$[Pt(NH_3)_2(tu)_2]^{2+}$.

Furthermore, the *cis*- and *trans*-$[PtL_2X_2]$ complexes (where L = monodentate thiourea, X = Cl^- and Br^-), have been reported and examined by ^{195}Pt NMR[32]. It was recently reported[33] that the reaction of *N*-propyl-*N'*-benzoylthiourea with K_2PtCl_4 yields mixtures of *cis*- and *trans*-bis(*N*-propyl-*N'*-benzoylthioureato)-dichloroplatinum(II), *cis*-$[PtX_2L_2]$ and *trans*-$[PtX_2L_2]$. Accordingly, in the case of the formation of a square planar $[PtL_2]$ complex, two configurations, *cis* and *trans*, may be possible while the corresponding protonated *cis* and *trans* species, $[PtL(LH)]^+$ and $[Pt(LH)_2]^{2+}$, may be postulated as shown below:

$$[PtCl_4]^{2-} + 2LH \rightarrow \textit{cis/trans}\text{-}[Pt(LH)_2]Cl_2 + 2Cl^-$$
$$[Pt(LH)_2]Cl_2 \rightarrow [Pt(LH)L]Cl + HCl$$
$$[Pt(LH)L]Cl \rightarrow [PtL_2] + HCl$$

In general, for complexes of the type $[PtX_2L_2]$ the *cis* isomers are enthalpy favoured, but entropy changes in solution favour the *trans* form[34]. The free energy differences between the *cis* and *trans* forms are usually quite small and changes in ligand, solvent or temperature can effect the equilibrium position.

$$\text{cis-}[PtX_2L_2] \underset{H\ -ve}{\overset{S\ +ve}{\rightleftharpoons}} \text{trans-}[PtX_2L_2]$$

It may thus be reasonable to anticipate that protonation of *cis*-$[PtL_2]$, with mineral acid, HX, may yield complexes of the type *cis*-$[PtX_2L_2]$. Hence, the question arises as to whether the isomerisation of *cis*-$[PtX_2L_2]$, under favourable conditions, may take place in solution to yield the corresponding *trans*-$[PtX_2L_2]$. Following deprotonation under appropriate conditions, it may be possible to isolate the corresponding neutral *cis*-$[PtL_2]$ and *trans*-$[PtL_2]$ isomers.

Due to our interest in *trans*-bis(*N,N*-dialkyl-*N'*-benzoylthioureato)metal(II) complexes as metallomesogens[19], we decided to examine the effect of protonation on *cis*-bis(*N,N*-dibutyl-*N'*-benzoylthioureato)platinum(II). The effect of protonation on this complex was studied by means of high resolution ^{1}H and ^{195}Pt NMR spectroscopy. The ^{1}H spectra of complex reactions are not always easy to unravel hence the latter technique is particularly useful. This is because reactions involving platinum ions can readily be studied as the metal chemical shift is sensitive to the types of ligand within the coordination sphere[35]. Moreover, there is a dependence of the ^{195}Pt chemical shift on the complex geometry. The sensitivity of the chemical shift to molecular structure is sufficient to ensure that there is seldom overlap of signals; geometric and stereo-isomers can easily be separated by hundreds and tens of ppm, respectively. Furthermore, the metal shift dispersion is relatively large thereby facilitating identification of the reaction complexes[35].

It is noteworthy that both solvent and temperature affect the ^{195}Pt chemical resonance. A change in solvent can result in shifts amounting to several hundred parts per million[36]. It is therefore obvious that conclusions as to molecular structure which are based on small differences in chemical shifts in the ^{195}Pt NMR spectra, are drawn from measurements made in the same solvent.

A recent report by Koch[11] *et al* discussed the acid-base chemistry of bis(*cis-N,N*-dibutyl-*N'*-benzoylthioureato)platinum(II) in solution. They reported that neutral *cis*-$[PtL_2]$ complexes may readily be protonated to yield a distribution of *cis*-$[Pt(HL)L]^{+}$ and *cis*-$[Pt(HL)_2)]^{2+}$ cationic species which were characterised by high resolution multinuclear NMR. They also reported that the ^{195}Pt chemical shift of the cationic species were strongly dependent on the nature of the uncoordinated anion (Cl^-, Br^-, I^-) present, and suggested that this was due to tight ion-pair formation in solution. However, recent work in our laboratory (see Chapter 6) has led us to question the existence of such cationic species, prompting a more detailed examination of the nature of these species.

In this section of the thesis it is necessary that we distinguish between a deprotonated chelating ligand coordinated to a metal through both the *S*- and *O*-atoms, represented as (L-*S,O*), and a protonated ligand that is bonded to the metal *via* the *S*-atom only, (HL-*S*).

Experimental Procedure

All ^{1}H and ^{195}Pt NMR spectra were recorded in $CDCl_3$ solution at 25 °C. The following experimental procedure was performed and the ^{1}H and ^{195}Pt NMR spectra recorded.

(a) The *cis*-$[Pt(L\text{-}S,O)_2]$ complex, between 25 and 75 mg, was dissolved in 0.6 ml $CDCl_3$, to give a clear, pale yellow solution. The ^{1}H and ^{195}Pt NMR spectra were recorded.

(b) Aliquots of 100 μL concentrated hydrochloric acid was added to the NMR tube containing the *cis*-[Pt(L-*S,O*)$_2$] complex in $CDCl_3$. After vigorous shaking the phases were allowed to separate. Where necessary the distinctly darker yellow/range organic phase was filtered through a microfibre glasswool, resulting in a clear solution prior to NMR spectroscopy.

(c) After spectral acquisition, the aqueous phase was removed and the $CDCl_3$ solution washed with water, followed by re-acquisition of the spectra.

(d) Finally the NMR solution was washed with concentrated ammonia, filtered, and the NMR spectra re-acquired.

The effect of protonation on *cis*-bis(*N,N*-dibutyl-*N'*-benzoylthioureato)platinum(II)

The ^{195}Pt spectra, in $CDCl_3$, of *cis*-bis(*N,N*-dibutyl-*N'*-benzoylthioureato)platinum(II), *cis*-[Pt(L-*S,O*)$_2$], shows a single sharp resonance at -2727 ppm (Figure 4.3(a)). The corresponding ^1H NMR spectrum is consistent with only a single deprotonated complex species in solution, as confirmed by the absence of the characteristic N - H resonance in the 8 - 10 ppm range.

Addition of 100 μL of *conc.* HCl directly to the NMR tube, containing the *cis*-bis(*N,N*-dibutyl-*N'*-benzoylthioureato)platinum(II) complex, yields a spectrum consisting of two ^{195}Pt resonances at -3218 ppm (rel. int. 78 %) and -3034 (22 %) (Figure 4.3(b)). In the corresponding ^1H NMR spectrum of this solution, two signals at 11.14 ppm (rel. int. 82%) and 10.79 (18 %) assigned to the N - H resonances, confirm protonation of the coordinated ligands. The two N - H resonances imply that either different complexes exist in solution or that the sites of protonation of the coordinated ligand are in-equivalent and in slow exchange on the NMR time scale, in the same complex. The latter possibility is, however, ruled out by the presence of two resonances in the ^{195}Pt NMR spectra which indicate at least two distinctly different complex species in solution.

Removal of the excess mineral acid from the $CDCl_3$ solution and subsequent washing with distilled water yields a spectrum consisting of three ^{195}Pt resonances at -3218 (rel. int. 43 %), -3034 (3 %) and -2968 (54 %) ppm (Figure 4.3(c)). In the corresponding ^1H NMR spectrum of this solution, three resonances at 11.14 (rel. int. 40%), 10.79 (4%) and 11.27 ppm (56%) assigned to the N - H protons, confirm protonation of the coordinated ligands.

Washing of the NMR solution with 5 M ammonia solution yields ^1H and ^{195}Pt NMR spectra identical to that of the starting neutral *cis*-[Pt(L-*S,O*)$_2$] complex. There is no evidence of any other species in solution.

Figure 4.3 ^{195}Pt NMR spectrum acquired during protonation of *cis*-bis(*N,N*-dibutyl-*N'*-benzoylthioureato)-platinum(II), *cis*-[Pt(L-*S,O*)$_2$], in $CDCl_3$ at 30 °C.

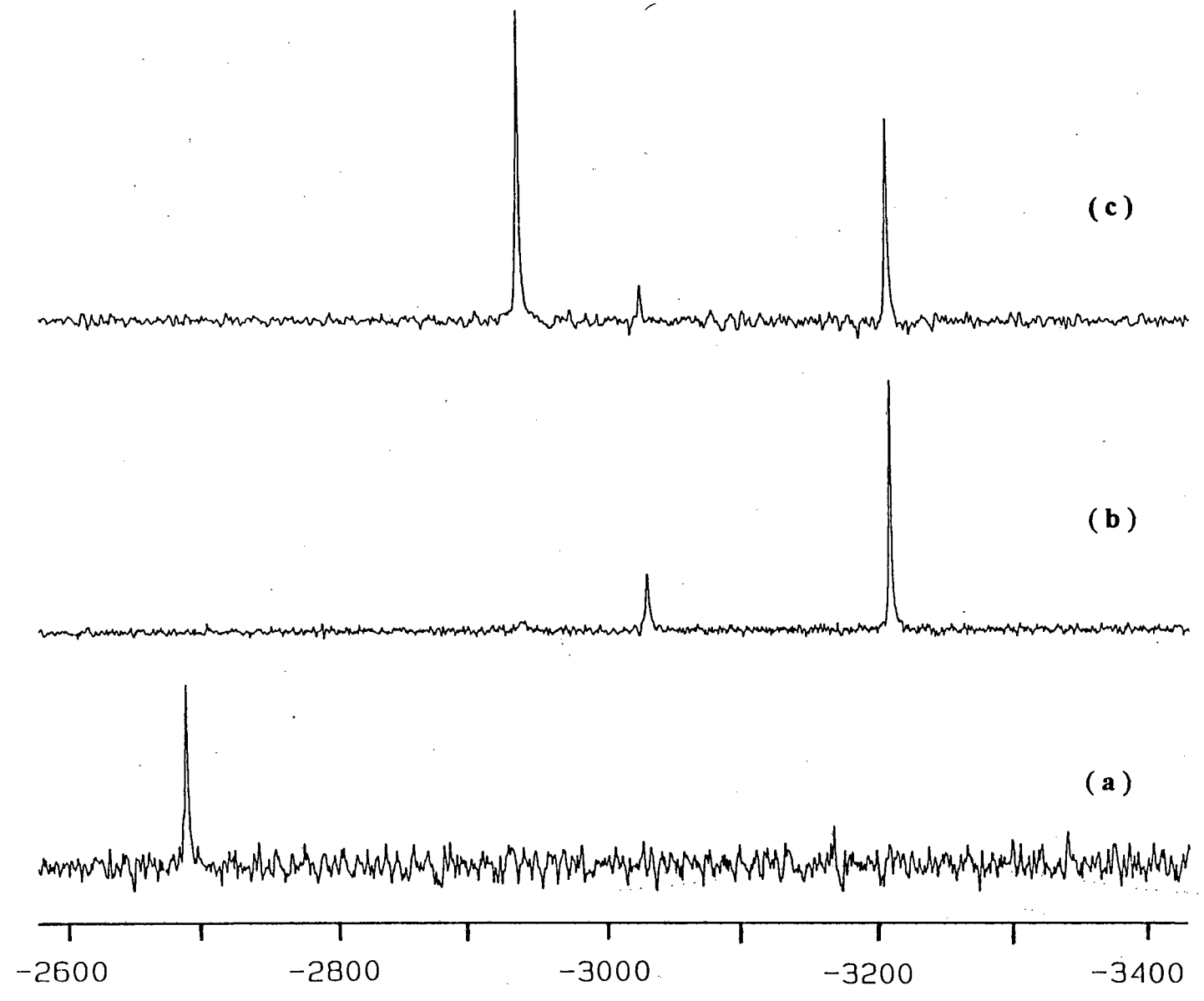

(a) *cis*-[Pt(L-*S,O*)$_2$] **(b)** *cis*-[Pt(L-*S,O*)$_2$] + HCl **(c)** *cis*-[Pt(L-*S,O*)$_2$] + HCl + H_2O.

Consideration of the ^{195}Pt and ^{1}H NMR spectra obtained on addition of HCl to a solution of the *cis*-[Pt(L-*S,O*)$_2$] complex suggests that protonation of the bound ligand in the presence of coordinating Cl^- anions, leads to ring opening of the *S,O*-chelate such that the *N,N*-dialkyl-*N'*-benzoylthiourea ligand remains bound to Pt through the *S*-atom only. The dramatic upfield shift of the resonances in the ^{195}Pt spectrum suggests the coordination of chloride anions. Pregnosin[36] reported that the ^{195}Pt shift moves to high field in the order S > Cl^- > O. Kerrison and Sadler[37] reported upfield shifts on sequential replacement of oxygen-bonded DMSO by Cl^- in *cis*-[Pt(SOMe$_2$)$_2$(OSMe$_2$)$_2$]$^{2+}$ from -3070 to -3459 ppm. It is thus reasonable to postulate that the peaks at -3218 and -3034 ppm represent di-coordinated Cl^- complexes. Thus, the *O*-atom of the *N*-acyl moiety of the ligand is displaced from the coordination sphere of the Pt(II) atom by the Cl^- anion. Strong support for this postulate is obtained from the ^{195}Pt spectrum of a mixture of *cis*- and *trans*-bis(*N*-propyl-*N'*-benzoylthioureato)dichloroplatinum(II), in $CDCl_3$, which shows peaks at -3219 and -3040 ppm respectively[38]. The resonance at -3219 ppm represents *cis*-bis(*N*-propyl-*N'*-benzoythioureato)dichloro-platinum(II), which has been characterised crystallographically[33]. It is therefore reasonable to assign the resonance at -3218 ppm to the *cis*-[Pt(HL-*S*)$_2$Cl$_2$] complex and the resonance at -3034 ppm to the *trans*-[Pt(HL-*S*)$_2$Cl$_2$] isomer, in which the protonated ligands, HL, are coordinated *via* the *S*-atom to the Pt(II) atom.

Assignment of the relatively small ^{195}Pt peak at -3034 ppm to the *trans*-[Pt(HL-*S*)$_2$Cl$_2$] isomer is further supported by the work of Castan[32] *et al* who reported similar ^{195}Pt shift trends for *cis*- and *trans*-[PtL$_2$X$_2$] complexes in DMSO-d_6 solution (where L = monodentate thiourea ligands and X = Cl^- and Br^-). Furthermore the ^{195}Pt peak at -3034 ppm is at an intermediate chemical shift between the deprotonated, chelated *cis*-[Pt (L-*S,O*)$_2$] complex at -2708 ppm, and the *cis*-[Pt(HL-*S*)$_2$Cl$_2$] complex at -3216 ppm. The assignment is in accordance with the fact that the sequential addition of chloride coordinating ligands results in upfield platinum chemical shifts and the general observation that the chemical shifts of *trans* platinum species are usually downfield compared to the corresponding *cis* platinum species[36].

Interpretation of the ^{1}H and ^{195}Pt spectra suggests that the ^{195}Pt peak at -2968 ppm, present after washing the NMR solution with distilled water, represents the *cis*-[Pt(L-*S,O*)(HL-*S*)Cl] complex. In the corresponding ^{1}H NMR spectrum of this solution, only one N - H signal at 11.27 ppm is evident for this species. The ^{195}Pt signal at -2968 ppm is slightly upfield from the signal of the neutral *cis* isomer which is consistent with Pregosin's observed upfield shifts on coordination of chloride ligands[36].

The formation of only the *cis*-[Pt(L-*S,O*)$_2$] complex on washing of a previously acid treated solution with 5 M ammonia, implies that rapid isomerisation of the *trans*-[Pt(HL-*S*)$_2$Cl$_2$] complex must accompany deprotonation and / or ring closure to yield exclusively the *cis*-[Pt(L-*S,O*)$_2$] complex. This is because no evidence of any other resonances in either the ^{1}H or ^{195}Pt NMR spectra corresponding to a *trans*-[Pt(L-*S,O*)$_2$] isomer could be found (excluding undetectable trace amounts).

It is interesting to note the remarkably rapid chelate-ring opening, following protonation of the chelated ligand, and chelate-ring closure, following deprotonation of the *S*-coordinated ligand. Presumably deprotonation results in the *N*-acyl carbonyl donor atom becoming substantially more nucleophilic (existing essentially in a O^- form) toward Pt (II) coordination. Moreover, the pendant *N*-acyl moiety is clearly held in a favourable position within the coordination sphere of the Pt (II) atom, resulting in rapid closure of the chelate ring. The effects of protonation on *cis*-bis(*N,N*-dialkyl-*N'*-benzoylthioureato)platinum(II) are summarised diagrammatically in Figure 4.4. The present results therefore suggest that chelation can be pH controlled and hence these ligands may have interesting and potentially useful industrial applications.

Figure 4.4 Schematic representation of the effects of addition of *conc.* HCl to a solution of *cis*-[Pt(L-*S,O*)$_2$] complex in $CDCl_3$ (L = *N,N*-dialkyl-*N'*-benzoylthiourea).

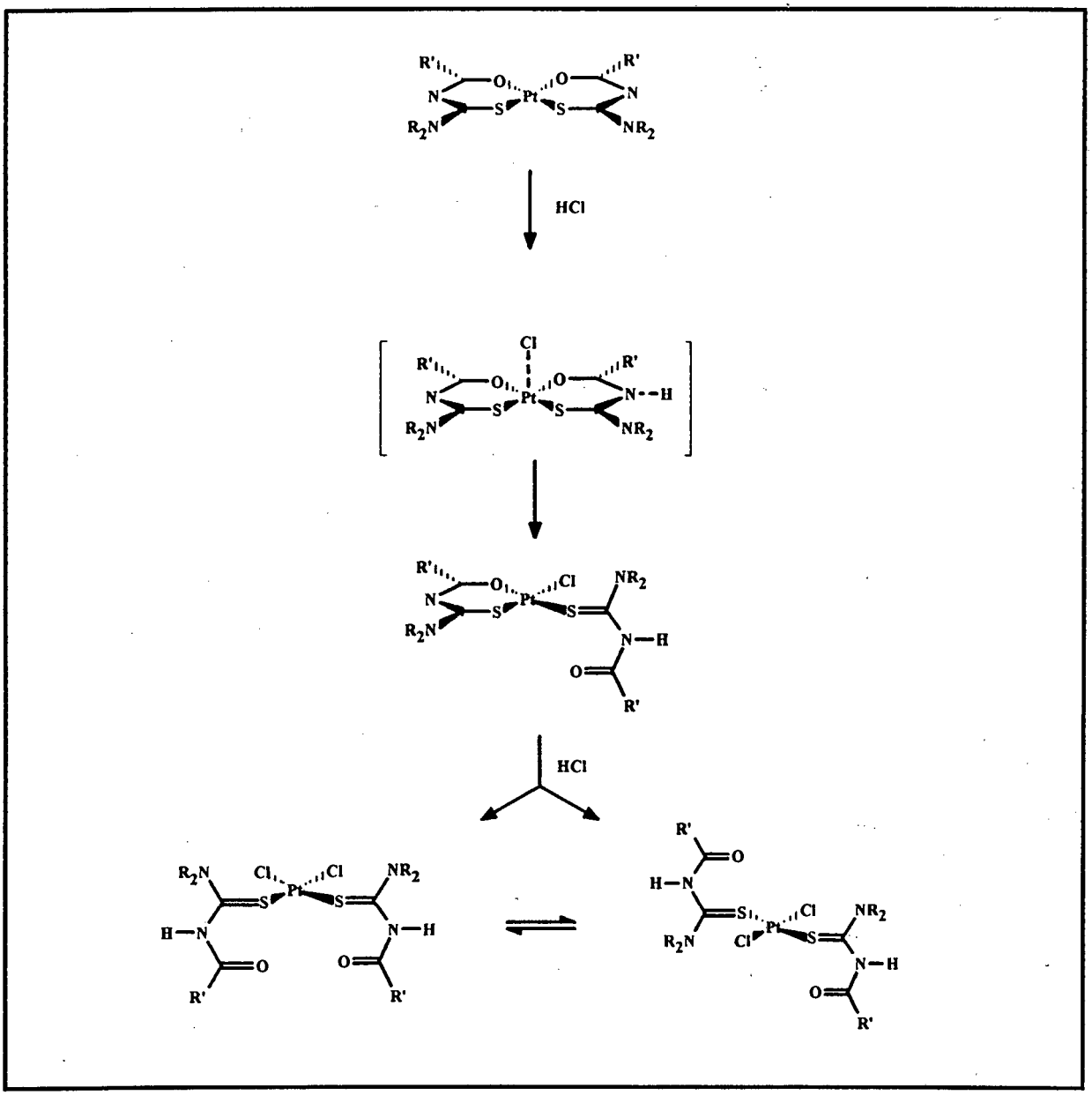

Unfortunately, protonation of *cis*-bis(*N,N*-dialkyl-*N'*-benzoylthioureato)metal(II) does not yield any of the corresponding *trans*-bis(*N,N*-dialkyl-*N'*-benzoylthioureato)metal(II) complex. The latter complex may have proved to have interesting physical properties as a result of the elongated rod-shaped structure and *trans* arrangement of ligands around the central square-planar metal atom.

4.2.3 Coordination chemistry of *N,N*-dialkyl-*N'*-naphthoylthiourea and *N,N*-dialkyl-*N'*-anthracoylthiourea

The naphthyl and anthracyl groups introduce to *N*-acylthioureas a potentially fluorescent probe and a sterically demanding acyl group. These properties could prove interesting with respect to the coordination chemistry of *N*-alkyl- and *N,N*-dialkyl-*N'*-acylthiourea compounds. The use of *N*-acylthioureas for the selective solvent extraction of the platinum group metals is well known[6-10]. Fluorescent probes could have exciting applications in this regard for the analytical determination of the platinum group metals. Furthermore, in view of the recently described isolation of the first *trans* *N*-acylthiourea platinum (II) complex[29], in which the coordinated ligand incorporates a naphthyl moiety, we decided to examine the effect of a bulky acyl group on the coordination chemistry of the nickel (II) and copper (II) derivatives of *N,N*-dialkyl-*N'*-naphthoylthiourea and *N,N*-dialkyl-*N'*-anthracoylthiourea. Trans metal complexes of *N*-naphthoyl- or *N*-anthracoylthiourea could potentially yield fluorescent metal-containing liquid crystals.

The nickel (II) and copper (II) complexes of *N,N*-dibutyl-, *N,N*-dihexyl- and *N,N*-dioctyl-*N'*-naphthoylthiourea and *N,N*-dioctyl-*N'*-anthracoylthiourea were synthesised by reacting two equivalents of ligand with one equivalent of metal acetate in DMF/water[1]. The products were obtained in 70 - 90 % yield and characterised by C, H and N elemental analysis. ^{1}H and ^{13}C NMR spectra of selected nickel complexes were recorded in $CDCl_3$, at 25 °C. The physical and analytical data are recorded in the experimental section.

The ^{1}H NMR spectra of *cis*-bis(*N,N*-dialkyl-*N'*-naphthoylthioureato)nickel(II) and *cis*-bis(*N,N*-dialkyl-*N'*-anthracoylthioureato)nickel(II) are consistent with only one deprotonated complex, as confirmed by the absence of the N - H resonance in the 8 - 9 ppm region. The chemical shifts of the naphthyl protons of the nickel complexes are in accordance with those observed by Koch[29] *et al* for the *cis* isomer of bis(*N,N*-dibutyl-*N'*-naphthoylthioureato)platinum(II). No evidence of any *trans* species was evident in the ^{1}H NMR spectrum. We have not been able to unambiguously ascertain from a crystal structure determination, that the bis(*N,N*-dialkyl-*N'*-anthracoylthioureato)nickel(II) complex has the *cis* conformation of ligands around the nickel atom. However, the similarity between the carbonyl and thiocarbonyl signals in the ^{13}C NMR spectra of bis(*N,N*-dialkyl-*N'*-anthracoylthioureato)nickel(II) and *cis*-bis(*N,N*-dialkyl-*N'*-naphthoylthioureato)nickel(II) suggests that the complex is the *cis* isomer. The NMR spectra of *cis*-bis(*N,N*-dialkyl-*N'*-anthracoyl-thioureato)nickel(II) did not show evidence of any other species in solution.

The melting point of the nickel (II) and copper (II) complexes *N,N*-dialkyl-*N'*-naphthoylthiourea are lower than that of the corresponding ligands (Table 4.2), with the exception of *cis*-bis(*N,N*-dibutyl-*N'*-naphthoyl-thioureato)nickel(II). Interestingly, the copper and nickel complexes of the dihexyl derivative are both liquids at room temperature, whereas the analogous dibutyl and dioctyl derivatives are all solids. In general, the melting point of the nickel and copper complexes decrease with an increase in alkyl chain length.

Table 4.2 A comparison of the melting points (°C) of the nickel and copper complexes of *N,N*-dialkyl-*N'*-naphthoylthiourea with respect to the uncomplexed ligand.

n (chain length)	**Ligand**	**Ni(II)L_2**	**Cu(II)L_2**
4	97 - 99	109 -111	81 - 83
6	71 - 72	liquid	liquid
8	82 - 83	40 - 44	48 - 50

In Chapter 2 we reported that the melting point of *N,N*-dioctyl-*N'*-anthracoylthiourea is lower than that of the corresponding benzyl and naphthyl derivatives. However, it is interesting to note that the melting point of the nickel and copper complexes of the anthracyl derivatives are significantly higher than that of the analogous benzyl and naphthyl complexes (Table 4.3). In view of these results, future work comparing the X-ray crystal structures of analogous benzyl, naphthyl and anthracyl complexes could prove most illuminating with respect to intermolecular contacts and packing of molecules in the solid state.

Table 4.3 The melting points (°C) of nickel and copper complexes of *N,N*-dioctyl-*N'*-benzoylthiourea, *N,N*-dioctyl-*N'*-naphthoylthiourea and *N,N*-dioctyl-*N'*-anthracoylthiourea.

acyl moiety	**n (chain length)**	**ligand (LH)**	**Ni(II)L_2**	**Cu(II)L_2**
benzyl	8	52 - 54	75 - 77	liquid
naphthyl	8	82 - 83	40 - 44	48 - 50
anthracyl	8	43 - 47	143 - 145	132 - 134

It was thus with great delight that we discovered that 1,6-bis(*N,N*-dioctylthiourea)-hexan-1,6-dione displays mesogenic behaviour. Heating of the solid crystalline material results in a direct solid to isotropic liquid transition at 77 °C. Slow cooling of the isotropic liquid to 48 °C allows for the formation of highly coloured *spherulites* each carrying a familiar cross of extinction. Upon further cooling, the spherulites coalesce to form a pronounced *pseudo-focal-conic texture*[39] **(photograph 12)**. The backs of the fans of the focal-conic texture are smooth. The mesophase appears at a relatively slow rate on cooling of the isotropic liquid and remains in this liquid-crystalline state for several hours at room temperature. The structure of this monotropic mesophase with the spherulitic texture is not currently known and deserves further investigation.

Recently, Stebani and Lattermann[39] synthesised 3,4-bis(alkoxy)benzoyl substituted diethylenetriamine compounds which show monotropic liquid-crystalline phases exhibiting a pseudo-focal-conic texture similar to that observed for compound 7. Their preliminary X-ray measurements indicated a smectic / lamellar structure. It is thus apparent that X-ray measurements must be performed in order to identify the structure of the monotropic mesophase of 1,6-bis(*N,N*-dioctylthiourea)-hexan-1,6-dione.

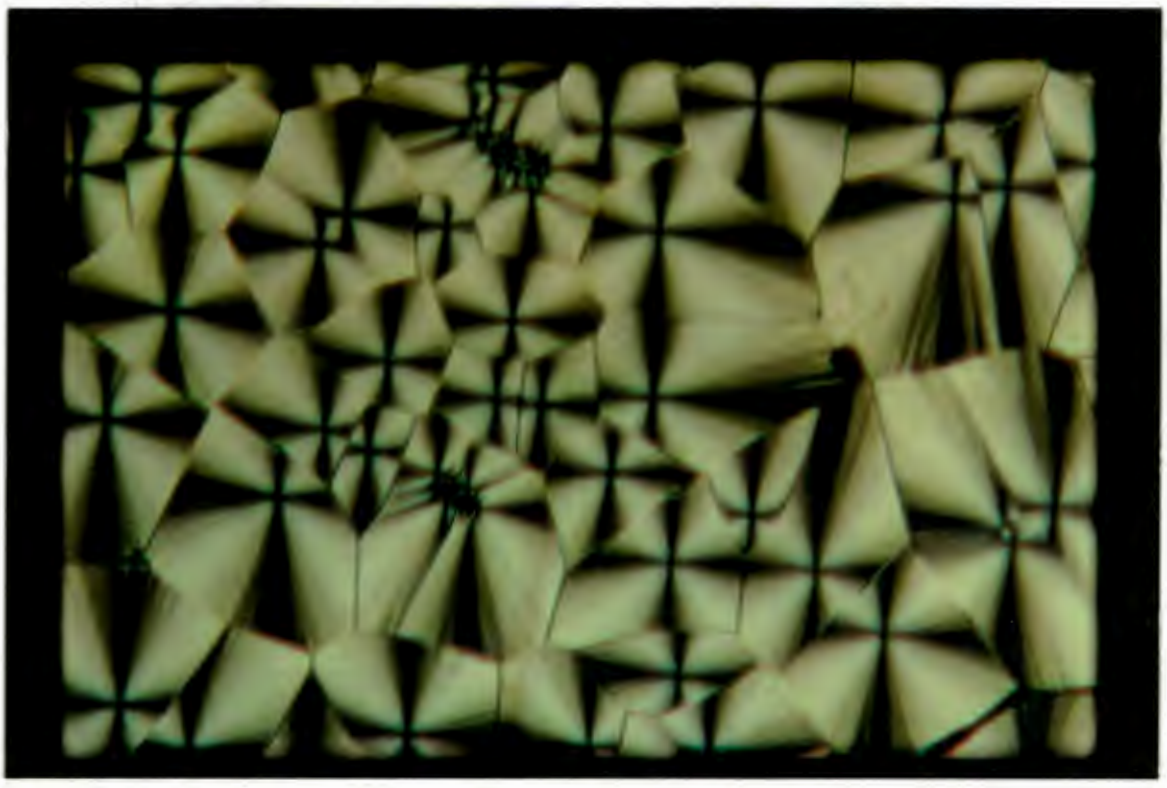

Photograph 12 Pseudo-focal-conic texture of 1,6-bis(*N,N*-dioctylthiourea)-hexan-1,6-dione (7) after standing for several hours at room temperature.

Interestingly, the nickel complexes of *N,N*-dialkyl-*N'*-benzoylthiourea are not stable to silica gel chromatography. The nickel (II) complex decomposes to yield the corresponding *N,N*-dialkyl-*N'*-benzoyl-thiourea ligand, which can be recovered quantitatively after chromatography. Accordingly, one could anticipate that the metal complex is protonated in the presence of acidic silica gel. This could result in chelate ring opening and decomposition to yield the corresponding ligand. Whether decomposition occurs due to the breaking of the nickel-sulfur or the nickel-oxygen bond is not known at this stage. However, based on the fact that hard acids (nickel) prefer hard bases (oxygen) (HSAB principle)[23], we propose that the nickel-sulfur bond will be more readily broken (hard acid / soft base) than the stronger nickel-oxygen bond (hard acid / hard base).

In conclusion, we found no evidence for the formation of the corresponding *trans* isomers of *cis*-bis(*N,N*-dioctyl-*N'*-naphthoylthioureato)nickel(II) and *cis*-bis(*N,N*-dioctyl-*N'*-anthracoylthioureato)nickel(II). This result was surprising and disappointing, in view of the recently reported isolation of *trans*-bis(*N,N*-dibutyl-*N'*-naphthoylthioureato)platinum(II)[29]. It therefore seems reasonable to propose that the lack of formation of any *trans* species may be ascribed either to the manner in which the complexes were prepared, or to the influence of the metal on the *cis-trans* isomerism. The present nickel (II) complexes were synthesised using nickel (II) acetate which implies that a base is present throughout the reaction, whereas the preparation of the *trans*-bis(*N,N*-dibutyl-*N'*-naphthoylthioureato)platinum(II) involved the synthesis of the protonated platinum complex, followed by deprotonation of the crude product with dilute NaOH[29]. Moreover, the reactions were performed in different solvents and it is known that changes in solvent can effect the *cis-trans* equilibrium position[36]. Further work aimed at understanding and exploiting the *cis/trans* isomerism deserves attention.

4.2.4 Coordination chemistry of *N*-alkyl-*N'*-benzoylthiourea

On the basis of the X-ray crystal structure of *N*-butyl-*N'*-benzoylthiourea, one may anticipate that the coordination chemistry of the *N*-alkyl-*N'*-benzoylthiourea ligands will be different to that of the *N,N*-dialkyl-*N'*-benzoylthioureas. In continuation of our original idea of preparing metal-containing liquid crystals, we attempted to synthesise the *N*-alkyl-*N'*-benzoylthiourea complexes of copper (II) and nickel (II). The resulting complexes were studied with the aid of ^{1}H and ^{13}C NMR spectroscopy, C, H and N elemental analysis and +FAB spectrometry. The characterisation of the complexes is recorded in the experimental section.

Nickel complexes of N-alkyl-N'-benzoylthiourea

The remarkable difference in coordination chemistry between *N,N*-dialkyl-*N'*-benzoylthiourea and *N*-alkyl-*N'*-benzoylthiourea is clearly illustrated in the reaction with nickel(II)acetate. The *N,N*-dialkyl-*N'*-benzoyl-thiourea compounds form stable *cis*-[NiL_2] complexes whereas the *N*-alkyl-*N'*-benzoylthioureas do not form stable complexes under any conditions.

Copper complexes of N-alkyl-N'-benzoylthiourea

The reaction of two equivalents of *N*-dodecyl-*N'*-benzoylthiourea or *N*-tetradecyl-*N'*-benzoylthiourea with one equivalent of copper (II) acetate in DMF[1], produced a yellow crystalline material. The product was purified by means of preparative chromatography, using $CHCl_3$ as eluent, and recrystallised from $CHCl_3$ / EtOH to yield a yellow copper complex. The yellow colour of the complex, in addition to the sharp ^1H NMR signals, implies that copper is in an oxidation state of +I which implies that copper (II) is reduced to Cu(I) in the course of the reaction.

No mesogenic behaviour is observed (polarising optical microscopy) for the copper (I) complex of *N*-dodecyl-*N'*-benzoylthiourea or *N*-tetradecyl-*N'*-benzoylthiourea. The complexes show a direct transition from the solid state into the isotropic liquid at a sharp melting point, and slow cooling of this liquid results in a direct transition to the solid phase without passing through any liquid-crystalline phase. These observations were confirmed from the DSC thermograms.

Sharp resonances are observed in the ^1H and ^{13}C NMR spectra of the copper complex of *N*-tetradecyl-*N'*-benzoylthiourea. No amidic N - H signal is observed in the proton spectrum, which indicates that the ligand is deprotonated. The proton spectrum is not straightforward and clearly shows two sets of resonances in a 2 : 1 ratio. This suggests that either the ligand is in two different environments in the same metal complex, or that two different complex species are present in solution. The latter possibility is, however, ruled out by the fact that the complex is chromatographically homogeneous (silica gel sheets / variety of solvents) and only one species is evident in the ^{13}C NMR spectrum. Further evidence supporting a single species are the observed elemental analyses (Table 4.4), which suggest that the ligand and metal are in a 1 : 1 ratio, and the +FAB spectrum which shows *m/z* signals at 411.2 and 827.2 representing $[Cu(LH_2)]^+$ and $[Cu_2(LH_2)_2]^{2+}$ respectively (Table 4.5).

Table 4.4 Calculated and observed % C, H and N elemental analyses for the copper (I) complex of *N*-dodecyl-*N'*-benzoylthiourea (LH_2)[1e] and *N*-tetradecyl-*N'*-benzoylthiourea (LH_2)[1f].

		% C	% H	% N
Cu(LH)[1e]	observed	58.9	7.4	6.9
Cu(LH)[1e]	calculated	58.4	7.6	6.8
Cu(LH)[1f]	observed	60.2	8.1	6.4
Cu(LH)[1f]	calculated	60.1	8.0	6.4

Table 4.5 Selected peaks observed in the +FAB spectrum (NOBA) of the copper (I) complex of *N*-dodecyl-*N'*-benzoylthiourea (1e) and *N*-tetradecyl-*N'*-benzoylthiourea (1f).

assignment	calculated mass	observed mass
$[Cu(LH_2)^{1e}]^+$	411.7	411.0
$[Cu_2(LH_2{}^{1e})_2]^{2+}$	823.4	827.2
$[Cu(LH_2{}^{1f})]^+$	438.8	438.6
$[Cu_2(LH_2{}^{1f})_2]^{2+}$	877.6	881.3

In view of the isolation of a copper (I) complex from the reaction of *N*-tetradecyl-*N'*-benzoylthiourea with copper (II) acetate, we decided to synthesise a copper (I) complex from $Cu^1(CH_3CN)_4PF_6$ to verify that the copper (I) complex formed in this reaction is the same copper (I) complex formed in the reaction of *N*-tetradecyl-*N'*-benzoylthiourea with copper (II) acetate. Characterisation of the two independently synthesised copper complexes shows that the products have identical melting points, C, H and N elemental analyses and ^1H and ^{13}C NMR spectra. This confirms that copper (II) is reduced to copper (I) in the reaction with *N*-alkyl-*N'*-benzoylthiourea to form a copper (I) *N*-acylthiourea complex.

In order to determine the structure of the yellow *N*-tetradecyl-*N'*-benzoylthiourea copper (I) complex, attempts were made to isolate suitable crystals for an X-ray crystallographic study. However recrystallisation from a variety of solvents failed to yield a crystal of diffraction quality. Hence, given the present data, the structure of the copper (I) complex of *N*-dodecyl-*N'*-benzoylthiourea and *N*-tetradecyl-*N'*-benzoylthiourea remains uncertain. It is evident that a more detailed investigation, including a study of the redox chemistry, is

required for a full understanding of the chemistry of the system and to elucidate the nature of the copper (I) complex.

In addition to the yellow copper (I) complex obtained from the reaction of *N*-tetradecyl-*N'*-benzoylthiourea with copper (II) acetate, a white compound was isolated from the aqueous solution and characterised. The white compound melts at 86 - 88 °C, whereas the melting point of the corresponding ligand is 51 - 52 °C. This suggests that the isolated product is not the uncomplexed ligand.

The results of NMR spectroscopy and elemental analysis suggest that the isolated product is the oxidised derivative of the ligand i.e. $(LH)_2.2HCl$, (Figure 4.5). The ^1H NMR spectrum is very similar to the parent ligand spectrum. However, two N - H peaks, a broad singlet at 8.74 ppm and a broad triplet, which implies coupling with the protons of the alkyl chain adjacent to nitrogen at 8.64 ppm, are evident in the ^1H NMR spectrum. These two N - H peaks must not be confused with the N - H signals of the ligand at 10.79 and 9.42 ppm. Of particular significance are the two signals at 167.8 and 153.7 ppm in the ^{13}C NMR spectrum. The peak at 167.8 ppm is in agreement with the carbonyl resonance of *N*-tetradecyl-*N'*-benzoylthiourea, at 166.8 ppm, and the signal at 153.7 ppm corresponds favourably with other -N=C-S- ^{13}C signals, e.g. thiazole at 152.7 ppm[39]. The C, H and N elemental analyses are in agreement with the proposed hydrochloride disulfide structure. Support for the disulfide derivative is strengthened by reports on the formation of disulfides of related compounds. Studies by Harris[40] *et al* have shown that *N*-benzoylthioureas are readily oxidised to the corresponding disulfide in the presence of bromine. Moreover, Kolthoff and Stricks[41] have reported that the reaction between cysteine (RSH) and cupric copper in ammoniacal solution, yields cuprous cysteinate (RSCu) and cystine (RSSR), i.e. cysteine is oxidised to cystine and copper (II) is reduced to Cu (I). Accordingly, these reports together with the results of NMR spectroscopy and C, H and N elemental analysis suggest that the white compound isolated is the hydrochloride disulfide derivative of the parent ligand.

Figure 4.5 Schematic representation of the hydrochloride disulfide derivative, one of the products of the reaction of *N*-alkyl-*N'*-benzoylthiourea with Cu(II) acetate.

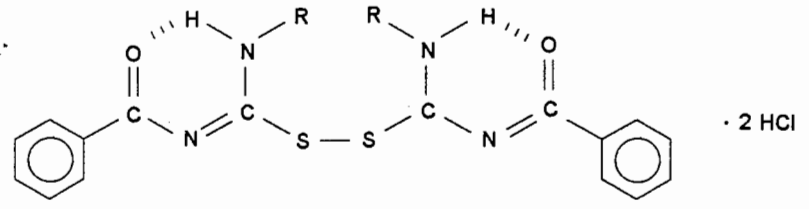

In summary, we have shown that two products are isolated from the reaction of *N*-alkyl-*N'*-benzoylthiourea with copper (II) acetate. These include a copper (I) complex and the hydrochloric disulfide derivative of the ligand, which implies that copper (II) is reduced to copper (I) and the ligand is oxidised.

Platinum complexes of N,N-dialkyl-N'-benzoylthiourea

In order to further exemplify the differences in coordination chemistry of the *N,N*-dialkyl- and *N*-alkyl-*N'*-benzoylthioureas, the reaction of these ligands with *cis*-$[Pt(PEt_2Ph)_2Cl_2]$ was investigated. The *cis*-$[Pt(PEt_2Ph)_2Cl_2]$ complex was selected for its high reactivity and good solubility in $CDCl_3$. It may be reasonable to anticipate that the reactive *cis*-$[Pt(PEt_2Ph)_2Cl_2]$ complex will coordinate with *N,N*-dialkyl-*N'*-benzoylthiourea to yield the corresponding *cis*-$[Pt(PEt_2Ph)_2(L\text{-}S,O)]$ complex, where L-*S,O* represents the ligand coordinated through the sulfur and oxygen atoms (Figure 4.6). On the other hand, a significantly different coordination chemistry is postulated for the reaction of *cis*-$[Pt(PEt_2Ph)_2Cl_2]$ with *N*-alkyl-*N'*-benzoylthiourea on the basis of the X-ray crystal structure of *N*-butyl-*N'*-benzoylthiourea.

The reaction of *N,N*-dialkyl- and *N*-alkyl-*N'*-benzoylthiourea with *cis*-$[Pt(PEt_2Ph)_2Cl_2]$ was studied with the aid of proton decoupled ^{31}P NMR spectroscopy. The experimental procedure is recorded in the experimental section. Phosphorus NMR spectroscopy is very useful for following complex reactions because the spectra are usually relatively simple and therefore easier to interpret than the corresponding proton NMR spectra. Interpretation of the spectra is based on the fact that the chemically equivalent phosphorus atoms couple with ^{195}Pt (i = ½, natural abundance = 33.7 %) and appear as a singlet with satellites. On the other hand, chemically non-equivalent phosphorus atoms couple with one another and with the platinum atom, and appear as two sets of doublets with satellites. Moreover, the coupling constant of chemically non-equivalent phosphorus atoms is known to be dependent on whether the atoms are *cis* or *trans* to one another[42]. The $^1J(Pt, P)$ coupling constant varies according to the *trans*-influence of the ligand opposite to the Pt - P bond[42]. Therefore by varying the ligand *trans* to phosphorus from something with a small *trans*-influence (e.g. a halogen or oxygen ligand) to one with a much larger *trans*-influence (e.g. another phosphorus ligand or sulfur ligand), large changes in the NMR parameters can be induced. The general trend that has emerged from the inspection of vast numbers of $^1J(Pt - P)$ coupling constants shows that phosphorus atoms *trans* to each other have $^1J(Pt - P)$ values of approximately 2200 - 2400 Hz, whereas phosphorus atoms *cis* to one another have $^1J(Pt - P)$ values in the range 3200 - 3600 Hz[42].

It is noteworthy that no reaction between *N,N*-dibutyl-*N'*-benzoylthiourea and one equivalent *cis*-$[Pt(PEt_2Ph)_2Cl_2]$, in $CDCl_3$, is evident from the ^{31}P NMR spectrum in the absence of a base. This result was surprising based on the reactivity of *cis*-$[Pt(PEt_2Ph)_2Cl_2]$. The ^{31}P NMR spectrum shows a singlet, with platinum satellites, at 3.04 ppm with a coupling constant $^1J(P - Pt)$ of 3545 Hz. This signal represents the unreacted *cis*-$[Pt(PEt_2Ph)_2Cl_2]$ complex (Figure 4.7(a)).

However, evidence of a reaction is visible in the ^{31}P NMR spectrum after the addition of triethylamine (Figure 4.7(b)). Two signals, each a doublet with satellites at -3.52 and 14.64 ppm, with a $^{1}J(P - Pt)$ coupling constant of 3588 and 3047 Hz respectively, are observed in the ^{31}P NMR spectrum. These two signals continue to grow with the further addition of triethylamine until, after addition of one equivalent of base, i.e. 1L : 1Pt : 1Et_3N, these are the only two peaks evident in the ^{31}P NMR spectrum (Figure 4.7(c)). No minor products are observed in the ^{31}P NMR spectrum.

Figure 4.6 Schematic representation of the proposed reaction of *N,N*-dialkyl-*N'*-benzoylthiourea with *cis*-$[Pt(PEt_2Ph)_2Cl_2]$ in the presence of triethylamine. Note the *cis* arrangement of the atoms in the metal complex.

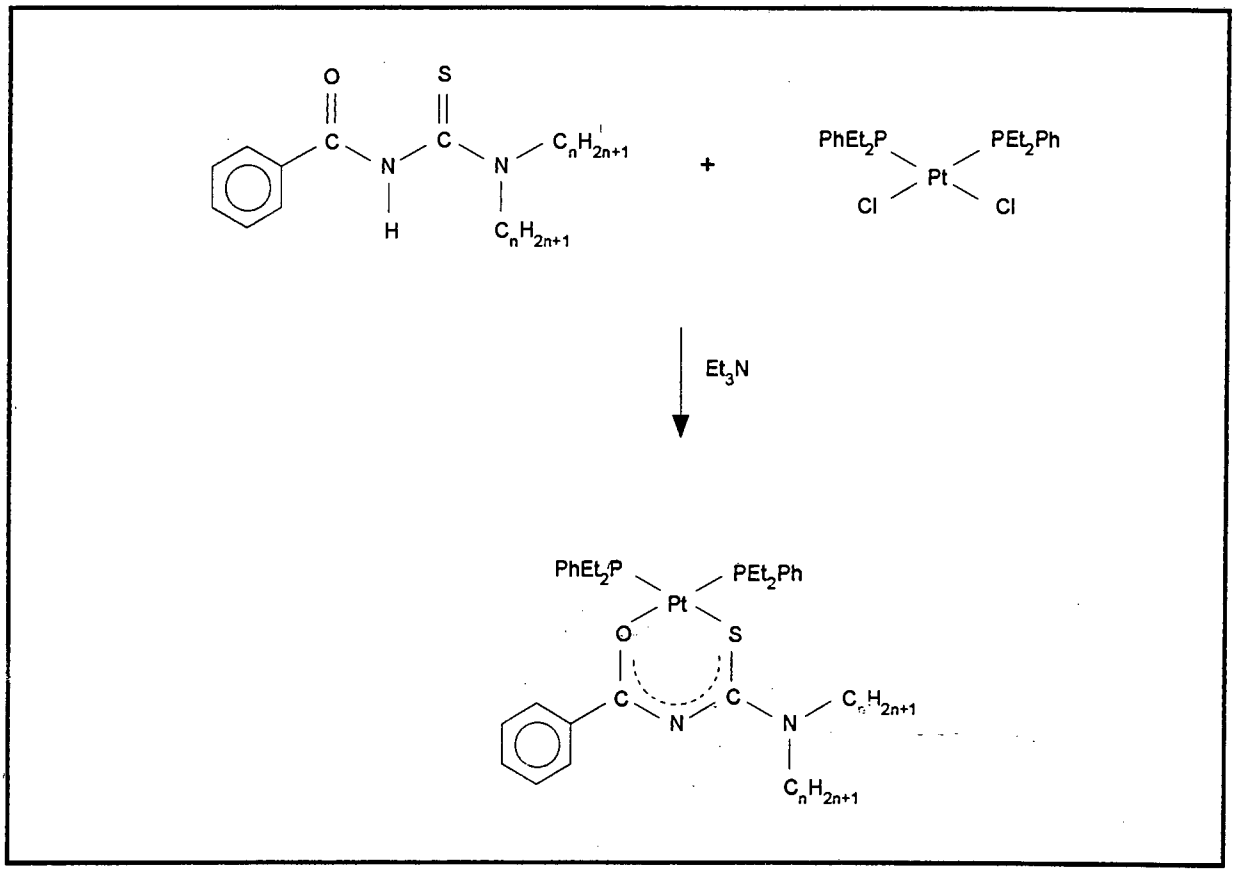

Based on the fact that only one species is present in solution and that the one bond coupling constants of the signals at -3.52 and 14.64 ppm are consistent with a *cis* arrangement of phosphorus atoms[55], the present results confirm that *N,N*-dibutyl-*N'*-benzoylthiourea reacts quantitatively with an equimolar amount of *cis*-$[Pt(PEt_2Ph)_2Cl_2]$, in the presence of triethylamine, to yield exclusively the stable *cis*-$[Pt(PEt_2Ph)_2(L\text{-}S,O)]$ complex. No change in the ^{31}P NMR spectrum is observed on heating of the reaction mixture containing *cis*-$[Pt(PEt_2Ph)_2(L\text{-}S,O)]$, for 24 hours at 50 °C.

Figure 4.7 $^{31}P\{^{1}H\}$ NMR spectrum acquired during the reaction of *N,N*-dibutyl-*N'*-benzoylthiourea (LH) with *cis*-$[Pt(PEt_2Ph)_2Cl_2]$ upon the addition of base, Et_3N.

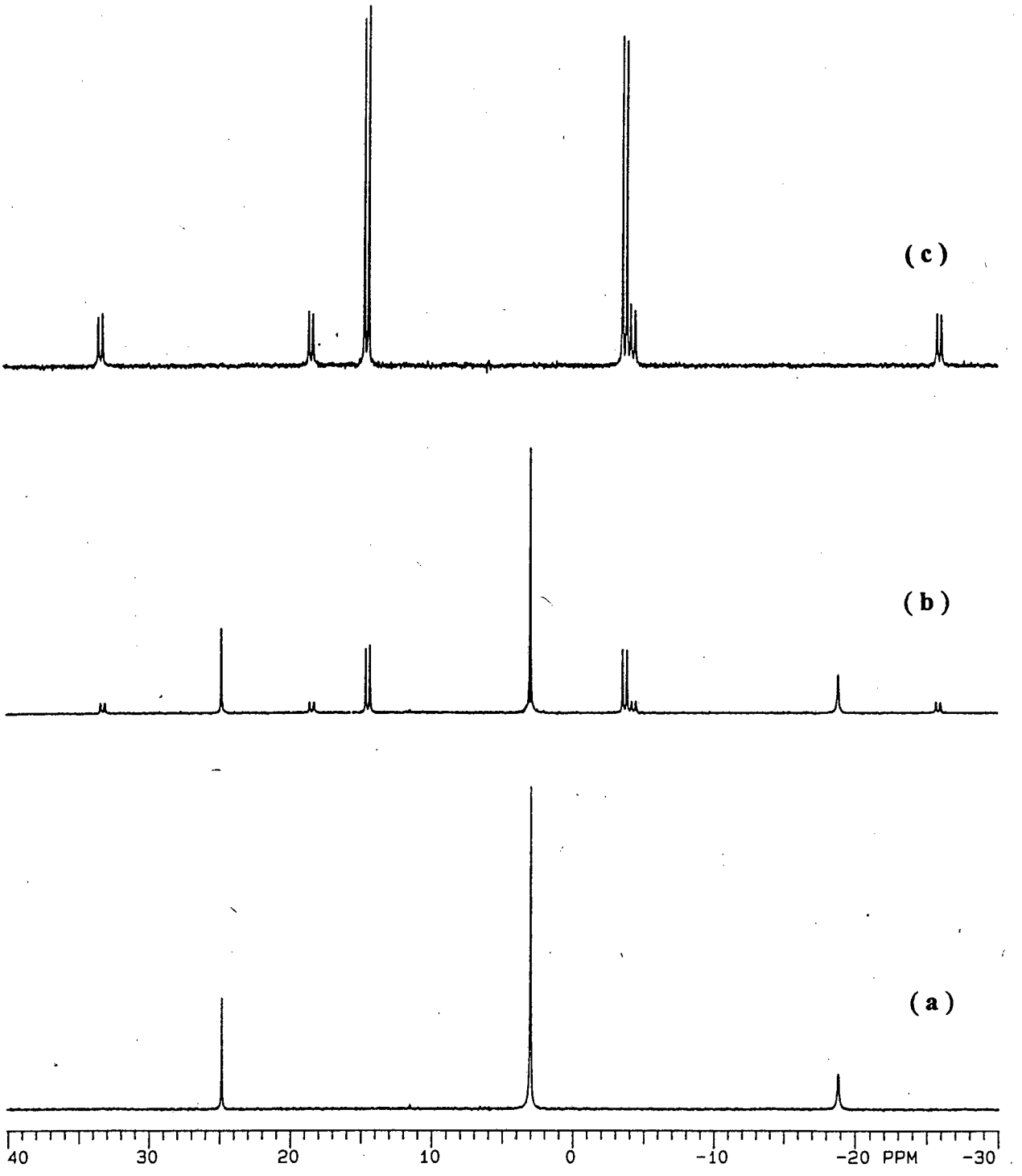

(**a**) Molar equivalents of LH and *cis*-$[Pt(PEt_2Ph)_2Cl_2]$– no Et_3N.

(**b**) Molar equivalents of LH and *cis*-$[Pt(PEt_2Ph)_2Cl_2]$ – 0.3 equivalents of Et_3N.

(**c**) Molar equivalents of LH, *cis*-$[Pt(PEt_2Ph)_2Cl_2]$ and Et_3N.

Platinum complexes of N-alkyl-N'-benzoylthiourea

Consequent to the *intra*molecular hydrogen bond observed in the crystal structure of *N*-butyl-*N'*-benzoylthiourea, we postulated that the platinum coordination chemistry of *N*-alkyl-*N'*-benzoylthiourea would be significantly different to that observed for the *N,N*-dialkyl-*N'*-benzoylthiourea analogues. The experimental conditions were similar to that followed for the analogous experiment involving *N,N*-dialkyl-*N'*-benzoylthiourea.

No reaction occurs between *N*-butyl-*N'*-benzoylthiourea and *cis*-$[Pt(PEt_2Ph)_2Cl_2]$ in the absence of triethylamine. The only resonance observed in the ^{31}P NMR spectrum, a singlet at 3.04 ppm, represents the unreacted *cis*-$[Pt(PEt_2Ph)_2Cl_2]$. In the presence of base however, a number of complex species are observed in solution. Two small doublets with satellites, at 14.32 and -3.34 ppm with a coupling constant $^1J(P - Pt)$ of 3002 and 3608 Hz respectively, and at 8.47 and -3.68 ppm with a coupling constant $^1J(P - Pt)$ of 2875 and 3188 Hz respectively are evident. Three singlets at 11.02 ppm with a coupling constant $^1J(P - Pt)$ of 2591 Hz, at 8.21 ppm with a coupling constant $^1J(P - Pt)$ of 2550 Hz and at 3.04 ppm representing *cis*-$[Pt(PEt_2Ph)_2Cl_2]$ are observed in the ^{31}P NMR spectrum. (Figure 4.8(a)).

No new peaks are observed in the ^{31}P NMR spectrum on the addition of an excess amount of base, however the relative sizes of the existing peaks change with time and an increase in base concentration. The singlets at 11.02 and 8.21 ppm increase in size whereas the singlet at 3.04 and the doublets at 14.32 and -3.34 ppm, and 8.47 and -3.68 ppm, decrease in size. Three major species, singlets at 11.02, 8.21 and 3.04 ppm, are evident in the ^{31}P NMR spectrum of the reaction mixture, after standing for 24 hours at 50 °C (Figure 4.8(b)). The signal at 3.04 ppm represents the unreacted *cis*-$[Pt(PEt_2Ph)_2Cl_2]$ complex.

Careful inspection of the ^{31}P NMR spectra obtained upon sequential addition of triethylamine, together with the general trend that phosphorus atoms *trans* to each other have coupling constants in the region 2500 Hz, whereas phosphorus atoms *cis* to each other have larger coupling constants ~ 3500 Hz[42], suggests the reaction species diagrammatically summarised in Figure 4.9.

Figure 4.8 $^{31}P\{^{1}H\}$ NMR spectra acquired during the reaction of *N*-alkyl-*N'*-benzoylthiourea, (LH_2), with *cis*-$[Pt(PEt_2Ph)_2Cl_2]$. The alphabetical letters correspond to the species illustrated in Figure 4.9.

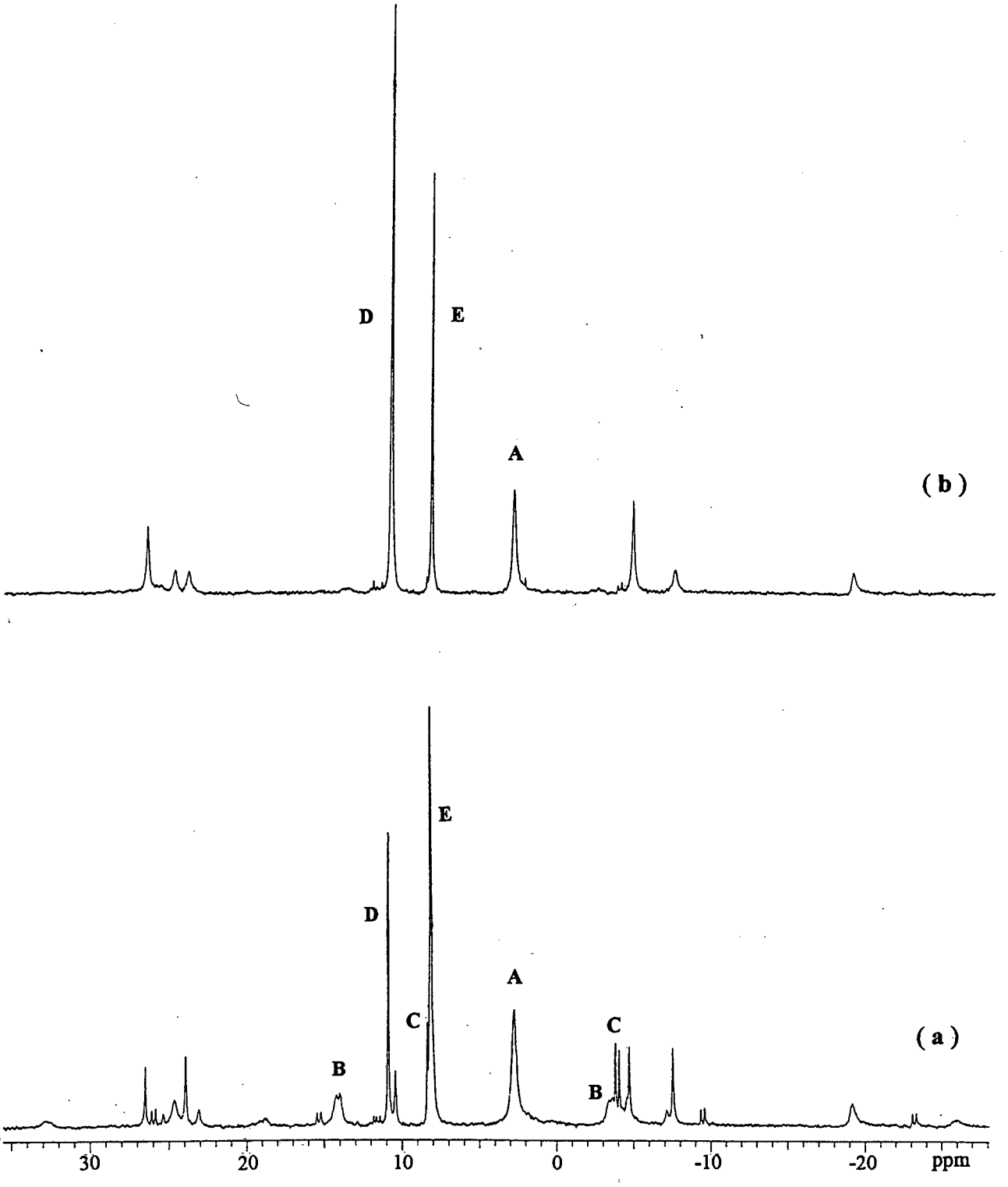

(**a**) Molar equivalents of LH_2, *cis*-$[Pt(PEt_2Ph)_2Cl_2]$ and Et_3N at 25 °C.

(**b**) Molar equivalents of LH_2, *cis*-$[Pt(PEt_2Ph)_2Cl_2]$ and Et_3N after standing for 24 hours at 50 °C.

Figure 4.9 Schematic representation of reaction of *N*-alkyl-*N'*-benzoylthiourea (LH_2) with *cis*-$[Pt(PEt_2Ph)_2Cl_2]$ in the presence of triethylamine.

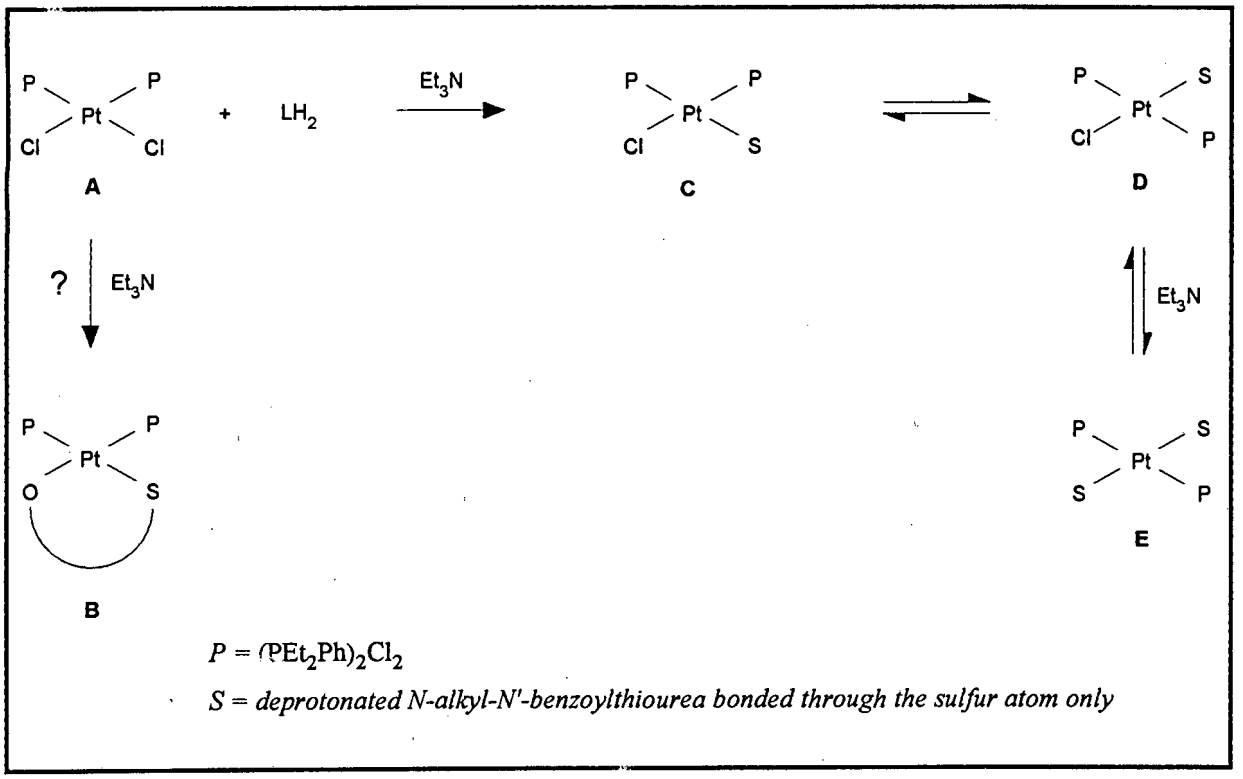

Interpretation of the ^{31}P NMR spectra suggests that addition of triethylamine to a solution of *cis*-$[Pt(PEt_2Ph)_2Cl_2]$ and *N*-butyl-*N'*-benzoylthiourea yields four platinum complexes. The relatively small signals at 14.32 and -3.34 ppm have remarkably similar chemical shifts and coupling constants to those observed for the reaction of *cis*-$[Pt(PEt_2Ph)_2Cl_2]$ with *N,N*-dibutyl-*N'*-benzoylthiourea. The chemical shifts and coupling constants strongly suggest the presence of *cis*-$[Pt(PEt_2Ph)_2(L\text{-}S,O)]$. However, this assignment is not consistent with the work described earlier in this chapter, and with the proposed *intra*molecular hydrogen bond controlled coordination of *N*-alkyl-*N'*-benzoylthiourea, this suggests that the assignment is unlikely.

The doublets at 8.47 and -3.68 ppm are assigned to *cis*-$[Pt(PEt_2Ph)_2(L\text{-}S)Cl]$, where L-*S* represents the deprotonated ligand coordinated through the sulfur atom only. Such an arrangement of ligands is reminiscent of one of the products of protonation of *cis*-bis(*N,N*-dibutyl-*N'*-benzoylthioureato)platinum(II), *cis*-$[Pt(L\text{-}S,O)(HL\text{-}S)Cl]$, where (HL-*S*) represents the protonated ligand coordinated through the sulfur atom only. The transient appearance of *cis*-$[Pt(PEt_2Ph)_2(L\text{-}S)Cl]$ in the ^{31}P NMR spectrum suggests time dependent and/or thermal dependent processes in solution, which reach a steady state only after approximately 24 hours and 50 °C.

The singlets at 8.21 and 11.02 ppm are assigned to *trans*-[Pt(PEt_2Ph)$_2$(L-*S*)$_2$] and *trans*-[Pt(PEt_2Ph)$_2$(L-*S*)Cl] respectively, and represent the major species present in the reaction mixture after standing for 24 hours at 50 °C (Figure 4.7(b)). These species were assigned the *trans* conformation on the basis of their coupling constants. Evidence in strong support of these assignments comes from the recorded $^{31}P\{^1H\}$ NMR spectrum of the reaction of a mixture of the *cis* and *trans* isomers of bis(*N*-propyl-*N'*-benzoylthioureato)dichloro-platinum(II) with two equivalents of diethylphenylphosphine. The $^{31}P\{^1H\}$ NMR spectrum of the reaction products shows two singlets at 8.27 and 11.56 ppm assigned to *trans*-[Pt(PEt_2Ph)$_2$(L-*S*)$_2$] and *cis*-[Pt(PEt_2Ph)$_2$(L-*S*)$_2$] respectively[61]. Therefore in the experiment with *N*-butyl-*N'*-benzoylthiourea the ^{31}P signal at 8.21 ppm is assigned to *trans*-[Pt(PEt_2Ph)$_2$(L-*S*)$_2$].

In view of the complexity of the present ^{31}P NMR spectra we conclude that the *N*-alkyl-*N'*-benzoylthioureas show substantially different coordination chemistries to that observed for the *N,N*-dialkyl-*N'*-benzoylthioureas. The results suggest that the described *intra*molecular hydrogen bond controls unidentate coordination of these types of ligands, accounting for the substantial differences in coordination chemistry between the *N*-alkyl-*N'*-benzoylthioureas and *N,N*-dialkyl-*N'*-benzoylthioureas.

4.3 CONCLUSION

We have synthesised and characterised the copper (II), nickel (II), platinum (II) and palladium (II) complexes of *N,N*-dibutyl-, *N,N*-dihexyl- and *N,N*-dioctyl-*N'*-benzoylthiourea. Unfortunately, these complexes do not show any liquid-crystalline properties. In retrospect, the *cis* conformation of ligands around the central metal atom may account for the absence of liquid-crystalline character.

The present study has shown that HCl protonation of the coordinated ligand in *cis*-[Pt(L-*S,O*)$_2$] complexes, where L is *N,N*-dialkyl-*N'*-benzoylthiourea, results in the reversible opening of the 6-membered chelate ring, with concomitant coordination of the Cl^- ion to the Pt (II) atom. We found by means of ^{195}Pt and ^1H NMR spectroscopy that protonation of *cis*-[Pt(L-*S,O*)$_2$] with HCl to yields a mixture of complexes of type *cis*- and *trans*-[Pt(HL-*S*)$_2$Cl$_2$] in which the protonated ligand, (HL-*S*), is coordinated to the metal *via* the *S*-atom only with the *O*-donor atom of the *N*-acyl moiety being pendent. Treatment of the mixture of these *cis* and *trans* complexes with ammonia, leads to the rapid formation of exclusively the *cis*-[Pt(L-*S,O*)$_2$] complex.

Furthermore, the we demonstrated the substantial difference in coordination chemistry between the *N,N*-dialkyl-*N'*-benzoylthioureas and the *N*-alkyl-*N'*-benzoylthioureas. The reaction of *N,N*-dialkyl-*N'*-benzoylthiourea with copper (II) acetate yields a bis-chelated, green copper (II) complex. On the other hand, the reaction of copper (II) acetate with *N*-alkyl-*N'*-benzoylthiourea results in the reduction of Cu (II) to Cu (I) and in the oxidation of the ligand. A yellow copper (I) complex, in which the metal and ligand are present in a ratio of 1 : 1, and the hydrochloride disulfide salt of the ligand were isolated. Moreover, where *N,N*-dialkyl-*N'*-benzoylthiourea forms stable neutral nickel (II) complexes, we have not been able to isolate a well-defined nickel (II) complex with *N*-alkyl-*N'*-benzoylthiourea under any circumstances.

The difference in coordination chemistry between *N*-alkyl- and *N,N*-dialkyl-*N'*-acylthiourea is further illustrated by the proton decoupled ^{31}P NMR spectrum of the reaction of the ligand with *cis*-[Pt(PEt$_2$Ph)$_2$Cl$_2$] in the presence of base. A straightforward spectrum, suggesting that *cis*-[Pt(PEt$_2$Ph)$_2$(L-*S,O*)] is the only product, is observed for the *N,N*-dibutyl-*N'*-benzoylthiourea ligand. However, a complex spectrum is evident for *N*-butyl-*N'*-benzoylthiourea. Interpretation of the spectrum suggests that the major products of the reaction are *trans*-[Pt(PEt$_2$Ph)$_2$(L-*S*)$_2$] and *trans*-[Pt(PEt$_2$Ph)$_2$(L-*S*)Cl].

In conclusion, the present study has demonstrated the profound effect the *intra*molecular hydrogen bond has on the coordination of these types of ligands, accounting for the substantial differences in coordination behaviour between *N*-alkyl- and *N,N*-dialkyl-*N'*-acylthioureas. Further work aimed at understanding and exploiting these differences for the possible control of selectivity of these ligands, may prove most illuminating.

4.4 Experimental

The nickel (II) and copper (II) complexes were prepared according to the general method reported by Beyer[1] *et al.* A DMF / H_2O solution (20 cm^3) of metal acetate (0.0011 mol) was added dropwise to a stirred, warm (50 °C) solution of the ligand (0.002 mol) in the same solvent (20 cm^3). The reaction mixture was stirred for 60 minutes with gentle heating. The addition of water to the reaction mixture resulted in precipitation of the product which was filtered and recrystallised from $CHCl_3$ / EtOH unless specifically stated otherwise.

***cis*-bis(*N,N*-dibutyl-*N'*-benzoylthioureato)nickel(II)** 76 % yield, mp 132 - 134 °C. Anal. Calcd for $C_{32}H_{46}N_4O_2S_2.Ni$: C, 59.9; H, 7.2; N, 8.7. Found C, 59.8; H, 7.4; N, 8.7.

***cis*-bis(*N,N*-dihexyl-*N'*-benzoylthioureato)nickel(II)** 85 % yield, mp 74 - 76 °C. Anal. Calcd for $C_{40}H_{62}N_4O_2S_2.Ni$: C, 63.7; H, 8.3; N, 7.4. Found C, 63.8; H, 8.0; N, 7.4.

***cis*-bis(*N,N*-dioctyl-*N'*-benzoylthioureato)nickel(II)** 78 % yield, mp 75 - 77 °C. Anal. Calcd for $C_{48}H_{78}N_4O_2S_2.Ni$: C, 66.6; H, 9.1; N, 6.5. Found C, 67.0; H, 9.3; N, 6.5. NMR ($CDCl_3$) ^1H δ 0.88 (12H, t, CH_3), 1.24 - 1.78 (48H, b.m, CH_2), 3.71 (8H, m, NCH_2) 7.37 (4H, q, H(3) / H(5)), 7.46 (2H, t, H(4)), 8.13 (4H, d, H(2) / H(6)); ^{13}C δ 14.08, 22.63, 26.97, 27.08, 27.29, 27.91, 29.25, 29.39, 31.80, 51.32, 51.94, 127.83, 129.19, 131.30, 136.85, 172.25, 172.95.

***cis*-bis(*N,N*-dibutyl-*N'*-benzoylthioureato)copper(II)** Recrystallisation of the crude product from H_2O / EtOH gave a dark green crystalline product (81 %), mp 94 - 96 °C. Anal. Calcd for $C_{32}H_{46}N_4O_2S_2.Cu$: C, 59.5; H, 7.2; N, 8.7. Found C, 59.3; H, 7.3; N, 8.5.

***cis*-bis(*N,N*-dihexyl-*N'*-benzoylthioureato)copper(II)** 84 % yield, mp 39 - 41 °C. Anal. Calcd for $C_{40}H_{62}N_4O_2S_2.Cu$: C, 63.3; H, 8.2; N, 7.4. Found C, 63.4; H, 8.4; N, 7.3.

***cis*-bis(*N,N*-dioctyl-*N'*-benzoylthioureato)copper(II)** Product is a liquid (88 %). Anal. Calcd for $C_{48}H_{78}N_4O_2S_2.Cu$: C, 66.2; H, 9.0; N, 6.4. Found C, 66.7; H, 9.3; N, 6.7.

The platinum (II) and palladium (II) complexes were prepared according to the method previously reported by Koch[33] *et al.* A solution of K_2MCl_4 (0.1 mmol) in H_2O - dioxane (1 : 1 v/v) was added slowly to a warm (50 °C) solution of the ligand (0.2 mmol) in dioxane (20 cm^3) - H_2O (10 cm^3). Sodium acetate (0.4 mmol) was added and the reaction mixture stirred for a further 60 min at 50 °C. Excess water was added while cooling the solution and the precipitate collected by filtration. The crude product was recrystallised from chloroform-acetonitrile.

***cis*-bis(*N,N*-dibutyl-*N'*-benzoylthioureato)platinum(II)** 84 % yield, mp 162 - 163 °C (lit. 164 - 166 °C)[26]. Anal. Calcd for $C_{32}H_{46}N_4O_2S_2.Pt$: C, 49.4; H, 6.0; N, 7.2. Found C, 49.2; H, 5.8; N, 7.2.

***cis*-bis(*N,N*-dihexyl-*N'*-benzoylthioureato)platinum(II)** 79 % yield, mp 95 - 97 °C. Anal. Calcd for $C_{40}H_{62}N_4O_2S_2.Pt$: C, 54.0; H, 7.0; N, 6.3. Found C, 53.9; H, 6.8; N, 6.3.

***cis*-bis(*N,N*-dioctyl-*N'*-benzoylthioureato)platinum(II)** 73 % yield, mp 91 - 93 °C. Anal. Calcd for $C_{48}H_{78}N_4O_2S_2.Pt$: C, 57.5; H, 7.9; N, 5.6. Found C, 57.7; H, 7.7; N, 5.5. NMR ($CDCl_3$) ^1H δ 0.86 (6H, t, CH_3), 0.89 (6H, t, CH_3'), 1.26 - 1.80 (48H, b.m, CH_2), 3.73 (8H, m, NCH_2), 7.40 (4H, q, H(3) / H(5)), 7.46 (2H, t, H(4)), 8.24 (4H, d, H(2) / H(6)); ^{13}C δ 14.09, 22.63, 27.05, 27.10, 27.18, 27.92, 29.25, 29.39, 31.78, 51.82, 51.87, 128.01, 129.40, 131.29, 137.66, 167.39, 168.31.

***cis*-bis(*N,N*-dibutyl-*N'*-benzoylthioureato)palladium(II)** 78 % yield, mp 142 - 144 °C. Anal. Calcd for $C_{32}H_{46}N_4O_2S_2.Pd$: C, 55.8; H, 6.7; N, 8.1. Found C, 55.5; H, 6.9; N, 8.0.

***cis*-bis(*N,N*-dihexyl-*N'*-benzoylthioureato)palladium(II)** 86 % yield, mp 83 - 84 °C. Anal. Calcd for $C_{40}H_{62}N_4O_2S_2.Pd$: C, 60.0; H, 7.8; N, 7.0. Found C, 60.2; H, 7.9; N, 6.9.

***cis*-bis(*N,N*-dioctyl-*N'*-benzoylthioureato)palladium(II)** 79 % yield, mp 92 - 94 °C. Anal. Calcd for $C_{48}H_{78}N_4O_2S_2.Pd$: C, 63.1; H, 8.6; N, 6.1. Found C, 63.4; H, 8.6; N, 6.1. NMR ($CDCl_3$) ^1H δ 0.87 (12H, q, CH_3), 1.25 - 1.80 (48H, b.m, CH_2), 3.76 (8H, q, NCH_2), 7.41 (4H, q, H(3) / H(5)), 7.51 (2H, t, H(4)), 8.26 (4H, d, H(2) / H(6)); ^{13}C δ 14.09, 22.61, 27.02, 27.11, 27.44, 27.93, 29.23, 29.38, 31.80, 51.95, 53.10, 127.88, 129.70, 131.37, 137.16, 170.49, 171.53.

***cis*-bis(*N,N*-dibutyl-*N'*-naphthoylthioureato)nickel(II)** 84 % yield, mp 109 - 111 °C. Anal. Calcd for $C_{40}H_{50}N_4O_2S_2.Ni$: C, 64.8; H, 6.8; N, 7.6. Found C, 65.1; H, 6.7; N, 7.6.

***cis*-bis(*N,N*-dihexyl-*N'*-naphthoylthioureato)nickel(II)** Product is a purple liquid (66 %). Anal. Calcd for $C_{48}H_{66}N_4O_2S_2.Ni$: C, 67.5; H, 7.8; N, 6.6. Found C, 67.8; H, 7.6; N, 6.5.

***cis*-bis(*N,N*-dioctyl-*N'*-naphthoylthioureato)nickel(II)** 79 % yield, mp 40 - 44 °C. Anal. Calcd for $C_{56}H_{82}N_4O_2S_2.Ni$: C, 69.6; H, 8.6; N, 5.8. Found C, 69.4; H, 8.8; N, 5.8. NMR ($CDCl_3$) ^1H δ 0.85, 0.91 (12H, t, CH_3), 1.22 - 1.35 (40H, m, CH_2), 1.71 (8H, m, $NCH_2\underline{CH_2}$), 3.71 (8H, m, NCH_2), 6.96 (2H, t, H(7)), 7.32 (2H, t, H(3)), 7.38 (2H, t, H(6)), 7.78 (2H, d, H(5)), 7.87 (2H, d, H(4)), 8.09 (2H, d, H(2)), 8.88 (2H, d, H(8)); ^{13}C δ 14.04, 14.09, 22.57, 22.63, 26.95, 27.29, 28.02, 29.20, 29.28, 31.74, 31.80, 51.14, 51.75, 124.36, 125.43, 126.50, 127.14, 127.90, 128.93, 131.22, 133.85, 134.73, 172.61, 175.23.

***cis*-bis(*N,N*-dibutyl-*N'*-naphthoylthioureato)copper(II)** 73 % yield, mp 81 - 83 °C. Anal. Calcd for $C_{40}H_{50}N_4O_2S_2.Cu$: C, 64.4; H, 6.8; N, 7.5. Found C, 64.4; H, 6.7; N, 7.5.

***cis*-bis(*N,N*-dihexyl-*N'*-naphthoylthioureato)copper(II)** Product is a dark green liquid (78 %). Anal. Calcd for $C_{48}H_{66}N_4O_2S_2.Cu$: C, 67.1; H, 7.8; N, 6.5. Found C, 67.3; H, 7.7; N, 6.4.

***cis*-bis(*N,N*-dioctyl-*N'*-naphthoylthioureato)copper(II)** Recrystallisation of the crude product from H_2O / EtOH gave a dark green crystalline product (87 %), mp 48 - 50 °C. Anal. Calcd for $C_{56}H_{82}N_4O_2S_2.Cu$: C, 69.3; H, 8.5; N, 5.8. Found C, 69.5; H, 8.7; N, 5.7.

The anthracyl metal derivatives were synthesised according to the general method. However, molar equivalents of metal acetate and ligand were reacted together.

***cis*-bis(*N,N*-dioctyl-*N'*-anthracoylthioureato)nickel(II)** 82 % yield, mp 143 - 145 °C. Anal. Calcd for $C_{64}H_{86}N_4O_2S_2.Ni$: C, 72.1; H, 8.1; N, 5.3. Found C, 72.2; H, 8.1; N, 5.3. NMR ($CDCl_3$) ^1H δ 0.80 (6H, t, CH_3), 0.91 (6H, t, CH_3'), 1.02 - 1.78 (48H, b.m, CH_2), 3.48 (4H, t, NCH_2), 3.74 (4H, t, NCH_2'), 7.26 (4H, t, H(3) / H(9)), 7.28 (4H, t, H(4) / H(8)), 7.82 (4H, d, H(5) / H(7)), 8.23 (4H, d, H(2) / H(10)), 8.25 (2H, s, H(6)); ^{13}C δ 14.04, 14.12, 22.50, 22.66, 26.62, 27.01, 27.25, 28.29, 29.01, 29.10, 29.22, 29.29, 31.65, 31.83, 50.92, 51.79, 124.82, 125.43, 126.55, 127.24, 127.95, 128.18, 131.17, 172.51, 176.24.

***cis*-bis(*N,N*-dioctyl-*N'*-anthracoylthioureato)copper(II)** 79 % yield, mp 132 - 134 °C. Anal. Calcd for $C_{64}H_{86}N_4O_2S_2.Cu$: C, 71.8; H, 8.1; N, 5.2. Found C, 72.0; H, 8.4; N, 5.3.

The copper (I) complexes were synthesised according to the general method where one molar equivalent of copper (II) acetate is reacted with two molar equivalents of ligand.

Cu (I) complex of *N*-dodecyl-*N'*-benzoylthiourea Pure copper (I) complex was obtained after preparative layer chromatography of the crude product, using $CHCl_3$ as eluent. The product was recrystallised from $CHCl_3$ / EtOH to give yellow block-like crystals (45 %), mp 92 - 95 °C. Anal. Calcd for $C_{20}H_{31}N_2OS.Cu$: C, 58.4; H, 7.6; N, 6.8. Found C, 58.9; H, 7.4; N, 6.9. +FAB (NOBA) Calc for $Cu(LH_2)^+$ 411.7; $Cu_2(LH_2)_2^{2+}$ 823.4. Found 411.0, 827.2. NMR ($CDCl_3$) ^1H δ major : 0.87 (3H, t, CH_3), 1.15 - 1.54 (20H, m, CH_2), 2.90 (2H, q, NCH_2), 7.30 - 7.38 (3H, m, H(3) / H(4) / H(5)), 8.17 (2H, d, H(2) / H(6)), 11.94 (1H, t, H(10)); minor : 0.86 (3H, t, CH_3), 1.19 - 1.54 (20H, m, CH_2), 3.01 (1H, m, NCH_2), 3.26 (1H, m, NCH_2), 7.38 - 7.47 (3H, m, H(3) / H(4) / H(5)), 7.96 (2H, d, H(2) / H(6)), 12.01 (1H, t, N(10) - H(10)).

Cu (I) complex of *N*-tetradecyl-*N'*-benzoylthiourea Pure copper (I) complex was obtained after preparative layer chromatography of the crude product, using $CHCl_3$ as eluent. The product was recrystallised from $CHCl_3$ / EtOH to give yellow block-like crystals (47 %), mp 85 - 87 °C. Anal. Calcd for $C_{22}H_{35}N_2OS.Cu$: C, 60.2; H, 8.0; N, 6.4. Found C, 60.2; H, 8.1; N, 6.4. +FAB (NOBA) Calc for $Cu(LH_2)^+$ 438.8; $Cu_2(LH_2)_2^{2+}$ 877.6. Found 438.6, 881.3. NMR ($CDCl_3$) ^1H δ major : 0.88 (3H, t, CH_3), 1.20 - 1.54 (24H, m, CH_2), 2.91 (2H, q, NCH_2), 7.29 - 7.38 (3H, m, H(3) / H(4) / H(5)), 8.18 (2H, d, H(2) / H(6)), 11.93 (1H, t, N(10) - H(10)); minor : 0.86 (3H, t, CH_3), 1.20 - 1.54 (24H, m, CH_2), 2.99 (1H, m, NCH_2), 3.25 (1H, m, NCH_2'), 7.38 - 7.47 (3H, m, H(3) / H(4) / H(5)), 7.93 (2H, d, H(2) / H(6)), 12.03 (1H, t, N(10) - H(10)). ^{13}C δ 14.09, 22.67, 26.90, 28.78, 29.18, 29.33, 29.47, 29.61, 31.90, 46.93, 127.70, 128.17, 130.84, 138.11, 177.14, 178.62.

The hydrochloride salt of *N*-tetradecyl-*N'*-benzoylthiourea disulfide was obtained from the aqueous solution after evaporating the water under reduced pressure (azeotrope with MeOH). The white solid was recrystallised from EtOH to give a pure white product, mp 86 - 88 °C. Anal. Calcd for $C_{44}H_{70}N_4O_2S_2.2HCl$: C, 64.0; H, 9.0; N, 6.8. Found C, 64.6; H, 9.3; N, 6.7. NMR ($CDCl_3$) ^1H δ 0.87 (6H, t, CH_3), 1.25 - 1.58 (48H, m, CH_2), 3.35 (4H, q, NCH_2), 7.48 (4H, t, H(3) / H(5)), 7.59 (2H, t, H(4)), 7.89 (4H, d, H(2) / H(6)), 8.64 (2H, t, N(10) - H(10)), 8.74 (2H, b.s, N(8) - H(8)); ^{13}C δ 14.10, 22.68, 26.94, 29.29, 29.34, 29.53, 29.59, 29.64, 31.91, 40.00, 127.47, 128.89, 132.51, 133.06, 153.71, 167.81.

***N*-tetradecyl-*N'*-benzoylthiourea Cu (I) complex from $Cu(CH_3CN)_4PF_6$** A solution of the ligand (0.02 mol) in CH_3CN was added dropwise to a stirred, warm solution of $Cu(CH_3CN)_4PF_6$ (0.011 mol) in CH_3CN. The reaction mixture was heated to reflux and stirred for 15 minutes at which point sodium acetate (0.04 mol) was added and the solution heated to reflux for an additional 1 hour. Excess water was added while cooling the solution and the precipitate collected by filtration. The crude product was recrystallised from $CHCl_3$ / CH_3CN to give a yellow crystalline product (92 %), mp 85 - 87 °C. Analytical data was identical to that recorded above for Cu (I) complex of *N*-tetradecyl-*N'*-benzoylthiourea.

Protonation of *cis*-bis(*N,N*-dibutyl-*N'*-benzoylthioureato)platinum(II) with concentrated HCl

All ^1H and ^{195}Pt NMR spectra were recorded in 5mm tubes in $CDCl_3$ solution, using a Varian UNITY-400 spectrometer operating at 400 and 85.8 MHz respectively. The ^1H spectra were recorded at 25 °C. The ^{195}Pt NMR spectra were recorded at 30 °C using 100 kHz spectral widths using 20μs pulses (~ 90 °) with 0.5 s pulse delay, since T_1 of the nucleus was < ca 0.1 s; the range between 2048 and 16000 pulses gave excellent spectra. All ^{195}Pt shifts are quoted relative to external H_2PtCl_6 (500 mg / ml in 30 % v / v D_2O / 1M HCl) and are estimated to be accurate to ± 2 ppm.

Complexation of *N*-alkyl- and *N,N*-dialkyl-*N'*-benzoylthiourea with $Pt(PEt_2Ph)_2Cl_2$ - $^{31}P\{^1H\}$ NMR spectroscopy

The proton decoupled ^{31}P NMR spectra were recorded in $CDCl_3$ using 5 mm tubes and a Varian VXR-200 Fourier transform spectrometer operating at 81 MHz. All $^{31}P\{^1H\}$ shifts are given relative to 85 % phosphoric acid / D_2O and are estimated to be accurate to ± 0.1 ppm. Spectra were obtained using a 20 kHz spectral width and data was processed with a line broadening of 1 Hz.

Aliquots of 20 μL triethylamine were directly added to the NMR tube containing 0.1 mmol of *N*-alkyl- or *N,N*-dialkyl-*N'*-benzoylthiourea and $Pt(PEt_2Ph)_2Cl_2$ (0.1 mmol) in 1 mL $CDCl_3$. The $^{31}P\{^1H\}$ NMR spectra were recorded at 25 °C. After the addition of a molar equivalent of Et_3N, the temperature was raised to 50 °C and the $^{31}P\{^1H\}$ NMR spectrum recorded. The NMR tube containing the reaction mixture, was allowed to stand for 24 hours at 50 °C, and the $^{31}P\{^1H\}$ NMR spectrum re-acquired.

REFERENCES

1 Beyer, L.; Hoyer, E.; Hennig, H.; Kirmse, R.; Hartmann, H.; Liebscher, J.; *J. Prakt. Chem.*, 1975, **317**, 829.

2 Beyer, L.; *Z. Chem.*, 1980, **20**, 268.

3 Beyer, L.; Hoyer, E.; Liebscher, J.; Hartmann, H.; *Z. Chem.*, 1981, **21**, 81.

4 Behrendt, S.; Beyer, L.; Dietze, F.; Kleinpeter, E.; Hoyer, E.; Ludwig, E.; Uhleman, E.; *Inorg. Chim. Acta*, 1980, **43**, 141.

5 Kleinpeter, E.; Behrendt, S.; Beyer, L.; *Z. Anorg. Allg. Chem.*, 1982, **495**, 105.

6 Vest, P.; Schuster, M.; König, K.-H.; *Fresenius' Z. Anal. Chem.*, 1989, **335**, 759.

7 König, K.-H.; Schuster, M.; Schneeweis, G.; Steinbrech, B.; *Fresenius' Z. Anal. Chem.*, 1984, **325**, 621.

8 Schuster, M.; *Fresenius' Z. Anal. Chem.*, 1992, **342**, 791.

9 König, K.-H.; Schuster, M.; Steinbrech, B.; Schneeweis, G.; Schlodder, R.; *Fresenius' Z. Anal. Chem.*, 1985, **321**, 457.

10 Vest, P.; Schuster, M.; Konig, K.-H.; *Fresenius J. Anal. Chem.*, 1991, **341**, 566.

11 Irving, A.; Koch, K.R.; Matoetoe, M.; *Inorg. Chim. Acta,* 1993, **206**, 193.

12 Pidcock, A.; Richards, R.E.; Venanzi, L.M.; *J. Chem. Soc. A*, 1966, 1707.

13 Pearson, R.G.; *Inorg. Chem.*, 1973, **12**, 712.

14 Richter, R.; Beyer, L.; Kaiser, J.; *Z. Anorg. Allg. Chem.*, 1980, **461**, 67.

15 Knuuttilla, P.; Knuuttilla, H.; Hennig, H.; Beyer, L.; *Acta Chem. Scand., Ser. A,* 1982, **36**, 541.

16 Fitzl, G.; Beyer, L.; Sieler, J.; Richter, R.; Kaiser, J.; Hoyer, E.; *Z. Anorg. Allg. Chem.*, 1977, **433**, 237.

17 Sieler, J.; Richter, R.; Hoyer, E.; Beyer, L.; Lindqvist, O.; Andersen, L.; *Z. Anorg. Allg. Chem.*, 1990, **580**, 167.

18 Bensch, W.; Schuster, M.; *Z. Anorg. Allg. Chem.*, 1992, **615**, 93.

19 Giroud-Godquin, A-M.; Maitlis, P.M.; *Angew. Chem. Int. Ed. Engl.*, 1991, **30**, 375.

20 Vorländer, D.; *Ber.*, 1910, **43**, 3120.

21 Sacconi, L.; Mani, F.; Bencini, A.; *Comprehensive Coordination Chemistry - The synthesis, reactions, properties and applications of coordination compounds*, vol. 5, (eds.), Wilkinson, G., Gillard, R.D., McCleverty, J.A., Pergamon Press, Oxford, 1987.

22 *Comprehensive Coordination Chemistry - The Late Transition Metals*, vol. 2, (eds.), Wilkinson, G.; Gillard, R.D.; McCleverty, J.A.; Pergamon Press, New York, 1987.

23 Ho, T.-L.; *Hard and Soft Acids and Bases Principle in Organic Chemistry*, Academic Press, New York, 1977.

24 Sidgwick, N.V.; *Chemical Elements and their Compounds*, vol 1, Claredon, Oxford, 1949.

25 Massey, A.; *Comprehensive Inorganic Chemistry*, vol 3, (eds.), Bailar, J.C.; Emeléus, H.J.; Nyholm,R.S.; Trotman-Dickenson, A.F.; Pergamon, Oxford, 1973.

26 Hughes, M.N.; *Inorganic Chemistry of Biological Systems*, 2nd edn., Wiley, Chichester, 1981.

27 Hatfield, W.E.; Whyman, R.; *Transition Met. Chem.*, 1969, **47**, 5.

28 Jardin, F.H.; *Adv. Inorg. Chem. Radiochem.*, 1975, **17**, 115.

29 Koch, K.R.; du Toit, J.; Caira, M.; Sacht, C.; *J. Chem. Soc., Dalton Trans,* 1994, 785.

30 Koch, K.R.; Matoetoe, M.C.; *Mag. Res. Chem.*, 1991, **29**, 1158.

31 Huheey, J.E.; *Inorganic Chemistry - Principles of Structure and Reactivity*, Harper & Row, New York, 1978.

32 Bret, J-M.; Castan, P.; Commenges, G.; Laurent, J-P.; *Polyhedron*, 1983, **2**, 901.

33 Bourne, S.; Koch, K.R.; *J. Chem. Soc., Dalton Trans.*, 1993, 2071.

34 Anderson, G.K.; Cross, R.J.; *Chem. Soc. Rev.*, 1980, **9**, 185.

35 Pregosin, P.S.; *Studies in Inorganic Chemistry 13. Transition Metal Nuclear Magnetic Resonance,* Elsevier, New York, 1991.

36 Pregosin, P.S.; *Coord. Chem. Rev.*, 1982, **44**, 247.

37 Kerrison, S.J.S.; Sadler, P.J.; *Inorg. Chim. Acta,* 1985, **104**, 197.

38 Koch, K.R.; Sacht, C.; unpublished results.

39 Johnson, L.F.; Jankowski, W.C.; *Carbon -13 NMR spectra. A collection of assigned, coded and indexed spectra*, John Wiley & Sons, New York, 1972.

40 Harris, R.L.N.; Oswald, L.T.; *Aust. J. Chem.*, 1974, **27**, 1531.

41 Kolthoff, I.M.; Stricks, W.; *J. Am. Chem. Soc.*, 1951, **73**, 1728.

42 Pregosin, P.S.; Kunz, R.W.; *^{31}P and ^{13}C NMR of Transition Metal Phosphine Complexes*, (eds.), Diehl, P.; Fluck, E.; Kosfeld, R.; Springer-Verlag, Berlin, Heidelberg, New York, 1979.

CHAPTER 5

MACROCYCLIC *N*-ACYLTHIOUREAS

5.1 Introduction

The first crown ether, dibenzo-18-crown-6 (Figure 5.1), was discovered in 1967[1] by the industrial chemist Charles J. Pedersen. Pedersen's interest was aroused by the unusual solubility of the macrocyclic polyether - it was only slightly soluble in methanol, but on addition of sodium salts, it was readily soluble. At the time Pedersen undertook his work, neutral complexing agents for transition metals were already well known, but complexing of alkali metals by neutral species was an uncommon phenomenon. Strong stoichiometric complexes with alkali metals had only been observed with biological materials[2,3].

Figure 5.1 Pedersen's first crown ether - dibenzo-18-crown-6[1].

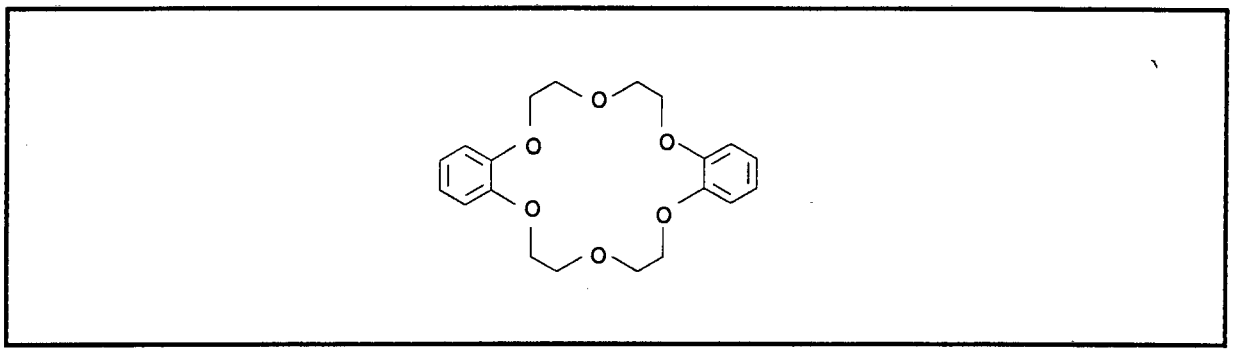

Pedersen's reports on the synthesis of a variety of macrocyclic polyethers and his observations that Group IA and IIA cations significantly increased the dissolution of the macrocyclic compounds in methanol, led to the discovery of the complexing power of macrocyclic polyether compounds and to the synthesis of other macrocyclic polyethers[4]. Furthermore, Pedersen announced that macrocyclic crown ethers were remarkably selective towards certain alkali and alkali earth metals[4]. Since these functionalities are closely related to those observed with biological ionophores, naturally occurring ion transport phenomena were successfully mimicked by these synthetic materials[5]. This property encouraged work in the field of selective complexation since it was anticipated that such approaches could open new aspects of membrane biology and could lead to the development of a variety of applications[6].

From the very beginning, Pedersen recognised that systematic nomenclature was absurdly complicated for discussion of such complex macrocyclic molecules, e.g. the structure in Figure 5.1 has the name 2,3,11,12-dibenzo-1,4,7,10,13,16-hexaoxacyclooctadeca-2,11-diene[7]. The most popular and widely used nomenclature, and the one referred to in this work, is based on Pedersen's original nomenclature. Hence, Pedersen's first macrocyclic polyether (Figure 3.1), can be named as follows:

(i) the total number of atoms in the ring is given in square brackets, e.g. [18]

(ii) the family name 'crown' then follows

(iii) finally, the total number of heteroatoms in the ring portion of the structure is given, e.g. 6, representing the six oxygen donor atoms in the ring

(iv) additional substituents are affixed at the beginning of the whole name, e.g. dibenzo.

In this thesis the name 'crown ether' shall refer to a mono-cyclic compound containing only oxygen as the donor atom whereas the term aza- and diaza-crown ether (Figure 5.2) shall refer to a mono-cyclic compound containing, in addition to the oxygen donor atoms, one and two nitrogen donor atoms respectively.

Figure 5.2 Schematic representation of aza-18-crown-6 and diaza-18-crown-6[8].

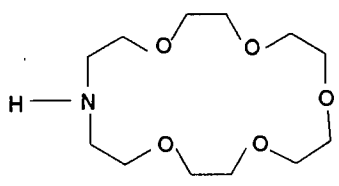

aza-18-crown-6

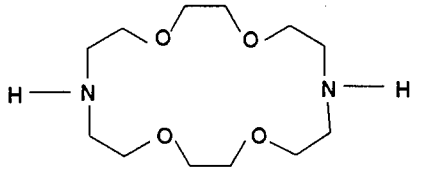

diaza-18-crown-6

In view of the selective complexing abilities of macrocyclic crown ethers, a correlation between structure and properties was sought and all parameters in the classical crown ether were varied[8-14]. The structural modifications included variations in ring size and number of rings, molecular flexibility and type and number of donor atoms in the ring. Consequently, these investigations have resulted in a plethora of publications including extensive review articles[8].

Since the discovery of Pedersen's crown ether, a variety of macrocyclic molecules have been prepared and widely applied in chemistry, industry and related fields. The ability to form complexes with salts and certain other compounds is the most remarkable property of the cyclic polyethers. Accordingly, it is necessary to understand how structural modifications effect the properties and complexing abilities of crown ether compounds.

In a hydrophilic medium, the oxygen atoms of the ring point outwards, creating a lipophilic carbon centre[15]. In a lipophilic medium, the oxygen atoms point inwards, with the hydrophobic CH_2 groups turned outwards. For optimal complexation of cations, the donor atoms must all point inward towards the macrocycle's hole. Unless the macrocycle adopts this conformation, solvation of the ring-bound cation will not occur and complexation will fail. Thus, the nature of the surrounding solvent determines the extent to which complexation of cations occurs[7]. Furthermore, other factors, including crown ether *ring size*, ligand *topology* and the *donor atoms* present also effect the degree of cation complexation.

In substituting nitrogen for oxygen the size and shape of the molecule remain essentially similar, but the acid-base properties of the compound are substantially altered[5]. Moreover, the *cation binding selectivity* is changed because nitrogen and oxygen have inherently different affinities for cations[5]. Accordingly, complexation of alkali metals falls dramatically when the ring oxygen atoms are replaced with nitrogen atoms, but rises significantly in this order in the case of transition metal ions such as Ag^+. This observation is in accordance with the HSAB principle[16], which predicts that energetically, hard oxygen atoms and hard alkali metal ions on the one hand, and soft nitrogen atoms and soft transition metal ions on the other, will afford better binding pairs[16].

Complexation processes between crown ethers and various cations have been studied extensively and can be detected in solution in many different ways, such as spectral changes, altered solubilities and electrochemically. Of the numerous approaches used over the years, a few have emerged as most convenient or most useful. These methods include the extraction technique, the ion selective electrode technique, and ^1H NMR spectroscopy[8,17-19].

Finally, interest in the structure and binding behaviour of valinomycin[20], a macrocyclic antibiotic, has led to the study of macrocyclic compounds possessing cation-ligating arms[6]. The amine group of a simple aza- or diaza-crown ether provides a convenient location for the modification of crown ethers allowing for the synthesis of 'armed' macrocycles[5,21] (Figure 5.3). Various studies have concentrated on the design and synthesis[22-26] of new crown ethers as well as the effect substituents[27-30] have on the properties of crown ethers. Quite a number of studies have focused on the complexation and selectivity profiles of single-armed aza-crown ethers[21,31-36] and two-armed diaza-crown ethers[21,35-39].

Figure 5.3 Examples of single- and two-armed nitrogen pivot aza-crown ethers[5].

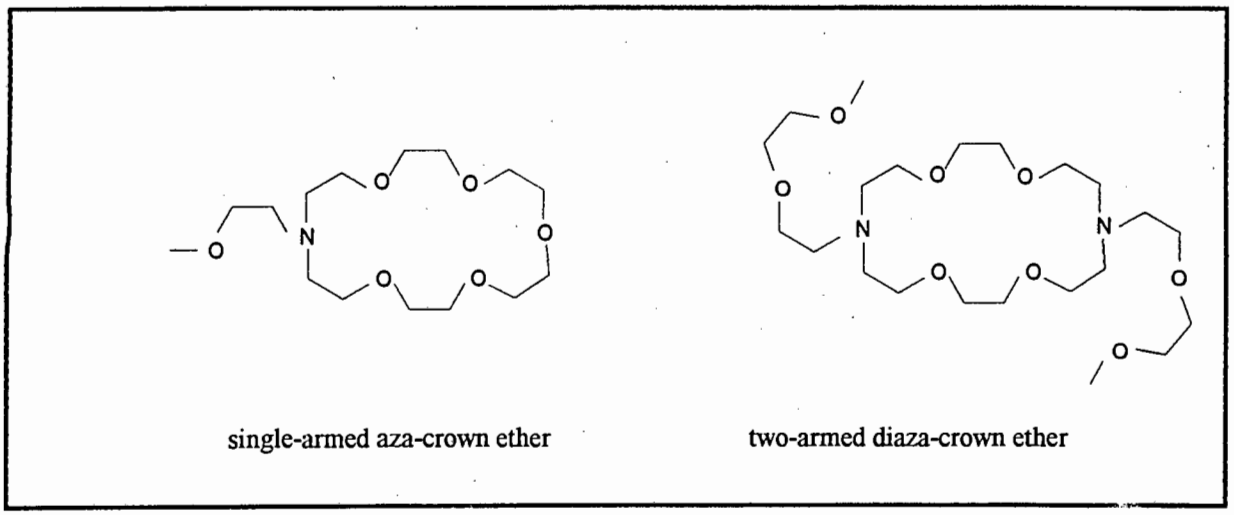

The recent interest in 'armed' macrocyclic molecules[5] encouraged us to attempt the preparation of macrocyclic compounds incorporating *N*-acylthiourea sidearms. Our original approach to macrocyclic *N*-acylthioureas was two-fold. Firstly, we anticipated that once a cation was bound in the macrocyclic ring, the *N*-acylthiourea sidearm bearing the neutral carbonyl donor group would provide a third dimension of solvation (Figure 5.4). Recent reports have revealed that three dimensional coordination with spherical cations gives rise to more stable complexes compared to only two dimensional complexation[29,40]. Secondly, macrocyclic *N*-acylthiourea compounds incorporate two potential sites for cation complexation, i.e. the chelate moiety for complexing transition metals and the macrocyclic ring for complexing, amongst others, Group IA and IIA metals, and selected organic molecules[41,42] (Figure 5.5).

Figure 5.4 Schematic representation of third dimension solvation of a cation in a macroring[32].

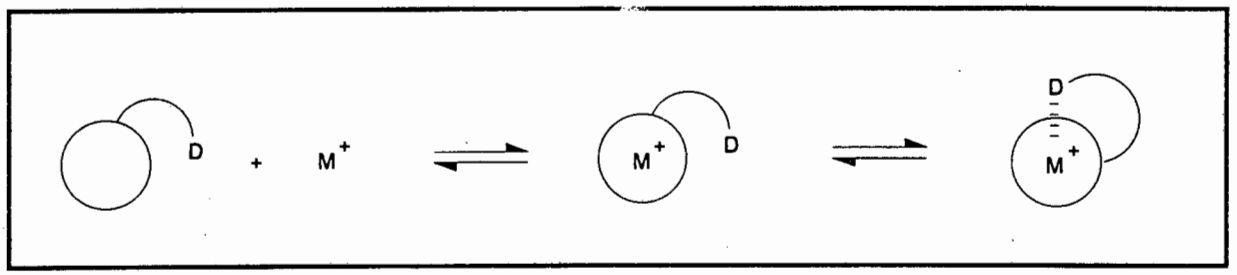

The present study includes the synthesis and characterisation of two novel, potentially fluorescent macrocyclic *N*-acylthioureas, these being *N*-aza-18-crown-6-*N'*-naphthoylthiourea and *N,N*-diaza-18-crown-6-*N'*-naphthoylthiourea, and a heterocyclic derivative, *N*-morpholino-*N'*-naphthoylthiourea. UV spectroscopy and picrate extraction studies indicated poor binding between K^+ and NH_4^+ cations and the aza-crown ether moieties of *N*-aza-18-crown-6-*N'*-naphthoylthiourea and *N,N*-diaza-18-crown-6-*N'*-naphthoylthiourea. The X-ray crystal structures of these compounds were therefore determined with particular interest in the conformation of the macrocyclic rings. Finally, proton NMR experiments were performed to ascertain whether *any* degree of complexation between *N*-aza-18-crown-6-*N'*-naphthoylthiourea and K^+ and $CH_3NH_3^+$ cations could be observed in solution. The experiments were performed at low temperatures due to the poor binding affinities indicated by preliminary experiments.

Figure 5.5 Schematic representation of the potentially fluorescent *N*-aza-18-crown-6-*N'*-naphthoylthiourea compound illustrating the presence of a transition metal binding site and a potential alkali metal binding site.

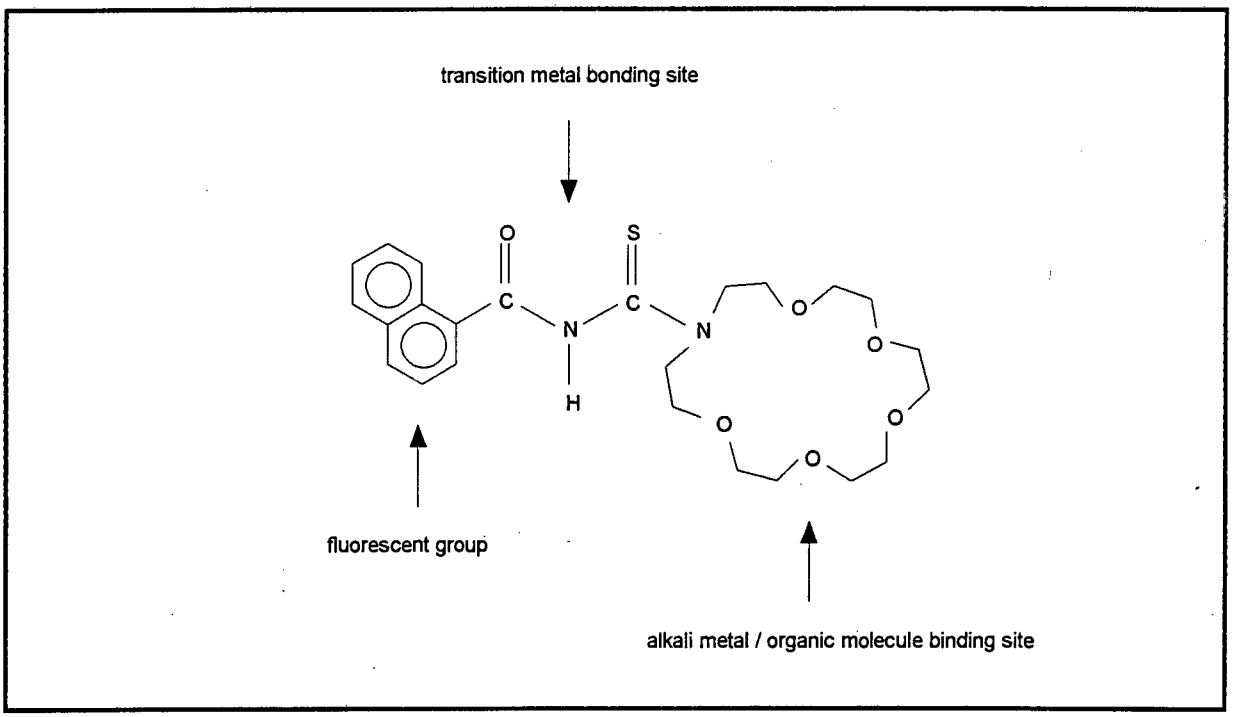

5.2 Results and Discussion

5.2.1 Synthesis and Characterisation of *N*-morpholino- (1), *N*-aza-18-crown-6- (2), *N,N*-diaza-18-crown-6-*N'*-naphthoylthiourea (3)

The compounds, *N*-morpholino-*N'*-naphthoylthiourea (**1**), *N*-aza-18-crown-6-*N'*-naphthoylthiourea (**2**) and *N,N*-diaza-18-crown-6-*N'*-naphthoylthiourea (**3**) (Figure 5.6), were prepared employing the general method[43] of preparation of *N*-acylthioureas. The products were isolated as colourless crystals and in fairly good yields of 70 - 80 %. The compounds were satisfactorily characterised by C, H and N elemental analysis, mass spectrometry, and ^{1}H and ^{13}C NMR spectroscopy. It is interesting to note that the ^{1}H NMR spectra and elemental analyses of **2** and **3** revealed the inclusion of chloroform and/or water molecules. Accordingly, to gain further insight into the extent to which these macrocyclic *N*-acylthiourea compounds include solvent molecules, Thermogravimetric Analysis (TGA) and Differential Scanning Calorimetry (DSC) investigations were performed.

The ^{1}H NMR spectrum, elemental analyses, and TGA thermogram of *N*-aza-18-crown-6-*N'*-naphthoyl-thiourea, suggests the inclusion of one mole of water per mole of **2**, irrespective of the recrystallising solvent. It is evident from the TGA thermogram (Figure 5.7) that a decrease in the weight of sample **2** occurs in the temperature range from 70 - 130 °C. The decrease in weight agrees with the loss of one mole of water per mole of **2**. A single broad endotherm in this temperature range, due to melting of the sample and the resulting loss of solvent, is observed in the DSC heating thermogram.

On the other hand, consideration of the ^{1}H NMR spectrum, elemental analyses, and the TGA thermogram of *N,N*-diaza-18-crown-6-*N'*-naphthoylthiourea (**3**), suggests that recrystallisation of **3** from $CHCl_3$ / EtOH results in the inclusion of one mole of water and two moles of chloroform. A substantial decrease in the weight of sample of **3** between 90 and 150 °C, is evident from the TGA thermogram (Figure 5.8(a)). The decrease in weight is in agreement with the loss of one mole of water and two moles of chloroform per mole of **3**.

Three endothermic peaks at 99, 108 and 159 °C, are observed in the DSC heating curve of *N,N*-diaza-18-crown-6-*N'*-naphthoylthiourea (Figure 5.8(b)). The overlapping endotherms at 99 and 108 °C represent the loss of chloroform and water from the crystal lattice. We propose that the larger endothermic peak at 99 °C represents the loss of chloroform on the basis of its lower boiling point compared to water, and the size of the endotherm. The smaller endotherm at 108 °C could therefore represent the loss of water. The loss of chloroform and water occurs at temperatures in excess of their boiling points which suggests that these solvent molecules are strongly bound in the crystal lattice. The melting transition of **3** is represented by the endothermic peak at 159 °C. An interesting point to note is that the inclusion of solvent molecules is solvent

dependent, as no evidence for the inclusion of solvent molecules is observed when **3** is recrystallised from $CHCl_3$ / CH_3CN (see section 5.2.3).

Figure 5.6 Schematic representation of *N*-morpholino-*N'*-naphthoylthiourea (**1**) *N*-aza-18-crown-6-*N'*-naphthoylthiourea (**2**) and *N,N*-diaza-18-crown-6-*N'*-naphthoylthiourea (**3**).

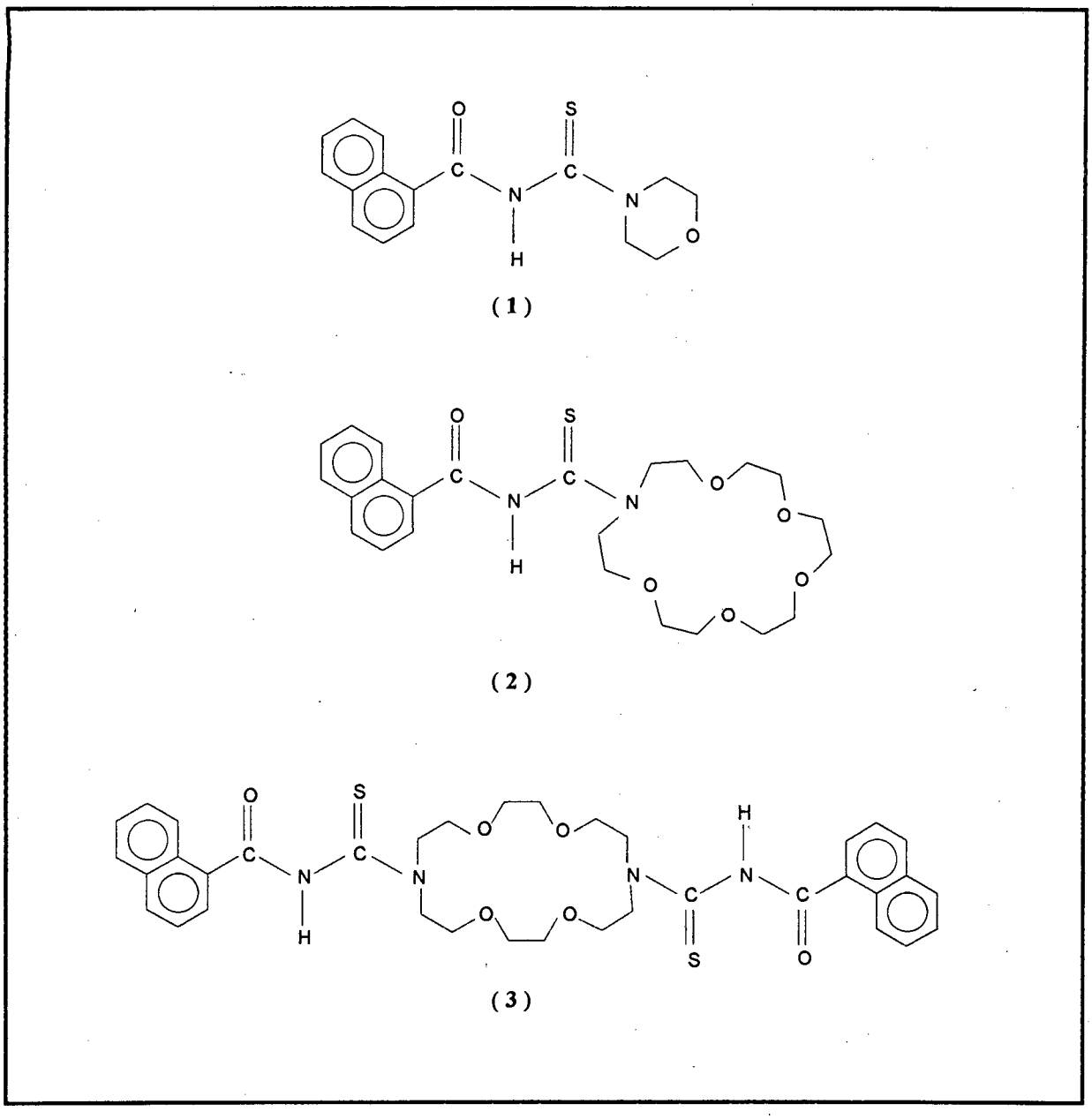

(**1**)

(**2**)

(**3**)

Figure 5.7 The TGA thermogram of *N*-aza-18-crown-6-*N'*-naphthoylthiourea, recrystallised from $CHCl_3$ / CH_3CN, illustrates the loss of water.

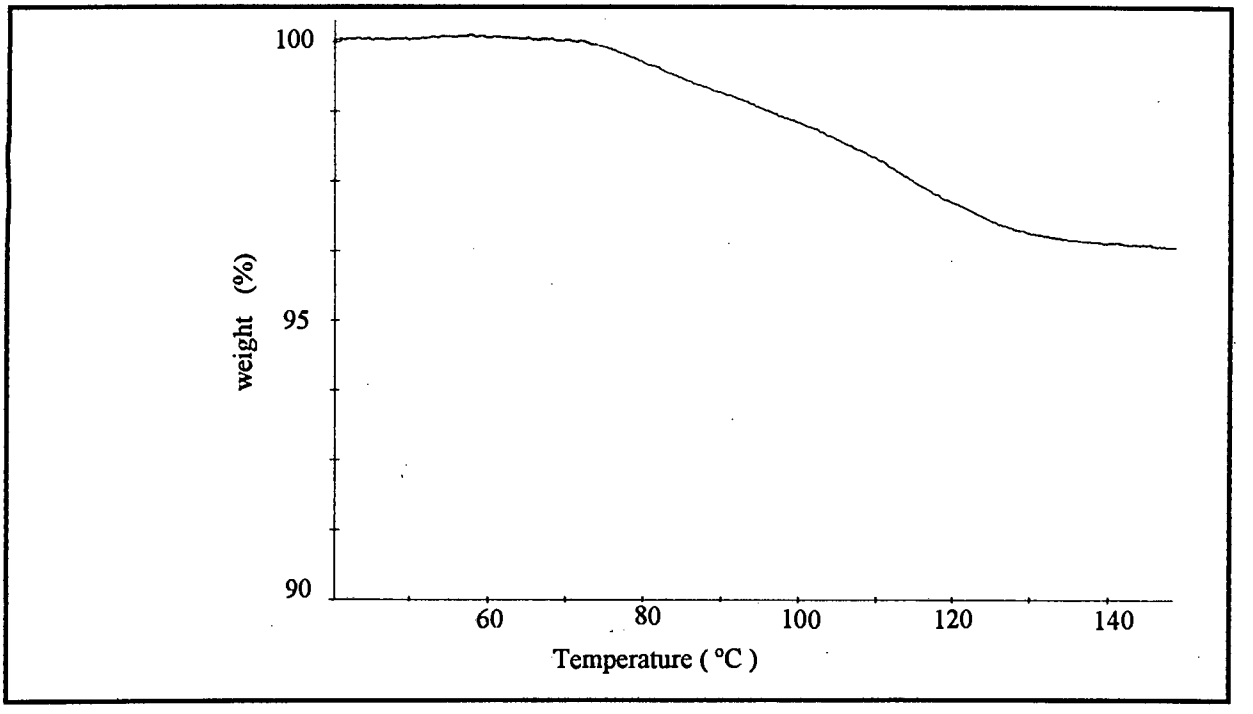

Figure 5.8(a) The TGA thermogram of **3**, recrystallised from $CHCl_3$ / EtOH, illustrating the loss of one mole of water and two moles of chloroform per mole of *N,N*-diaza-18-crown-6-*N'*-naphthoylthiourea.

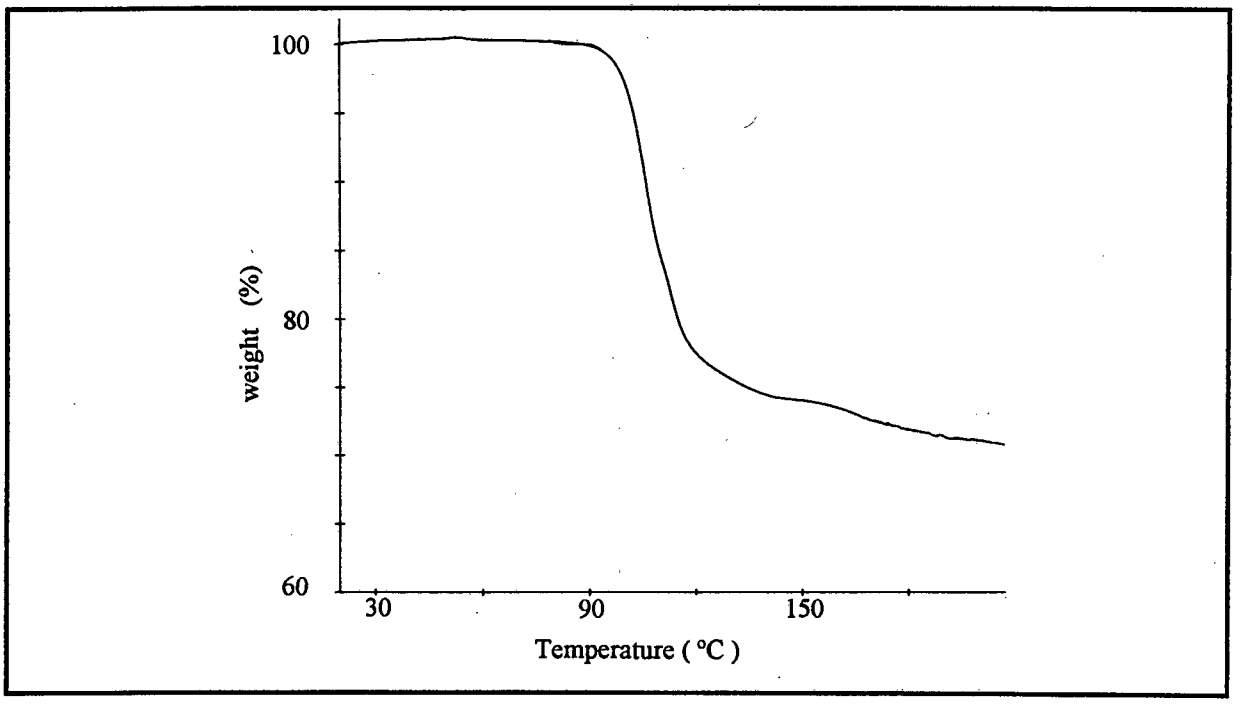

Figure 5.8(b) The DSC heating curve of **3**. The endotherms between 90 and 110 °C represent the loss of solvent.

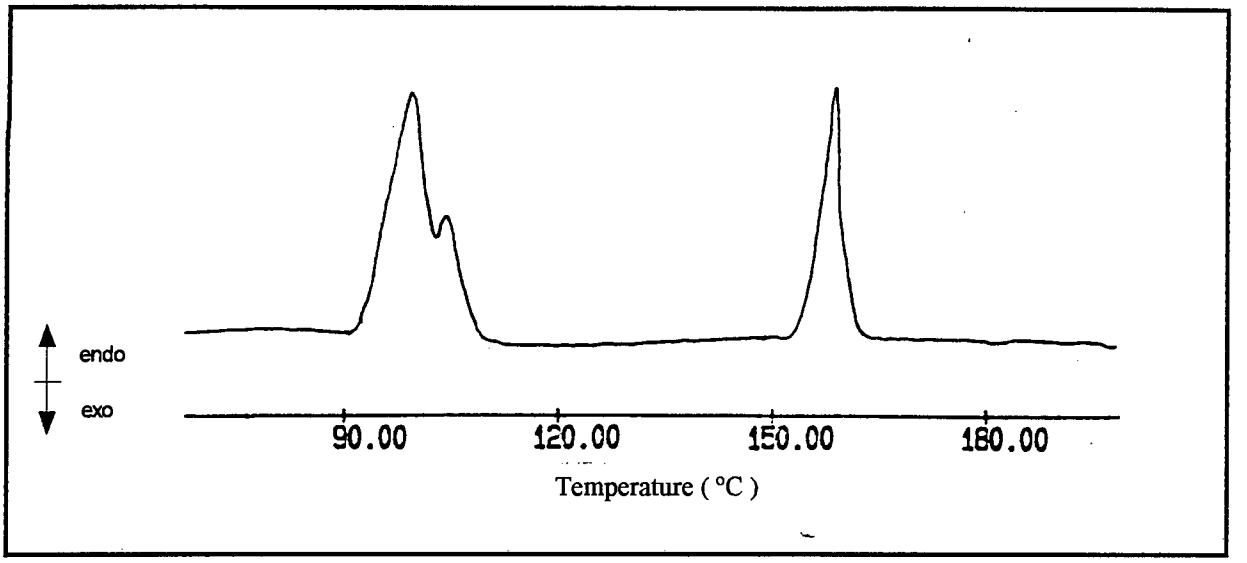

5.2.2 Complexation Studies

In view of the remarkable complexing behaviour of crown ethers, the types of complexes formed are now known to be multifarious and varied. Various reports have shown that K^+ and NH_4^+ cations are suitably sized for complexation into the cavity of aza-18-crown-6 and diaza-18-crown-6[22,31,37,41,44]. The compounds under study, *N*-aza-18-crown-6-*N'*-naphthoylthiourea and *N,N*-diaza-18-crown-6-*N'*-naphthoylthiourea, have a polyether ring that we therefore believed was appropriately sized for complexation with K^+ and NH_4^+ cations, and a sidearm bearing a neutral carbonyl group that we envisioned would interact with the cation once it was bound to the aza-crown ether ring, and thus provide a third dimension of solvation. In the present work the interaction of the aza- and diaza-crown ether moieties of *N*-aza-18-crown-6-*N'*-naphthoylthiourea and *N,N*-diaza-18-crown-6-*N'*-naphthoylthiourea with K^+ and NH_4^+ cations was studied with the aid of metal picrate extraction studies and UV spectroscopy.

5.2.2.1 K^+ and NH_4^+ Picrate Extraction Studies

Complexing of cations by crown ethers can be detected in solution in many different ways. One of the simplest qualitative, and under certain conditions, quantitative approaches utilises the extraction technique[8,17]. Most crown ethers are insoluble or relatively insoluble in aqueous solutions and most metal salts are insoluble or relatively insoluble in organic solvents. Equal volumes of an organic solvent (e.g. dichloromethane) and water containing a metal salt (e.g. potassium picrate) may be mixed and the aqueous layer will be yellow due to the presence of the dissolved potassium picrate, and the organic layer colourless. However on addition of a crown ether which dissolves in the organic layer, the organic layer becomes yellow

as a result of the crown ether's complexation with the potassium cation so that the potassium picrate salt partitions into the organic phase. The extent to which extraction occurs can be detected visibly or, under certain conditions, quantitatively by ultraviolet spectroscopy[45].

The disadvantage of the extraction method however, is that for crown ethers with a cavity ring size larger than 21 ring atoms, water can interfere with complexation[46]. Furthermore, the technique is sensitive to the hydrophobic / hydrophilic balance and this may affect conclusions[8]. The nature of the solvent also effects the extent to which complexation between a macrocyclic ring and a cation occurs[5]. The technique must therefore be used with attention to detail and with due caution.

In the present study comparative solvent extractions of aqueous K^+ and NH_4^+ picrates were performed, employing previously reported methods[17,47,48]. Two different sets of experiments were performed, the first involving an equimolar amount of cation and macrocyclic compound, and the second, involving a ten times excess of the macrocyclic compound. The solvents, dichloromethane and water, were saturated with each other prior to use in order to prevent volume changes of both phases during extraction. Equal volumes (10 cm^3) of a dichloromethane solution of aza-18-crown-6, diaza-18-crown-6, *N*-aza-18-crown-6-*N'*-naphthoylthiourea or *N,N*-diaza-18-crown-6-*N'*-naphthoylthiourea and an aqueous solution of K^+ or NH_4^+ picrate were introduced into an Erlenmeyer flask, which was stoppered and then shaken vigorously for 40 minutes in a thermostated water bath at 25.0 ± 0.5 °C. The mixture was then centrifuged in order to complete phase separation. Part of the dichloromethane phase was withdrawn and the percentage extraction was determined spectrophotometrically (λ_{max} = 356 nm). Similar extraction experiments were performed under basic conditions i.e. in the presence of KOH / K^+ picrate and NH_3 / NH_4^+ picrate.

The percentage extractability of K^+ and NH_4^+ picrate by *N*-aza-18-crown-6-*N'*-naphthoylthiourea and *N,N*-diaza-18-crown-6-*N'*-naphthoylthiourea is listed in Table 5.1, along with the corresponding data for their parent compounds, aza-18-crown-6 and diaza-18-crown-6. In blank experiments, there was no detectable extraction of the metal picrate into the organic phase in the absence of the crown ether compounds.

Table 5.1 Percentage extractability of K^+ and NH_4^+ picrate by *N*-aza-18-crown-6-*N'*-naphthoylthiourea, (**2**), and *N,N*-diaza-18-crown-6-*N'*-naphthoylthiourea, (**3**), compared to aza-18-crown-6 and diaza-18-crown-6.

Compound	**% Extractability**	
	K^+	NH_4^+
Aza-18-crown-6	29.8	30.4
N-aza-18-crown-6-*N'*-naphthoylthiourea (**2**)	0	0
diaza-18-crown-6	20.9	19.9
N,N-diaza-18-crown-6-*N'*-naphthoylthiourea (**3**)	0	0

No evidence of metal picrate extraction into the organic phase was detected for **2** and **3**. No changes in the degree of cation extraction were observed in the presence of KOH/K^+ picrate and NH_3/NH_4^+ picrate. Moreover, a ten times excess of compound **2** and **3** with respect to the cation had no effect on the degree of metal picrate extraction.

Based on the foregoing results it is evident that *N*-aza-18-crown-6-*N'*-naphthoylthiourea and *N,N*-diaza-18-crown-6-*N'*-naphthoylthiourea do not extract K^+ and NH_4^+ metal picrates into dichloromethane solutions. However, it is necessary to mention that Iwachido[17] *et al* have reported that the *hydrophobicity* of a compound shows virtually *no effect* on the *stability* of a metal crown complex, whereas it does have an effect on the *extraction equilibrium constant*, K_{ex}. Accordingly, the hydrophobicity of *N*-aza-18-crown-6-*N'*-naphthoylthiourea and *N,N*-diaza-18-crown-6-*N'*-naphthoylthiourea may have profound effects on their ability to extract appropriately sized cations from aqueous solutions.

5.2.2.2 Ultraviolet Spectroscopic Studies

Potential K^+ and NH_4 cation complexation with *N*-aza-18-crown-6-*N'*-naphthoylthiourea and *N,N*-diaza-18-crown-6-*N'*-naphthoylthiourea, was studied with the aid of UV spectroscopy. The experimental approach was based on the observation that cyclic polyethers frequently exhibit pronounced shifts in their optical spectra in the presence of a coordinating cation. Complexation with a cation generally results in a hypsochromic shift of the peak maxima or in the appearance of a new peak[4,41]. The new peak is usually not clearly separated from the main band and is therefore not suitable for precise quantitative measurements. However it's appearance has been used extensively for qualitative detection of complexation[4]. Complexation of a cation into the aza- and diaza-crown ether cavities of **2** and **3** respectively, is therefore expected to result in a shift in the peak maxima or in the appearance of a new peak.

N-aza-18-crown-6-*N'*-naphthoylthiourea and *N,N*-diaza-18-crown-6-*N'*-naphthoylthiourea show an absorption maximum at 215 nm (in acetonitrile) in the UV spectrum. A small 'shoulder' on the peak at 215 nm was observed in the UV spectra of compounds **2** and **3** in the presence of equimolar amounts of KSCN or KI. Although this is not conclusive evidence, the appearance of the 'peak shoulder' nevertheless suggests a degree of complexation between K^+ and the aza- and diaza-crown ether moieties of **2** and **3** respectively.

A similar experiment, based on the observation that salts of picric acid in low polarity media frequently exhibit pronounced shifts in their optical spectra in the presence of crown ethers[42], was attempted. Unfortunately, complexation of *N*-aza-18-crown-6-*N'*-naphthoylthiourea and *N,N*-diaza-18-crown-6-*N'*-naphthoylthiourea with potassium or ammonium picrate could not be followed by UV spectroscopy because of peak overlap of the picrate and *N*-acylthiourea compounds in the UV spectra.

In summary, the poor interaction between the polyether rings of *N*-aza-18-crown-6-*N'*-naphthoylthiourea and *N,N*-diaza-18-crown-6-*N'*-naphthoylthiourea and K^+ and NH_4^+ cations was disappointing. Hence, in order to rationalise these weak interactions, the X-ray crystal structures of *N*-aza-18-crown-6-*N'*-naphthoylthiourea and *N,N*-diaza-18-crown-6-*N'*-naphthoylthiourea were determined.

5.2.3 Crystal and molecular structures of *N*-aza-18-crown-6-*N'*-naphthoylthiourea and *N,N*-diaza-18-crown-6-*N'*-naphthoylthiourea

The crystals of *N*-aza-18-crown-6-*N'*-naphthoylthiourea and *N,N*-diaza-18-crown-6-*N'*-naphthoylthiourea were grown from solutions containing huge excesses of K^+ cations with the hope of isolating a K^+ complex. However, the noticeable absence of K^+ from the solid state structures clearly demonstrates the poor binding affinity of the aza- and diaza-crown ether rings of *N*-aza-18-crown-6-*N'*-naphthoylthiourea and *N,N*-diaza-18-crown-6-*N'*-naphthoylthiourea towards alkali metals.

The structures of *N*-aza-18-crown-6-*N'*-naphthoylthiourea (**2**) and *N,N*-diaza-18-crown-6-*N'*-naphthoylthiourea (**3**) were determined by Dr Susan Bourne (Department of X-ray Crystallography, UCT). The structures were determined by single crystal X-ray diffraction and were solved by direct methods using SHELXS-86[49] and refined using SHELX-76[50]. The final model included anisotropic refinement of all non-hydrogen atoms. The hydrogens atoms involved in hydrogen bonding were located in the difference Fourier map and refined isotropically with constrained bond lengths. All the other hydrogens were placed in calculated positions and linked to shared isotropic temperature factors. The crystal data, experimental data and refinement parameters are summarised in Table 3.1 of Appendix 3, and the fractional atomic coordinates and thermal parameters for all non-hydrogen atoms are listed in Tables 3.2 and 3.3 of Appendix 3.

Description of the molecular structure of N-aza-18-crown-6-N'-naphthoylthiourea

Colourless cubic crystals of *N*-aza-18-crown-6-*N'*-naphthoylthiourea (**2**) were obtained from an acetone / KI / D_2O solution on slow evaporation of the solvent at room temperature. The molecular structure contains discrete molecules of **2** and solvent water molecules. The presence of solvent water molecules in the crystal structure confirms the results of elemental analyses and TGA (described in section 5.2.1) which indicated the presence of one mole of water per mole of **2**. The molecular structure and atom numbering is illustrated in Figure 5.9. The bond lengths and bond angles all fall within the expected ranges and are reported in Table 3.4 of Appendix 3.

Figure 5.9 Perspective view of the molecular structure of *N*-aza-18-crown-6-*N'*-naphthoylthiourea showing the atom numbering scheme for the non-hydrogen atoms. The dashed line represents *intra*molecular hydrogen bonding. The H atoms are omitted for clarity.

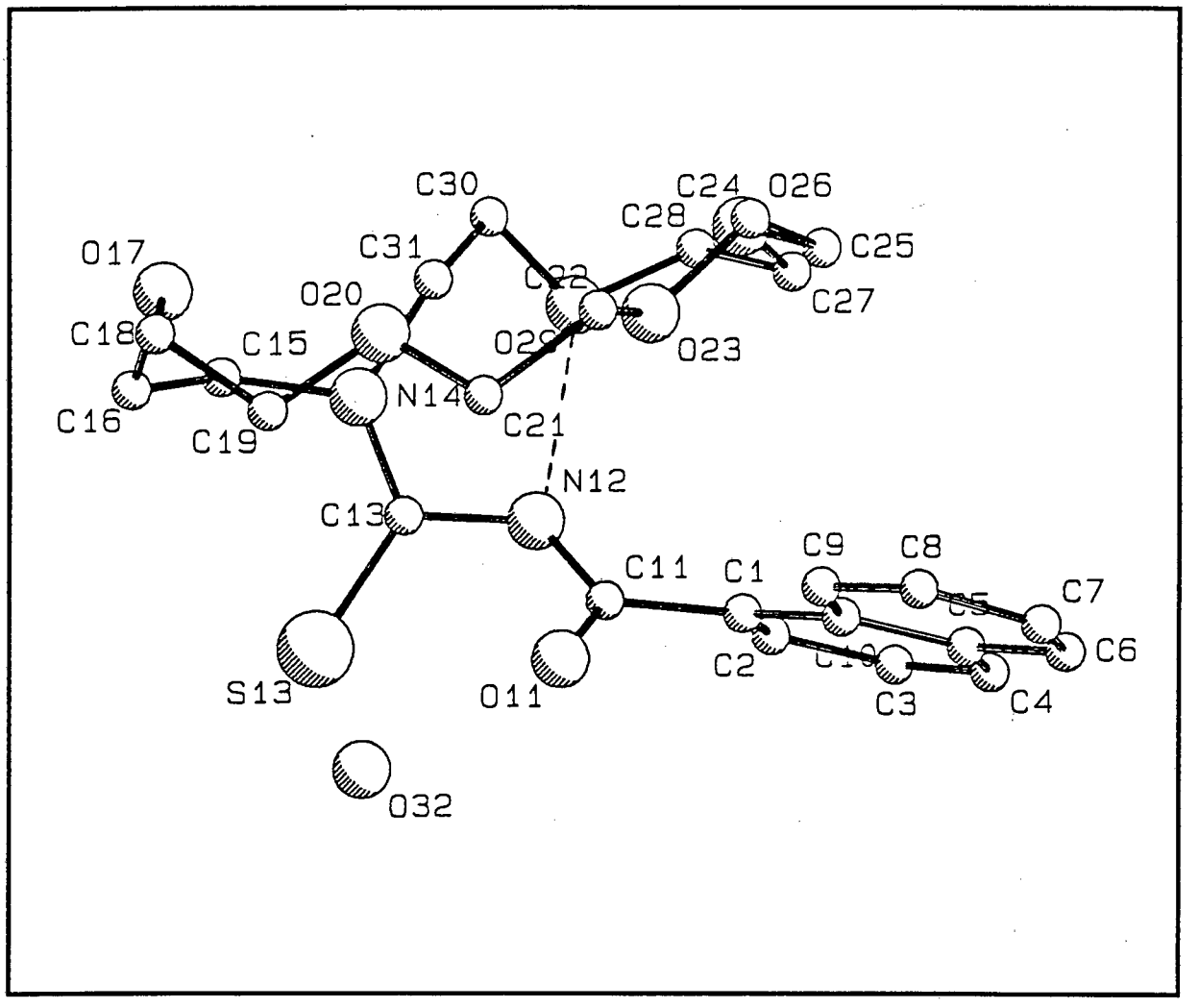

The naphthyl group of *N*-aza-18-crown-6-*N'*-naphthoylthiourea (**2**) is planar, with a mean deviation of atoms from the plane of 0.024 Å. The bond distances and bond angles of the aromatic system are unexceptional and will not be discussed further.

The C(13) – N(14) bond of **2** is 1.331(5) Å, 0.14 Å shorter than the observed length of the N(14) - C(15) bond. The N(14) - C(15) bond distance, 1.473(4) Å, is similar to that observed for an average C - N single bond, 1.472 Å[51]. On the other hand, the length of the C(13) - N(14) bond is significantly longer than the average single C - N bond but shorter that the average C - N double bond, 1.29 Å[51]. The partial double bond character of C(13) - N(14) may be attributed to delocalisation of the N(14) lone pair of electrons into this bond. The bond distances of **2** are in good agreement with those recently recorded by Sacht[52] *et al* for the related *N,N*-diethanolamino-*N'*-benzoylthiourea compound. The observed C(15) - N(14) - C(31), C(15) - N(14) - C(13) and C(31) - N(14) - C(13) bond angles are 115.7, 120.4 and 123.8° respectively. The approach of these angles to 120° infers a degree of sp^2 hybridisation of the N(14) orbitals, which strengthens the proposal for delocalisation of the nitrogen lone pair of electrons into the C(13) - N(14) bond (Figure 5.10).

Furthermore, the observed C(13) – S(13) bond distance is 1.667(4) Å, which is shorter than a single, 1.81 Å, but longer than a double, 1.56 Å, C – S bond[51]. This suggests that the thio-amide is closer to a dipolar zwitterionic canonical form where the sulfur atom has a partial negative charge and the bond is intermediate between that of a single and double bond.

Figure 5.10 Schematic representation of the delocalisation of the nitrogen lone pair of electrons into the C(13) - N(14) bond of *N*-acylthiourea.

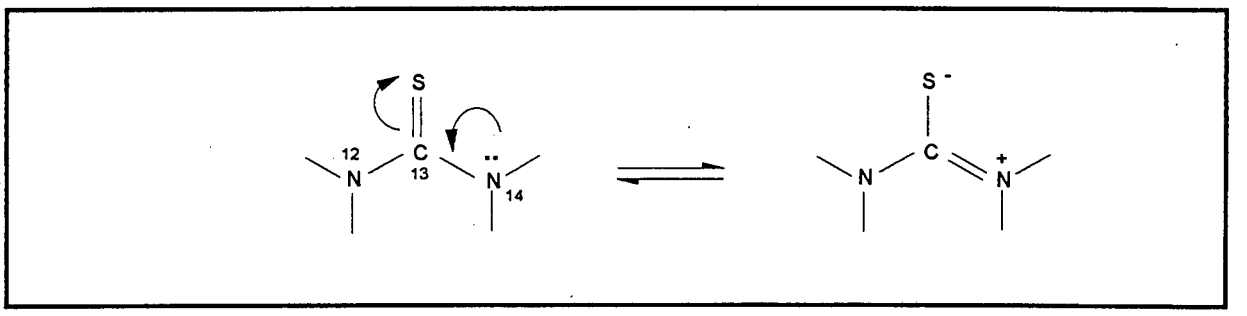

The bond distances, angles and torsion angles of the aza-18-crown-6 ring of **2** are summarised in Table 5.2. The O-C-C-O torsion angles of the aza-18-crown-6 ring indicate a skew conformation (not completely staggered) of the hydrogens of the oxyethylene groups. Interestingly, the X-C-C-X (X = O or N) torsion angles are all *gauche* (mean 64°, range 54 - 76°) with a +,+,–,+,–,– pattern. This contrasts with the familiar D_{3d} conformation of 18-crown-6 rings which have the *gauche* pattern +,–,+,–,+,–. The conformation of the aza-crown ring of **2**, +,+,–,+,–,–, thus represents an unusual conformation of the 18-membered ring not

usually found in 18-crown-6 structures[53,54]. The O-C-C-O torsion angle of 75.6° is significantly larger than the O-C-C-N torsion angles (-61.2, 62.9°), presumably a consequence of the shorter C - O bond lengths[55].

Table 5.2 Bond distances (Å), bond angles (°) and torsion angles (°) of the aza-18-crown-6 ring of *N*-aza-18-crown-6-*N'*-naphthoylthiourea with e.s.d's in parentheses.

A	B	C	D	B-C (Å)	A-B-C (°)	A-B-C-D (°)
N14	C15	C16	O17	1.503(5)	113.3(3)	62.9(5)
C15	C16	O17	C18	1.420(5)	109.1(3)	
C16	O17	C18	C19	1.424(5)	113.9(3)	
O17	C18	C19	O20	1.481(6)	114.0(3)	65.6(5)
C18	C19	O20	C21	1.418(5)	110.1(4)	
C19	O20	C21	C22	1.415(5)	112.5(3)	
O20	C21	C22	O23	1.486(6)	109.9(3)	-75.6(4)
C21	C22	O23	C24	1.409(4)	109.5(3)	
C22	O23	C24	C25	1.422(5)	111.9(3)	
O23	C24	C25	O26	1.493(5)	109.1(3)	67.2(4)
C24	C25	O26	C27	1.420(5)	108.9(3)	
C25	O26	C27	C28	1.414(5)	113.7(3)	
O26	C27	C28	O29	1.488(5)	108.3(3)	-54.1(4)
C27	C28	O29	C30	1.428(4)	111.7(3)	
C28	O29	C30	C31	1.441(4)	114.1(3)	
O29	C30	C31	N14	1.511(5)	110.4(3)	-61.2(4)

It is noteworthy that compound **2** is folded so that the macrocyclic moiety is above the C(11) - N(12) - C(13) backbone of the chelate ring with the carbonyl and thiocarbonyl groups pointing away from the macrocyclic cavity. The molecule is held in this position by an *intra*molecular hydrogen bond between the hydrogen of the amide nitrogen and an oxygen atom of the crown macrocycle, N(12) - H(12)...O(29) (Figure 5.9). The observed N(12) - H(12) bond distance is 0.84 (3) Å and the N(12) ... O(29) bond length 2.900 (4) Å (Table 5.3). The latter bond distance is in accordance with the average N - H...O bond length, 2.98 Å, reported by Kuleshova[56] *et al.* The N(12) - H(12)...O(29) bond angle is 143(5) °.

Table 5.3 The observed N - H and N...O bond lengths (Å) and the bond angle (°) of *N*-aza-18-crown-6-*N'*-naphthoylthiourea with e.s.d. in parentheses.

Assignment	**Bond length (Å)**
N(12) – H(12)	0.84(3)
N(12) ... O(29)	2.900(4)
O(32)-H(32A)	0.97(3)
O(32)...O(20)	2.970(5)*
O(32)-H(32B)	1.03(3)
O(32)...O(11)	2.922(5)
Assignment	**Bond angle (°)**
N(12)-H(12)...O(29)	143(5)
O(32)-H(32A)...O(20)	134(4)
O(32)-H(32B)...O(11)	173(6)

** via (x, y-1, z)*

A novel aspect of the present structure is that the molecular packing of *N*-aza-18-crown-6-*N'*-naphthoyl-thiourea is characterised by infinite ribbons of molecules related by translation along [010], (Figure 5.11). These ribbons are held in place by *inter*molecular hydrogen bonding between a water molecule and two adjacent molecules of **2**. Each bridging water molecule is hydrogen bonded to the carbonyl group of one molecule of **2** and to an oxygen atom of the aza-crown ether ring of an adjacent molecule of **2**. Such an arrangement of bridging water molecules is reminiscent of *t*-$BuNH_3^+$ crown ether complexes which, under certain conditions, form dimers in which water molecules serve as additional and indispensable building blocks[46].

The hydrogen bonded water molecule is located above the cavity of the aza-crown ring of **2** with its oxygen atom forming essentially equidistant bonds with the *oxygen atom* of the aza-crown ring, O(32)...O(20), 2.970(5) Å and the oxygen atom of the *carbonyl group* of an *adjacent* molecule, O(32)...O(11), 2.922(5) Å. These observed O_{water} ... O_{ring} and O_{water} ... $O_{carbonyl}$ separation distances are in accordance with those reported by Willey[57] *et al* between a protonated aza-crown molecule and a water solvate molecule. However, Willey found that the water molecule was located above the aza-crown cavity with its oxygen atom forming hydrogen bonds with the *nitrogen atom* and two of the *oxygen atoms* of the *same* aza-crown ether ring[57].

The bond angle between the water molecule and the carbonyl oxygen atom of **2** is approximately linear, 173 °, whereas the observed hydrogen bond angle between the water molecule and the oxygen atom of the macrocyclic ring is 134 °. The hydrogen bonding data is given in Table 5.3.

It is interesting to note that a crystalline sample of **2** is converted into a colourless *liquid* if heated to 40 °C under vacuum. The absence of water in the liquid sample was confirmed by ^{1}H NMR spectroscopy. The compound remained a liquid under anhydrous conditions but solidified under atmospheric conditions. These results, together with the solid state structure, suggest that water molecules play an integral part in the crystallisation of a solid material.

Figure 5.11 Molecular packing of *N*-aza-18-crown-6-*N'*-naphthoylthiourea is characterised by infinite ribbons of molecules held in place by *inter*molecular hydrogen bonding (dashed lines) between bridging water molecules.

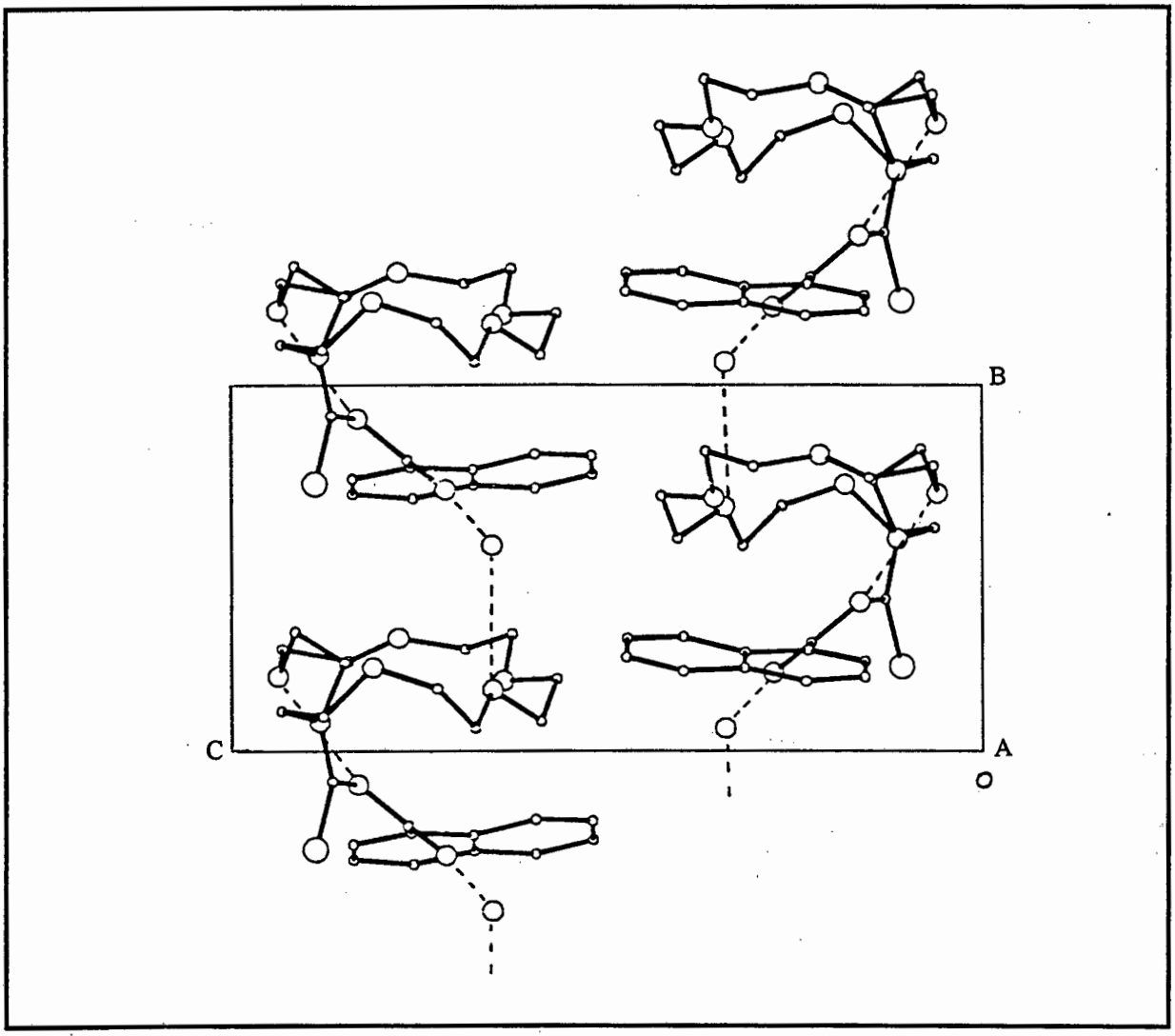

Description of the molecular structure of N,N-diaza-18-crown-6-N'-naphthoylthiourea

Colourless cubic crystals of *N,N*-diaza-18-crown-6-*N'*-naphthoylthiourea (**3**) were obtained from a solution of $CHCl_3/CH_3CN$/KSCN on slow evaporation of the solvent at room temperature. Each molecule of **3** is located at a centre of inversion at the Wyckoff position *h*, (½ ½ ½) and hence half the molecule constitutes the asymmetric unit. The molecular structure and atom numbering is illustrated in Figure 5.12. The bond lengths and bond angles all fall within the expected limits and are reported in Table 3.5 of Appendix 3.

Figure 5.12 Perspective view of the molecular structure of *N,N*-diaza-18-crown-6-*N'*-naphthoylthiourea, showing the atom numbering scheme for the non-hydrogen atoms. The dashed lines represent the *intra*molecular hydrogen bonds. The H atoms are omitted for clarity.

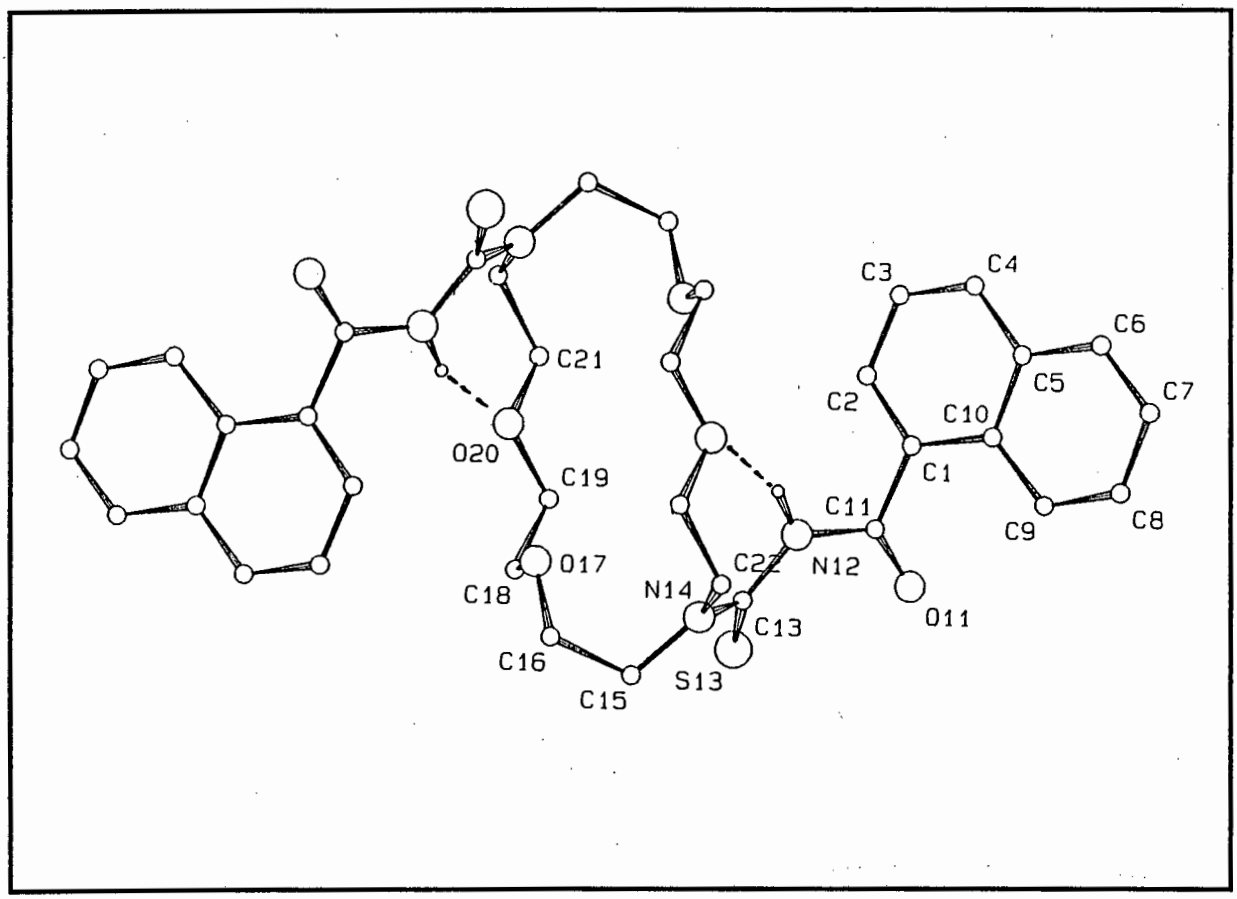

The aromatic ring is essentially planar, with a maximum deviation from the mean plane of 0.06 Å. The bond distances and bond angles of the naphthyl moiety all fall within the expected ranges and will not be discussed further. The bond distances, bond angles and torsion angles of the chelate moiety of *N,N*-diaza-18-crown-6-*N'*-naphthoylthiourea are similar to those observed for *N*-aza-18-crown-6-*N'*-naphthoylthiourea. Particularly noticeable from the X-ray crystal structure of *N,N*-diaza-18-crown-6-*N'*-naphthoylthiourea is the approach of

the N(14) bond angles to 120°, indicating sp^2 hybridisation of the N(14) orbitals. Further evidence supporting sp^2 hybridisation is the apparent partial double bond character of the C(13) - N(14) bond.

The bond distances, angles and torsion angles of the diaza-18-crown-6 ring of **3** are summarised in Table 5.4. The bond distances and bond angles along the ethyleneoxy chain are similar to those observed for *N*-aza-18-crown-6-*N'*-naphthoylthiourea (Table 5.2). Four of the C-X-C-C (X = O or N) torsion angles are *trans* with angles within 3° of 180 °. Of the four remaining C-X-C-C torsion angles, two are 73.3° and two are -145.7°. It is interesting to note that the X-C-C-X torsion angles are all *gauche* (mean 58°, range 49 - 68°) with a +,–,–,+,–,– pattern. This pattern follows an order not usually found in 18-crown-6 structures[53,54] and differs from the *gauche* pattern, +,+,–,+,–,–, observed for *N*-aza-18-crown-6-*N'*-naphthoylthiourea. The O-C-C-O torsion angle of -67.8° observed for **3**, is significantly larger than the O-C-C-N torsion angle of 48.5°. A similar relationship was observed for the analogous torsion angles of *N*-aza-18-crown-6-*N'*-naphthoylthiourea and is presumably a consequence of the shorter C - O bond distances[55].

Table 5.4 Bond distances (Å), bond angles (°) and torsion angles (°) of the diaza-18-crown-6 ring of **3** with e.s.d's in parentheses.

A	B	C	D	B-C (Å)	A-B-C (°)	A-B-C-D (°)
N14	C15	C16	O17	1.519(5)	113.04(28)	48.5(4)
C15	C16	O17	C18	1.419(4)	112.55(29)	73.3(4)
C16	O17	C18	C19	1.421(3)	114.62(25)	-145.7(3)
O17	C18	C19	O20	1.489(4)	110.07(27)	-67.8(3)
C18	C19	O20	C21	1.425(5)	110.84(29)	-177.6(3)
C19	O20	C21	C22	1.427(3)	109.91(27)	-178.7(3)

It is interesting to note that each molecule of **3** is folded so that the crown ether macrocyclic moiety is 'sandwiched' between the two C(11) - N(12) - C(13) sidearms (Figure 5.13). The *N*-acylthiourea sidearms are in an anti relationship about the macrocycle's plane with the oxygen and sulfur atoms of the two carbonyl and thiocarbonyl groups pointing away from the diaza-crown ether cavity. The diaza-18-crown-6 ring adopts a chair-like conformation, held in place by two *intra*molecular hydrogen bonds between each amide hydrogen and an oxygen atom of the macrocyclic ring, N(12) - H(12)...O(20). This hydrogen-bonded conformation is reminiscent of the structure of *N*-aza-18-crown-6-*N'*-naphthoylthiourea. The bond distances of the *intra*molecular hydrogen bonds are similar to the analogous *intra*molecular hydrogen bonds observed for *N*-aza-18-crown-6-*N'*-naphthoylthiourea. However, the N(12) - H(12)...O(20) angle is 156(2)°, 13° larger than the analogous angle, N(12) - H(12)...O(29), for *N*-aza-18-crown-6-*N'*-naphthoylthiourea.

White[35] *et al* reported the presence of *intra*molecular hydrogen bonds in the X-ray crystal structure of L,L-*N,N*-bis[*O*-methylglycylglycyl]-4,13-diaza-18-crown-6. However, an interesting point to note is that the *intra*molecular hydrogen bonds reported by White were observed between the amide hydrogen and the *nitrogen* atom of the diaza-crown ring. A novel aspect of the X-ray structures of *N*-aza-18-crown-6-*N'*-naphthoylthiourea and *N,N*-diaza-18-crown-6-*N'*-naphthoylthiourea is that the observed *intra*molecular hydrogen bonds are between the amide hydrogen and the *oxygen* atom of the aza- or diaza-crown ether ring respectively.

Figure 5.13 Molecular structure of *N,N*-diaza-18-crown-6-*N'*-naphthoylthiourea showing the anti relationship of the sidearms about the macrocycle's plane.

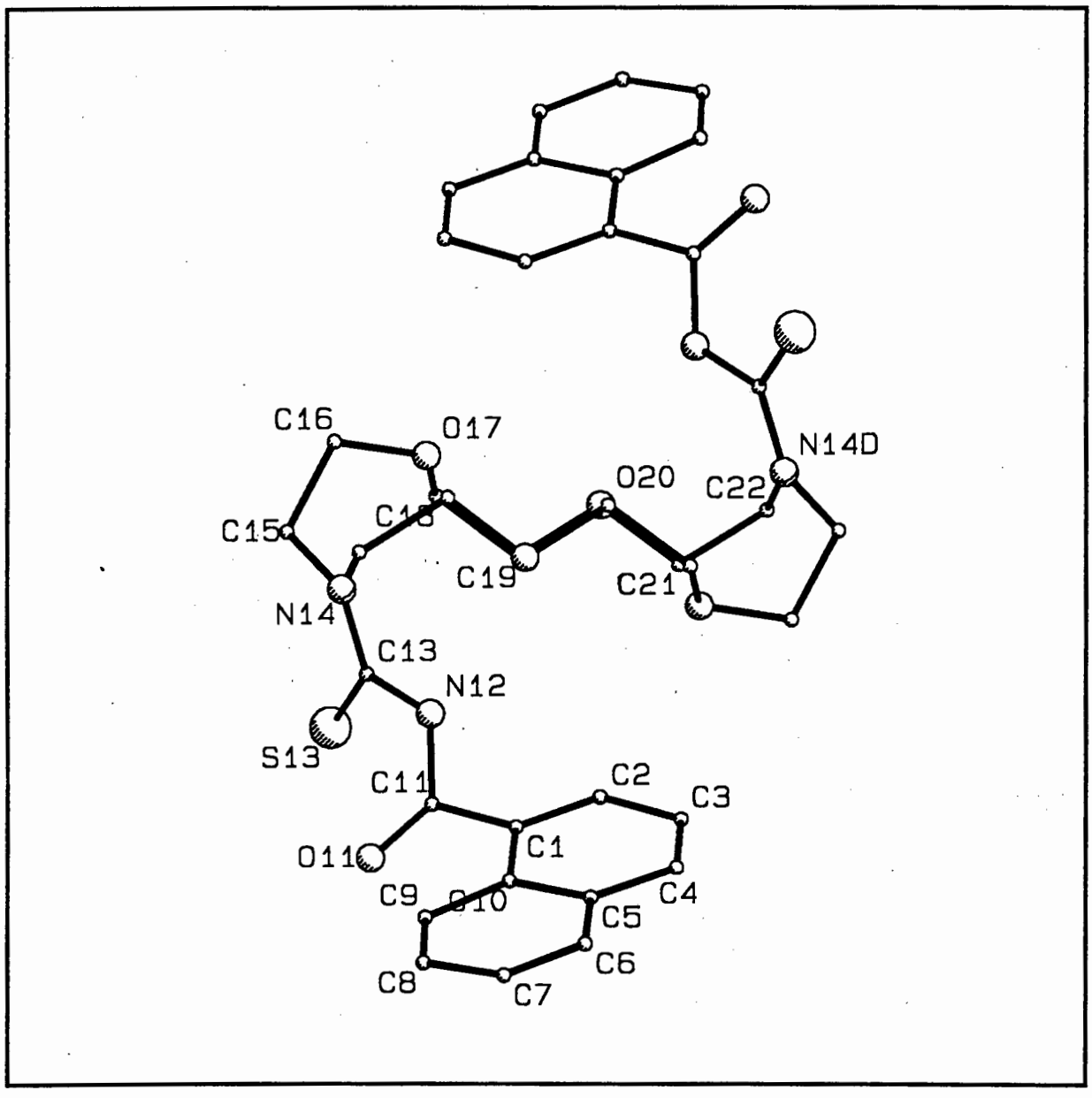

In summary, the X-ray crystal structure determination of *N*-aza-18-crown-6-*N'*-naphthoylthiourea and *N,N*-diaza-18-crown-6-*N'*-naphthoylthiourea has clearly demonstrated that K^+ cations are not complexed into the aza- and diaza-18-crown ether moieties upon crystallisation from solutions containing excesses of KI or KSCN respectively.

It is evident from the C(13) - N(14) bond distances and N(14) bond angles that the N(14) atom of the macrocyclic rings of **2** and **3** tend towards sp^2 hybridisation. This implies a decrease in the availability of the nitrogen lone pair of electrons for cation complexation. Moreover, we have been able to establish that the aza- and diaza-crown ether rings are bound to the amide hydrogen *via* an *intra*molecular hydrogen bond which results in an unusual conformation of the 18-membered rings. Furthermore, the carbonyl functional groups of **2** and **3** point away from the cavity of the macrocyclic ring. Hence, third dimension solvation can only occur if this conformation is disrupted and the carbonyl group rotated so that the oxygen atom bonds to the alkali metal ion. It is evident that the above mentioned factors may have important implications with regard to the cation binding ability of *N*-aza-18-crown-6-*N'*-naphthoylthiourea and *N,N*-diaza-18-crown-6-*N'*-naphthoyl-thiourea. These factors may be used to rationalise the weak binding interactions of **2** and **3** observed with K^+ and NH_4^+ cations.

5.2.4 NMR spectroscopy

NMR spectroscopy can be used to study reversible reactions in which two nuclei exchange chemical environments, because the line shape of NMR signals is sensitive to chemical exchange processes[58]. The line shape of the NMR signal is therefore dependent on dynamic processes and the rates at which these processes occur in solution. Accordingly, one obtains different line shapes depending on the life time of the exchangeable nuclei in the different environments[58] (Figure 5.14). If the life time of the exchangeable nuclei in two different magnetic environments is long with respect to the NMR time scale, then two separate signals are observed. This is called the area of slow exchange. On the other hand, in the area of fast exchange the life time of the exchangeable nuclei in the two different environments is short with respect to the NMR time scale, and the spectrum becomes a single signal with a normal relaxed line width. At the coalescence point the two signals merge into a broad band (intermediate exchange).

Figure 5.14 Theoretical nuclear magnetic resonance spectra for an exchange process A ↔ B as a function of the life time of the exchangeable protons in two different chemical environments[58].

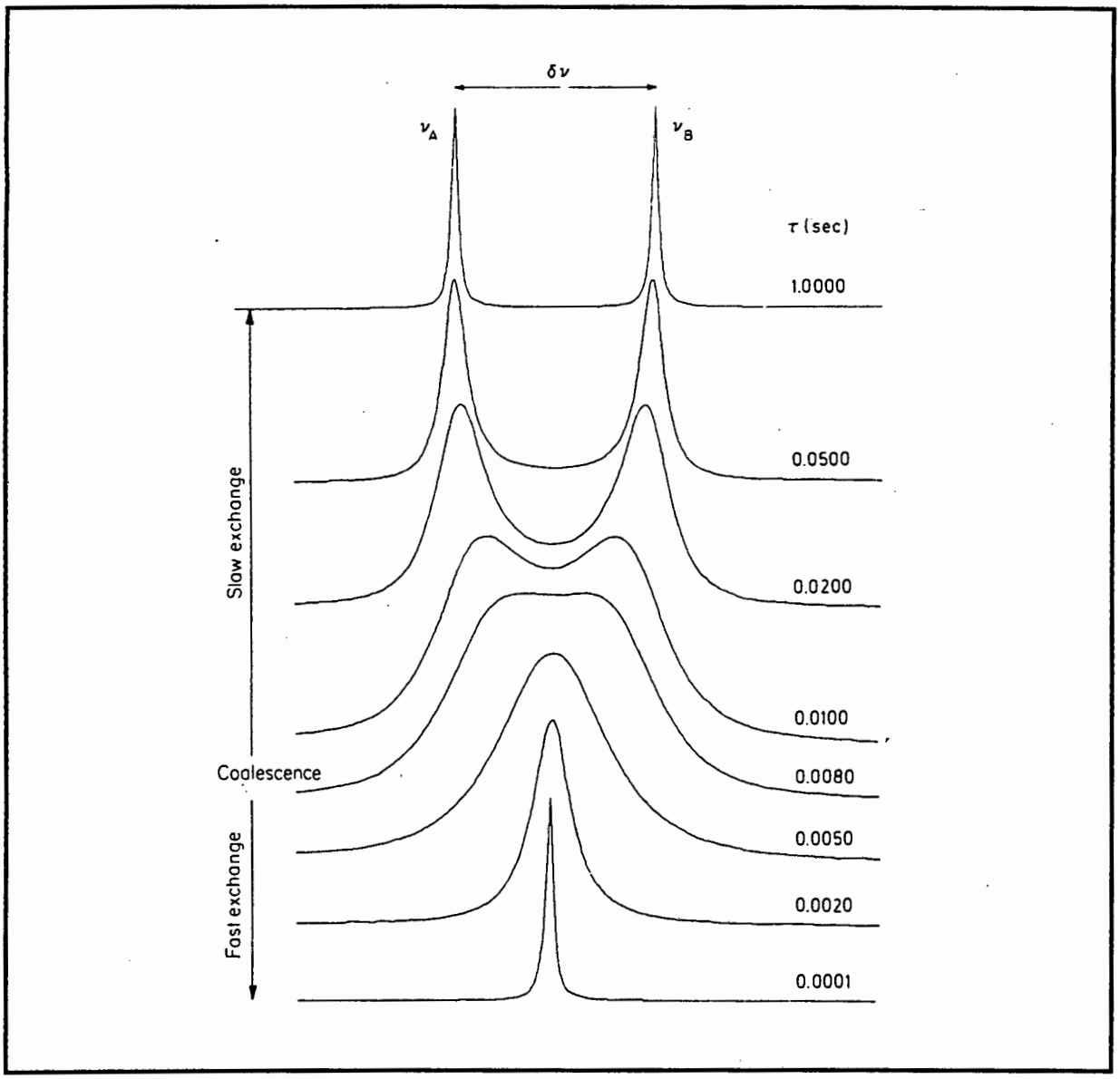

The thio-amidic bond of *N*-acylthioureas has significant double bond character[59]. Consequently, the rate of rotation around this bond, and therefore the bond order, influences the line shape of the NMR signals of the methylene protons attached to the nitrogen atom. The interpretation of the proton spectra of the oxyethylene region of *N*-aza-18-crown-6-*N'*-naphthoylthiourea is not straightforward because at least two dynamic processes must be considered at any one time, i.e. rotation around the C - N bond and conformational motion of the oxyethylene ring. It is not possible to distinguish between these two motions of the oxyethylene ring and therefore interpretation of the proton spectra in this chapter will be confined to the influences of restricted rotation. The concept of restricted rotation associated with a thio-amidic C - N bond was addressed in Chapter 2. It is noteworthy that in this thesis an increase in restricted rotation is synonymous with an

increase in the C - N bond order, i.e. an increase in double bond character. Conversely, a decrease in restricted rotation refers to a decrease in the C - N bond order, i.e. an increase in single bond character.

The flexibility of the macrocyclic aza-crown ether ring and rotation about the C - N bond will allow the molecule to adopt different conformations in solution. Accordingly, the ^{1}H NMR spectrum represents the weighted average of the different conformations of the aza-crown ether ring in solution at a given temperature. It is thus reasonable to expect that the relative populations of the various conformers of the macrocyclic ring in solution will be *temperature* dependent.

The *N*-aza- and *N,N*-diaza-18-crown-6-*N'*-naphthoylthioureas have a macrocyclic ring that we anticipated could be suitable for complexation with K^+ and RNH_3^+ cations[22,31,37,41,44] and a sidearm bearing the carbonyl functional group which we envisioned could provide a third dimension of solvation. However, we did not anticipate the existence of the *intra*molecular hydrogen bond(s) between the amide hydrogen and the oxygen atom of the aza- and diaza-crown ether ring. Accordingly, the hydrogen bond may prevent rotation of the carbonyl group toward the macroring-bound cation and thus decrease solvation of the cation and ultimately the extent of cation complexation. Furthermore, the *intra*molecular hydrogen bond(s) may prevent the macrocyclic rings from assuming a conformation necessary for cation complexation. Nevertheless, proton NMR spectroscopy was employed to ascertain whether *any* interaction between the macrocyclic ring of *N*-aza-18-crown-6-*N'*-naphthoylthiourea and K^+ and $CH_3NH_3^+$ cations could be detected in solution.

The proton NMR experiments were performed in acetone-d_6. Due to the poor interactions previously observed between K^+ / NH_3^+ cations and *N*-aza-18-crown-6-*N'*-naphthoylthiourea, the NMR experiments were performed in the temperature range 25 to -30 °C. The low temperature NMR spectra of *N*-aza-18-crown-6-*N'*-naphthoylthiourea (**2**) will be addressed and compared to the analogous spectra of **2** in the presence of KI and CH_3NH_3Cl. Standard solutions of KI and CH_3NH_3Cl were prepared in D_2O since these salts are relatively insoluble in acetone.

5.2.4.1 ^{1}H NMR spectroscopy of *N*-aza-18-crown-6-*N'*-naphthoylthiourea

The ^{1}H NMR spectrum of *N*-aza-18-crown-6-*N'*-naphthoylthiourea, in CD_3COCD_3 at 25 °C, consists of the characteristic N - H resonance in the region 10 - 11 ppm, four doublets and three triplets representing the naphthyl moiety in the 7 - 9 ppm region and the oxyethylene signals in the 3 - 5 ppm range (Figure 5.15).

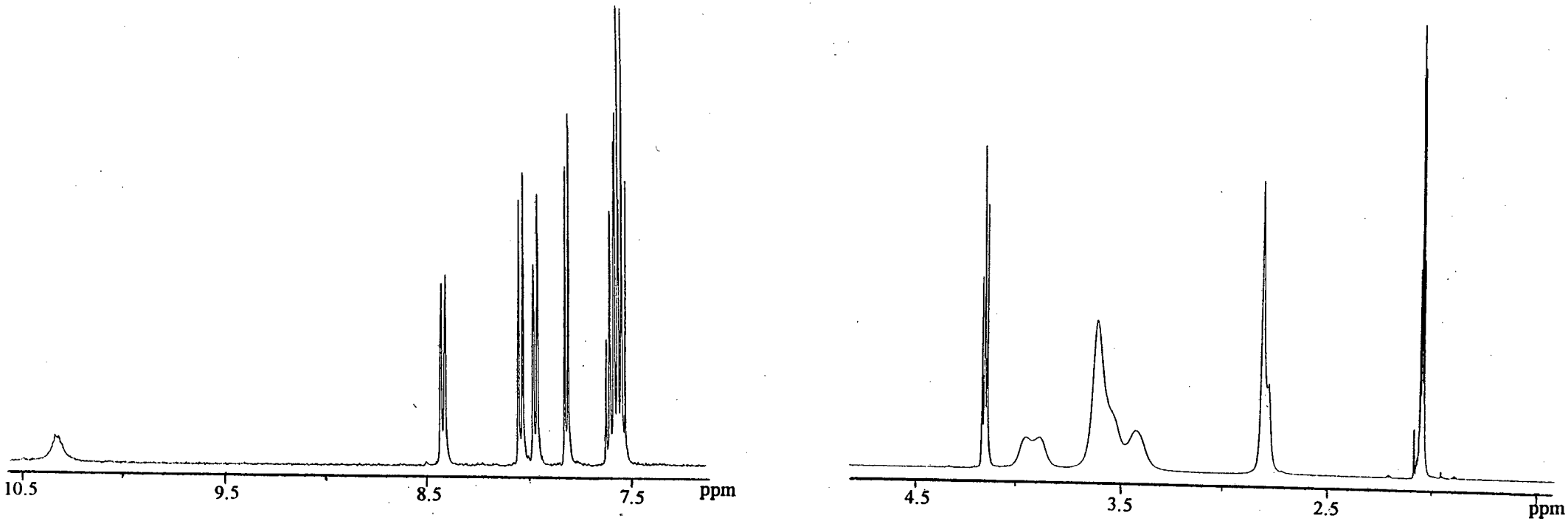

Figure 5.15 Proton NMR spectrum of *N*-aza-18-crown-6-*N'*-naphthoylthiourea in CD_3COCD_3 at 25 °C.

The NMR assignments of the aza-crown ether ring are based on the numbering scheme in Figure 5.16. The ^{1}H NMR resonances of the aza-crown ether ring were assigned with the aid of a HETCOR experiment. Assignment of the carbon atoms in the ^{13}C NMR spectrum was relatively straightforward and hence, knowing these assignments, we could assign the signals representing H(15)/H(31) and H(16)/H(30) from the HETCOR experiment. However, we were not able to unambiguously differentiate between the resonances representing H(15) and H(31). Similarly, H(16) could not be unambiguously assigned from H(30). The oxyethylene resonances assigned to H(15) / H(31) and H(16) / H(30) will be discussed in some detail. The broad, unresolved resonances in the region 3.1 - 3.7 ppm, representing the remaining 16 protons of the oxyethylene ring will not be addressed, since the proton spectrum is poorly resolved and these methylene groups are subject to rapid conformational motion of the aza-crown ether ring.

Figure 5.16 Numbering scheme for the aza-crown ether ring of *N*-aza-18-crown-6-*N'*-naphthoylthiourea.

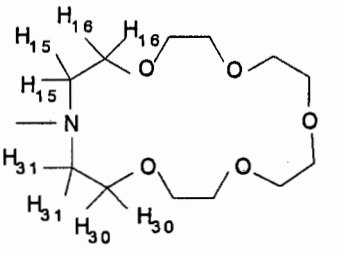

The effect of temperature on the ^{1}H NMR spectrum of *N*-aza-18-crown-6-*N'*-naphthoylthiourea

The ^{1}H NMR spectra of *N*-aza-18-crown-6-*N'*-naphthoylthiourea (**2**) were recorded in acetone-d_6 in the temperature range from 25 to -30 °C, in increments of 5 °C. Smaller increments of 1 °C were used to accurately determine the coalescence temperature. No significant shifts in the naphthyl protons of the ^{1}H spectra were observed with a change in temperature. However, pronounced changes in the aza-crown ether resonances in the region 3 - 4.5 ppm, were evident with changes in temperature. The proton spectra of the oxyethylene region of **2**, recorded in CD_3COCD_3 in the temperature range 25 to -30 °C, are illustrated in Figure 5.17. The ^{1}H NMR spectrum, (CD_3COCD_3), at 25 °C shows a sharp triplet at 4.15 ppm assigned to H(15) / H(31) and two broad signals at 3.96 and 3.87 ppm assigned to H(16) and H(30). The spectrum at 25 °C suggests that H(15) and H(31) are in fast exchange on the NMR time scale and accordingly only one environment is observed. On the other hand, the two broad signals representing H(16) and H(30) appear to be in relatively slow exchange and two signals are evident.

As the temperature is reduced from 25 °C to -30 °C, the H(15) / H(31) *triplet* at 4.15 ppm becomes broad and at low temperature separates into a *pair of triplets* at 4.19 and 4.06 ppm, the *broad* H(16) and H(30) signals at 3.96 and 3.87 ppm separate into two *well-defined triplets* at 3.94 and 3.83 ppm. The approximate coalescence temperature for H(15) / H(31) and H(16) / H(30) is 4 and 32 °C respectively. (The coalescence temperature of H(16) / H(30) was obtained from the proton spectrum recorded in the temperature range from 25 °C to 60 °C). Accordingly, as the NMR solution is cooled to -30 °C, internal rotation around the C - N bond becomes slow on the NMR time scale and "freezing out" of the four different methylene environments ensues, as is apparent from the four sets of triplets observed in the proton spectrum at -30 °C.

$\Delta G_c^{\ddagger}$ values for rotation around the C - N bond were approximated at the coalescence temperature, since a comparison of these values in the absence and presence of cations may indicate whether complexation is occurring in solution. Constant linewidth (width at half-height) measurements were observed between -30 and -40 °C which suggests that the limit of slow exchange due to restricted rotation around the C - N bond had been reached. Hence using a form of the Eyring equation[58],

$$\Delta G_c^{\ddagger} = 19.14 \times T_c \, (9.97 + \log T_c / \Delta\upsilon) \ \text{J.mol}^{-1},$$

$\Delta G_c^{\ddagger}$ for rotation about the C - N bond of *N*-aza-18-crown-6-*N'*-naphthoylthiourea was estimated.

The accuracy of the derived $\Delta G_c^{\ddagger}$ value depends mainly on the accuracy with which the coalescence temperature (T_c) can be measured[60]. A reasonable error in T_c is ± 2 °C and this corresponds to an error in $\Delta G_c^{\ddagger}$ of ± 0.5 kJ.mol^{-1}.[60] The sample temperatures in the present experiment are accurate to within 0.5 °C. The $\Delta G_c^{\ddagger}$ for rotation about the thio-amidic C - N bond of *N*-aza-18-crown-6-*N'*-naphthoylthiourea was estimated to be 57 kJ.mol^{-1}, T_c = 277 K (for H(15) and H(31)). It is interesting to note that this thio-amidic C - N value is lower than that reported for the barriers to rotation about conventional amide links[61]. Furthermore, the $\Delta G_c^{\ddagger}$ was calculated using information regarding H(16) and H(30) and estimated to be 63 kJ.mol^{-1}, T_c = 305 K. These two different $\Delta G_c^{\ddagger}$ values suggest that two dynamic processes[62] are involved with the macrocyclic ring, since the free energies of activation differ by 6 kJ.mol^{-1} which is well outside experimental error[44].

Figure 5.17 Proton NMR spectra of the oxyethylene region, 3.8 - 4.3 ppm, of *N*-aza-18-crown-6-*N'*-naphthoylthiourea in CD_3COCD_3 in the temperature range 25 to -30 °C.

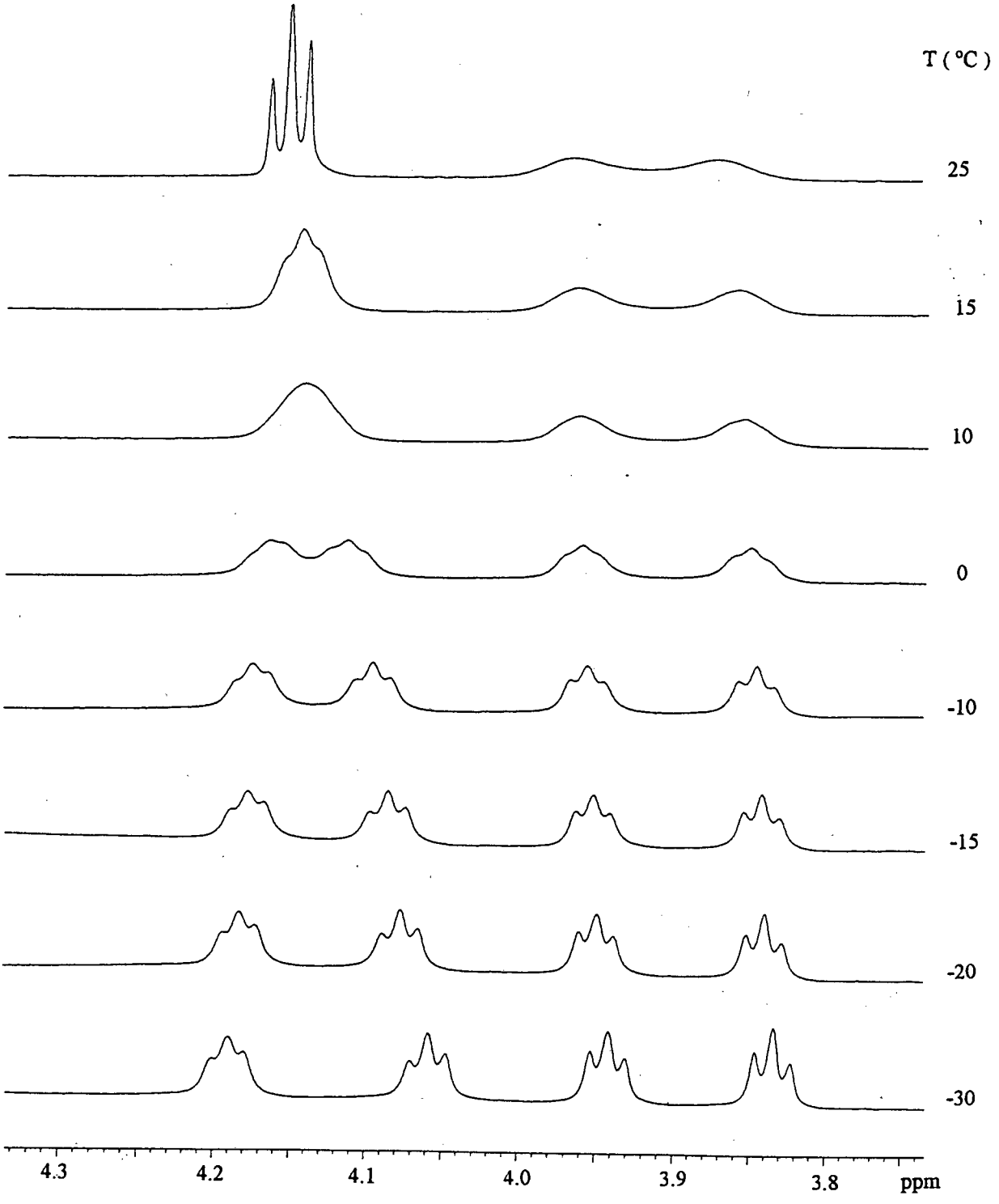

5.2.4.2 ^{1}H NMR study of the interaction of K^+ and $CH_3NH_3^+$ with *N*-aza-18-crown-6-*N'*-naphthoylthiourea

Any potential interaction between the aza-crown ether ring of *N*-aza-18-crown-6-*N'*-naphthoylthiourea and K^+ and $CH_3NH_3^+$ cations was studied by adding one equivalent of the cation, in 20 μl D_2O, directly to the NMR tube containing one equivalent of *N*-aza-18-crown-6-*N'*-naphthoylthiourea in 1 mL CD_3COCD_3.

The nitrogen-hydrogen bonds of amides are known to be acidic (pK_a of acetamide $\approx$ 15)[63], thus *N*-acylthiourea may act as a weak acid. It is therefore reasonable to assume that the addition of D_2O to an acetone solution of *N*-aza-18-crown-6-*N'*-naphthoylthiourea may result in the formation of hydronium ions. These have been shown to interact with aza-crown ethers[46]. Accordingly, the effect of 20 μl D_2O on the ^{1}H NMR spectrum of *N*-aza-18-crown-6-*N'*-naphthoylthiourea was investigated.

An aliquot of 20 μl of D_2O was added directly to the NMR tube containing an acetone-d_6 solution of *N*-aza-18-crown-6-*N'*-naphthoylthiourea. The proton NMR spectra were recorded in the temperature range from 25 to -30 °C. No significant differences in the ^{1}H NMR spectrum of the aromatic and oxyethylene regions of *N*-aza-18-crown-6-*N'*-naphthoylthiourea in the presence of D_2O were observed, compared to the analogous spectrum in the absence of D_2O, in the temperature range 25 to -30 °C. Interestingly, these results suggest that the addition of 20 μl D_2O does not effect the observed proton NMR spectrum of *N*-aza-18-crown-6-*N'*-naphthoylthiourea. Therefore any effect that may be observed in the oxyethylene region of the ^{1}H NMR spectrum on the addition of a cation in 20 μl D_2O, is due to the interaction of the cation with the aza-crown ether ring and not due to the presence of D_2O / hydronium ions.

Interaction of N-aza-18-crown-6-N'-naphthoylthiourea with KI

Delocalisation of the nitrogen lone pair of electrons into the C(13) - N(14) bond increases the bond order[59] and therefore the C - N rotational energy barrier. Interaction between a cation and the aza-crown ether ring is expected to decrease the C(13) - N(14) bond order, since the nitrogen lone pair of electrons is less likely to be delocalised into the bond if it is involved in cation complexation. Accordingly, a degree of complexation between the aza-crown ether ring and the K^+ cation is deemed to exist, if a decrease in the C - N bond order is indicated by proton NMR spectroscopy.

An aliquot of 20 μl of D_2O containing one equivalent of KI was added directly to the NMR tube containing an acetone-d_6 solution of one equivalent of *N*-aza-18-crown-6-*N'*-naphthoylthiourea. The ^{1}H NMR spectra were recorded in the temperature range from 25 to -30 °C, in increments of 5 °C. The chemical shifts and line shape of the naphthyl signals in the NMR proton spectrum do not change on the addition of KI in the temperature range 25 to -30 °C, and are thus not discussed further. However, significant changes are observed

in the oxyethylene region of the proton spectrum as a function of temperature. The proton spectra of the oxyethylene region of *N*-aza-18-crown-6-*N'*-naphthoylthiourea, in the presence of an equimolar amount of KI, are illustrated in Figure 5.18.

At 25 °C, the ^{1}H NMR spectrum of the oxyethylene region of *N*-aza-18-crown-6-*N'*-naphthoylthiourea in the presence of one molar equivalent of KI, shows *two sharp triplets* at 4.19 and 3.93 ppm, representing H(15) / H(31) and H(16) / H(30) respectively. This region of the spectrum is different to the analogous spectrum in the absence of KI, where *one sharp triplet* at 4.15 ppm, representing H(15) / H(31), and *two broad signals* at 3.96 and 3.87 ppm, representing H(16) and H(30), are observed. These results suggest that in the presence of KI, the C(13) - N(14) bond order decreases and H(15) and H(31) are in fast exchange with respect to the NMR time scale. Similarly, the life time of H(16) and H(30) in their two different environments is relatively short and the two environments cannot be distinguished from each other.

Cooling of the NMR solution, containing **2** in the presence of an equimolar amount of KI to -30 °C, yields a proton NMR spectrum significantly different to that observed for **2** in the absence of KI. The ^{1}H NMR spectrum in the presence of KI, shows two pairs of broad signals at 4.29 and 4.22 ppm for H(15) and H(31) and 3.96 and 3.91 ppm for H(16) and H(30). At this low temperature the exchange of H(15) with H(31), and H(16) with H(30), is relatively slow and thus four different environments are observed. However, at -30 °C these resonances are not the well-defined triplets observed for **2** in the absence of KI, but broad signals. Thus, further cooling, to a temperature lower than -30 °C, is required to effectively "freeze out" the four methylene environments to obtain sharp, well-defined triplets.

Furthermore a change, albeit small, in the chemical shift positions of H(15) / H(31) and H(16) / H(30) (Table 5.5) is evident from the proton spectrum at -30 °C. Wong[64] *et al* have reported that complexation with an alkali cation induces downfield shifts of the polyether ring protons due to the increased electronegativity of the oxygen atoms. At -30 °C, small downfield shifts of approximately 0.1 ppm are observed for the oxyethylene signals of *N*-aza-18-crown-6-*N'*-naphthoylthiourea in the presence of KI, compared to the spectrum in the absence of KI.

Figure 5.18 Proton NMR spectra (CD_3COCD_3) of the oxyethylene region, 3.8 - 4.4 ppm, of *N*-aza-18-crown-6-*N'*-naphthoylthiourea in the presence of an equimolar amount of KI in 20 µl D_2O in the temperature range 25 to -30 °C.

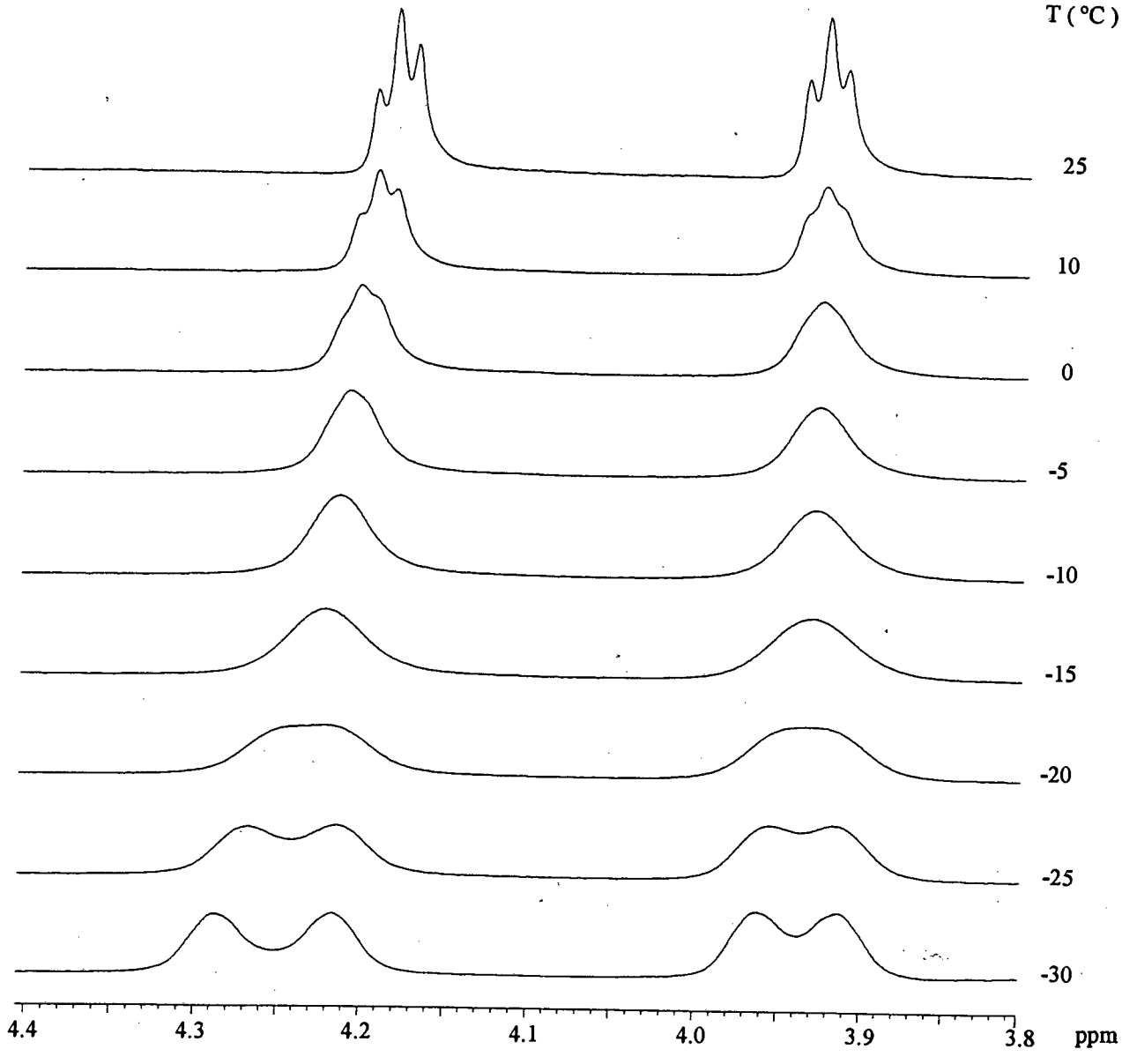

Table 5.5 ^{1}H NMR data, in acetone-d_6, of *N*-aza-18-crown-6-*N'*-naphthoylthiourea (**2**) in the absence of KI and on addition of an equimolar amount of KI in 20 µl D_2O at -30 °C.

	(**2**)	(**2**) + **KI**
H(15) / H(31)	4.19; 4.06 (t)	4.29; 4.22 (b.s)
H(16) / H(30)	3.94; 3.83 (t)	3.96; 3.91 (b.s)

(t) *represents a triplet*

(b.s) *represents a broad singlet*

The coalescence temperature of the signals representing the H(15) / H(31) and H(16) / H(30) protons of *N*-aza-18-crown-6-*N'*-naphthoylthiourea is altered in the presence of KI. Coalescence of the signals of the methylene peaks, H(15) / H(31) and H(16) / H(30), is observed at 4 and 32 °C respectively in the absence of KI, whereas in the presence of KI coalescence of these signals occurs at -20 °C. Using a form of the Eyring equation[58], $\Delta G_c^{\ddagger} = 19.14 \times T_c (9.97 + \log T_c / \Delta\upsilon)$, the $\Delta G_c^{\ddagger}$ value for rotation around the C(13) - N(14) bond of *N*-aza-18-crown-6-*N'*-naphthoylthiourea in the presence of KI, was estimated to be 53 kJ.mol^{-1} using either the H(15) / H(31) or the H(16) / H(30) experimental results. Although this $\Delta G_c^{\ddagger}$ value of 53 kJ.mol^{-1} is slightly lower than the value calculated in the absence of KI (57 kJ.mol^{-1}), and hence suggests that the C(13) - N(14) bond order decreases in the presence of KI, it must be stressed that these are only approximate values and that errors are involved in the $\Delta G_c^{\ddagger}$ calculations using the present method. Nevertheless, the difference in coalescence temperatures of the H(15) / H(31) and H(16) / H(30) signals in the presence of KI, compared to the spectrum in the absence of KI, clearly illustrates that KI is associated with the aza-crown ether ring.

In summary, interpretation of the ^{1}H NMR spectra of *N*-aza-18-crown-6-*N'*-naphthoylthiourea in the presence of KI, compared to the spectrum in the absence of KI, suggests that

- the C(13) - N(14) bond order decreases in the presence of KI
- the line shape of H(15) / H(31) and H(16) / H(30), is modified
- small downfield shifts for H(15), H(16), H(30) and H(31) are observed
- the coalescence temperature of H(15) / H(31) and H(16) / H(30) is altered.

These factors indicate that a degree of complexation occurs between the aza-crown ring of **2** and K^+ in acetone-d_6.

Complexation of N-aza-18-crown-6-N'-naphthoylthiourea with CH_3NH_3Cl.

The potential interaction between *N*-aza-18-crown-6-*N'*-naphthoylthiourea (**2**) and CH_3NH_3Cl was studied in acetone-d_6 with the aid of proton NMR spectroscopy. The experiment is based on the observation that the exchange between complexed and free $CH_3NH_3^+$, which is fast on the NMR time scale at room temperature, becomes sufficiently slow on cooling to produce line broadening and peak separation of the methyl signal in the ^1H NMR spectrum[58,65]. Accordingly, if complexation between the aza-crown ether ring and $CH_3NH_3^+$ occurs in solution, then two signals for complexed and free $CH_3NH_3^+$ are expected in the ^1H NMR spectrum at low temperatures. The methyl peak of CH_3NH_3Cl is thus an excellent spectroscopic "handle" to confirm whether cation complexation occurs in solution.

One equivalent of CH_3NH_3Cl, in 20 μL D_2O, was added directly to the NMR tube containing an acetone-d_6 solution of an equimolar amount of *N*-aza-18-crown-6-*N'*-naphthoylthiourea. The ^1H NMR spectra were recorded in a temperature array from 25 to -30 °C. The proton spectra of the oxyethylene region of **2**, in the presence of an equimolar amount of CH_3NH_3Cl, are illustrated in Figure 5.19 and the corresponding proton spectra of the methyl group of CH_3NH_3Cl, are illustrated in Figure 5.20.

The spectrum at 25 °C shows a singlet at 2.63 ppm assigned to the methyl peak of CH_3NH_3Cl. Consequently, if $CH_3NH_3^+$ is complexed to the aza-crown ether ring, the complexed and free methyl peaks are in fast exchange and are evident as a single line in the ^1H NMR spectrum.

If the temperature of the NMR solution containing *N*-aza-18-crown-6-*N'*-naphthoylthiourea and CH_3NH_3Cl is reduced to 0 °C, three sets of well-defined triplets are observed at 4.14 ppm representing H(15) / H(31), and at 3.94 and 3.85 ppm representing H(16) and H(30). Further cooling of the NMR solution to -30 °C results in peak separation of these signals in the proton spectrum. At -25 °C the H(15) / H(31) protons are observed as a broad multiplet, whereas the H(16) and H(30) resonances are evident as a pair of quartets (Figure 5.19). The large signal at 3.8 ppm in the proton spectrum at -30 °C is due to the water in solution; the signal moves downfield on cooling of the NMR solution. The complicated aza-crown ether region in the ^1H NMR spectrum suggests that more than one species persists in solution. It seems reasonable to anticipate that these signals are due to complexed and uncomplexed aza-crown ether rings.

Figure 5.19 Proton NMR spectra (CD_3COCD_3) of the oxyethylene region, 3.8 - 4.2 ppm, of *N*-aza-18-crown-6-*N'*-naphthoylthiourea in the presence of an equimolar amount of CH_3NH_3Cl, in 20 µl D_2O, in the temperature range 25 to -30 °C.

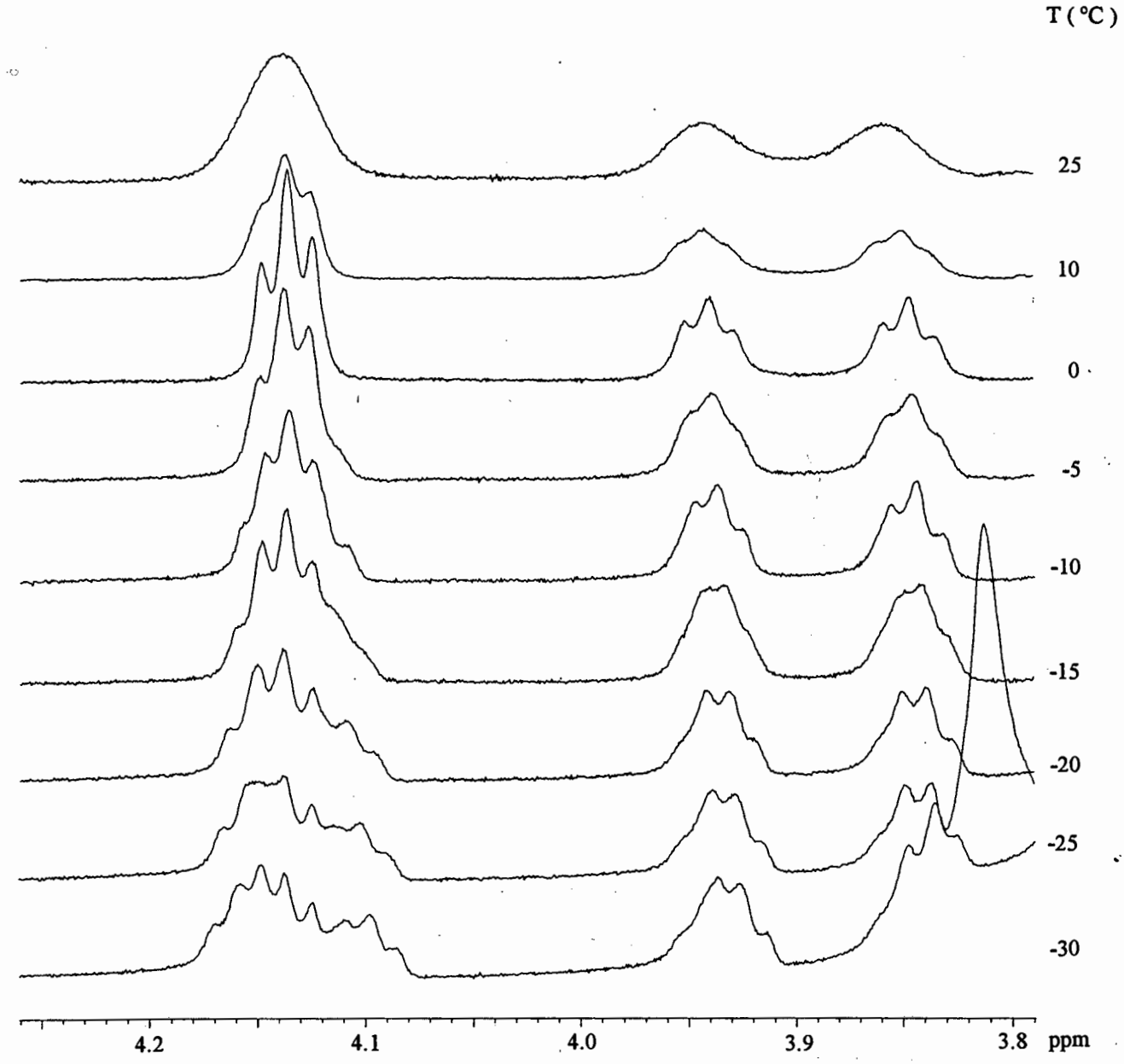

Figure 5.20 Proton NMR spectra (CD_3COCD_3) of the methyl group of CH_3NH_3Cl in the presence of an equimolar amount of *N*-aza-18-crown-6-*N'*-naphthoylthiourea in the temperature range 25 to -30 °C.

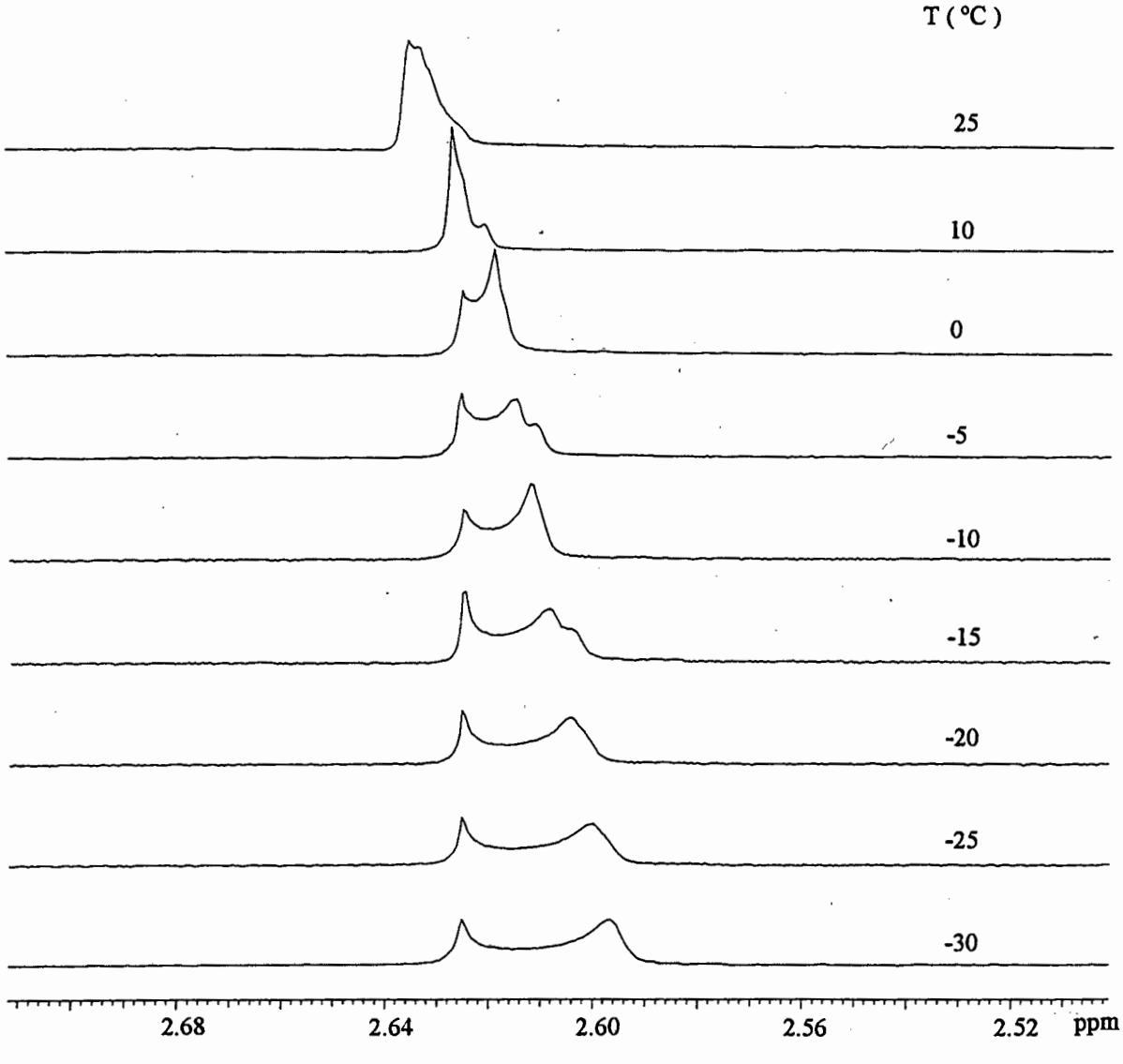

Furthermore two singlets, at 2.63 and 2.60 ppm, are evident in the proton spectrum on cooling of the NMR solution to -30 °C. These signals are assigned to free and complexed $CH_3NH_3^+$ and exist in an approximate ratio of 1 : 3 (measured by integration) respectively. The complexed methyl peak at 2.60 ppm, moves upfield (Δ 0.036 ppm) as a function of temperature, the free methyl peak remaining in approximately the same chemical shift position (Figure 5.20). This upfield shift which is indicative of shielding, may be attributed to the fact that in the $CH_3NH_3^+$ complex, the methyl group is located in the shielding zone of the aromatic moiety of *N*-aza-18-crown-6-*N'*-naphthoylthiourea. The solid state structure of compound **2** has shown that the aza-crown ether ring is folded over the chelate moiety. It is therefore reasonable to postulate that such relative orientations of the aza-crown ether ring persist in solution. Hence, the complexed cation may experience an anisotropic shielding effect due to the proximity of the naphthyl rings. Reinhoudt[19] *et al* have observed similar upfield shifts of *t*-$BuNH_3^+$ on complexation with crown ether compounds that contain aromatic groups.

It is interesting to note that at -30 °C more than one set of naphthyl signals are observed in the proton spectrum. This further suggests that the naphthyl groups are in close proximity to the aza-crown ether ring and are sensitive to aza-crown ether - cation interactions.

Kinetic and thermodynamic data was roughly approximated using Reinhoudt's[18] direct ^1H NMR method. The chemical shift of the complexed methyl group was determined from the recorded proton NMR spectra at 0, -5, -10, -15, -20, -25, -30 °C . At each temperature K was estimated using the equation,

$$K = \frac{[\,N\text{-aza-18-crown-6-}N'\text{-naphthoylthiourea} \cdot CH_3NH_3^+\,]}{[\,N\text{-aza-18-crown-6-}N'\text{-naphthoylthiourea}\,] \times [\,CH_3NH_3^+\,]}$$

From a plot of ln K vs. T^{-1} (Figure 5.21) the enthalpy and entropy of complexation were estimated using the equation:

$$\ln K = \Delta S^\circ / R - \Delta H^\circ / RT$$

From the plot of ln K vs. T^{-1}, the approximate enthalpy and entropy of formation were calculated to be -3.7 kcal.mol^{-1} and +11 cal.mol^{-1}K^{-1} respectively. From the ΔH° contribution to ΔG° it can be concluded that the complex is enthalpy stabilised in acetone[19]. In acetone a positive ΔS° was measured. This is unexpected because the overall ΔS° is usually negative for a cation complexation process[19]. The positive ΔS° strongly indicates significant solvent reorganisation and conformational change of the aza-crown ether moiety of *N*-aza-18-crown-6-*N'*-naphthoylthiourea prior to complexation.

Reinhoudt[19] *et al* observed ΔH° values of -3.4 and -5.4 kcal.mol^{-1}, and ΔS° values of -3.0 and -0.7 cal.mol^{-1}K^{-1}, for *t*-$BuNH_3ClO_4$ complexation with 1,3-xylyl-18-crown-6 and 18-crown-6 respectively, in acetone. The present ΔH° calculated for *N*-aza-18-crown-6-*N'*-naphthoylthiourea is similar to that obtained by Reinhoudt, whereas the ΔS° calculated for *N*-aza-18-crown-6-*N'*-naphthoylthiourea is positive and substantially larger than the values reported by Reinhoudt. This indicates a greater degree of disorder of *N*-aza-18-crown-6-*N'*-naphthoylthiourea upon cation complexation compared to Reinhoudt's 18-crown-6 ligands, i.e. the aza-crown ether moiety of compound **2** must undergo significant conformational reorganisation before cation complexation can occur. This is in accordance with the observed torsion angles of the aza-crown ether ring of *N*-aza-18-crown-6-*N'*-naphthoylthiourea which is in contrast to the familiar D_{3d} conformation usually found in 18-crown-6 rings[53,54] and in the K^+ complex of diaza-18-crown-6[66]. It is reasonable to postulate that the conformation of the aza-crown ether ring persists in solution and hence a degree of conformational change is required to obtain the desired D_{3d} conformation necessary for complexation.

The free energy of activation ($\Delta G_c^{\ddagger}$) of the exchange process between the complexed and free $CH_3NH_3^+$, described by the equation, $\Delta G_c = 4.57 \times T_c (9.97 + \log (T_c / \Delta\upsilon))$ cal.mol^{-1}, was estimated at the coalescence temperature (283 K) of the methyl probe to give a $\Delta G_c^{\ddagger}$ value of approximately 14 kcal.mol^{-1}. Reinhoudt[19] *et al* calculated $\Delta G_c^{\ddagger}$ values of 8.8 and 11.5 kcal.mol^{-1} for the exchange process of *t*-$BuNH_3ClO_4$ with 1,3-xylyl-18-crown-6 and 18-crown-6 respectively, in acetone-d_6. Thus these values suggest that the complexation of CH_3NH_3Cl with *N*-aza-18-crown-6-*N'*-naphthoylthiourea is less spontaneous than that of 1,3-xylyl-18-crown-6 or 18-crown-6 with *t*-$BuNH_3ClO_4$.

Hence the proton NMR studies of the reaction of CH_3NH_3Cl with *N*-aza-18-crown-6-*N'*-naphthoylthiourea suggest that:

- complexed and free *N*-aza-18-crown-6-*N'*-naphthoylthiourea species exist in solution
- complexed and free CH_3NH_3Cl exist in solution.

This indicates that a degree of complexation, between the aza-crown ether ring of *N*-aza-18-crown-6-*N'*-naphthoylthiourea and $CH_3NH_3^+$, occurs in solution.

Figure 5.21 Graphical representation of ln K vs. T^{-1} for the [*N*-aza-18-crown-6-*N'*-naphthoylthiourea · $CH_3NH_3^+$] complex in CD_3COCD_3.

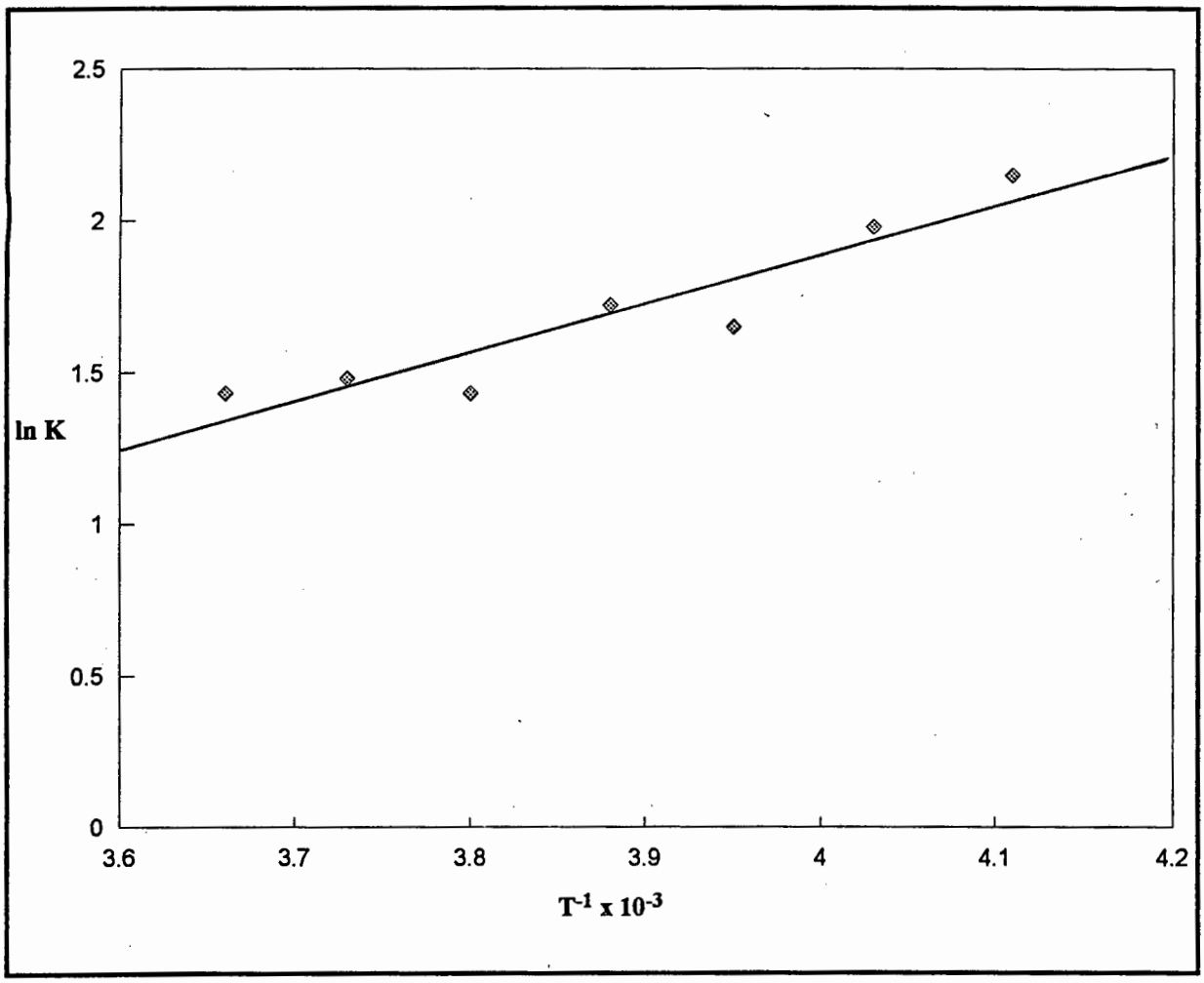

The proton NMR spectra indicate that the observed spectral changes are dependent on the cation under study. This may be explained in view of the fact that different binding mechanisms are involved for K^+ and $CH_3NH_3^+$ cations. Metal ions such as the tetrahedral K^+ are sequestered within the macrocyclic ring, whereas the spherical $CH_3NH_3^+$ cations hydrogen bond to ring donor atoms[66,67]. Ammonium is a " directional " cation while K^+ is not[32]. These differences in binding ability, i.e. ion - dipole interactions and hydrogen bonding, may account for the differences in the observed proton spectra of *N*-aza-18-crown-6-*N'*-naphthoylthiourea in the presence of K^+ and $CH_3NH_3^+$.

In view of the two *intra*molecular hydrogen bonds and unusual conformation of the diaza-crown ether ring observed in the crystal structure of *N,N*-diaza-18-crown-6-*N'*-naphthoylthiourea, we predicted a decrease in diaza-crown ether / cation interaction with respect to *N*-aza-18-crown-6-*N'*-naphthoylthiourea. Accordingly, the interaction of K^+ and $CH_3NH_3^+$ cations with *N,N*-diaza-18-crown-6-*N'*-naphthoylthiourea was not studied with the aid of ^1H NMR spectroscopy.

5.3 Conclusion

We have successfully synthesised and characterised the first *N*-acylthiourea compounds incorporating a crown ether moiety, *N*-aza-18-crown-6-*N'*-naphthoylthiourea and *N,N*-diaza-18-crown-6-*N'*-naphthoylthiourea. Although it has not been possible to extract K^+ and NH_4^+ picrate salts from an aqueous phase into an organic phase with *N*-aza-18-crown-6-*N'*-naphthoylthiourea and *N,N*-diaza-18-crown-6-*N'*-naphthoylthiourea, or to grow crystals of a potassium complex of these compounds, it is nevertheless clear from proton NMR studies that cations are to some degree, complexed by *N*-aza-18-crown-6-*N'*-naphthoylthiourea in acetone-d_6. However, the interaction of K^+ and $CH_3NH_3^+$ cations with the aza-crown ether moiety of *N*-aza-18-crown-6-*N'*-naphthoylthiourea was significantly less than we anticipated.

The crystal structure determinations of *N*-aza-18-crown-6-*N'*-naphthoylthiourea and *N,N*-diaza-18-crown-6-*N'*-naphthoylthiourea have revealed a number of factors that may account for the weak binding between the macrocyclic moieties and K^+ and $CH_3NH_3^+$ cations. These include:

- the unusual conformation of the aza- and diaza-crown ether rings
- the presence of one and two *intra*molecular hydrogen bond(s) respectively, which may have a profound effect on the conformation of the aza- and diaza-18-crown-6 rings and hence hinder cation complexation
- the *intra*molecular hydrogen bonds may prevent sidearm interaction of the carbonyl moiety with a cation once it is bound in the oxyethylene ring, and therefore reduce the complexing ability of the aza- and diaza-crown ether rings
- the oxyethylene ring is folded over the chelate C - N - C backbone with the carbonyl groups pointing away from the aza-crown cavity
- the C - N bond length and bond angles of the nitrogen atom of the aza-crown ether ring suggest that the nitrogen lone pair of electrons are delocalised into the C - N bond and therefore less available for complexation.

Gokel[36] *et al* observed similar decreased K^+ and NH_4^+ cation complexation with aza- and diaza-18-crown-6 ethers having an amidic group present on the macrocyclic ring nitrogen. They attributed this to the fact that an amide nitrogen is less flexible and less basic than a tertiary nitrogen and will therefore be less able to encapsulate a cation. It seems plausible that the thio-amidic moiety of *N*-aza-18-crown-6-*N'*-naphthoyl-

thiourea and *N,N*-diaza-18-crown-6-*N'*-naphthoylthiourea may have the same effect on the properties of the aza- and diaza-crown ether rings.

Future research aimed at synthesising a macrocyclic *N*-acylthiourea that incorporates an amine macrocyclic ring nitrogen, as opposed to a thia-amide ring nitrogen, could potentially exhibit substantially improved properties with respect to cation binding .

5.4 Experimental

Aza-18-crown-6 (1,4,7,10,13-pentaoxa-16-azacyclooctadecane) was prepared employing the method reported by Maeda[23] *et al* in a 22 % yield. Diaza-18-crown-6 (1,4,10,13-tetraoxa-7,16-aza-cyclooctadecane) and morpholine (1-oxa-4-aza-cyclohexane) were obtained from Aldrich Chemical company and used without further purification.

^{1}H NMR experiments were performed on a Varian UNITY-400 spectrometer operating at 400 MHz.

Aza-18-crown-6[23] Freshly distilled dichlorotetraethyleneglycol (0.04 mol) was added dropwise to a stirred solution of potassium metal (0.1 mol) in 600 ml refluxing (60 °C) *tert*-butyl alcohol and diethanolamine (0.08 mol). The mixture was heated at 60 °C for 48 hours, cooled and filtered. The crude product was distilled by Kugelröhr apparatus (143 - 145 °C, 0.1 mmHg) to give a colourless liquid which solidified on cooling. The solid was recrystallised from hexane to give colourless crystals, (23% yield), mp 47 - 49°C (lit. mp 48 - 51°C)[23]. NMR ($CDCl_3$) ^{1}H δ 2.63 (1H, s, N - H), 2.78 (4H, t, NCH_2), 3.56 - 3.69 (20H, m, CH_2).

The *N*-acylthioureas were prepared according to the method reported by Douglass and Dains[43] as described in Chapter 2. All crude products were recrystallised from $CHCl_3$ / EtOH to yield colourless crystalline products.

***N*-morpholino-*N'*-naphthoylthiourea** (**1**) 83 % yield, mp 165 - 167 °C. Anal. Calcd for $C_{16}H_{16}N_2O_2S$: C, 63.97; H, 5.37; N, 9.33. Found C, 64.03; H, 5.37; N, 9.40. NMR ($CDCl_3$) ^{1}H δ 3.81 (2H, b.s, NCH_2), 3.87 (4H, b.s, OCH_2), 4.22 (2H, b.s, NCH_2'), 7.50 (1H, t, H(7)), 7.55 (1H, t, H(3)), 7.63 (1H, t, H(6)), 7.78 (1H, d, H(5)), 7.91 (1H, d, H(4)), 8.02 (1H, d, H(2)), 8.42 (1H, d, H(8)), 8.47 (1H, s, NH); ^{13}C δ 52.37, 52.53, 124.44, 124.95, 126.29, 126.45, 126.88, 127.99, 128.64, 131.08, 132.79, 133.86, 164.78, 178.86.

***N*-aza-18-crown-6-*N'*-naphthoylthiourea** (**2**) 71 % yield, mp 69 - 71 C. Anal. Calcd for $C_{24}H_{32}N_2O_6S.H_2O$: C, 58.20; H, 6.93; N, 5.66. Found C, 58.17; H, 6.83; N, 5.65. NMR ($CDCl_3$) ^{1}H δ 3.08 - 3.61 (16H, m, OCH_2CH_2O), 3.91 (4H, s, H(16)/H(30)), 4.03, 4.17 (4H, b.s, H(15)/H(31)), 7.45 (1H, t, H(7)), 7.51 (1H, t, H(3)), 7.57 (1H, t, H(6)), 7.74 (1H, d, H(5)), 7.85 (1H, d, H(4)), 7.93 (1H, d, H(2)), 8.45 (1H, d, H(8)), 10.44 (1H, s, NH); ^{13}C δ 53.21, 55.07, 69.05, 69.13, 70.41, 77.37, 124.47, 125.66, 126.02, 126.50, 127.39, 128.26, 130.41, 131.45, 133.69, 133.71, 167.80, 180.33.

***N,N*-diaza-18-crown-6-*N'*-naphthoylthiourea** (**3**) 85 % yield, mp 159 - 162 °C. Anal. Calcd for $C_{36}H_{40}N_4O_6S_2.H_2O.2CHCl_3$: C, 48.25; H, 4.69; N, 5.93. Found : C, 48.31; H, 4.63; N, 6.09. NMR (DMSO-d_6) ^{1}H δ 3.57 (8H, t, OCH_2CH_2O), 3.80 (8H, b.d, $NCH_2\underline{CH_2}O$), 3.97 (4H, b.s, NCH_2), 4.23 (4H, b.s, NCH_2'), 7.56 (2H, t, H(7)), 7.58 (2H, t, H(3)), 7.60 (2H, t, H(6)), 7.72 (2H, d, H(5)), 7.80 (2H, d, H(4)), 8.07 (2H, d, H(2)), 8.27 (2H, d, H(8)), 10.85 (2H, s, NH); ^{13}C δ 52.94, 53.35, 66.90, 68.84, 69.80, 124.62, 124.86, 125.91, 126.18, 126.92, 128.16, 129.70, 130.69, 132.49, 133.03, 166.25, 181.44.

Solvent Extraction Studies

The general procedure was similar to that reported in previous studies[17,47,48]. Potassium and ammonium picrates were prepared according to the procedure of Coplan and Fuoss[68]. The solvents, dichloromethane and water, were saturated with each other prior to use in order to prevent volume changes of both phases during extraction. Equal volumes (10 cm^3) of dichloromethane solutions of aza-18-crown-6, diaza-18-crown-6, *N*-aza-18-crown-6-*N'*-naphthoylthiourea and *N,N*-diaza-18-crown-6-*N'*-naphthoylthiourea, and an aqueous solution of K^+ or NH_4^+ picrate, were introduced into an Erlenmeyer flask which was stoppered and then shaken vigorously for 40 minutes in a thermostated water bath at 25.0 ± 0.5 °C. The mixture was then centrifuged in order to complete phase separation. Part (3 cm^3) of the dichloromethane phase was withdrawn and the percentage extraction was determined spectrophotometrically (λ_{max} = 356 nm). A similar extraction experiment was performed under basic conditions i.e. in the presence of KOH / K^+picrate and NH_3 / NH_4^+ picrate. In blank experiments, there was no detectable extraction into the organic phase in the absence of the crown ether ligand. The picrate concentration in the aqueous phase was determined spectrophotometrically. The absorbances were measured on a Philips UV/visible spectrophotometer PU 8620 series at 356 nm. The ε was calculated from the absorbance of the blank solution with the aid of the Beer Lambert Law[45]. Thereafter this value was used to calculate the aqueous picrate concentrations (Beer Lambert Law) and the %-extraction was determined using the equation:

$$\% \text{ extraction} = ([\text{aq picrate}]_i - [\text{aq picrate}]_f) \div [\text{aq picrate}]_i \times 100$$

where 'i' is the initial picrate concentration and 'f' is the final picrate concentration after extraction.

UV Spectroscopic Studies

The *N*-aza-18-crown-6-*N'*-naphthoylthiourea and *N,N*-diaza-18-crown-6-*N'*-naphthoylthiourea compounds were dissolved in acetonitrile. The solutions were diluted to obtain a solution of molarity 1.8 x 10^{-5} M. In a separate experiment equimolar amounts of KI and *N*-aza-18-crown-6-*N'*-naphthoylthiourea, KSCN and *N*-aza-18-crown-6-*N'*-naphthoylthiourea, KI and *N,N*-diaza-18-crown-6-*N'*-naphthoylthiourea, and KSCN and *N,N*-diaza-18-crown-6-*N'*-naphthoylthiourea, were dissolved in acetonitrile and diluted to obtain a final molarity of 1.8 x 10^{-5} M. The UV spectra of these solutions were recorded on a Varian Superscan 3 UV/visible spectrophotometer using 1.00 cm matching quartz cells.

^{1}H NMR Experiments: Interaction of KI and CH_3NH_3Cl with *N*-aza-18-crown-6-*N'*-naphthoylthiourea

Standard solutions of potassium iodide and methyl ammonium chloride were prepared in 1 cm^3 D_2O to give a final molarity of 0.5095M. *N*-aza-18-crown-6-*N'*-naphthoylthiourea (0.01 mmol) was dissolved in 0.6 cm^3 CD_3COCD_3. 20 μL of the cation dissolved in D_2O was added directly to the NMR tube containing 0.6 cm^3 of *N*-aza-18-crown-6-*N'*-naphthoylthiourea in CD_3COCD_3 (i.e. equimolar amounts of cation and macrocycle). The proton spectra were recorded in the temperature range from 25 to -40 °C, in increments of 5 °C and in increments of 1 °C to accurately determine the coalescence temperatures.

REFERENCES

1 Pederson, C.J.; *J. Am. Chem. Soc.*, 1967, **89**, 2495.

2 Stefanac, Z.; Simon, W.; *J. Microchem.*, 1967, **12**, 125.

3 Pioda, L.A.R.; Wachter, H.A.; Dohner, R.E.; Simon, W.; *Helv. Chim. Acta,* 1967, **50**, 1373.

4 Pederson, C.J.; *J. Am. Chem. Soc.*, 1967, **89**, 7071.

5 Gokel, G.W.; *Monographs in Supramolecular Chemistry - Crown Ethers and Cryptands*, ed. Stoddart, J.F., Royal Society of Chemistry, Cambridge, 1991.

6 Tsukube, H.; *J. Coord. Chem.*, 1987, **B-16**, 101.

7 Vögtle, F.; *Supramolecular Chemistry*, John Wiley & Sons, Chichester, England, 1991.

8 Gokel, G.W.; Korzeniowski, S.J. (eds.), *Macrocyclic Polyether Synthesis*, Springer, Berlin, Heidelberg, New York, 1982.

9 Dietrich, B.; Lehn, J.-M.; Sauvage, J.P.; *Chem.Unserer Zeit*, 1973, **7**, 120.

10 Lehn, J.-M.; *Pure Appl. Chem.*, 1977, **49**, 857.; 1978, **50**, 871.

11 Vögtle, F.; Weber, E.; *Angew. Chem. Int. Ed. Engl.*, 1979, **18**, 753.

12 Bradshaw, J.S.; Hui, J.Y.K.; *J. Heterocycl. Chem.*, 1974, **11**, 649.

13 Gokel, G.W.; Dishong, D.M.; Schultz, R.A.; Gatto, V.J.; *Synthesis*, 1982, 997.

14 Christensen, J.J.; Eatough, D.J.; Izatt, R.M.; *Chem. Rev.*, 1974, **74**, 351.

15 Izatt, R.M.; Christensen, J.J.; (eds.), *Synthetic Multidentate Macrocyclic Compounds*, Academic Press, San Francisco, 1978.

16 Ho, T.-L.; *Hard and Soft Acids and Bases Principle in Organic Chemistry*, Academic Press, New York, 1977.

17 Iwachido, T.; Sadakane, A.; Tôei, K.; *Bull. Chem. Soc. Jpn.*, 1978, **51**, 629.

18 de Jong, F.; Reinhoudt, D.N.; Smit, C.J.; Huis, R.; *Tetrahedron Lett.*, 1976, 4783.

19 de Boer, J.A.A.; Reinhoudt, D.N.; *J. Am. Chem. Soc.*, 1985, **107**, 5347.

20 Brockmann, H.; Schmidt-Kastner, G.; *Chem. Ber.*, 1955, **88**, 57.

21 White, B.D.; Arnold, K.A.; Gokel, G.W.; *Tetrahedron Lett.*, 1987, 1749.

22 Kulstad, S.; Malmsten, L.A.; *Acta Chem. Scand.*, 1979, **B33**, 469.

23 Maeda, H.; Furuyoshi, S.; Nakatsuji, Y.; Okahara, M.; *Bull. Chem. Soc. Jpn.*, 1983, **56**, 212.

24 Matsumoto, K.; Minatogawa, H.; Munakata, M.; Toda, M.; Tsukube, H.; *Tetrahedron Lett.*, 1990, 3923.

25 Balch, A.L.; Neve, F.; Olmstead, M.M.; *Inorg. Chem.*, 1991, **30**, 3395.

26 Toda, M.; Tsukube, H.; Minatogawa, H.; Munakata, M.; Hirotsu, K.; Miyahara, I.; Higuchi, T.; Matsumoto, K.; *Supramolecular Chem.*, 1993, **2**, 289.

27 Lockhart, J.C.; Thompson, M.E.; *J. Chem. Soc. Perkin Trans. I*, 1977, 202.

28 Kotzyba-Hibert, F.; Lehn, J.-M.; Vierling, P.; *Tetrahedron Lett.*, 1980, 941.

29 Masuyama, A.; Nakatsuji, Y.; Ikeda, I.; Okahara, M.; *Tetrahedron Lett.*, 1981, 4665.

30 Tsukube, H.; *J. Chem. Soc., Chem. Commun.*, 1983, 970.

31 Dishong, D.M.; Diamond, C.J.; Cinoman, M.I.; Gokel, G.W.; *J. Am. Chem. Soc.*, 1983, **105**, 586.

32 Schultz, R.A.; White, B.D.; Dishong, D.M.; Arnold, K.A.; Gokel, G.W.; *J. Am. Chem. Soc.*, 1985, **107**, 6659.

33 Calverley, M.J.; Dale, J.; *Acta Chem. Scand., Ser.B.*, 1982, **36**, 241.

34 Masuyama, A.; Nakatsuji, Y.; Ikeda, I.; Okahara, M.; *Tetrahedron Lett.*, 1981, 4665.

35 White, B.D.; Mallen, J.; Arnold, K.A.; Fronczek, F.R.; Gandour, R.D.; Gehrig, L.M.B.; Gokel, G.W.; *J. Org. Chem.*, 1989, **54**, 937.

36 Zinic, M.; Frkanec, L.; Škaric, V.; Trafton, J.; Gokel, G.W.; *Supramolecular Chem.*, 1992, **1**, 47.

37 Gatto, V.J.; Gokel, G.W.; *J. Am. Chem. Soc.*, 1984, **106**, 8240.

38 Gatto, V.J.; Arnold, K.A.; Viscariello, A.M.; Miller, S.R.; Morgan, C.R.; Gokel, G.W.; *J. Org. Chem.*, 1986, **51**, 5373.

39 Kulstad, S.; Malmsten, L.A.; *J. Inorg. Nucl. Chem.*, 1981, **43**, 1299.

40 Schultz, R.A.; Schlegel, E.; Dishong, D.M.; Gokel, G.W.; *J. Chem. Soc., Chem. Commun.*, 1982, 242.

41 Pedersen, C.J.; Frensdorff, H.K.; *Angew. Chem. Int. Ed. Engl.*, 1972, **11**, 16.

42 Bourgoin, M.; Wong, K.H.; Hui, J.Y.; Smid, J.; *J. Am. Chem. Soc.*, 1975, **97**, 3462.

43 Douglass, I.B.; Dains, F.B.; *J. Am. Chem. Soc.*, 1934, **56**, 719.

44 Lynn, B.C.; Tsesarskaja, M.; Schall, O.F.; Hernandez, J.C.; Watanabe, S.; Takahashi, T.; Kaifer, A.; Gokel, G.W.; *Supramolecular Chem.*, 1993, **1**, 253.

45 Skoog, D.A.; West, D.M.; Holler, F.J.; *Fundamentals of Analytical Chemistry*, 5th edn., Saunders College Publishing, New York, 1988.

46 de Jong, F.; Reinhoudt, D.N.; Smit, C.J.; *Tetrahedron Lett.*, 1976, 1371.

47 Inoue, Y.; Nakagawa, K.; Hakushi, T.; *J. Chem. Soc., Dalton Trans.*, 1993, 2279.

48 Takeda, Y.; Namisaki, T.; Fujiwara, S.; *Bull. Chem. Soc. Jpn.*, 1984, **57**, 1055.

49 Sheldrick, G.M.; SHELXS-86 in *Crystallographic Computing 3*, (eds.), Sheldrick, G.M.; Kruger, C.; Goddard, R.; Oxford University Press, 1985.

50 Sheldrick, G.M.; SHELXL-93. In preparation for *J. Appl. Cryst.*, 1993.

51 March, J.; *Advanced Organic Chemistry: Reactions, Mechanisms and Structure*, McGraw-Hill Company, 1968.

52 Koch, K.R.; Sacht, C.; unpublished results.

53 Santos, M.A.; Drew, M.G.B.; *J. Chem. Soc., Faraday Trans.*, 1991, 1321.

54 Wipff, G.; Weiner, P.; Kollman, P.; *J. Am. Chem. Soc.*, 1982, **104**, 3249.

55 Beer, P.D.; Crowe, D.B.; Ogden, M.I.; Drew, M.G.B.; Main, B.; *J. Chem. Soc., Dalton Trans.*, 1993, 2107.

56 Kuleshova, L.N.; Zorkii, P.M.; *Acta Cryst.*, 1981, **B37**, 1363.

57 Willey, R.W.; Rudd, M.D.; Alcock, N.W.; *J. Chem. Soc., Dalton Trans.*, 1993, 2359.

58 Günter, H.; *An Introduction to NMR Spectroscopy*, John Willey & Sons, Chichester, New York, Brisbane, Toronto, 1980.

59 Beyer, L.; Behrendt, S.; Kleinpeter, E.; Borsdorf, R.; Hoyer, E.; *Z. Anorg. Allg. Chem.*, 1977, **437**, 282.

60 Sandström, J.; *Dynamic NMR Spectroscopy*, Academic Press, London, 1982.

61 Buhleier, E.; Wehner, W.; Vögtle, F.; *Chem. Ber.*, 1979, **112**, 559.

62 Hammond, P.J.; Bell, A.P.; Hall, C.D.; *J. Chem. Soc., Perkin Trans. I*, 1983, 707.

63 Streitweiser, J.R.; Heathcock, C.H.; *Introduction to Organic Chemistry*, 3rd edn., Macmillan Publishing Company, New York, 1985.

64 Wong, K.H.; Konizer, G.; Smid, J.; *J. Am. Chem. Soc.*, 1970, **92**, 666.

65 de Jong, F.; Reinhoudt, D.N.; Smit, C.J.; *Tetrahedron Lett.*, 1976, 1375.

66 White, B.D.; Fronczek, F.R.; Gandour, R.D.; Gokel, G.W.; *Tetrahedron Lett.*, 1987, 1753.

67 Izatt, R.M.; Lamb, J.D.; Izatt, N.E.; Rossiter, B.E.; Christensen, J.J.; Haymore, B.L.; *J. Am. Chem. Soc.*, 1979, **101**, 6273.

68 Coplan, M.A.; Fuoss, R.M.; *J. Phys. Chem.*, 1964, **68**, 1177.

CHAPTER 6

PLATINUM (II) COORDINATION CHEMISTRY OF *N*-MORPHOLINO-*N'*-NAPHTHOYLTHIOUREA AND *N*-AZA-18-CROWN-6-*N'*-NAPHTHOYLTHIOUREA

6.1 Introduction

In the previous chapter, we demonstrated the disappointingly low binding affinity of *N*-aza-18-crown-6-*N'*-naphthoylthiourea to cations such as K^+ and $CH_3NH_3^+$. Firstly, we attributed this low binding to the presence of the strong *intra*molecular hydrogen bond which holds the macrocyclic moiety above the C(11) - N(12) - C(13) backbone of the chelate ring in an usual conformation, and secondly, to delocalisation of the aza-crown ether nitrogen lone pair of electrons into the C(13) - N(14) bond rendering these electrons less available for cation complexation.

In Chapter 4 we prepared neutral platinum (II) complexes with ligands based on the *N,N*-dialkyl-*N'*-acylthiourea motif. Metal (II or III) coordination is likely to render the N - H proton of the ligand more acidic. Therefore it is reasonable to expect that a ligand coordinated to the metal atom via the sulfur and oxygen donor atoms will be deprotonated, as illustrated in Chapter 4. Hence metal coordination with concomitant loss of the proton involved in the *intra*molecular hydrogen bond of the *N*-aza-18-crown-6-*N'*-naphthoylthiourea ligand, may activate the aza-crown ether moiety to bind K^+ or NH_4^+ cations. The aza-crown ether moiety of *cis*- or *trans*-bis(*N*-aza-18-crown-6-*N'*-naphthoylthioureato)metal(II) may complex K^+ and NH_4^+ cations to a greater degree than in the corresponding ligand, since the macrocyclic moiety will no longer be involved with an *intra*molecular hydrogen bond and may be freer to assume the desired D_{3d} conformation required for cation complexation[1-3].

Furthermore, it has been shown that metal coordination of the chelate ring increases the N(12) - C(13) bond order with respect to the uncomplexed ligand[4]. This implies a decrease in double bond character of the C(13) - N(14) bond once the ligand is coordinated, which may have a profound effect on the availability of the lone pair of electrons of the aza-crown ether nitrogen for cation binding.

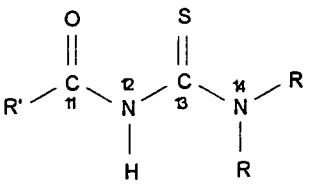

Accordingly, we decided to examine whether the interaction between appropriately sized cations and the aza-crown ether ring of *N*-aza-18-crown-6-*N'*-naphthoylthiourea was effected by platinum (II) coordination of the chelate ring. Employing a reported method[5], the synthesis of the platinum complexes of *N*-morpholino-*N'*-naphthoylthiourea and *N*-aza-18-crown-6-*N'*-naphthoylthiourea (Figure 6.1) was undertaken as described in the experimental section of this chapter.

Figure 6.1 Schematic representation of *cis*-bis(*N*-morpholino-*N'*-naphthoylthioureato)platinum(II) (**IV**) and *cis*-bis(*N*-aza-18-crown-6-*N'*-naphthoylthioureato)platinum(II) (**V**).

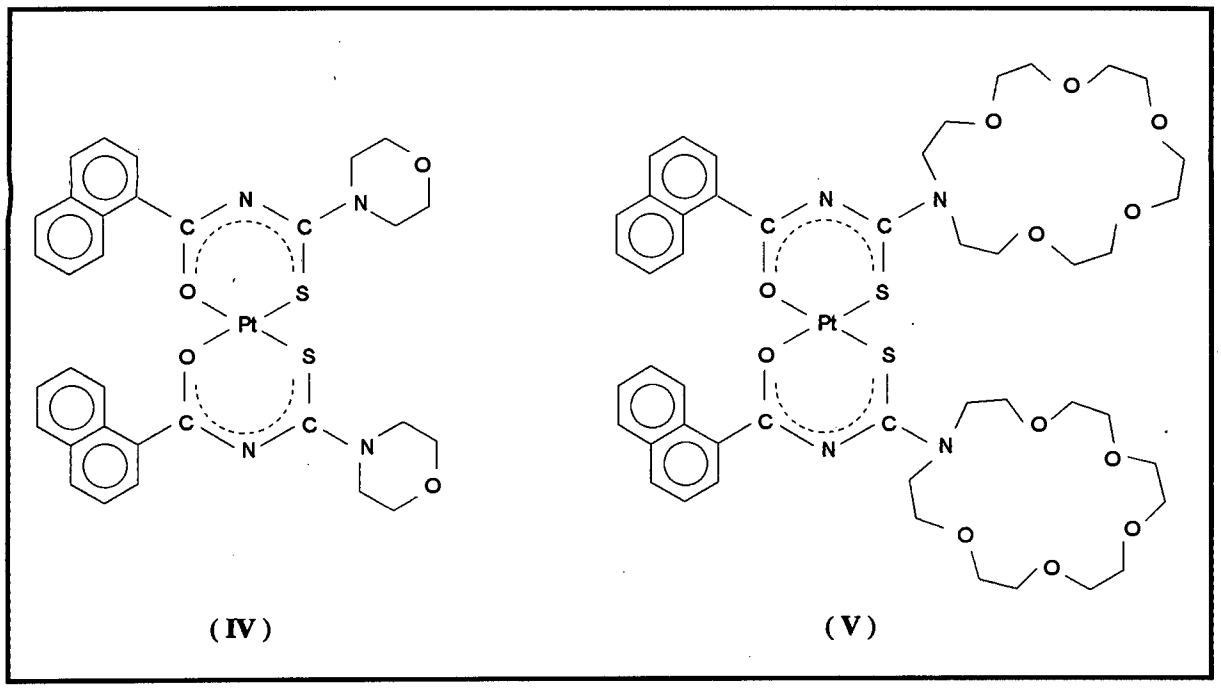

6.2 Results and Discussion

6.2.1 Synthesis and characterisation of *cis*-bis(*N*-morpholino-*N'*-naphthoyl-thioureato)platinum(II) and *cis*-bis(*N*-aza-18-crown-6-*N'*-naphthoylthioureato)-platinum(II).

Complex Preparation

The *cis*-bis(*N*-morpholino-*N'*-naphthoylthioureato)platinum(II) (**IV**) and *cis*-bis(*N*-aza-18-crown-6-*N'*-naphthoylthioureato)platinum(II) (**V**) complexes (Figure 6.1) were prepared according to a previously reported method[5]. The addition of two molar equivalents of *N*-morpholino-*N'*-naphthoylthiourea to one molar equivalent of a K_2PtCl_4 solution resulted in an immediate colour change from a clear, colourless solution to a bright yellow solution. Sodium acetate was added and a precipitate was immediately evident. The precipitate was collected and the complex isolated as a bright yellow solid **IV**, in 91 % yield.

The addition of two equivalents of *N*-aza-18-crown-6-*N'*-naphthoylthiourea to one molar equivalent of a K_2PtCl_4 solution in the presence of sodium acetate did not result in any colour change. The reaction solution turned yellow after stirring for a few hours at room temperature. The reaction mixture was stirred for two days during which a yellow solid precipitated out of the solution. The yellow solid **V** was isolated in 67 % yield. ^1H NMR spectroscopy of the mother liquor showed the presence of mainly unreacted ligand.

These results suggest that at room temperature, the reaction of *N*-morpholino-*N'*-naphthoylthiourea with platinum (II) occurs more readily than the analogous reaction with *N*-aza-18-crown-6-*N'*-naphthoylthiourea. It seems reasonable to predict that the *intra*molecular hydrogen bond observed from the X-ray crystal structure of *N*-aza-18-crown-6-*N'*-naphthoylthiourea persists in solution and may thus affect the acidity of the N - H proton. Furthermore, steric factors may influence the rate of the reaction; the morpholino moiety being less sterically demanding than the aza-crown ether moiety.

Complex Characterisation

The platinum complexes were characterised by ^{1}H, ^{13}C and ^{195}Pt NMR spectroscopy and C, H and N elemental analysis. A detailed account of the physical and elemental data is given in the experimental section. An interesting point to note is the observed elemental analyses of the platinum complex of *N*-aza-18-crown-6-*N'*-naphthoylthiourea (**V**) (Table 6.1). The elemental analyses were determined after repeated recrystallisations of the complex from acetonitrile / diethylether solutions.

Table 6.1 Analytical data (% C, H, N) of *cis*-bis(*N*-aza-18-crown-6-*N'*-naphthoylthioureato)-platinum(II).2KCl.4H_2O.

	Calculated	Observed 1	Observed 2	Observed 3	Observed 4	Average
% C	42.15	42.23	42.31	42.33	42.14	42.20
% H	5.16	5.06	4.99	5.00	5.17	5.06
% N	4.10	4.11	4.15	4.11	4.05	4.10

The C, H and N elemental analyses of complex **V** indicates that two moles of KCl and four moles of water are associated with one mole of *cis*-bis(*N*-aza-18-crown-6-*N'*-naphthoylthioureato)platinum(II). The thermogravimetric analysis of **V** indicates a loss in weight of 5.16 %, which corresponds favourably with a loss of four water molecules per molecule of **V** (calculated 5.27 %). Furthermore, integration of the water signal in the proton NMR spectrum of **V** (anhydrous $CDCl_3$) indicates the presence of approximately four water molecules per molecule of **V**. The involvement of water molecules in crown ether cation complexation is not an unknown phenomenon; the role of water molecules as bridging units in the complexation of alkylammonium salts by crown ethers has previously been mentioned[6] (Chapter 5). In summary, when considering all the analytical data together, it is evident that two moles of KCl and four moles of H_2O are associated with one mole of *cis*-bis(*N*-aza-18-crown-6-*N'*-naphthoylthioureato)platinum(II).

^1H and ^{13}C NMR Spectroscopy

The chemical shifts of the naphthyl protons of **IV** and **V** are similar to the analogous protons reported for *cis*-bis(*N,N*-dibutyl-*N'*-naphthoylthioureato)platinum(II)[5]. Hence **IV** and **V** were assigned the *cis* conformation. The remarkable difference between the observed chemical shifts of the naphthyl protons of *cis*-$[PtL_2]$ and *trans*-$[PtL_2]$[5] is illustrated in Figure 6.2.

Evidence for the complexation of K^+ into the aza-crown ether ring of *cis*-bis(*N*-aza-18-crown-6-*N'*-naphthoylthioureato)platinum(II).2KCl.$4H_2O$ is apparent from the oxyethylene region of the proton NMR spectrum. Significant downfield shifts are observed for the protons of the aza-crown ether ring with respect to the corresponding ligand spectrum (Figure 6.3). These shifts may be due to K^+ complexation into the aza-crown ether ring, since it has been reported that complexation of a cation with a crown ether moiety induces downfield shifts in the resonances of the oxyethylene protons. This is due to the increased electronegativity of the oxygen atoms[7].

Furthermore, sharp signals representing the protons of the aza-crown ether rings are observed in the ^1H NMR spectrum of **V**. The sharpness of the oxyethylene signals suggests that motion of the aza-crown ether moiety is either very slow or fast on the NMR time scale. As previously discussed in Chapter 5, at least two motions, rotation around the C - N bond and conformational motion of the macrocyclic ring, must be considered when interpreting the proton spectrum of macrocyclic *N*-acylthiourea molecules. It is reasonable to postulate that K^+ cation complexation of the aza-crown ether ring will result in a relatively 'rigid' conformation of the macrocyclic moiety. Thus if K^+ is complexed into the macrocyclic ring of **V**, the conformation motion of the aza-crown ether ring will be slow on the NMR time scale and accordingly sharp signals are expected in the proton NMR spectrum.

On the other hand, one may argue that complexation of the chelate moiety is expected to decrease the C - N bond order (N of aza-crown ether ring), which implies an increase in the rotation of the aza-crown ether ring around this bond. However, this argument is ruled out by the fact that separate signals are observed for the protons adjacent to nitrogen, H(15) and H(31), and for the protons adjacent to oxygen, H(16) and H(30) (Figure 6.3). The observed decrease in rotation about the C - N bond could be due to the bulky aza-crown ether rings which sterically hinder rotation around this bond.

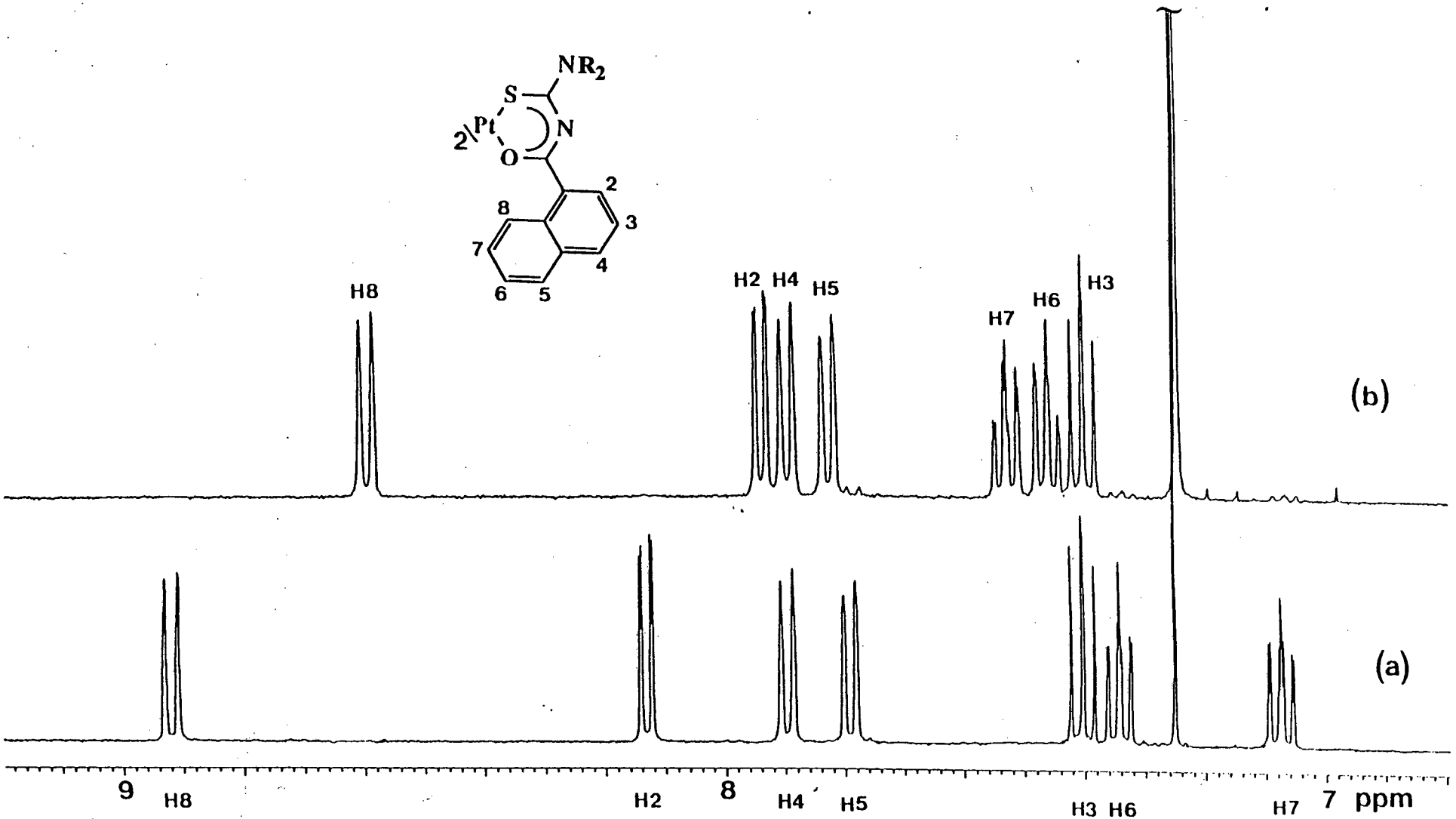

Figure 6.2 The proton NMR spectra of the aromatic region of (a) *cis*-bis(*N*-aza-18-crown-6-*N'*-naphthoylthioureato)platinum(II) and (b) *trans*-bis(*N,N*-dibutyl-*N'*-naphthoylthioureato)platinum(II) in $CDCl_3$ at 25 °C[5]. The spectrum of *trans*-PtL_2 is reproduced with the permission of K.R.Koch.

Figure 6.3 ^{1}H NMR spectra of the oxyethylene region of (**a**) *cis*-bis(*N*-aza-18-crown-6-*N'*-naphthoyl-thioureato)platinum(II) and (**b**) *N*-aza-18-crown-6-*N'*-naphthoylthiourea in $CDCl_3$ at 25 °C.

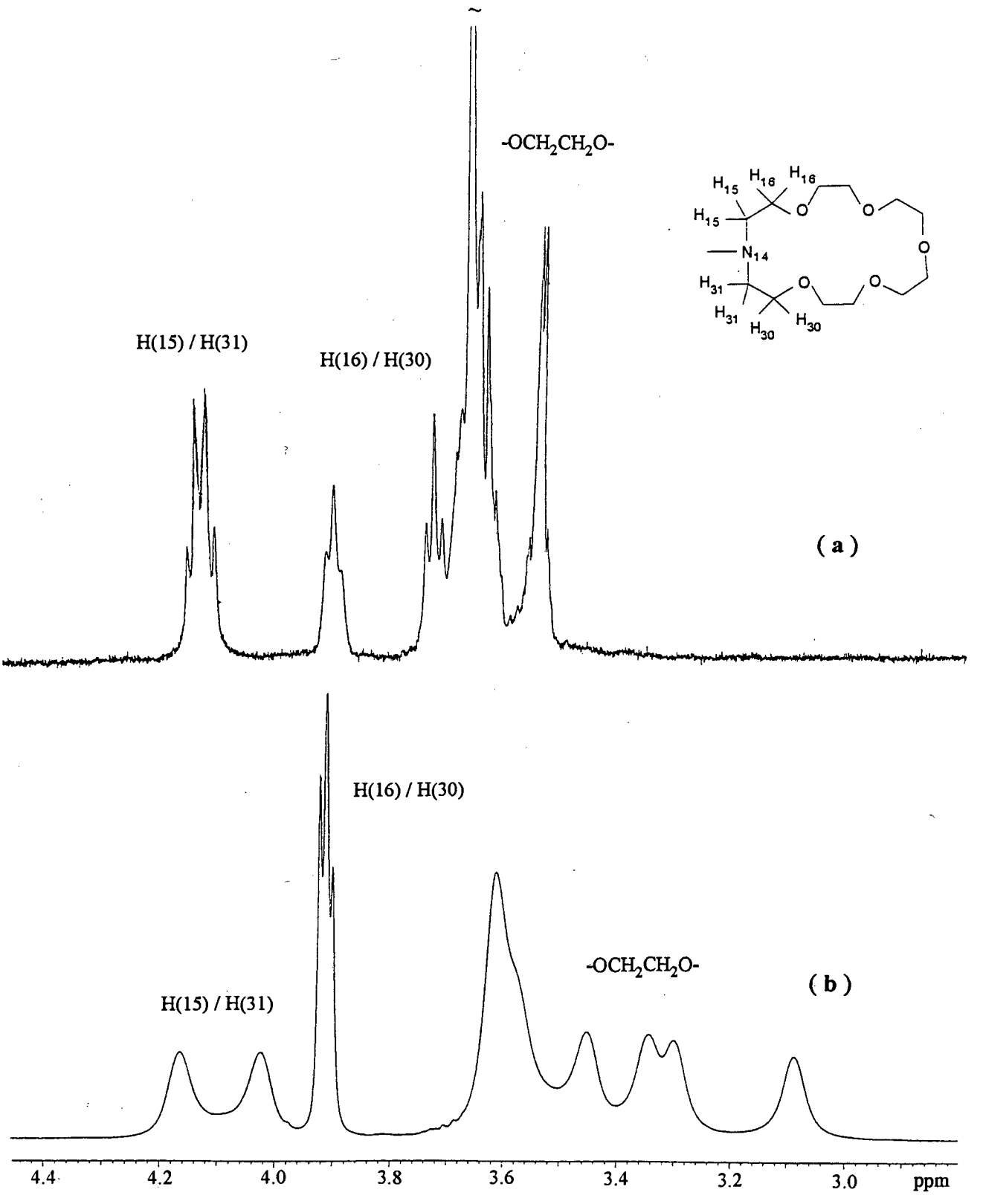

In summary, the observed downfield shifts of the aza-crown ether signals in the proton NMR spectrum of **V** compared to the corresponding ligand spectrum, indicate K^+ complexation. The sharpness of the signals in the oxyethylene region of the proton spectrum may firstly, be due to the rigid conformation of the aza-crown ether ring as a result of K^+ complexation, and secondly, to a decrease in rotation about the C - N bond as a result of the steric bulkiness of the aza-crown ether rings.

In comparison, the signals of the oxyethylene region in the proton spectrum of *cis*-bis(*N*-morpholino-*N'*-naphthoylthioureato)platinum(II) do not show any significant shifts or an increase in sharpness compared to the uncomplexed ligand spectrum. Thus the observed changes in the oxyethylene signals discussed above, are not the result of bidentate platinum coordination.

Unambiguous evidence for K^+ cation complexation into the aza-crown ether moieties of *cis*-bis(*N*-aza-18-crown-6-*N'*-naphthoylthioureato)platinum(II).2KCl.$4H_2O$ requires an X-ray crystal structure determination. However, despite numerous attempts to obtain crystals from a variety of solvents and utilising a number of crystallisation techniques, we were not able to isolate crystals of diffraction quality. Nevertheless, the elemental analyses and the observed ^1H NMR spectrum suggest that K^+ cations are complexed into the aza-crown ether rings of *cis*-bis(*N*-aza-18-crown-6-*N'*-naphthoylthioureato)platinum(II).2KCl.$4H_2O$.

6.2.2 Crystallographic study of *cis*-bis(*N*-morpholino-*N'*-naphthoylthioureato)-platinum(II)

Although we were unable to isolate crystals of *cis*-bis(*N*-aza-18-crown-6-*N'*-naphthoylthioureato)-platinum(II).2KCl.$4H_2O$ of diffraction quality, the structure of *cis*-bis(*N*-morpholino-*N'*-naphthoyl-thioureato)platinum(II) (**IV**) was determined by single-crystal X-ray diffraction. Bright yellow crystals were obtained by dissolving the complex in a chloroform - ethanol solution and allowing very slow evaporation of the solvent at room temperature. The structure was determined Ms Anita Coetzee (Department of X-ray Crystallography, UCT). The Pt and S atoms were located by direct methods using SHELXS-86[8]. The remaining atoms were located in a difference Fourier map and refined by full-matrix least squares based on F^2 using SHELXL-93[9]. The Pt, S, N and O atoms were treated anisotropically, as well as C7A, C8A, C10A, C11A, C7B, C8B, C10B and C11B. All hydrogen atoms were placed in geometrically calculated positions and linked to a common temperature factor for chemically equivalent positions. The crystal data, experimental and refinement parameters are summarised in Table 4.1 of Appendix 4 and the fractional coordinates for all non-hydrogen atoms are listed in Table 4.2 of Appendix 4.

Each molecule of *cis*-bis(*N*-morpholino-*N'*-naphthoylthioureato)platinum(II) is located in a general position and therefore a whole molecule constitutes the asymmetric unit. The unit cell is monoclinic and contains four molecules. The bond lengths and bond angles all fall within the expected limits and are reported in

Table 4.3 of Appendix 4. The molecular structure and atom numbering scheme for the non-hydrogen atoms is shown in Figure 6.4.

Figure 6.4 Perspective view of the molecular structure of *cis*-bis(*N*-morpholino-*N'*-naphthoylthioureato)-platinum(II) showing the atom numbering scheme for the non-hydrogen atoms. The H atoms are omitted for clarity.

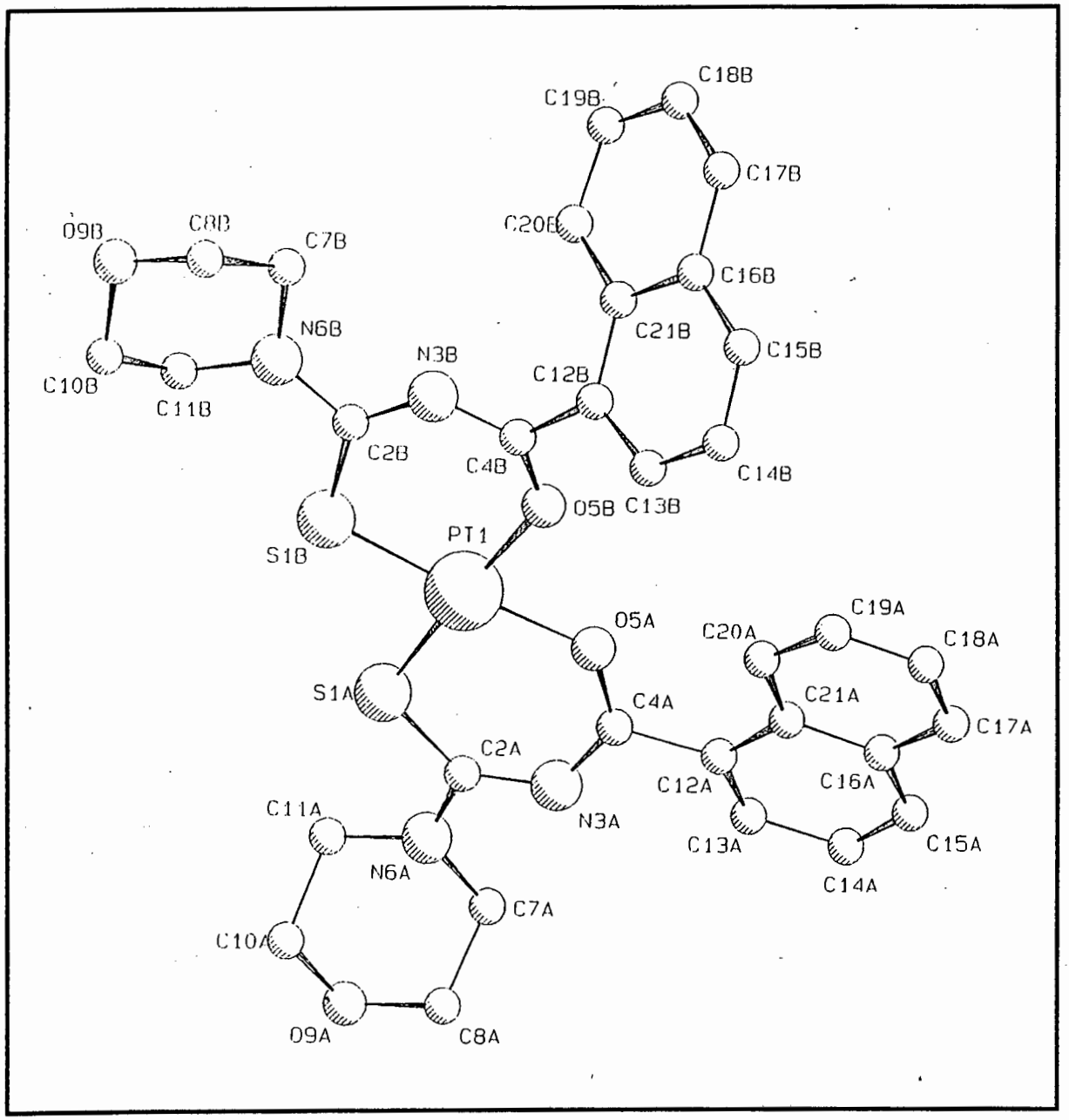

The X-ray crystal structure of *cis*-bis(*N*-morpholino-*N'*-naphthoylthioureato)platinum(II) confirms the proposed *cis* conformation of the ligands around the central metal atom and square-planar *O,S*-bidentate coordination of the ligand to the platinum atom. The observed Pt-O bond lengths are very close to 2.0 Å and are in agreement with the Pt-O bond lengths reported for Pt(acetylacetonato)$_2$[10,11]. The bond distances and bond angles of *cis*-bis(*N*-morpholino-*N'*-naphthoylthioureato)platinum(II) are similar to those reported for *trans*-bis(*N,N*-dibutyl-*N'*-naphthoylthioureato)platinum(II)[5].

A comparison of the structure of *cis*-bis(*N*-morpholino-*N'*-naphthoylthioureato)platinum(II) with the related structure of *N*-aza-18-crown-6-*N'*-naphthoylthiourea discussed in the previous chapter, shows that the carbonyl and thiocarbonyl bond lengths in the complex are significantly longer than those in the free ligand derivative. However the average two consecutive C - N bond lengths, N(3) - C(2) and N(3) - C(4) of the chelate ring of the complex, are approximately 0.06 and 0.04 Å shorter than the analogous bonds of the free ligand derivative. These changes in bond length on complexation indicate extensive delocalisation of electrons within the chelate ring of *cis*-bis(*N*-morpholino-*N'*-naphthoylthioureato)platinum(II), similar to that reported for the *cis*-bis(*N,N*-dibutyl-*N'*-benzoylthioureato)platinum(II)[4] and *trans*-bis(*N,N*-dibutyl-*N'*-naphthoylthioureato)platinum(II)[5] complexes.

Table 6.2 The bond distances (Å) observed for *cis*-bis(*N*-morpholino-*N'*-naphthoylthioureato)-platinum(II) (**IV**) and *N*-aza-18-crown-6-*N'*-naphthoylthiourea (**2**).

bond	(2)	(IV)
C=O	1.212(4)	1.254(11); 1.270(11)
C=S	1.667(4)	1.724(11); 1.705(11)
N(3) - C(2)	1.396(5)	1.339(12); 1.339(12)
N(3) - C(4)	1.372(4)	1.334(12); 1.319(11)

No significant differences are observed in the bond angles of the morpholino ring nitrogen atom of *cis*-bis(*N*-morpholino-*N'*-naphthoylthioureato)platinum(II) compared to the analogous angles observed for *N*-aza-18-crown-6-*N'*-naphthoylthiourea. These results, together with the similar C - N bond lengths, suggest sp^2 hybridisation of the nitrogen atom of the morpholino ring of *cis*-bis(*N*-morpholino-*N'*-naphthoyl-thioureato)platinum(II).

The six-membered coordination rings, Pt-S(1B)-C(2B)-N(3B)-C(4B)-O(5B) and Pt-S(1A)-C(2A)-N(3A)-C(4A)-O(5A), were found to be essentially planar with an angle of 2.14(0.27)° between the two planes. The aromatic groups were tested for planarity and deviated less than 0.05 Å from the mean plane. It is interesting to note that the naphthyl moieties are orientated at different angles to the coordination plane of

platinum (Figure 6.5). Naphthyl ring A is orientated at an angle of 16.85 °, whereas naphthyl ring B is orientated at an angle of 52.85 ° with respect to the coordination plane of platinum. The angle between the two aromatic groups is 62.36 °.

The crystal structure of *trans*-bis(*N,N*-dibutyl-*N'*-naphthoylthioureato)platinum(II)[5] and *cis*-bis(*N,N*-dibutyl-*N'*-benzoylthioureato)platinum(II)[4] show the naphthyl and benzyl moieties to be approximately co-planar with the square plane of coordination. It thus seems evident that steric interactions between the naphthyl moieties prevent co-planar orientation of these rings in *cis*-bis(*N*-morpholino-*N'*-naphthoylthioureato)-platinum(II).

In a recent report[5], the chemical shift positions of the naphthyl protons of *cis*- and *trans*-bis(*N,N*-dibutyl-*N'*-naphthoylthioureato)platinum(II) were shown to be remarkably different in $CDCl_3$ at 25 °C. The authors postulated that these differences were due to differing orientations of the naphthyl groups in the *cis* and *trans* isomers. Thus the X-ray crystal structure of *cis*-bis(*N*-morpholino-*N'*-naphthoylthioureato)platinum(II) confirms that the orientation of the naphthyl groups of *cis*-$[PtL_2]$ is different to that of *trans*-$[PtL_2]$, in the solid state. It is reasonable to postulate that such relative orientations of the naphthyl moieties will persist in solution and result in significant differences in the naphthyl signals of the proton NMR spectra.

Figure 6.5 Perspective view of *cis*-bis(*N*-morpholino-*N'*-naphthoylthioureato)platinum(II) showing the different orientation of the naphthyl moieties with respect to the square plane of coordination. The morpholino moieties are omitted for clarity.

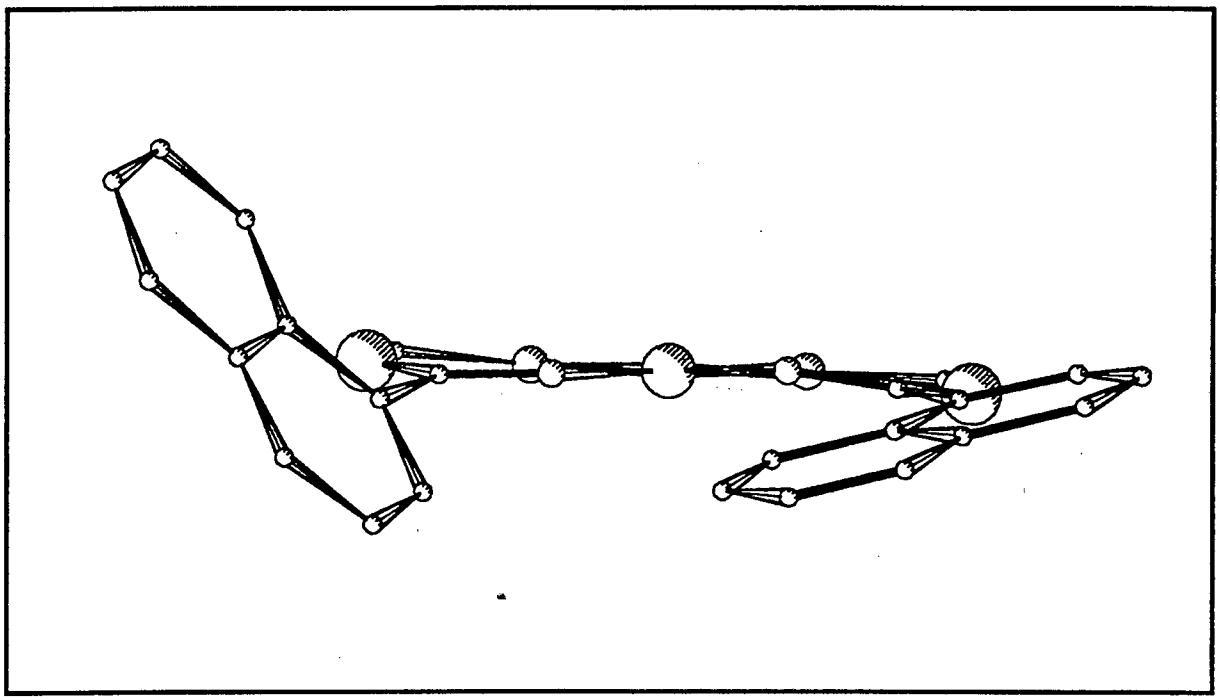

The morpholino moieties of *cis*-bis(*N*-morpholino-*N'*-naphthoylthioureato)platinum(II) are approximately co-planar with the square plane of coordination (Figure 6.6). The morpholino rings exist in a chair conformation.

Figure 6.6 Perspective view of *cis*-bis(*N*-morpholino-*N'*-naphthoylthioureato)platinum(II) showing the co-planarity of the morpholino rings with the platinum coordination plane. The naphthyl moieties are omitted for clarity.

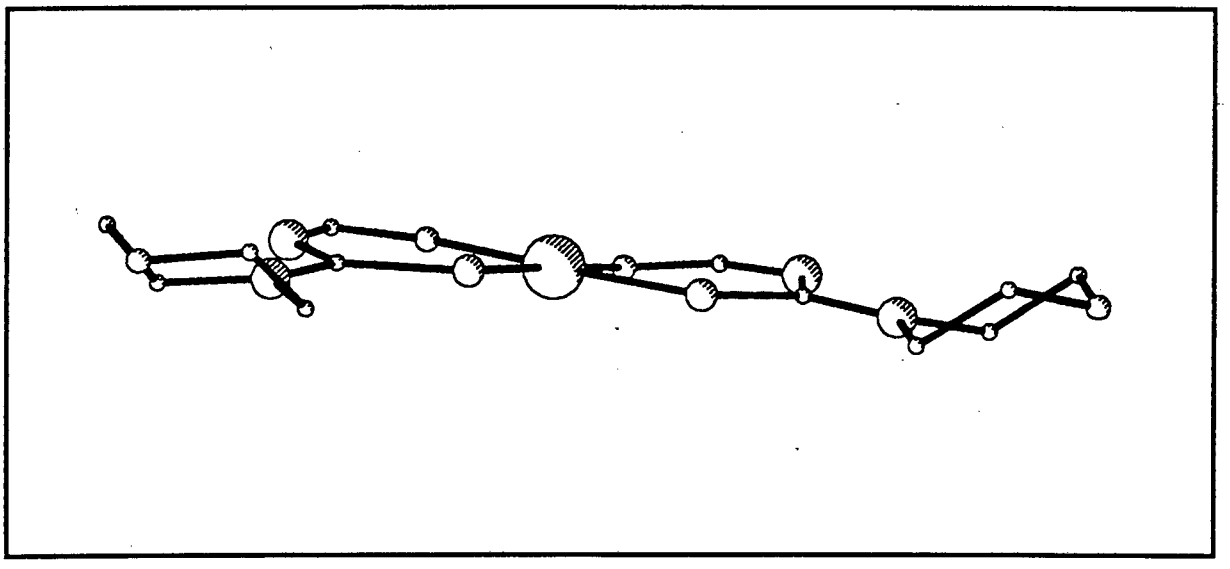

In summary, the X-ray crystal structure determination of *cis*-bis(*N*-morpholino-*N'*-naphthoylthioureato)-platinum(II) is consistent with a *cis* square-planar configuration of ligands around the central platinum atom. Furthermore, the crystal structure has shown that the naphthyl groups are not in the plane of platinum coordination. The naphthyl groups are orientated at angles of 16.85 and 52.85 ° to the square plane of coordination, whereas the *trans*-$[PtL_2]$[5] complex shows the naphthyl groups to be essentially co-planar with the square of coordination. The different orientations of the naphthyl groups thus explain the observed differences in the naphthyl proton chemical shifts in the ^1H NMR spectra of *cis*- and *trans*-$[PtL_2]$ complexes[5].

6.2.3 Protonation Studies

In chapter 4 it was shown that protonation of the coordinated ligand in *cis*-Pt(L-*S,O*)$_2$] complexes, where L is *N,N*-dialkyl-*N'*-benzoylthiourea, with HCl, results in the reversible opening of the 6-membered chelate ring with concomitant coordination of the Cl^- ion to the Pt (II) atom. A mixture of complexes of type *cis*- and *trans*-[Pt(HL-*S*)$_2$Cl$_2$] in which the protonated ligand, (HL), is coordinated to the metal through the *S*-atom only, with the *O*-donor atom of the *N*-benzoyl moiety being pendent, was identified from the chemical shifts of the signals in the ^{1}H and ^{195}Pt NMR spectra. Treatment of the mixture of these *cis* and *trans* complexes with concentrated NH_3, leads to the rapid formation of exclusively *cis*-[Pt(L-*S,O*)$_2$] complexes.

Furthermore, we synthesised *cis*-bis(*N,N*-dialkyl-*N'*-naphthoylthioureato)copper(II) and nickel (II) complexes and found no evidence for the formation of the corresponding *trans* isomer. This was surprising in view of the recently isolated *trans*-bis(*N,N*-dibutyl-*N'*-naphthoylthioureato)platinum(II) complex[5]. We postulated that the lack of formation of any *trans* isomer was due to the manner in which the complexes were prepared. (The complexes reported in Chapter 4 were prepared in the presence of acetate ions whereas the *trans*-bis(*N,N*-dibutyl-*N'*-naphthoylthioureato)platinum(II) complex[5] was isolated under acidic conditions.)

Given our interest in the question of *cis* / *trans* isomerism and the preparation of *trans*-bis(*N,N*-dialkyl-*N'*-acylthioureato)metal(II) complexes (for the preparation of metal-containing liquid crystals), we decided to examine the effect of protonation on complexes that include ligands with relatively bulky naphthyl groups. The effect of protonation on *cis*-bis(*N*-morpholino-*N'*-naphthoylthioureato)platinum(II) (**IV**) and *cis*-bis(*N*-aza-18-crown-6-*N'*-naphthoylthioureato)platinum(II) (**V**), was investigated.

Protonation Experiments

All ^{1}H and ^{195}Pt NMR spectra were recorded in $CDCl_3$ at 25 °C. The following experimental procedure was performed:

(a) The *cis*-[Pt(L-*S,O*)$_2$] complex, between 25 and 75 mg, was dissolved in 0.6 ml $CDCl_3$ to give a clear, pale yellow solution. The ^{1}H and ^{195}Pt NMR spectra were recorded.

(b) Aliquots of 100 μL concentrated hydrochloric acid were added to the NMR tube containing the *cis*-[Pt(L-*S,O*)$_2$] complex in $CDCl_3$. After vigorous shaking the phases were allowed to separate, which was complete after *ca* 5 - 10 min. Where necessary the distinctly darker yellow/ orange organic phase was filtered through a microfibre glasswool, resulting in a clear solution prior to NMR spectroscopy.

(c) After spectral acquisition, the mineral acid was removed and the $CDCl_3$ solution washed with water, followed by re-acquisition of the spectra.

(d) Finally the NMR solution was washed with concentrated ammonia, filtered, and the NMR spectra re-acquired.

The effects of protonation on *cis*-bis(*N*-morpholino-*N'*-naphthoylthioureato)platinum(II)

The ^{195}Pt NMR spectrum of the neutral *cis*-bis(*N*-morpholino-*N'*-naphthoylthioureato)platinum(II) complex, (**IV**), in $CDCl_3$, shows only a single sharp resonance at -2708 ppm, corresponding to *cis*-[Pt(L-*S,O*)$_2$] (Figure 6.7(a)). This resonance has a similar chemical shift to the analogous ^{195}Pt signal observed for *cis*-bis(*N,N*-dibutyl-*N'*-benzoylthioureato)platinum(II) (Chapter 4). The corresponding ^1H NMR spectrum of **IV** is consistent with only one deprotonated complex species in solution, as confirmed by the absence of the characteristic N - H resonance in the 8 - 10 ppm range. The full detailed ^1H NMR assignments of the neutral *cis* complex **IV** are recorded in the experimental section.

Addition of 100 μL *conc.* HCl directly to the NMR tube containing **IV**, yields a spectrum consisting of two ^{195}Pt resonances at -3215 (rel. int. 67 %) and -3019 ppm (33 %), (Figure 6.7(b)). No signal representing deprotonated *cis*-[Pt(L-*S,O*)]$_2$] is evident. The dramatic upfield shift of the resonances in the ^{195}Pt spectrum suggests the coordination of chloride anions to yield two species in solution[12]. The peak at -3215 ppm is assigned to the *cis*-[Pt(HL-*S*)$_2$Cl$_2$] complex and the peak at -3019 ppm assigned to the *trans*-[Pt(HL-*S*)$_2$Cl$_2$] complex. In the proton NMR spectrum of this solution, two corresponding ^1H resonances at 11.37 (rel. int. 71 %) and 10.99 (29 %) ppm assigned to the N - H moieties, confirm protonation of the coordinated ligands. The signals in the ^1H and ^{195}Pt NMR spectra of the present *cis*-[Pt(HL-*S*)$_2$Cl$_2$] and *trans*-[Pt(HL-*S*)$_2$Cl$_2$] complexes are similar to the analogous complexes observed on protonation of *cis*-bis(*N,N*-dibutyl-*N'*-benzoylthioureato)platinum(II) discussed in Chapter 4.

Removal of the excess mineral acid from the $CDCl_3$ solution of the complex, followed by washing with distilled water, yields a spectrum consisting of three ^{195}Pt resonances at -3215 (rel. int. 46 %), -3019 (21 %) and -2952 ppm (33 %), (Figure 6.7(c)). These signals represent *cis*-[Pt(HL-*S*)$_2$Cl$_2$], *trans*-[Pt(HL-*S*)$_2$Cl$_2$] and *cis*-[Pt(L-*S,O*)(HL-*S*)Cl] respectively. In the corresponding ^1H NMR spectrum of this solution three N - H resonances at 11.38 (rel int. 50 %), 10.99 (16 %) and 11.58 (34 %) ppm respectively, confirm these assignments.

Figure 6.7 The observed ^{195}Pt spectra of *cis*-bis(*N*-morpholino-*N'*-naphthoylthioureato)platinum(II) on protonation with HCl and subsequent part deprotonation with H_2O.

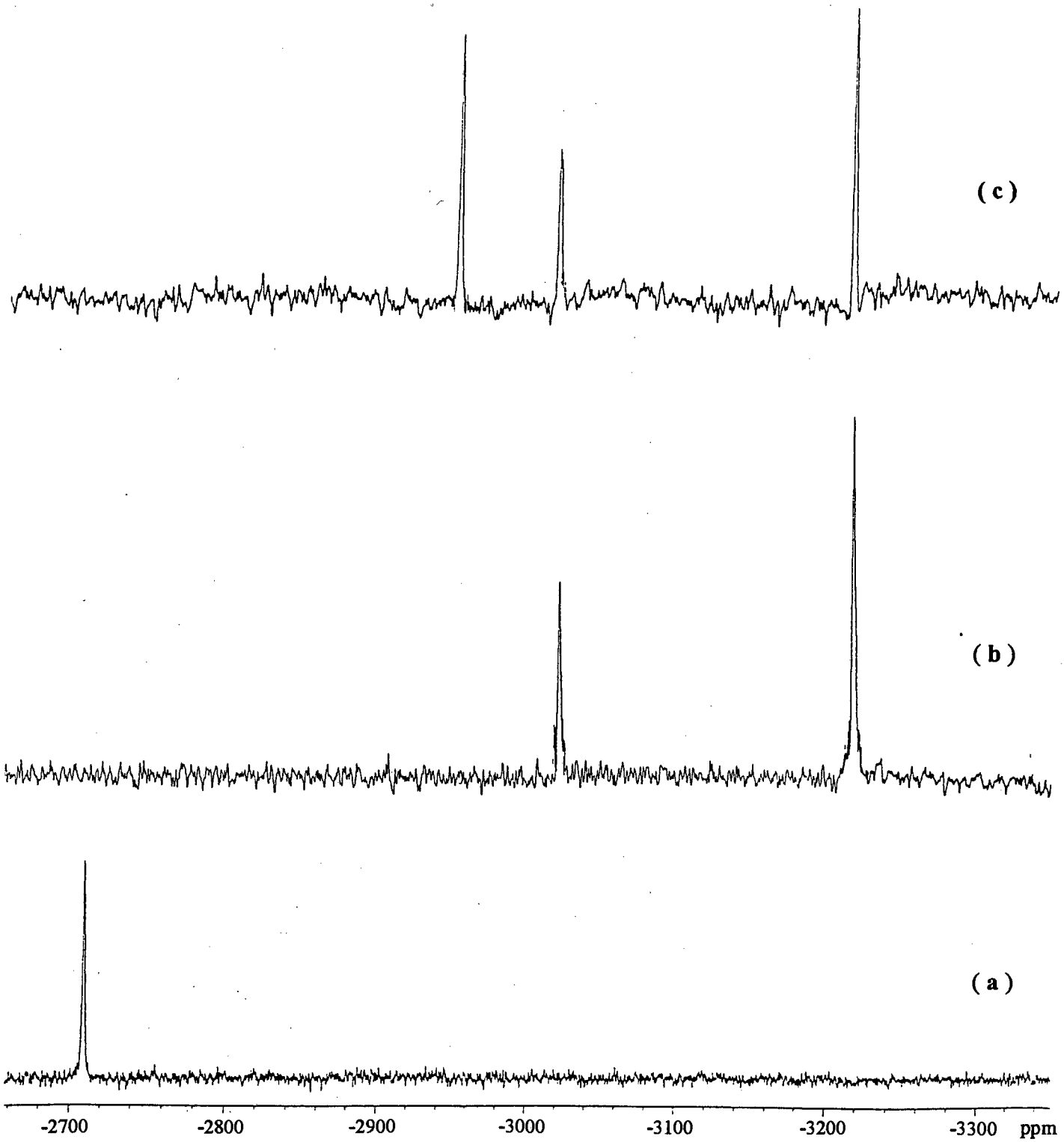

(**a**) Neutral *cis*-[Pt(L-*S,O*)$_2$].

(**b**) Addition of HCl yields *cis*-[Pt(HL-*S*)$_2$Cl$_2$] and *trans*-[Pt(HL-*S*)$_2$Cl$_2$].

(**c**) Addition of H_2O yields, in addition to the species observed in (**b**), *cis*-[Pt(L-*S,O*)(HL-*S*)Cl].

Subsequent washing of the NMR solution with 5 M ammonia yields a ^{195}Pt spectrum identical to that of the starting deprotonated *cis*-[Pt(L-*S,O*)$_2$] complex. In the ^1H spectrum of this solution the corresponding ^1H resonances are consistent with only one deprotonated complex species in solution, as confirmed by the absence of any N - H resonances in the 8 - 10 ppm region. However, the presence of a minor (< 5 %) species not previously observed in the spectra, was evident.

Synthesis of the platinum (II) complex of *N*-morpholino-*N'*-naphthoylthiourea in the presence of HCl.

The platinum (II) complex of *N*-morpholino-*N'*-naphthoylthiourea, (**IV**), was synthesised under acidic conditions to investigate whether the formation of the complex *in the presence of acid*, had any effect on the *cis-trans* isomerism of the products. If the postulate is correct that under acidic conditions the ligands are coordinated monodentately to the metal via the sulfur atom, then it is reasonable to predict that the presumably less stable *trans* isomer could be formed, on deprotonation, along a kinetically favoured route.

Protonated **IV** was prepared by the dropwise addition of *N*-morpholino-*N'*-naphthoylthiourea, in an CH_3CN / 2 M HCl solution, to a stirred, warm solution of K_2PtCl_4 in the same solvent. After 24 hours, the solvent was removed and the yellow solid isolated. The ^{195}Pt spectrum of the isolated complex in $CDCl_3$, shows two sharp resonances at -3213 (rel. int. 70 %) and -3019 (30 %) ppm, (Figure 6.8(a)). In the ^1H NMR spectrum of this solution, two corresponding N - H resonances at 11.32 (rel. int. 73 %) and 10.97 (27 %) ppm, confirm the presence of protonated species in solution. These species were assigned to *cis*-[Pt(HL-*S*)$_2$Cl$_2$] and *trans*-[Pt(HL-*S*)$_2$Cl$_2$] respectively, since the chemical shifts of the observed resonances in the ^{195}Pt and ^1H spectra are identical to those obtained when the neutral *cis*-[Pt(L-*S,O*)$_2$] complex is protonated with concentrated HCl. Furthermore, integration of the ^1H and ^{195}Pt signals suggest that the ratio of the *cis* and *trans* isomers present, are approximately the same as that obtained when the neutral *cis*-[Pt(L-*S,O*)$_2$] complex is protonated with concentrated HCl.

Washing with water and the addition of a few drops of 5M ammonia directly to the NMR tube containing the protonated sample, yields a spectrum consisting of two sharp ^{195}Pt resonances at -2708 (rel. int. 72 %), assigned to *cis*-[Pt(L-*S,O*)$_2$], and -2952 ppm (28 %), assigned to *cis*-[Pt(L-*S,O*)(HL-*S*)Cl] (Figure 6.8(b)). No signals at -3213 and -3019 ppm are observed. The corresponding ^1H NMR spectrum of this solution is consistent with one deprotonated complex species as confirmed by the absence of the characteristic N - H resonance, and one mono-protonated complex species, *cis*-[Pt(L-*S,O*)(HL-*S*)Cl], as confirmed by the presence of a N - H resonance at 11.57 ppm.

Storage of the above solution for 24 hours followed by treatment with an additional 100 µL 5M NaOH, yields a spectrum consisting of a ^{195}Pt resonance at -2708 ppm (rel. int. 48 %) and a previously unobserved signal at -3027 ppm (52 %) (Figure 6.8(c)).

Figure 6.8 The observed ^{195}Pt spectra of *cis*-bis(*N*-morpholino-*N'*-naphthoylthioureato)platinum(II) prepared under acidic conditions.

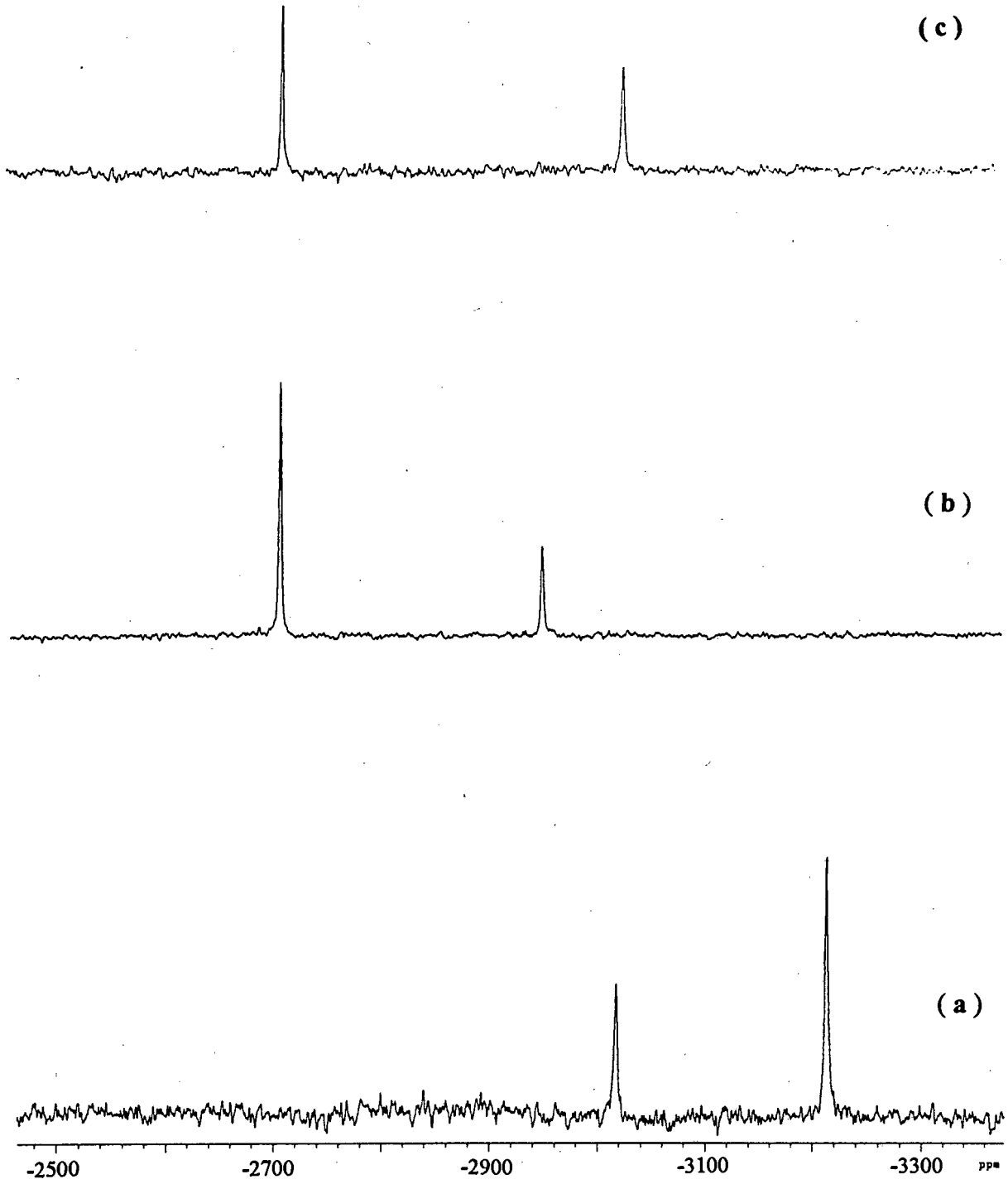

(**a**) (**IV**) prepared in the presence of HCl yields *cis*-$[Pt(HL\text{-}S)_2Cl_2]$ and *trans*-$[Pt(HL\text{-}S)_2Cl_2]$.

(**b**) Washing with H_2O / NH_3 yields *cis*-$[Pt(L\text{-}S,O)_2]$ and *cis*-$[Pt(L\text{-}S,O)(HL\text{-}S)Cl]$.

(**c**) Storage of solution in (**b**) for 24 hours followed by the addition of NaOH, yields *cis*-$[Pt(L\text{-}S,O)_2]$, *trans*-$[Pt(L\text{-}S,O)_2]$ and an unidentified organic species.

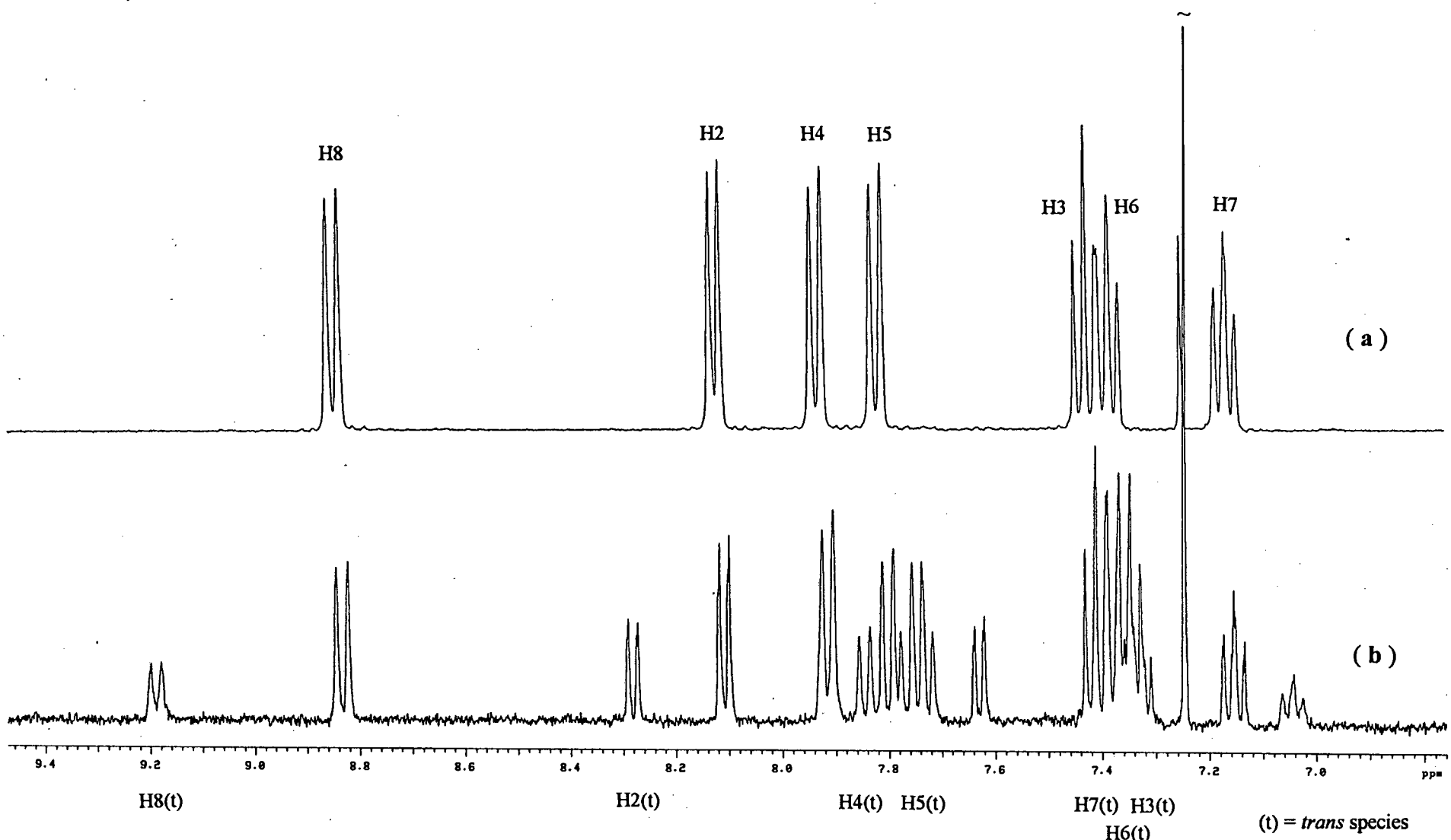

Figure 6.9 ^{1}H NMR spectrum, ($CDCl_3$), of (**a**) *cis*-bis(*N*-morpholino-*N'*-naphthoylthioureato)platinum(II) and (**b**) the solution of *cis*-bis(*N*-morpholino-*N'*-naphthoylthioureato)platinum(II) previously protonated with HCl, left for 24 hours after addition of distilled water / NH_3 and then deprotonated with NaOH.

Careful inspection of the ^{1}H and ^{195}Pt NMR spectra suggests that, as for *cis*-bis(*N,N*-dibutyl-*N'*-benzoylthioureato)platinum(II), protonation of the bound ligand in the presence of coordinating Cl^- anions, leads to ring opening of the *S,O*-chelate such that the *N*-morpholino-*N'*-naphthoylthiourea ligand remains bound to Pt through the *S*-atom only. On deprotonation with water and ammonia, the peak which appears in the ^{195}Pt spectrum at -2952 ppm and corresponds to a peak at 11.57 ppm in the ^{1}H NMR spectrum, is assigned to *cis*-[Pt(L-*S,O*)(HL-*S*)Cl] in which one ligand molecule remains protonated and bound to the metal through the *S*-atom only, while the other ligand molecule is deprotonated and *S,O*-chelated to Pt(II).

Two signals are observed in the ^{195}Pt NMR spectrum after complete deprotonation with 5 M NaOH. Consideration of the ^{195}Pt and ^{1}H spectra (Figure 6.8 and 6.9) suggests that the resonance at -2708 ppm is consistent with the *cis*-[Pt(L-*S,O*)$_2$] complex whereas the resonance at -3027 ppm is postulated to represent *trans*-[Pt(L-*S,O*)$_2$]. Strong support for this postulate is obtained from the similarity of the naphthyl chemical shifts in the ^{1}H NMR spectrum of the *trans* complex in question here, with the previously published aromatic shifts of *trans*-bis(*N,N*-dibutyl-*N'*-naphthoylthioureato)platinum(II)[5]. (The present proton signals were assigned with the aid of a COSY experiment). The resonance at -3027 ppm, assigned to the *trans*-[Pt(L-*S,O*)$_2$] complex, should not be confused with the resonance at -3019 ppm assigned to the *trans*-[Pt(HL-*S*)$_2$Cl$_2$] complex.

The assignment of the *trans*-[Pt(L-*S,O*)$_2$] complex upfield of the corresponding *cis*-[Pt(L-*S,O*)$_2$] complex, is not consistent with the *generally* observed trend that, for complexes of type PtA_2X_2, the *cis* isomer is often more shielded (high field) compared to the corresponding *trans* isomer, typically by between 200 - 500 ppm for X = Cl^- [35]. However, this is a general trend and usually refers to monodentate A and X bound ligands. Furthermore, exceptions to this trend have been observed since Sadler[13] and McFarlane[14] have both reported ^{195}Pt NMR shifts of *cis* and *trans* complexes where the *trans* complex is upfield of the corresponding *cis* complex. Thus for the complexes *cis*-[Pt(SOMe$_2$)$_2$Cl$_2$] and *trans*-[Pt(SOMe$_2$)$_2$Cl$_2$], they find ^{195}Pt NMR shifts of -3459 and -3650 ppm respectively, in DMSO-d_6[14].

In addition to the ^{1}H NMR signals representing the protons of the *cis*-[Pt(L-*S,O*)$_2$] and *trans*-[Pt(L-*S,O*)$_2$] complexes, a third species is observed in the ^{1}H NMR spectrum. The identity of this species is presently unknown. No corresponding signal is evident in the ^{195}Pt NMR spectrum. The possibility of alkaline hydrolysis of the neutral or protonated complex **IV** was considered, since it is known that *N*-acylthioureas hydrolyse in NaOH solutions[15]. However, careful inspection of the ^{1}H NMR spectrum did not show any evidence of the hydrolysis products such as naphthyl carboxylic acid and *N*-morpholinothiourea. Furthermore, the experiment was repeated using concentrated ammonia as the base and the observed ^{195}Pt and ^{1}H NMR spectra were identical to the spectra obtained using NaOH as the base. Hence the minor species observed in the ^{1}H NMR spectrum is not the result of alkaline hydrolysis. Future work aimed at identifying this species warrants further attention.

In summary, protonation of neutral *cis*-bis(*N*-morpholino-*N'*-naphthoylthioureato)platinum(II) or preparation of the platinum (II) complex of *N*-morpholino-*N'*-naphthoylthiourea under acidic conditions, results in the formation of two species, *cis*-[Pt(HL-*S*)$_2$Cl$_2$] and *trans*-[Pt(HL-*S*)$_2$Cl$_2$], in which the protonated ligand is bound to the metal *via* the *S*-atom only. Deprotonation with H_2O / NH_3 or NaOH yields the deprotonated *cis*-[Pt(L-*S,O*)$_2$] complex and, under appropriate conditions, the corresponding *trans*-[Pt(L-*S,O*)$_2$] complex and an unknown organic species. A schematic representation of the deprotonation process is summarised in Figure 6.10.

The effect of protonation on *cis*-bis(*N*-aza-18-crown-6-*N'*-naphthoylthioureato)platinum(II)

The ^{195}Pt NMR spectrum of the *cis*-bis(*N*-aza-18-crown-6-*N'*-naphthoylthioureato)platinum(II) complex, (**V**), in $CDCl_3$, shows only a single relatively sharp resonance at -2699 ppm. This resonance is in the chemical shift region expected for a deprotonated *cis* complex and is assigned to *cis*-[Pt(L-*S,O*)$_2$]. The corresponding ^{1}H NMR spectrum is consistent with only one deprotonated complex species in solution, as confirmed by the absence of the characteristic N – H resonance in the 10 - 12 ppm range.

Addition of 100 μL *conc.* HCl directly to the NMR tube containing complex **V** yields a spectrum consisting of only one ^{195}Pt resonance at -3181 ppm. In the ^{1}H NMR spectrum of this solution the corresponding N - H peak at 11.08 ppm confirms protonation of the coordinated ligands. The chemical shift positions of the aromatic protons are similar to those observed for the di-protonated complex of **IV**, which together with the position of the ^{195}Pt signal, suggests that the species is *cis*-[Pt(HL-*S*)$_2$Cl$_2$]. The chemical shift difference in the ^{195}Pt signal representing the *cis*-[Pt(HL-*S*)$_2$Cl$_2$] complex of **IV** and **V** is 34 ppm, (**V** is 34 ppm downfield of the corresponding species of **IV**).

The removal of the excess mineral acid from the $CDCl_3$ solution, followed by washing with distilled water, yields a ^{195}Pt NMR spectrum consisting of two signals at -2935 (rel. int. 76 %) and -3181 ppm (24 %). The resonance at -2935 ppm is assigned to the *cis*-[Pt(L-*S,O*)(HL-*S*)Cl] complex and is 17 ppm downfield compared to the analogous protonated species of **IV**. The corresponding ^{1}H NMR spectrum is consistent with one di-protonated complex species *cis*-[Pt(HL-*S*)$_2$Cl$_2$], and one mono-protonated complex species *cis*-[Pt(L-*S,O*)(HL-*S*)Cl] in solution, as confirmed by the presence of the corresponding ^{1}H resonances at 11.08 and 11.21 ppm respectively.

Figure 6.10 Schematic representation of the formation of *cis*-[Pt(L-*S,O*)$_2$] and *trans*-[Pt(L-*S,O*)$_2$] on deprotonation with *conc.* NaOH or NH_3.

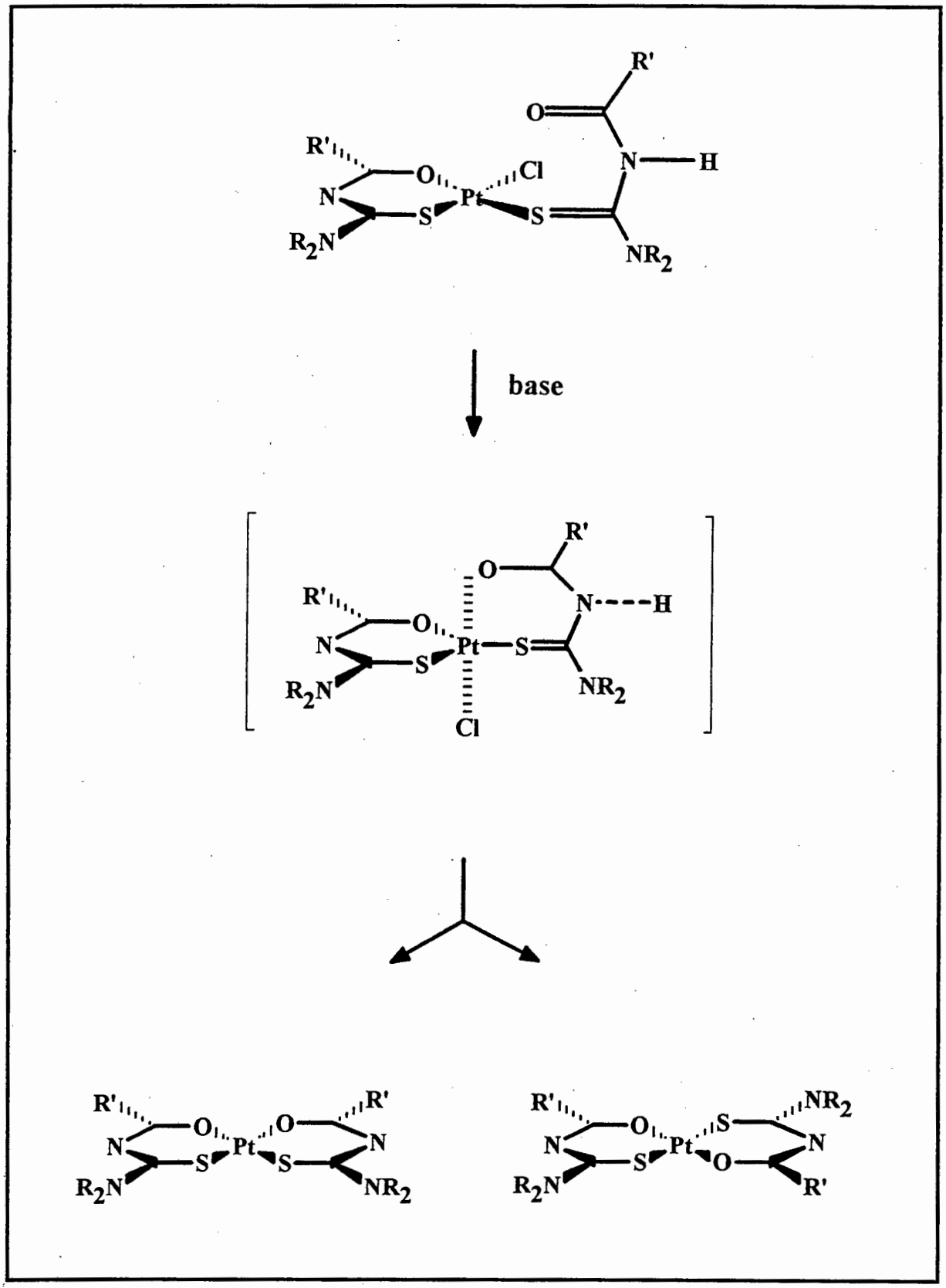

It is significant to note that on addition of 5 M ammonia, only a single resonance at -2700 ppm is observed in the ^{195}Pt spectrum which corresponds to the neutral *cis*-[Pt(L-*S,O*)$_2$] complex. The ^1H NMR spectrum is consistent with the neutral *cis*-[Pt(L-*S,O*)$_2$] complex. However, two minor species (< 5%) are also evident in the ^1H NMR spectrum. The chemical shifts of these minor species correspond with those observed in the experiment with *cis*-bis(*N*-morpholino-*N'*-naphthoylthioureato)platinum(II), i.e. a small amount of *trans*-[Pt(L-*S,O*)$_2$] and unidentified species.

Thus it is noteworthy that protonation of *cis*-bis(*N*-aza-18-crown-6-*N'*-naphthoylthioureato)platinum(II) with *conc.* HCl yields only the *cis*-[Pt(HL-*S*)$_2$Cl$_2$] complex. No evidence of the corresponding *trans* isomer was observed. This is interesting in view of the fact that both the *cis*- and *trans*-[Pt(HL-*S*)$_2$Cl$_2$] complexes were observed on protonation of *cis*-bis(*N*-morpholino-*N'*-naphthoylthioureato)platinum(II) under analogous conditions.

In conclusion, the effects of protonation on *cis*-[Pt(L-*S,O*)$_2$] complexes is summarised below:

- The neutral isomer, *cis*-[Pt(L-*S,O*)$_2$], upon protonation with HCl yields two species, *cis*-[Pt(HL-*S*)$_2$Cl$_2$] and *trans*-[Pt(HL-*S*)$_2$Cl$_2$].

- Addition of water results in a degree of deprotonation, and *cis*-[Pt(L-*S,O*)(HL-*S,*)Cl] is formed in addition to *cis*-[Pt(HL-*S*)$_2$Cl$_2$] and *trans*-[Pt(HL-*S*)$_2$Cl$_2$].

- Further deprotonation with NH_3 yields the deprotonated *cis*-[Pt(L-*S,O*)$_2$] complex. However, when L is *N*-morpholino-*N'*-naphthoylthiourea, the spectra suggest that the time-dependent *trans*-[Pt(L-*S,O*)$_2$] analogue is formed if the solution containing *cis*-[Pt(L-*S,O*)(HL-*S*)Cl] is allowed to stand for 24 hours, followed by deprotonation with NaOH or NH_3.

6.3 Conclusion

Although it has not been possible to establish unambiguously that K^+ is complexed into the aza-crown ether ring of *cis*-bis(*N*-aza-18-crown-6-*N'*-naphthoylthioureato)platinum(II), the elemental analyses and observed proton NMR spectra nevertheless suggest complexation of K^+ with the macrocyclic moiety of *cis*-bis(*N*-aza-18-crown-6-*N'*-naphthoylthioureato)platinum(II). Future research in this area could prove to be most illuminating.

We have gained insight into the X-ray crystal structure of *cis*-bis(*N*-morpholino-*N'*-naphthoylthioureato)-platinum(II). The structure clearly shows the *cis* configuration of ligands about the platinum atom and square-planar *O,S*-bidentate coordination of the ligand to the metal. The naphthyl moieties are not in the square plane of coordination, as reported for the *trans*-bis(*N,N*-dibutyl-*N'*-naphthoylthioureato)platinum(II) complex[5], but angled at 16.85 and 52.85 ° to the coordination plane of platinum. The different conformation of the naphthyl groups in the solid state structure of *cis*-bis(*N*-morpholino-*N'*-naphthoylthioureato)-platinum(II) and *trans*-bis(*N,N*-dibutyl-*N'*-naphthoylthioureato)platinum(II), substantiates the observed differences in the proton chemical shifts of *cis*- and *trans*-[Pt(L-*S,O*)$_2$] isomers in solution[5].

Furthermore, we have shown that protonation of the coordinated *N*-naphthoylthiourea ligand in *cis*-[Pt(L-*S,O*)$_2$] complexes in the presence of coordinating chloride ions, rapidly leads to the reversible ring-opening of the *S,O*-chelate ring, to yield complexes in which either one or both ligands are coordinated through the *S*-atom only, while the *O*-atom of the *N*-naphthoyl moiety is pendent. Moreover, we have been able to establish that deprotonation and subsequent chelate-ring closure of the coordinated *N*-naphthoylthiourea ligand in *cis*-[Pt(L-*S,O*)$_2$] complexes yields, in addition to the *cis* isomer, small amounts of the corresponding *trans* isomer. Such processes clearly have profound synthetic and mechanistic implications in the utilisation of these ligands for the potential solvent extraction[16] and/or chromatographic separations[17] of the platinum group metals. The effects of protonation on *cis*-[Pt(L-*S,O*)$_2$] complexes is diagrammatically summarised in Figure 6.11.

Figure 6.11 Schematic representation of the effects of addition of *conc.* HCl to a solution of *cis*-[Pt(L-*S,O*)$_2$] complex in $CDCl_3$ (L = *N,N*-dialkyl-*N'*-naphthoylthiourea).

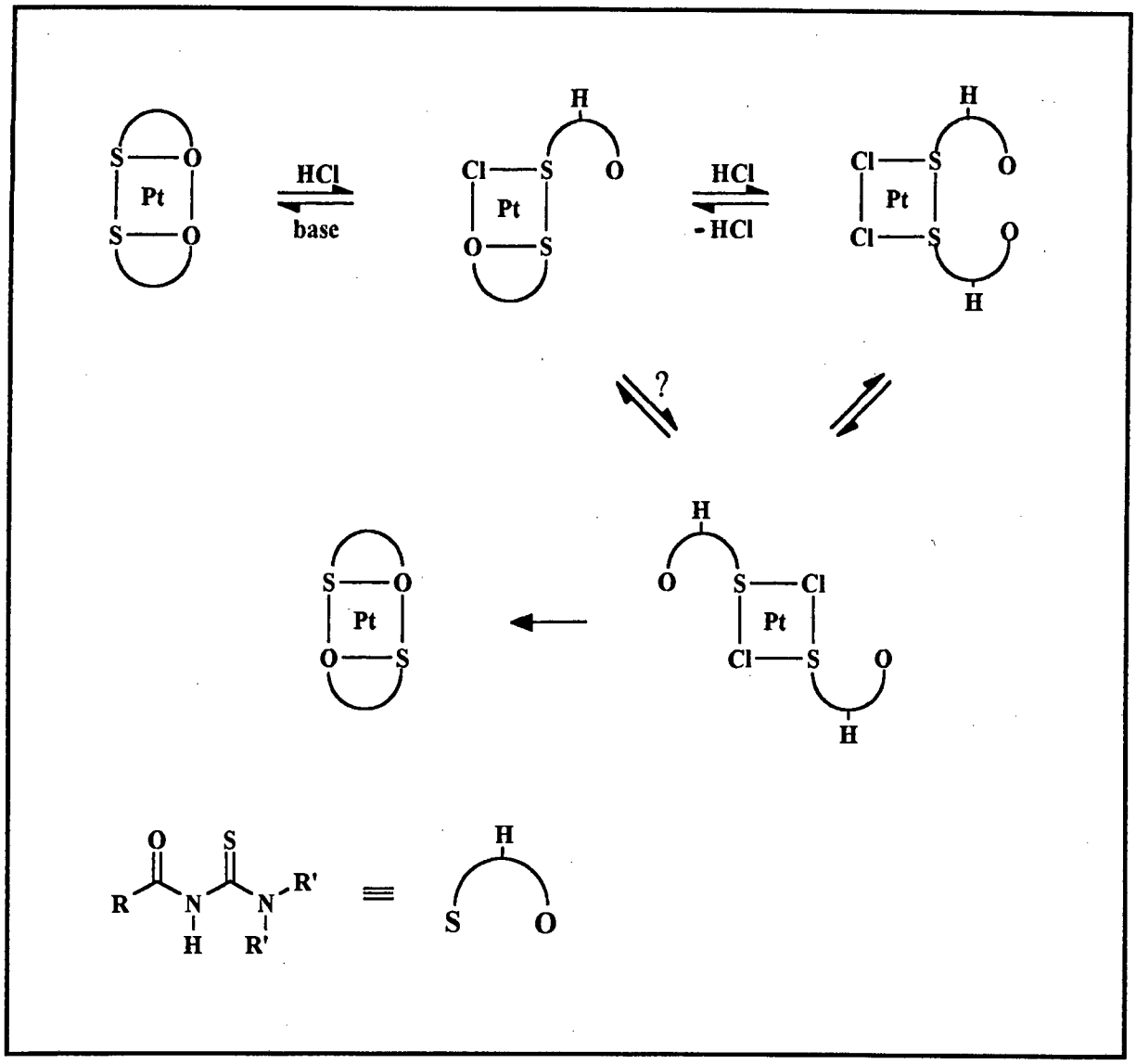

6.4 Experimental

***cis*-bis(*N*-morpholino-*N'*-naphthoylthioureato)platinum(II)** (This is a slight adaptation to the method reported by Koch[5] *et al*). A solution of *N*-morpholino-*N'*-naphthoylthiourea (0.24 mmol) in acetonitrile (40 cm^3) was added dropwise, over 10 - 15 min, to a stirred solution of K_2PtCl_4 (0.12 mmol) in the same solvent (40 cm^3). The solution was stirred for a further 15 min at room temperature. Sodium acetate (0.48 mmol), dissolved in 1 cm^3 water, was added and the reaction mixture stirred at room temperature for an additional 2 hours. The yellow precipitate was collected by filtration and recrystallised from CH_3CN / diethylether to give a bright yellow crystalline solid (**IV**) in 91 % yield. Decomposition, without melting, occurs above 190 °C. Anal. Calcd for $C_{32}H_{30}N_4O_4S_2Pt$: C, 48.40; H, 3.81; N, 7.06. Found : C, 48.05; H, 3.79; N, 7.16. NMR ($CDCl_3$): ^1H, δ 3.73 - 3.81 (4H, b.s, CH_2-O-CH_2), 4.11 (4H, b.s, N-CH_2), 7.17 (1H, t, H(7)), 7.38 (1H, t, H(6)), 7.43 (1H, t, H(3)), 7.82 (1H, d, H(5)), 7.93 (1H, d, H(4)), 8.12 (1H, d, H(2)), 8.84 (1H, d, H(8)); ^{13}C, δ 47.41, 49.81, 66.40, 124.59, 125.74, 126.65, 126.83, 128.20, 128.86, 131.11, 131.64, 134.02, 135.37, 168.14, 172.63.

***trans*-bis(*N*-morpholino-*N'*-naphthoylthioureato)platinum(II)** NMR ($CDCl_3$): ^1H, δ 3.74 (4H, b.s, CH_2-O-CH_2), 3.96 (4H, b.s, N-CH_2), 7.42 (1H, t, H(7)), 7.36 (1H, t, H(6)), 7.32 (1H, t, H(3)), 7.74 (1H, d, H(5)), 7.85 (1H, d, H(4)), 8.28 (1H, d, H(2)), 9.19 (1H, d, H(8)).

***cis*-bis(*N*-aza-18-crown-6-*N'*-naphthoylthioureato)platinum(II)** The general procedure followed that described for **IV**. However, the reaction mixture was stirred at room temperature for 2 days. The crude product was isolated and recrystallised from CH_3CN / diethylether to give a yellow solid (**V**) in 67 % yield. Melting, with decomposition, occurs at 145 - 147 °C. Anal. Calcd for $C_{48}H_{62}N_4O_{12}S_2.Pt.2KCl.4H_2O$: C, 42.15; H, 5.16; N, 4.10. Found : C, 42.20; H, 4.85; N, 4.10. NMR ($CDCl_3$): ^1H δ 3.55 - 3.67 (32H, m, CH_2CH_2-O-CH_2CH_2), 3.73 (4H, t, $NCH_2\underline{CH_2}$), 3.90 (4H, t, $NCH_2\underline{CH_2}$), 4.14 (8H, q, NCH_2), 7.09 (2H, t, H(7)), 7.37 (2H, t, H(6)), 7.42 (2H, t, H(3)), 7.81 (2H, d, H(5)), 7.92 (2H, d, H(4)), 8.12 (2H, d, H(2)), 8.85 (2H, d, H(8)); ^{13}C, δ 52.39, 53.48, 68.52, 69.21, 70.41, 70.49, 70.54, 70.57, 70.64, 70.68, 70.85, 70.91, 124.56, 125.64, 126.81, 127.01, 128.05, 128.72, 131.22, 131.36, 133.97, 135.49, 168.19, 171.86.

Preparation of platinum (II) complexes in acidic media: A solution of the *N*-morpholino-*N'*-naphthoylthiourea ligand (0.4 mmol) in 25 cm^3 acetonitrile - 2 $mol.dm^{-3}$ HCl (4:1 v/v), was added dropwise, over 10 - 15 min, to a stirred, warm (60 °C) solution of K_2PtCl_4 (0.2 mmol) in the same solvent (25 cm^3). The solution was stirred for a further 24 hours at 60 °C during which time the solution turned bright yellow. The solvent was removed under reduced vacuum and a yellow solid was isolated. The ^1H NMR showed the presence of two species. Assignment of the oxyethylene region was complex due to overlapping broad signals. NMR ($CDCl_3$): ^1H, δ **major species**: 7.22 (2H, t, H(7)), 7.35 (4H, b.t, H(3) / H(6)), 7.70 (2H, d, H(4)), 7.77 (2H, d, H(5)), 8.33 (2H, d, H(2)), 8.37 (2H, d, H(8)), 11.32 (2H, s, NH); **minor species**: 7.49 (6H, b.m, H(3) / H(6) / H(7)), 7.84 (2H, b.d, H(4)), 7.97 (2H, d, H(5)), 8.22 (2H, d, H(2)), 8.41 (2H, d, H(8)), 10.97 (2H, s, NH)

^1H and ^{195}Pt NMR Protonation Studies

All ^1H and ^{195}Pt NMR spectra were recorded in 5 mm tubes in $CDCl_3$ solution, using a Varian UNITY-400 spectrometer operating at 400 and 85.8 MHz respectively. The ^1H spectra were recorded at 25 °C. The ^{195}Pt NMR spectra were recorded at 30 °C using 100 kHz spectral widths using 20μs pulses (~ 90 °) with 0.5 s pulse delay, since T_1 of the nucleus was < ca 0.1 s; between 2048 and 16000 pulses gave excellent spectra. All ^{195}Pt shifts are quoted relative to external H_2PtCl_6 (500 mg / ml in 30 % v / v D_2O / 1M HCl) and are estimated to be accurate to ± 2 ppm.

Aliquots of 100 μL concentrated mineral acid (HX ; X = Cl) were added directly to the NMR tube containing 0.6 ml pale yellow solutions containing between 25 and 75 mg of *cis*-bis(*N*-morpholino-*N'*-naphthoylthioureato)platinum(II) **IV** or *cis*-bis(*N*-aza-18-crown-6-*N'*-naphthoylthioureato)platinum(II) **V** in $CDCl_3$. After vigorous shaking the phases were allowed to separate, which was complete after *ca* 5-10 min. Where necessary the distinctly darker yellow/orange organic phase was filtered through microfibre glass wool and a small quantity of EXTRELUT™ (Merck), resulting in a clear solution prior to NMR spectroscopy. After spectral acquisition, the mineral acid was removed, the $CDCl_3$ solution washed with water and ammonia solution, and filtered, followed by re-acquisition of the spectrum.

Protonated complex **IV**, prepared under acidic conditions, was dissolved in $CDCl_3$ to give a clear, yellow solution. After spectral acquisition, the $CDCl_3$ solution was washed with water and ammonia and filtered, followed by re-acquisition of the spectrum. The NMR solution was left for 24 hours at 25 °C, washed with NaOH and filtered, and the NMR spectra re-acquired.

REFERENCES

1 Izatt, R.M.; Lamb, J.D.; Izatt, N.E.; Rossiter, B.E.; Christensen, J.J.; Haymore, B.L.; *J. Am. Chem. Soc.*, 1979, **101**, 6273.

2 Santos, M.A.; Drew, M.G.B.; *J. Chem. Soc., Faraday Trans.*, 1991, 1321.

3 Wipff, G.; Weiner, P.; Kollman, P.; *J. Am. Chem. Soc.*, 1982, **104**, 3249.

4 Koch, K.R.; Irving, A.; Matoetoe, M.; *Inorg. Chim. Acta,* 1993, **206**, 193.

5 Koch, K.R.; du Toit, J.; Cairo, M.R.; Sacht, C.; *J. Chem. Soc., Dalton Trans.*, 1994, 785.

6 de Jong, F.; Reinhoudt, D.N.; Smit, C.J.; *Tetrahedron Lett.*, 1976, 1371.

7 Wong, K.H.; Konizer, G.; Smid, J.; *J. Am. Chem. Soc.*, 1970, **92**, 666.

8 Sheldrick, G.M.; SHELXS-86 in *Crystallographic Computing 3*, (eds.), Sheldrick, G.M.; Kruger, C.; Goddard, R. Oxford university Press, 1985.

9 Sheldrick, G.M.; SHELXL-93. In preparation for *J. Appl. Cryst.*, 1993.

10 Onuma, S.; Horioka, K.; Inoue, H.; Shibata, S.; *Bull. Chem. Soc. Jpn.*, 1980, **53**, 2679.

11 Katoh, M.; Miki, K.; Kai, Y.; Tanaka, N.; Kasai, N.; *Bull. Chem. Soc. Jpn.*, 1981, **54**, 611.

12 Pregosin, P.S.; *Coord. Chem. Rev.*, 1982, **44**, 247.

13 Kerrison, S.J.S.; Sadler, P.J.; *Inorg. Chim. Acta,* 1985, **104**, 197.

14 McFarlane, W.; *J. Chem. Soc., Dalton Trans.*, 1974, 324.

15 Congdon, W.I.; Edward, J.T.; *Can. J. Chem.*, 1974, **52**, 697.

16 Vest, P.; Schuster, M.; König, K.-H.; *Fresenius' Z. Anal. Chem.*, 1989, **335**, 759.

17 Schuster, M.; *Fresenius' Z. Anal. Chem.*, 1992, **342**, 791.

Concluding remarks

The work in this thesis has successfully illustrated the remarkable ease with which the *N*-alkyl- and *N,N*-dialkyl-*N'*-acylthioureas may be modified at either the amine or acyl moieties. Modification of the *N*-alkyl-*N'*-benzoylthiourea has allowed for the synthesis of a variety of liquid-crystalline compounds based on *N*-(*p*-alkyl)aniline-*N'*-(*p*-alkyloxy)benzoylthiourea, *N*-(*p*-alkyloxy)aniline-*N'*-(*p*-alkyl)benzoylthiourea and *N*-(*p*-alkyloxy)aniline-*N'*-(*p*-alkyloxy)benzoylthiourea. The position of the oxygen atom in the molecule has a significant influence on the type of mesophase exhibited by the liquid crystal compounds. The present mesogenic compounds exhibit nematic, smectic A or a combination of these liquid-crystalline phases. The crystal structure of *N*-(*p*-hexyloxy)aniline-*N'*-(*p*-methyloxy)benzoylthiourea has shown that the molecules are rod-shaped with planar aromatic and six-membered chelate rings. Furthermore, *inter*molecular contacts allow for the formation of dimers which results in an overall extension of the molecules. A comparison of the X-ray structures of the mesogenic and non-mesogenic *N*-acylthiourea compounds have shown that the following structural factors are important in determining liquid crystal behaviour in these compounds:

- the *intra*molecular hydrogen bond
- the presence of two benzyl groups
- an alkyloxy chain attached to one of the aromatic rings, preferably the aniline ring.

Complexation of *N,N*-dialkyl-*N'*-acylthiourea compounds with various d^8 metal atoms did not give rise to metal containing liquid crystals, probably as a result of the *cis* configuration of the ligands about the metal atom. Preparation of the corresponding *trans* isomers was unsuccessful. The synthesis of metal containing liquid crystals incorporating the *N*-alkyl-*N'*-benzoylthiourea ligands was also unsuccessful. On the other hand, this study highlighted the remarkable difference in coordination chemistry between the *N*-alkyl- and *N,N*-dialkyl-*N'*-acylthioureas. The *N,N*-dialkyl-*N'*-acylthioureas form stable *cis*-$[ML_2]$ complexes with nickel, copper, platinum and palladium whereas the *N*-alkyl-*N'*-acylthiourea ligands fail to form stable nickel (II) complexes under any conditions, and reduce copper (II) to copper (I) to form stable copper (I) complexes. These results, together with the ^{31}P NMR studies of the reaction between *cis*-$[Pt(PEt_2Ph)_2Cl_2]$ and *N*-alkyl- or *N,N*-dialkyl-*N'*-acylthiourea, illustrate the significant influence the *intra*molecular hydrogen bond has on the coordination chemistry of these types of molecules.

The first macrocyclic *N*-acylthioureas, *N*-aza-18-crown-6-*N'*-naphthoylthiourea and *N,N*-diaza-18-crown-6-*N'*-naphthoylthiourea, have been successfully synthesised and characterised. Unfortunately, the aza- and diaza-crown ether moieties of these compounds exhibit poor binding interactions with K^+ and NH_4^+ / $CH_3NH_3^+$ cations. The X-ray crystal structures of *N*-aza-18-crown-6-*N'*-naphthoylthiourea and *N,N*-diaza-18-crown-6-

N'-naphthoylthiourea have allowed us to predict the factors responsible for the weak cation binding interactions. These include:

- the presence of an *intra*molecular hydrogen bond between the amide hydrogen and the oxygen atom of the macrocyclic ring
- unusual conformation of the oxyethylene ring
- sp^2 hybridisation of the macrocyclic ring nitrogen atom
- macrocyclic moiety folded over the chelate backbone.
- neutral carbonyl donor groups point away from the crown cavity

The analysis of *cis*-bis(*N*-aza-18-crown-6-*N'*-naphthoylthioureato)platinum(II) suggests that KCl is associated with the complex. If K^+ is complexed into the aza-crown ether ring then it confirms the significant influence the *intra*molecular hydrogen bond of the ligand has on the conformation of the macrocyclic ring, and ultimately on the cation affinity of this ring.

Protonation studies of the *cis*-bis(*N,N*-dialkyl-*N'*-acylthioureato)platinum(II) have revealed that protonation of the coordinated *N*-acylthiourea ligand in the presence of coordinating chloride ions, rapidly leads to the reversible ring-opening of the *S,O*-chelate ring. The resulting products include complexes in which either one or both ligands are coordinated through the *S*-atom only, while the *O*-atom of the acyl group is held pendent. Deprotonation of the coordinated *N*-benzoylthiourea ligand and subsequent chelate-ring closure results in the formation of the *cis*-bis(*N,N*-dialkyl-*N'*-benzoylthioureato)platinum(II) complex exclusively. However, deprotonation of the coordinated *N*-naphthoylthiourea ligand results in the formation of the *cis*-bis(*N,N*-dialkyl-*N'*-naphthoylthioureato)platinum(II) complex, in addition to small amounts of the corresponding *trans*-bis(*N,N*-dialkyl-*N'*-naphthoylthioureato)platinum(II) complex.

In conclusion, the present work has illustrated the fascinating and extremely exciting chemistry involved in the study of the deceptively simple *N*-alkyl- and *N,N*-dialkyl-*N'*-acylthioureas. The challenge now lies in finding suitably applicable and economically viable industrial applications for these compounds.

Appendix 1

Table 1.1 A summary of the crystal data, details of data collection and final refinement for *N*-butyl-*N'*-benzoylthiourea.

Crystal data		
Molecular formula		$C_{12}H_{16}N_2OS$
Molecular mass (g mol^{-1})		236.34
Crystal system		monoclinic
Space group		$P2_1/c$
Unit cell dimensions	a (Å)	10.9779(7)
	b (Å)	6.1772(8)
	c (Å)	19.853(2)
	α (°)	90
	β (°)	102.464(8)
	γ (°)	90
V ($Å^3$)		1314.5(23)
Z		4
D_c (g cm^{-3})		1.194
μ (Mo Kα) (cm^{-1})		2.184
F(000)		504
Data collection		
Crystal dimensions (mm)		0.38 x 0.41 x 0.44
Scan mode		ω - 2θ
Scan width (°)		(0.85 + 0.35 tan θ)
Aperture width (mm)		(1.12 + 1.05 tan θ)
θ range scanned (°)		1 - 25
Range *h, k, l*		13, 7, ±23
Total time for data collections (hrs)		17.2
Intensity decay (%)		2.3
Empirical absorption correction, min / max / av, (%)		97.04, 99.96, 98.58
Number of unique reflections collected		2690
Number of observed reflections with I > 2σI		1593
Final refinement		
Number of parameters		134
Max LS shift to e.s.d.		0.112
Residual electron density (e $Å^{-3}$), max / min		0.44, -0.24
R1		0.0896
wR2		0.1233

Table 1.2 Fractional Atomic Coordinates (x 10^4) and thermal parameters ($Å^2$ x 10^3) of the non-hydrogen atoms, except H(10), of *N*-butyl-*N'*-benzoylthiourea with estimated standard deviations (e.s.d's) in parentheses.

Atom	*x/a*	*y/b*	*z/c*	U_{eq}*
C(1)	7021(5)	-3005(8)	3903(3)	61(2)
C(2)	7239(6)	-2873(12)	3248(3)	81(2)
C(3)	6742(7)	-4447(16)	2772(4)	105(3)
C(4)	6055(8)	-6111(14)	2935(5)	102(3)
C(5)	5878(6)	-6239(11)	3583(5)	96(3)
C(6)	6335(5)	-4706(9)	4078(3)	72(2)
C(7)	7629(4)	-1370(7)	4425(2)	57(2)
O(7)	8706(3)	-776(7)	4459(2)	79(2)
N(8)	6907(3)	-614(7)	4856(2)	59(2)
C(9)	7246(4)	835(8)	5396(2)	59(2)
S(9)	6172(1)	1602(3)	5833(1)	79(1)
N(10)	8416(4)	1491(7)	5543(2)	67(2)
H(10)	8971(46)	921(81)	5256(24)	66(14)
C(11)	8964(5)	2916(9)	6125(3)	69(2)
C(12)	9125(10)	5062(16)	5871(5)	126(3)
C(13)	9912(13)	6710(21)	6486(7)	158(4)
C(14)	8997(12)	7021(21)	6799(7)	151(4)

U_{eq} is defined as one third of the trace of the orthogonalised U_{ij} tensor*

Table 1.3 Selected torsion angles of *N*-butyl-*N'*-benzoylthiourea.

C(1) - C(7) - N(8) - C(9)	177.5(4)	C(2) - C(1) - C(6) - C(5)	-0.3(9)
O(7) - C(7) -N(8) - C(9)	-2.1(7)	C(6) - C(1) - C(2) - C(3)	1.1(10)
C(7) - N(8) - C(9) - S(9)	177.4(4)	C(7) - C(1) - C(2) - C(3)	176.3(6)
C(7) - N(8) - C(9) - N(10)	-3.8(7)	C(1) - C(2) - C(3) - C(4)	-0.3(12)
N(8) - C(9) - N(10) - C(11)	-176.0(4)	C(2) - C(3) - C(4) - C(5)	-1.3(13)
S(9) - C(9) - N(10) - C(11)	2.7(7)	C(3) - C(4) - C(5) - C(6)	2.2(13)
		C(4) - C(5) - C(6) - C(1)	-1.4(11)

Appendix 2

Table 2.1 A summary of the crystal data, details of data collection and final refinement for *N*-(*p*-hexyloxy)aniline-*N'*-(*p*-methyloxy)benzoylthiourea.

Crystal data		
Molecular formula		$C_{21}H_{26}N_2O_3S$
Molecular mass (g mol^{-1})		386.50
Crystal system		triclinic
Space group		$P\bar{1}$
Unit cell dimensions	a (Å)	9.203(2)
	b (Å)	11.0580(1)
	c (Å)	11.356(2)
	α (°)	72.890(10)
	β (°)	87.700(10)
	γ (°)	66.930(10)
V ($Å^3$)		1012.5(3)
Z		2
D_c ($mg.m^{-3}$)		1.268
μ (Mo Kα) (cm^{-1})		0.183
F(000)		412
Data collection		
Crystal dimensions (mm)		0.38 x 0.36 x 0.25
Scan mode		ω - 2θ
Scan width (°)		(0.85 + 0.35 tan θ)
Aperture width (mm)		(1.12 + 1.05 tan θ)
θ range scanned (°)		1.88 - 24.99
Range *h, k, l*		$-10 \le h \le 10$, $-12 \le k \le 13$, $0 \le l \le 13$
Total time for data collections (hrs)		26.2
Intensity decay (%)		< 1
Number of unique reflections collected		3750
Number of observed reflections with $I > 2\sigma I$		3554
Final refinement		
Number of parameters		259
Max LS shift to e.s.d.		0.001
Residual electron density (e $Å^{-3}$), min / max		-0.281, 0.281
R1		0.0510
wR2		0.1408

Table 2.2 Fractional Atomic Coordinates (x 10^4) and thermal parameters ($Å^2$ x 10^3) of the non-hydrogen atoms of *N*-(*p*-hexyloxy)aniline-*N'*-(*p*-methyloxy)benzoylthiourea.

Atom	*x/a*	*y/b*	*z/c*	U_{eq}^*
C(1)	226(2)	7800(2)	-2190(2)	43(1)
C(2)	1544(3)	9169(2)	-3610(2)	54(1)
C(3)	2190(3)	9692(3)	-4653(2)	58(1)
C(4)	3549(3)	8825(2)	-5019(2)	50(1)
O(4)	4295(2)	9225(2)	-6019(2)	69(1)
C(41)	3630(4)	10646(3)	-6748(3)	80(1)
C(5)	4231(3)	7449(2)	-4343(2)	49(1)
C(6)	3577(3)	6938(2)	-3305(2)	44(1)
C(7)	1490(3)	7331(2)	-1783(2)	44(1)
O(7)	119(2)	7983(2)	-1599(2)	59(1)
N(8)	2446(2)	6128(2)	-934(2)	47(1)
C(9)	2138(3)	5400(2)	200(2)	43(1)
S(9)	3614(1)	3937(1)	963(1)	65(1)
N(10)	685(2)	5975(2)	539(2)	45(1)
C(11)	1(3)	5576(2)	1652(2)	43(1)
C(12)	-1508(3)	6485(3)	1767(2)	54(1)
C(13)	-2266(3)	6212(3)	2822(2)	56(1)
C(14)	-1543(3)	5018(2)	3786(2)	45(1)
C(15)	-40(3)	4112(2)	3678(2)	55(1)
C(16)	715(3)	4394(2)	2619(2)	56(1)
O(17)	-2378(2)	4820(2)	4794(1)	53(1)
C(18)	-1668(3)	3539(2)	5764(2)	50(10
C(19)	-2792(3)	3474(3)	6754(2)	53(1)
C(20)	-2105(3)	2107(3)	7767(2)	59(1)
C(21)	-3146(3)	1925(3)	8802(2)	59(1)
C(22)	-2405(4)	597(3)	9849(3)	83(1)
C(23)	-3435(4)	437(3)	10884(3)	84(1)

Table 2.3 Bond distances (Å) and Bond angles (°) of *N*-(*p*-hexyloxy)aniline-*N'*-(*p*-methyloxy)benzoyl-thiourea, with estimated standard deviation in parenthesis

Bond distance	**(Å)**	**Bond angle**	**(°)**
C(1) - C(2)	1.380	C(2) - C(1) - C(6)	118.0(2)
C(1) - C(6)	1.391(3)	C(2) - C(1) - C(7)	118.5(2)
C(1) - C(7)	1.477(3)	C(6) - C(1) - C(7)	123.6(2)
C(2) - C(3)	1.378(3)	C(3) - C(2) - C(1)	121.8(2)
C(3) - C(4)	1.381(4)	C(2) - C(3) - C(4)	119.4(2)
C(4) - O(5)	1.356(3)	O(4) - C(4) - C(5)	115.8(2)
C(4) - C(5)	1.379(3)	O(4) - C(4) - C(3)	124.6(2)
O(4) - C(41)	1.432(3)	C(5) - C(4) - C(3)	119.6(2)
C(5) - C(6)	1.374(3)	C(4) - O(4) - C(41)	117.7(2)
C(7) - O(7)	1.229(3)	C(6) - C(5) - C(4)	120.5(2)
C(7) - N(8)	1.367(3)	C(5) - C(6) - C(1)	120.7(2)
N(8) - C(9)	1.389(3)	O(7) - C(7) - N(8)	121.6(2)
C(9) - N(10)	1.332(3)	O(7) - C(7) - C(1)	122.8(2)
C(9) - S(9)	1.661(2)	N(8) - C(7) - C(1)	115.6(2)
N(10) - C(11)	1.419(3)	C(7) - N(8) - C(9)	130.6(2)
C(11) - C(16)	1.373(3)	N(10) - C(9) - N(8)	115.3(2)
C(11) - C(12)	1.388(3)	N(10) - C(9) - S(9)	128.3(2)
C(12) - C(13)	1.377(3)	N(8) - C(9) - S(9)	116.4(2)
C(13) - C(14)	1.380(3)	C(9) - N(10) - C(11)	130.6(2)
C(14) - O(17)	1.364(3)	C(16) - C(11) - C(12)	118.0(2)
C(14) - C(15)	1.380(3)	C(16) - C(11) - N(10)	125.7(2)
C(15) - C(16)	1.382(3)	C(12) - C(11) - N(10)	116.3(2)
O(17) - C(18)	1.436(3)	C(13) - C(12) - C(11)	120.9(2)
C(18) - C(19)	1.502(3)	C(12) - C(13) - C(14)	120.6(2)
C(19) - C(20)	1.515(3)	O(17) - C(14) - C(15)	124.4(2)
C(20) - C(21)	1.504(3)	O(17) - C(14) - C(13)	116.9(2)
C(21) - C(22)	1.512(4)	C(15) - C(14) - C(13)	118.7(2)
C(22) - C(23)	1.493(4)	C(14) - C(15) - C(16)	120.4(2)
		C(11) - C(16) - C(15)	121.3(2)
		C(14) - O(17) - C(18)	116.9(2)
		O(17) - C(18) - C(19)	109.3(2)
		C(18) - C(19) - C(20)	110.6(2)
		C(21) - C(20) - C(19)	115.0(2)
		C(2) - C(21) - C(22)	114.6(2)
		C(23) - C(22) - C(21)	114.3(3)

Appendix 3

Table 3.1 A summary of the crystal data, details of data collection and final refinement for *N*-aza-18-crown-6-*N'*-naphthoylthiourea (**2**) and *N,N*-diaza-18-crown-6-*N'*-naphthoylthiourea (**3**).

Crystal data			
		2	**3**
Molecular formula		$C_{24}H_{34}N_2O_7S$	$C_{36}H_{40}N_4O_6S_2$
Molecular mass (g mol^{-1})		494.59	688.87
Crystal system		monoclinic	triclinic
Space group		$P2_1$	$P\bar{1}$
Unit cell dimensions	a (Å)	10.720(10)	9.387(4)
	b (Å)	7.509(3)	9.832(6)
	c (Å)	15.974(6)	10.339(1)
	α (°)	90	64.89(2)
	β (°)	108.09(8)	78.29(2)
	γ (°)	90	76.16(4)
V ($Å^3$)		1222.3(13)	833(11)
Z		2	1
D_c (g cm^{-3})		1.344	2.75
μ (Mo Kα) (mm^{-1})		0.179	4.056
F(000)		528	728
Data collection			
Crystal dimensions (mm)		0.31 x 0.31 x 0.28	0.35 x 0.40 x 0.40
Scan mode		ω - 2θ	ω - 2θ
Scan width (°)		(0.85 + 0.35 tan θ)	(0.85 + 0.35 tan θ)
Aperture width (mm)		(1.12 + 1.05 tan θ)	(1.12 + 1.05 tan θ)
θ range scanned (°)		1.34 - 24.97	1 - 25
Range *h, k, l*		±12, 0≤*k*≤8, 0≤*l*≤18,	±11, ± 11, 12
Total time for data collections (hrs)		18.1	23.6
Intensity decay (%)		22.4	3.7
Empirical absorption correction, min / max / av, (%)		N/A	97.02 / 99.94 / 98.50
Number of unique reflections collected		2319	3104
Number of observed reflections with I > 2σI		1953	2144
Final refinement			
Number of parameters		313	222
Max LS shift to e.s.d.		0.058	0.1
Residual electron density (e $Å^{-3}$), min / max		-0.244 / 0.390	-0.23 / 0.25
R1		0.0378	0.041
wR2		0.1025	0.046

Table 3.2 Fractional Atomic Coordinates (x 10^4) and equivalent isotropic displacement parameters ($Å^2$ x 10^3) for *N*-aza-18-crown-6-*N'*-naphthoylthiourea.

Atom	*x/a*	*y/b*	*z/c*	U_{eq}*
C(1)	6472(3)	2767(4)	2360(2)	33(1)
C(2)	6763(3)	2456(6)	1603(2)	40(1)
C(3)	8040(4)	2033(6)	1608(2)	47(1)
C(4)	9030(4)	1917(5)	2389(3)	46(1)
C(5)	8784(3)	2275(6)	3194(2)	38(1)
C(6)	9794(4)	2192(7)	4008(3)	54(1)
C(7)	9551(4)	2580(8)	4772(3)	65(1)
C(8)	8296(4)	3084(8)	4761(2)	59(1)
C(9)	7284(4)	3130(6)	4005(2)	43(1)
C(10)	7489(3)	2706(4)	3185(2)	35(1)
C(11)	5064(3)	2964(5)	2319(2)	36(1)
O(11)	4602(2)	2152(5)	2808(2)	51(1)
N(12)	4346(3)	4085(4)	1669(2)	38(1)
C(13)	2981(3)	4171(5)	1327(2)	36(1)
S(13)	2075(1)	2324(1)	1101(1)	50(1)
N(14)	2508(3)	5817(4)	1161(2)	35(1)
C(15)	1120(3)	6111(6)	656(2)	43(1)
C(16)	213(3)	5950(7)	1205(2)	47(1)
O(17)	528(2)	7294(4)	1864(2)	47(1)
C(18)	448(4)	6719(6)	2695(3)	50(1)
C(19)	1583(4)	5637(6)	3209(3)	49(1)
O(20)	2738(2)	6689(4)	3451(2)	44(1)
C(21)	3800(3)	5830(6)	4075(2)	46(1)
C(22)	4984(3)	6983(6)	4290(2)	46(1)
O(23)	5525(2)	6932(4)	3592(1)	41(1)
C(24)	6547(4)	8204(6)	3703(2)	46(1)
C(25)	7286(3)	7797(5)	3073(2)	44(1)
O(26)	6453(2)	8102(4)	2202(2)	46(1)
C(27)	6973(3)	7478(6)	1544(2)	44(1)
C(28)	5986(3)	7805(6)	669(2)	45(1)
O(29)	4741(2)	7050(3)	616(2)	40(1)
C(30)	3855(3)	8268(5)	839(2)	39(1)
C(31)	3275(3)	7420(5)	1492(2)	37(1)
O(32)	2552(4)	635(6)	3443(2)	74(1)

* *U_{eq} is defined as one third of the trace of the orthogonalised U_{ij} tensor*

Table 3.3 Fractional Atomic Coordinates (x 10^4) and equivalent isotropic displacement parameters ($Å^2$ x 10^3) for *N,N*-diaza-18-crown-6-*N'*-naphthoylthiourea.

Atom	*x/a*	*y/b*	*z/c*	U_{eq}*
C(1)	528(2)	6503(3)	2431(2)	34(1)
C(2)	504(3)	6620(3)	3711(3)	41(1)
C(3)	-496(3)	7753(3)	4068(3)	50(1)
C(4)	-1403(3)	8808(3)	3107(3)	48(1)
C(5)	-1380(3)	8782(3)	1747(3)	38(1)
C(6)	-2274(3)	9923(3)	714(3)	48(1)
C(7)	-2292(3)	9858(3)	-569(3)	52(1)
C(8)	-1433(3)	8634(3)	-870(3)	47(1)
C(9)	-548(2)	7519(3)	83(3)	39(1)
C(10)	-458(2)	7577(3)	1412(2)	33(1)
C(11)	1566(2)	5238(3)	2125(2)	36(1)
O(11)	1244(2)	4494(2)	1584(2)	54(1)
N(12)	2973(2)	5046(2)	2468(2)	36(1)
C(13)	4145(2)	3865(3)	2456(2)	33(1)
S(13)	3896(1)	2070(1)	3064(1)	48(0)
N(14)	5457(2)	4340(2)	1945(2)	34(1)
C(15)	6830(3)	3225(3)	2062(3)	43(1)
C(16)	7880(3)	3349(3)	2931(3)	45(1)
O(17)	7169(2)	3412(2)	4259(2)	46(1)
C(18)	6803(3)	2005(3)	5317(3)	49(1)
C(19)	5396(3)	2284(3)	6208(3)	49(1)
O(20)	5581(2)	3028(2)	7068(2)	38(1)
C(21)	4238(3)	3228(3)	7957(3)	44(1)
C(22)	4412(3)	4052(3)	8849(3)	41(1)

* *U_{eq} is defined as one third of the trace of the orthogonalised U_{ij} tensor*

Table 3.4 Bond distances (Å) and bond angles (°) for *N*-aza-18-crown-6-*N'*-naphthoylthiourea with estimated standard deviations in parentheses.

Bond lengths		**Bond angles**	
C(1) - C(2)	1.359(5)	C(2) - C(1) - C(10)	119.7(3)
C(1) - C(10)	1.426(5)	C(2) - C(1) - C(11)	119.0(3)
C(1) - C(11)	1.497(5)	C(10) - C(1) - C(11)	121.0(3)
C(2) - C(3)	1.403(5)	C(1) - C(2) - C(3)	121.8(3)
C(3) - C(4)	1.366(6)	C(4) - C(3) - C(2)	120.0(3)
C(4) - C(5)	1.416(5)	C(3) - C(4) - C(5)	120.4(3)
C(5) - C(6)	1.412(5)	C(6) - C(5) - C(4)	121.5(3)
C(5) - C(10)	1.420(5)	C(6) - C(5) - C(10)	119.2(4)
C(6) - C(7)	1.356(6)	C(4) - C(5) - C(10)	119.4(3)
C(7) - C(8)	1.393(7)	C(7) - C(6) - C(5)	120.8(4)
C(8) - C(9)	1.350(5)	C(6) - C(7) - C(8)	120.1(4)
C(9) - C(10)	1.431(5)	C(9) - C(8) - C(7)	121.6(4)
C(11) - O(11)	1.212(4)	C(8) - C(9) - C(10)	120.2(4)
C(11) - N(12)	1.372(4)	C(5) - C(10) - C(1)	118.8(3)
N(12) - C(13)	1.396(5)	C(5) - C(10) - C(9)	118.0(3)
C(13) - N(14)	1.331(5)	C(1) - C(10) - C(9)	123.2(3)
C(13) - S(13)	1.667(4)	O(11) - C(11) - N(12)	123.4(3)
N(14) - C(31)	1.461(5)	O(11) - C(11) - C(1)	122.0(3)
N(14) - C(15)	1.473(4)	N(12) - C(11) - C(1)	114.6(3)
C(15) - C(16)	1.503(5)	C(11) - N(12) - C(13)	126.8(3)
C(16) - O(17)	1.420(5)	N(14) - C(13) - N(12)	114.2(3)
O(17) - C(18)	1.424(5)	N(14) - C(13) - S(13)	124.7(3)
C(18) - C(19)	1.481(6)	N(12) - C(13) - S(13)	121.0(3)
C(19) - O(20)	1.418(5)	C(13) - N(14) - C(31)	123.8(3)
O(20) - C(21)	1.415(5)	C(13) - N(14) - C(15)	120.4(3)
C(21) - C(22)	1.486(6)	C(31) - N(14) - C(15)	115.7(3)
C(22) - O(23)	1.409(4)	N(14) - C(15) - C(16)	113.3(3)
O(23) - C(24)	1.422(5)	O(17) - C(16) - C(15)	109.1(3)
C(24) - C(25)	1.493(5)	C(16) - O(17) - C(18)	113.9(3)
C(25) - O(26)	1.420(5)	O(17) - C(18) - C(19)	114.0(3)
O(26) - C(27)	1.414(5)	O(20) - C(19) - C(18)	110.1(4)
C(27) - C(28)	1.488(5)	C(21) - O(20) - C(19)	112.5(3)
C(28) - O(29)	1.428(4)	O(20) - C(21) - C(22)	109.9(3)
O(29) - C(30)	1.441(4)	O(23) - C(22) - C(21)	109.5(3)
C(30) - C(31)	1.511(5)	C(22) - O(23) - C(24)	111.9(3)
		O(23) - C(24) - C(25)	109.1(3)
		O(26) - C(25) - C(24)	108.9(3)
		C(27) - O(26) - C(25)	113.7(3)
		O(26) - C(27) - C(28)	108.3(3)
		O(29) - C(28) - C(27)	111.7(3)
		C(28) - O(29) - C(30)	114.1(3)
		O(29) - C(30) - C(31)	110.4(3)
		N(14) - C(31) - C(30)	113.8(3)

Table 3.5 Bond distances (Å) and bond angles (°) for *N,N*-diaza-18-crown-6-*N'*-naphthoylthiourea with estimated standard deviations in parentheses

Bond lengths		**Bond angles**	
C(1) - C(2)	1.372(4)	C(2) - C(1) - C(10)	119.99(19)
C(1) - C(10)	1.437(3)	C(2) - C(1) - C(11)	119.29(22)
C(1) - C(11)	1.491(4)	C(10) - C(1) - C(11)	120.72(19)
C(2) - C(3)	1.402(4)	C(1) - C(2) - C(3)	121.18(28)
C(3) - C(4)	1.354(4)	C(4) - C(3) - C(2)	119.89(29)
C(4) - C(5)	1.412(5)	C(3) - C(4) - C(5)	121.27(32)
C(5) - C(6)	1.415(4)	C(6) - C(5) - C(4)	121.50(30)
C(5) - C(10)	1.418(4)	C(6) - C(5) - C(10)	118.94(26)
C(6) - C(7)	1.359(5)	C(4) - C(5) - C(10)	119.56(27)
C(7) - C(8)	1.395(4)	C(7) - C(6) - C(5)	121.21(32)
C(8) - C(9)	1.357(3)	C(6) - C(7) - C(8)	119.68(29)
C(9) - C(10)	1.419(4)	C(9) - C(8) - C(7)	121.24(29)
C(11) - O(11)	1.210(4)	C(8) - C(9) - C(10)	120.71(30)
C(11) - N(12)	1.385(3)	C(5) - C(10) - C(1)	117.82(21)
N(12) - C(13)	1.398(3)	C(5) - C(10) - C(9)	118.10(28)
C(13) - N(14)	1.348(3)	C(1) - C(10) - C(9)	124.07(28)
C(13) - S(13)	1.662(3)	O(11) - C(11) - N(12)	123.02(30)
N(14) - C(15)	1.467(3)	O(11) - C(11) - C(1)	124.21(29)
C(15) - C(16)	1.519(5)	N(12) - C(11) - C(1)	112.71(26)
C(16) - O(17)	1.419(4)	C(11) - N(12) - C(13)	126.58(27)
O(17) - C(18)	1.421(3)	N(14) - C(13) - N(12)	113.03(28)
C(18) - C(19)	1.489(4)	N(14) - C(13) - S(13)	125.11(27)
C(19) - O(20)	1.425(5)	N(12) - C(13) - S(13)	121.84(23)
O(20) - C(21)	1.427(3)	C(13) - N(14) - C(15)	120.19(26)
C(21) - C(22)	1.514(5)	N(14) - C(15) - C(16)	113.04(28)
C(22) - N(14)	1.476(2)	O(17) - C(16) - C(15)	112.55(29)
		C(16) - O(17) - C(18)	114.62(25)
		O(17) - C(18) - C(19)	110.07(27)
		O(20) - C(19) - C(18)	110.84(29)
		C(21) - O(20) - C(19)	109.91(27)
		O(20) - C(21) - C(22)	110.33(28)

Appendix 4

Table 4.1 A summary of the crystal data, details of data collection and final refinement for *cis*-bis(*N*-morpholino-*N'*-naphthoylthioureato)platinum(II).

Crystal data		
Molecular formula		$C_{32}H_{30}N_4O_4S_2Pt$
Molecular mass (g mol^{-1})		793.81
Crystal system		monoclinic
Space group		$P2_1/a$
Unit cell dimensions	a (Å)	9.146(2)
	b (Å)	23.761(6)
	c (Å)	13.770(4)
	α (°)	90
	β (°)	98.63(2)
	γ (°)	90
V ($Å^3$)		2958.6(13)
Z		4
D_c (g cm^{-3})		1.782
μ (Mo Kα) (mm^{-1})		4.929
F(000)		1568
Data collection		
Crystal dimensions (mm)		0.13 x 0.13 x 0.16
Scan mode		ω - 2θ
Scan width (°)		(0.80 + 0.35 tan θ)
Aperture width (mm)		(1.12 + 1.05 tan θ)
θ range scanned (°)		1.50 - 24.97
Range *h, k, l*		$0 \le h \le 10$, $0 \le k \le 28$, $-16 \le l \le 16$,
Total time for data collections (hrs)		45.6
Intensity decay (%)		+1.4
Empirical absorption correction, min / max / av, (%)		0.7720 / 0.9988 / 0.8977
Number of unique reflections collected		5200
Number of observed reflections with I > 2σI		3194
Final refinement		
Number of parameters		277
Residual electron density (e $Å^{-3}$), min / max		-1.151 / 2.025
R1		0.0486
wR2*		0.1090

* *in region of platinum atom*

Table 4.2 Fractional Atomic Coordinates (x 10^4) and equivalent isotropic displacement parameters ($Å^2$ x 10^3) for *cis*-bis(*N*-morpholino-*N'*-naphthoylthioureato)platinum(II).

Atom	*x/a*	*y/b*	*z/c*	U_{eq}*
Pt(1)	1957(1)	3531(1)	8662(1)	33(1)
S(1A)	3412(3)	3069(1)	9835(2)	47(1)
O(5A)	2444(7)	4294(2)	9257(5)	37(2)
N(3A)	3880(9)	4101(3)	10766(5)	33(2)
C(2A)	4159(11)	3550(5)	10709(7)	40(2)
C(4A)	3103(11)	4429(4)	10090(7)	34(2)
N(6A)	5136(11)	3353(3)	11447(6)	52(3)
C(7A)	5976(15)	3705(5)	12194(8)	58(4)
C(8A)	5991(15)	3457(5)	13165(9)	60(3)
O(9A)	6544(11)	2891(3)	13224(6)	75(3)
C(10A)	5691(19)	2559(5)	12524(10)	88(5)
C(11A)	5643(17)	2773(5)	11519(9)	77(5)
C(12A)	3095(11)	5042(4)	10363(7)	33(2)
C(13A)	4211(11)	5228(4)	11059(7)	35(2)
C(14A)	4335(13)	5801(4)	11331(8)	47(3)
C(15A)	3322(12)	6177(5)	10911(8)	48(3)
C(16A)	2133(11)	6010(4)	10199(8)	42(3)
C(17A)	1071(13)	6404(5)	9782(9)	56(3)
C(18A)	-60(14)	6252(5)	9101(9)	55(3)
C(19A)	-184(13)	5696(5)	8785(8)	49(3)
C(20A)	795(11)	5293(4)	9161(7)	38(2)
C(21A)	2004(11)	5437(4)	9886(7)	33(2)
S(1B)	1407(4)	2713(1)	7917(2)	62(1)
O(5B)	651(8)	3989(3)	7658(5)	42(2)
C(2B)	322(11)	2846(4)	6822(7)	38(2)
C(4B)	-194(10)	3829(4)	6890(7)	29(2)
N(3B)	-331(10)	3325(3)	6485(6)	40(2)
N(6B)	41(10)	2406(3)	6202(6)	46(2)
C(7B)	-765(14)	2445(5)	5216(9)	60(4)
C(8B)	-1800(16)	1978(5)	5002(12)	83(5)
C(9B)	-1114(9)	1454(3)	5141(6)	65(2)
C(10B)	-372(16)	1415(5)	6130(11)	79(4)
C(11B)	688(15)	1838(4)	6403(9)	67(4)
C(12B)	-1210(10)	4274(4)	6412(7)	27(2)
C(13B)	-1954(11)	4586(4)	6996(7)	35(2)
C(14B)	-2956(12)	5007(4)	6619(8)	44(3)
C(15B)	-3132(12)	5114(5)	5654(8)	46(3)
C(16B)	-2368(11)	4836(4)	5000(7)	35(2)
C(17B)	-2453(13)	4967(5)	3992(8)	51(3)
C(18B)	-1623(12)	4717(5)	3410(9)	50(3)
C(19B)	-650(13)	4293(5)	3762(9)	54(3)
C(20B)	-518(11)	4133(4)	4729(7)	33(2)
C(21B)	-1362(10)	4391(4)	5381(7)	30(2)

* *U_{eq} is defined as one third of the trace of the orthogonalised U_{ij} tensor*

Table 4.3 Bond distances (Å) and bond angles (°) for *cis*-bis(*N*-morpholino-*N'*-naphthoylthioureato)-platinum(II) with estimated standard deviations in parentheses.

Bond distance (Å)		**Bond angle (°)**	
Pt(1) - O(5B)	2.007(6)	O(5B) - Pt(1) - O(5A)	82.2(2)
Pt(1) - O(5A)	2.012(6)	O(5B) - Pt(1) - S(1B)	94.9(2)
Pt(1) - S(1B)	2.220(3)	O(5A) - Pt(1) - S(1B)	176.5(2)
Pt(1) - S(1A)	2.222(3)	O(5B) - Pt(1) - S(1A)	176.5(2)
S(1A) - C(2A)	1.724(11)	O(5A) - Pt(1) - S(1A)	94.5(2)
O(5A) - C(4A)	1.254(11)	S(1B) - Pt(1) - S(1A)	88.45(9)
N(3A) - C(4A)	1.334(12)	C(2A) - S(1A) - Pt(1)	108.1(4)
N(3A) - C(2A)	1.339(12)	C(4A) - O(5A) - Pt(1)	130.5(6)
C(2A) - N(6A)	1.334(13)	C(4A) - N(3A) - C(2A)	128.1(8)
C(4A) - C(12A)	1.504(12)	N(6A) - C(2A) - N(3A)	114.3(9)
N(6A) - C(11A)	1.452(13)	N(6A) - C(2A) - S(1A)	116.7(8)
N(6A) - C(7A)	1.454(13)	N(3A) - C(2A) - S(1A)	129.0(8)
C(7A) - C(8A)	1.46(2)	O(5A) - C(4A) - N(3A)	128.4(8)
C(8A) - O(9A)	1.435(13)	O(5A) - C(4A) - C(12A)	117.1(9)
O(9A) - C(10A)	1.390(14)	N(3A) - C(4A) - C(12A)	114.4(9)
C(10A) - C(11A)	1.47(2)	C(2A) - N(6A) - C(11A)	123.8(9)
C(12A) - C(13A)	1.365(13)	C(2A) - N(6A) - C(7A)	124.0(9)
C(12A) - C(21A)	1.453(13)	C(11A) - N(6A) - C(7A)	111.6(9)
C(13A) - C(14A)	1412(14)	N(6A) - C(7A) - C(8A)	110.2(10)
C(14A) - C(15A)	1.35(2)	O(9A) - C(8A) - C(7A)	112.7(10)
C(15A) - C(16A)	1.406(14)	C(10A) - O(9A) - C(8A)	109.5(9)
C(16A) - C(17A)	1.41(2)	O(9A) - C(10A) - C(11A)	113.1(11)
C(16A) - C(21A)	1.429(13)	N(6A) - C(11A) - C(10A)	110.9(11)
C(17A) - C(18A)	1.34(2)	C(13A) - C(12A) - C(21A)	119.9(9)
C(18A) - C(19A)	1.39(2)	C(13A) - C(12A) - C(4A)	117.3(9)
C(19A) - C(20A)	1.359(14)	C(21A) - C(12A) - C(4A)	122.8(9)
C(20A) - C(21A)	1.416(13)	C(12A) - C(13A) - C(14A)	121.4(10)
S(1B) - C(2B)	1.705(11)	C(15A) - C(14A) - C(13A)	120.0(11)
O(5B) - C(4B)	1.270(11)	C(14A) - C(15A) - C(16A)	121.4(11)
C(2B) - N(3B)	1.338(12)	C(15A) - C(16A) - C(17A)	120.8(10)
C(2B) - N(6B)	1.349(12)	C(15A) - C(16A) - C(21A)	119.9(10)
C(4B) - N(3B)	1.319(11)	C(17A) - C(16A) - C(21A)	119.3(10)
C(4B) - C(12B)	1.493(12)	C(18A) - C(17A) - C(16A)	121.3(12)
N(6B) - C(7B)	1.447(13)	C(17A) - C(18A) - C(19A)	119.7(12)
N(6B) - C(11B)	1.483(12)	C(20A) - C(19A) - C(18A)	122.2(12)
C(7B) - C(8B)	1.46(2)	C(19A) - C(20A) - C(21A)	119.8(10)
C(8B) - O(9B)	1.395(13)	C(20A) - C(21A) - C(16A)	117.7(9)
O(9B) - C(10B)	1.43(2)	C(20A) - C(21A) - C(12A)	125.0(9)
C(10B) - C(11B)	1.41(2)	C(16A) - C(21A) - C(12A)	117.3(9)
C(12B) - C(13B)	1.351(12)	C(2B) - S(1B) - Pt(1)	108.0(4)
C(12B) - C(21B)	1.434(12)	C(4B) - O(5B) - Pt(1)	129.6(6)
C(13B) - C(14B)	1.402(14)	N(3B) - C(2B) - N(6B)	114.0(9)
C(14B) - C(15B)	1.339(14)	N(3B) - C(2B) - S(1B)	129.3(8)
C(15B) - C(16B)	1.387(14)	N(6B) - C(2B) - S(1B)	116.6(7)
C(16B) - C(17B)	1.413(14)	O(5B) - C(4B) - N(3B)	129.0(9)
C(16B) - C(21B)	1.448(13)	O(5B) - C(4B) - C(12B)	114.6(8)
C(17B) - C(18B)	1.324(14)	N(3B) - C(4B) - C(12B)	116.3(8)

Table 4.3 Continued/...

Table 4.3 Continued.

Bond distance (Å)		Bond angle (°)	
C(18B) - C(19B)	1.38(2)	C(4B) - N(3B) - C(2B)	128.2(8)
C(19B) - C(20B)	1.373(14)	C(2B) - N(6B) - C(7B)	124.5(9)
C(20B) - C(21B)	1.409(13)	C(2B) - N(6B) - C(11B)	123.6(8)
		C(7B) - N(6B) - C(11B)	111.5(8)
		N(6B) - C(7B) - C(8B)	111.4(11)
		O(9B) - C(8B) - C(7B)	112.7(11)
		C(8B) - O(9B) - C(10B)	109.0(10)
		C(11B) - C(10B) - O(9B)	114.7(11)
		C(10B) - C(11B) - N(6B)	111.1(10)
		C(13B) - C(12B) - C(21B)	120.0(9)
		C(13B) - C(12B) - C(4B)	117.6(8)
		C(21B) - C(12B) - C(4B)	122.4(8)
		C(12B) - C(13B) - C(14B)	122.0(9)
		C(15B) - C(14B) - C(13B)	118.6(10)
		C(14B) - C(15B) - C(16B)	123.8(11)
		C(15B) - C(16B) - C(17B)	125.0(10)
		C(15B) - C(16B) - C(21B)	117.9(9)
		C(17B) - C(16B) - C(21B)	117.1(9)
		C(18B) - C(17B) - C(16B)	122.9(12)
		C(17B) - C(18B) - C(19B)	120.8(12)
		C(20B) - C(19B) - C(18B)	120.0(11)
		C(19B) - C(20B) - C(21B)	121.4(10)
		C(20B) - C(21B) - C(12B)	124.4(9)
		C(20B) - C(21B) - C(16B)	117.8(8)
		C(12B) - C(21B) - C(16B)	117.6(8)

Table 4.4 Selected torsion angles (°) for *cis*-bis(*N*-morpholino-*N'*-naphthoylthioureato)platinum(II).

	Torsion angle (°)
O(5A)-C(4A)-C(12A)-C(13A)	-155.97(0.90)
N(3A)-C(4A)-C(12A)-C(13A)	21.36(1.27)
O(5A)-C(4A)-C(12A)-C(21A)	21.06(1.36)
N(3A)-C(4A)-C(12A)-C(21A)	-161.61(0.87)
O(5B)-C(4B)-C(12B)-C(13B)	-46.50(1.21)
N(3B)-C(4B)-C(12B)-C(13B)	130.96(0.96)
O(5B)-C(4B)-C(12B)-C(21B)	130.68(0.94)
N(3B)-C(4B)-C(12B)-C(21B)	-51.87(1.28)